CHARACTERISATION OF PHOSPHOLIPASE C-η ENZYMES AND THEIR RELEVANCE TO DISEASE

Mohammed Arastoo

A Thesis Submitted for the Degree of PhD
at the
University of St Andrews

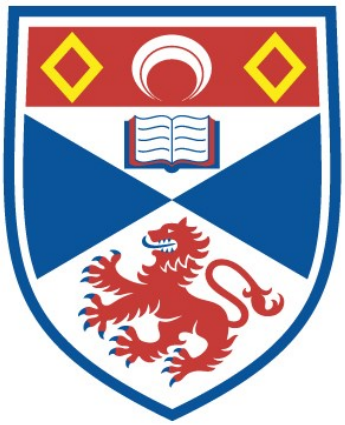

2016

Characterisation of Phospholipase C-η enzymes and their relevance to disease

Mohammed Arastoo, B.Sc. (Hons), M.Sc.

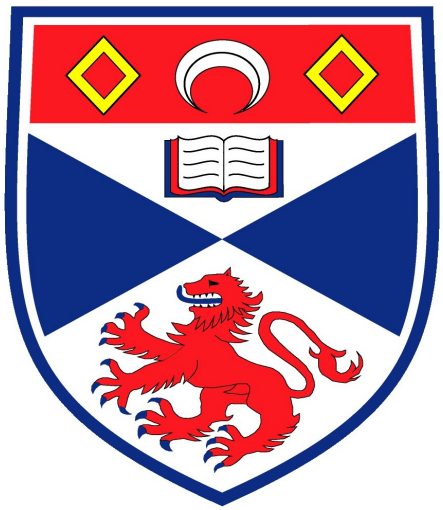

This thesis is submitted in partial fulfilment for the degree of
Doctor of Philosophy at the
University of St Andrews

Abstract

Phospholipase C enzymes are a class of enzymes that catalyse the cleavage of the membrane phospholipid, phosphatidylinositol bisphosphate (PtdIns(4,5)P_2) into the second messengers, inositol trisphosphate (Ins(4,5)P_3) and diacylglycerol (DAG). Six classes of PLC enzymes have been identified based on their structure and mechanism of activation.

PLCηs are the most recently identified family and consist of two isozymes, PLCη1 and PLCη2. The aim of this thesis is to further understand the mechanisms of PLCη activation, the role of PLCη2 in relation to neuritogenesis and their roles in certain disease states. Both isoforms were found to be activated by physiological concentrations of intracellular Ca^{2+}. Activation of PLCη2 by $G\beta_1\gamma_2$ was confirmed using a bacterial 2A co-expression system to allow expression of PLCη2, $G\beta_1$ and $G\gamma_2$ with a single plasmid. Localisation studies show a nuclear distribution for PLCη2, but a cytoplasmic distribution for PLCη1 in a neuroblastoma cells line (Neuro2A).

PLCη2 has been implicated in brain development and neurite formation. Building on this, a neuronal differentiation model using RA-treated Neuro2A cells stably expressing mutant forms of PLCη2 was utilised, revealing that PLCη2 activity is essential for neuritogenesis but that this process is independent of the enzymes high sensitivity towards Ca^{2+}. Furthermore, the direct interaction of PLCη2 and LIMK-1, a previously identified PLCη2 associated protein, is confirmed in the aforementioned neuronal model.

Due to the high sensitivity of PLCη enzymes to Ca^{2+} and because of their presence within neurons, they may be involved in Ca^{2+} dysregulation that occurs in certain diseases such as Alzheimer's disease (AD). The role of PLCη2 was assessed in amyloid-β (Aβ) treated differentiated Neuro2A cells, a cellular model for AD pathogenesis. Also a developmental role for PLCη1 was investigated due to a recently identified PLCη1 polymorphism in patients with holoprosencephaly, an embryonic midline defect.

Declaration

I, Mohammed Arastoo, hereby certify that this thesis, which is approximately 50,000 words in length, has been written by me, that it is the record of work carried out by me and that it has not been submitted in any previous application for a higher degree.

I was admitted as a research student in October, 2011 and as a candidate for the degree of Ph.D. in September, 2012; the higher study for which this is a record was carried out in the University of St Andrews between 2011 and 2015.

Date: October 22, 2015 Signature of candidate ……..

Supervisor's declarations

I hereby certify that the candidate has fulfilled the conditions of the Resolution and Regulations appropriate for the degree of Ph.D. in the University of St Andrews and that the candidate is qualified to submit this thesis in application for that degree.

Date: October 22, 2015 Signature of supervisor ……..

Copyright Declaration

In submitting this thesis to the University of St Andrews I understand that I am giving permission for it to be made available for use in accordance with the regulations of the University Library for the time being in force, subject to any copyright vested in the work not being affected thereby. I also understand that the title and the abstract will be published, and that a copy of the work may be made and supplied to any bona fide library or research worker, that my thesis will be electronically accessible for personal or research use unless exempt by award of an embargo as requested below, and that the library has the right to migrate my thesis into new electronic forms as required to ensure continued access to the thesis. I have obtained any third-party copyright permissions that may be required in order to allow such access and migration.

The following is an agreed request by candidate and supervisor regarding the electronic publication of this thesis:

Embargo on both of printed copy and electronic copy for the same fixed period of two years on the following grounds: publication would be commercially damaging to the researcher and to the supervisor and the University; publication would preclude future publication.

Date: October 22, 2015 Signature of Candidate:….....

Signature of Supervisor:….....

Acknowledgements

Completion of this thesis would not be possible without the support of many wonderful individuals.

First and foremost I would like to offer my sincerest appreciation to my supervisor Dr. Alan Stewart for his continuous assistance and support, for allowing me to be part of his group and for providing me with an opportunity to gain knowledge in a field of my interest. His kindness will always be remembered.

I would like to thank members of the lab and my group, both past and present who provided assistance, friendship and a lively atmosphere in the lab, especially Dr. Siavash Khazaipoul, Dr. Omar Kassar, Dagmara Wiatrek and particularly Dr. Petra Popovics whose research in the PLCη field helped me greatly throughout my project.

During this time I had the pleasure of meeting knowledgable staff who provided guidance and assistance towards my research. I would especially like to thank Prof. Frank Gunn-Moore, Dr. John Lucocq, Dr. Christian Hacker and Dr. Javier Tello for their help with experimental procedures and for sharing their knowledge with me.

Special recognition goes out to my close friends and my entire family, particularly my parents who have always encouraged me to seek knowledge, my siblings Amin and Sare who have given me so much joy over the years and especially my elder brother Ali who has supported me in every way possible. Finally I would like to thank my fiancée Zahra for her love, encouragement and patience during the write-up of my thesis.

"Every container becomes tightly packed with what is put in it, except for the container of knowledge, for surely it expands" IMAM ALI (as)

"Nothing in life is to be feared, it is only to be understood. Now is the time to understand more, so that we may fear less" MARIE CURIE

Contents

List of figures

List of tables

Abbreviations

AA	arachidonic acid
AC	adenlylate cyclase enzyme
AMPA	α-amino-3-hydroxyl-5-methyl-4-isoxazole propionate
ANT	adenine nucleotide translocase
APC	adenomatosis polyposis coli
ARC	arachidonic acid (AA) regulated Ca^{2+} channels
ATP	adenosine 5'-triphosphate
AP	action potentials
APC	streptavidin-tagged allophycocyanin
APOE4	apolipoprotein E4
BIFC	biomolecular fluorescence complementation
BDNF	brain-derived neurotrophic factor
BMP	bone morphogenic protein
C2 domain	constant 2 domain
cADPR	cyclic adenosine diphosphate ribose
CAMKs	Ca^{2+}/calmodulin-dependent protein kinases
cAMP	cyclic adenosine monophosphate
CDK	cyclicdependent kinase
CF	cleavage furrow
cGMP	cyclic guanosine monophosphate
CHYSEL	*cis*-acting hydrolase element
CICR	Ca^{2+}-induced Ca^{2+} release
CREB	cAMP responsive element binding protein
CycD	cyclophilin D
DAG	diacylglycerol
DAPI	4',6-diamidino-2-phenylindole
Disheveled	Dsh
DHP	dihydropyridine
DMEM	Dulbecco`s modified Eagle`s medium
ECACC	The European Collection of Cell Cultures
ECFP	enhanced cyan fluorescent protein
ECC	excitation contraction coupling
ECL	enhanced chemiluminescence
EMEM	Eagle's minimal essential medium
ER/SR	endo/sarcoplasmic reticulum
ERAV	equine rhinitis A virus
EV	empty vector
FAD	familial Alzheimer’s disease
EYFP	enhanced yellow flurescent protein
FRET	Förster resonance energy transfer
Fzd	Frizzled
GA	Golgi apparatus
GAP	GTPase-accelerating proteins
GDI	guanine nucleotide dissociation inhibitor
GEF	guanine nucleotide exchange factors
GFP	green fluorescent protein
GluRs	glutamate receptors

GRK	G-protein coupled receptor kinases
GPCR	G-protein-coupled receptor
Grp1	general receptor for phosphoinositides-1
GST	glutathione S-transferase
HCA	H^+/Ca^{2+} antiporter
HVA	high voltage activating
inaD	inactivation-no-afterpotential D
Ins(1,3,4)P3	inositol 1,3,4-trisphosphate
Ins(1,3,4,5)P4	inositol 1,3,4,5-tetrakisphosphate
Ins(1,4,5)P3	inositol 1,4,5-trisphosphate
Ins(4,5)P_3R	inositol 1,4,5-trisphosphate receptor
IP-assay	[^{3}H]Inositol-phosphate release assays
IRES	internal ribosomal entry site elements
K_s	Ca^{2+} binding ratio
LIMK-1	lim domain kinase-1
LPA	lysophosphatidic acid
LTD	long-term depression
LTP	long-term potentiation
LVA	low voltage activating
MAPK	mitogen activated protein kinase
MCU	mitochondrial Ca^{2+} uniporter
MTM1	myotubularin1
mPTP	mitochondrial permeability transition pore
MTMR	myotubularin related protein
MTT	3-(4,5-dimethylthiazol-2-yl)-2,5-diphenyltetrazolium bromide
NAADP	nicotinic acid adenine dinucleotide phosphate
nAChR	nicotinic variant of acetylcholine receptors
NCC	Neural crest cell
NCX	Na^+/Ca^{2+} exchanger
NCX_{mito}	mitochondrial Na^+/Ca^{2+} exchanger
NCX_{pm}	plasmamembrane Na^+/Ca^{2+} exchanger
NE	nuclear envelope
NLS	nuclear localisation sequence
NMDA	N-methyl-D-aspartic acid
PA	phosphatidic acid
PACAP	pituitary adenylate cyclase-activating polypeptide
PC	phosphatidylcholine
PDK1	3-phosphoinositide dependent protein kinase-1
PKG	cGMP-dependent protein kinase
PH	domain pleckstrin homology domain
Ptch	Patched
PtdCho	phosphatidylcholine
PtdEn	phosphatidylethanolamine
PTEN	phosphatase and tensin homolog
PtdIns	phosphatidylinositol
PtdIns(3)P	phosphatidylinositol 3-phosphate
PtdIns(3,4)P_2	phosphatidylinositol 3,4-bisphosphate
PtdIns(3,4,5)P_3	phosphatidylinositol 3,4,5-trisphosphate
PtdIns(4)P	phosphatidylinositol 4-phosphate
PtdIns(4,5)P_2	phosphatidylinositol 4,5-bisphosphate

PtdSer	phosphatidylserine
PKA	protein kinase A
PKC	protein kinase C
PLC	phospholipase C
PMCA	plasma membrane Ca^{2+}-ATPase
RA	retinoic acid
RARE	retinoic acid responsive element
RGS	regulator of G-protein signalling proteins
ROC	receptor-operated channel
RasGAP	RasGTPase activating protein
ROCC	receptor-operated calcium channel
RT	room temperature
RTK	receptor tyrosine kinase
RyR	ryanodine receptor
SEM	standard error of the mean
SERCA	sarco/endoplasmic reticulum ATPase
SH2	SRC homology 2
SKIP	ski-interacting protein
Shh	Sonic hedgehog
Smo	smoothened
SMOC	second messenger-operated channels
SPCA	secretory pathway Ca^{2+} ATPase
STIM1	stromal interaction protein 1
SM	sphingomyelin
SUR	systematic uniformrandom
t-tubules	transverse tubules
TaV	thosea asigna virus
TIM-barrel	triose phosphate isomerase-barrel
TPC	two-pore channels
TRITC	tetramethylrhodamine B isothiocyanate
TRPC	transient receptor potential channel
VDAC	voltage dependentanion channel
VOC	voltage-operated channels
VOCC	voltage-operated calcium channels
YFP	yellow fluorescent protein
Wt	wild type

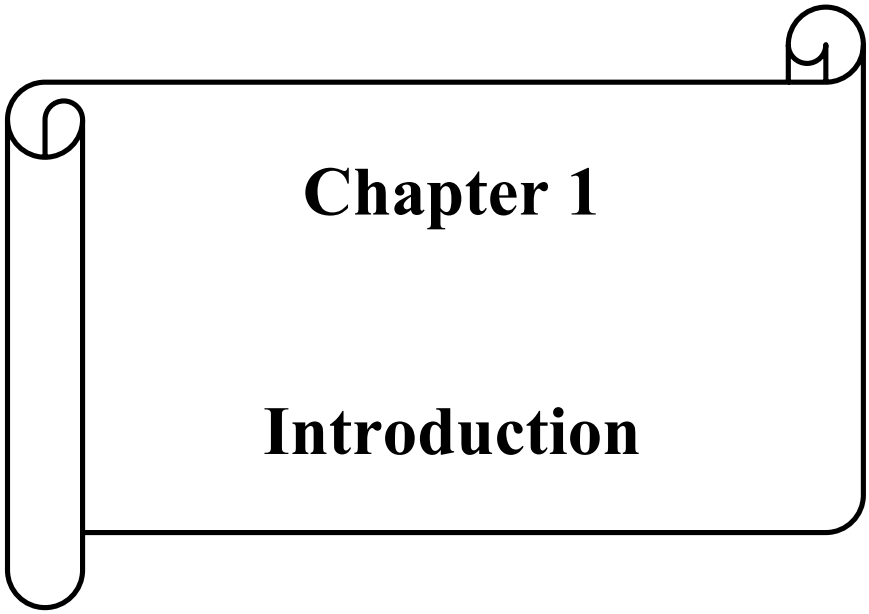

Chapter 1

Introduction

1.1. Overview of Calcium signalling

Ca^{2+} is a key intracellular signalling ion that activates a wide range of enzymes, ion channels and signalling pathways thereby controlling an array of cellular processes including neurotransmission (Simon and Llinas, 1985), muscle contraction (Szent-Gyorgyi, 1975) and fertilisation (Stricker, 1999), mechanisms of which will be discussed later. It plays a fundamental role in all cell types and is essential in key processes required for their specialised purpose. For example Ca^{2+} is essential in the functioning of neuronal cells by influencing processes such as excitability and synaptic strength thereby maintaining neuronal integrity and ensuring long term survival, allowing for normal brain physiology (Marambaud et al., 2009). In order to relay information received from an extracellular stimulus (such as hormones or neurotransmitters) to effectors that activate cellular responses, cells utilise many signalling pathways with Ca^{2+} being an integral part of several signalling systems. Without this versatile signalling ion many essential processes including membrane excitability, hormone and neurotransmitter secretion, enzyme activation, gene transcription, and muscle contraction would not be possible. Ca^{2+} functions over a wide temporal range, operating within minutes to hours in some processes such as gene transcription and cell growth or within microseconds for other processes such as triggering neurotransmitter release at the synaptic cleft (Dupont et al., 2007).

1.1.1. ON/OFF reactions

The regulation of Ca^{2+} signalling must be tightly controlled to allow efficient functioning of cells. This is maintained by a wide range of molecules that make up the Ca^{2+} signalling toolkit. Many of these molecules work to increase intracellular Ca^{2+} levels and collectively make up the ON reactions whereas others function to clear Ca^{2+} when it is not needed and make up the OFF reactions. The dynamics of Ca^{2+} signalling are therefore governed by an interaction between the ON and OFF reactions that control the fluctuations in Ca^{2+} across the plasma membrane and organelles (Berridge, 2012). The ON reactions are activated by increased cytosolic Ca^{2+} levels via entry through plasma membrane ion channels, exchangers and pumps or by release from organelles (Berridge et al., 2003). There are approximately 200 human proteins that act as Ca^{2+} effectors or buffers (Carafoli et al., 2001). A small portion of the Ca^{2+} that enters the cytoplasm goes on to activate effectors whereas the majority of the ion is taken up by cytosolic buffers such as parvalbumin, calretinin, and calbindin. Different cell types have different buffering capacities as determined by their Ca^{2+} binding ratio (K_s), which is the ratio

of buffer-bound Ca^{2+} to "free" Ca^{2+} in the cytosol. In the brain, motor neurons have a K_s value of 40 whereas Purkinje neurons have a value of 2000. The low Ca^{2+} buffering of motor neurons allows for generation of rapid Ca^{2+} signals which is required for efficient motor neuron functioning (Palecek et al., 1999). Also, upon reaching high Ca^{2+} concentrations, the ion itself functions as a negative feedback regulator, thereby preventing further Ca^{2+} release from ER stores (Finch et al., 1991), these protective strategies are in place to reduce the impact of the ON reaction and ensure a healthy physiological level of Ca^{2+}.

Maintaining a physiological level of Ca^{2+} is essential for cell survival so there are a number of different mechanisms that cells utilise to reset resting Ca^{2+} levels. These OFF reactions eliminate Ca^{2+} from the cytosol thus keeping Ca^{2+} at a basal level of ~100 nM. Ca^{2+} buffers in the lumen of the ER (such as calnexin and calreticulin) are a critical factor in the ability of ER/SR to store large levels of Ca^{2+} (Mery et al., 1996, Tjoelker et al., 1994). When cytosolic Ca^{2+} concentrations are at < 300 nM, mitochondria will take up Ca^{2+} via the mitochondrial Ca^{2+} uniporter (MCU) which is located in the mitochondrial inner membrane (Colegrove et al., 2000). Pumps and exchangers on the cell membrane and ER/SR also reduce cytosolic Ca^{2+} by either expelling it from the cell via the plasma membrane Ca^{2+} ATPase (PMCA) and the Na^{2+}/Ca^{2+} exchanger (NCX) or returning and storing into the ER/SR lumen via the sarco/endoplasmic reticulum Ca^{2+}-ATPase (SERCA) pump. In addition, once free Ca^{2+} concentrations return to normal levels, Ca^{2+} is slowly released from cytosolic buffers and mitochondria and is stored within the ER/SR (Berridge, 2001). Figure 1.1 shows the dynamics of Ca^{2+} movement within the cell.

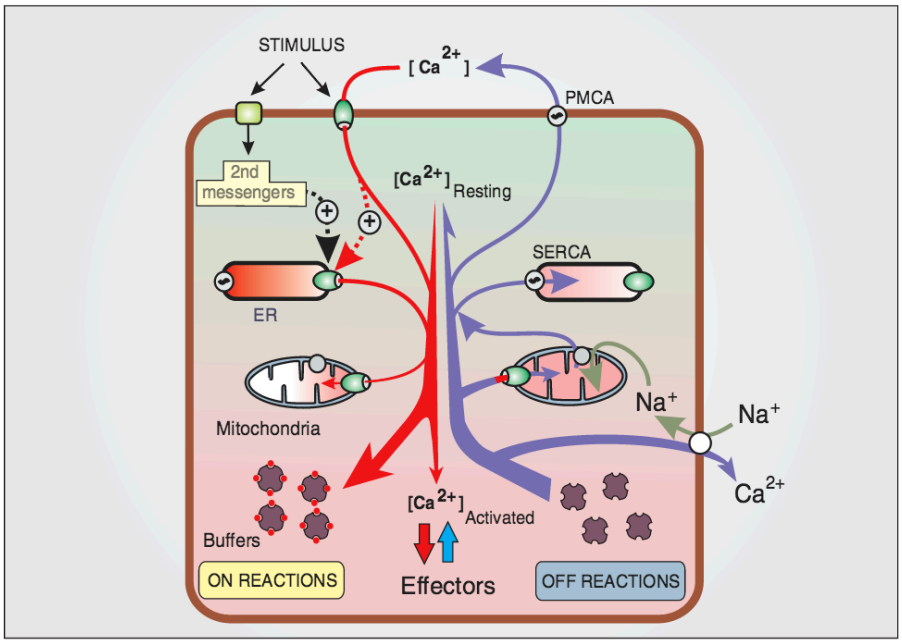

Figure 1.1: Factors controlling the ON and OFF reactions. The ON reaction is activated by external stimuli that introduce Ca^{2+} into the cytoplasm through channels and pumps on the cell membrane or by release through intracellular stores such as the ER/SR. Buffers adsorb most of the Ca^{2+} that enters the cytoplasm, leaving a small portion to activate effectors. The OFF reactions remove Ca^{2+} from the cytosol by uptake into organelles including the mitochondria via the mitochondria uniporter and ER/SR via the SERCA pump. Ca^{2+} can also be removed completely from the cell via the PMCA. Abbreviations: ER/SR, Endoplasmic reticulum/carcoplasmic reticulum. PMCA, plasma membrane Ca^{2+} ATPase. SERCA, sarco/endoplasmic reticulum Ca^{2+}-ATPase. Image taken from Berridge, 2012.

1.1.2. Mechanisms by which cells increase intracellular calcium

At rest, cells typically have a low concentration of intracellular Ca^{2+}, approximately 100-200 nM (Bygrave and Benedetti, 1996, Usachev et al., 1995). Ca^{2+} signalling occurs following increased intracellular concentrations upon arrival of a suitable stimulus that increases the Ca^{2+} concentration to above 500 nM (Verkhratsky, 2005). In this section, mechanisms of Ca^{2+} release from internal stores will be described followed by modes of Ca^{2+} entry through the extracellular space. For the most part, these mechanisms are the same for the ER and SR but for the purpose of this project the ER will be referred to.

1.1.2.1. Calcium release from the ER

The ER is the most important organelle involved in maintaining cellular Ca^{2+} homeostasis. Besides its important role in storing, modifying, and transporting newly synthesised proteins,

the ER is also a high capacity reservoir for intracellular Ca^{2+}, with concentrations ranging from high micromolar to low millimolar levels (Marambaud et al., 2009). Although the total Ca^{2+} store content may surpass 1 mM in some cells, it is estimated that [Ca^{2+}] ranges from 100-800 μM (Berridge et al., 1998) which is 3-4 orders of magnitude higher in comparison to the surrounding cytosol, creating a steep concentration gradient. This gradient is the primary driving force behind the movement of Ca^{2+} from the ER through receptors and channels. There are two main mechanisms by which Ca^{2+} is released from ER stores. This involves two types of receptors; inositol 1,4,5-trisphosphate receptors ($Ins(4,5)P_3Rs$) and ryanodine receptors (RyRs).

$Ins(4,5)P_3Rs$ are ligand gated Ca^{2+} channels made up of four subunits (Figure 1.2) that exist as homo- or heterotetramers and weigh approximately 1,200 kDa (Maeda et al., 1991, Patel et al., 1999). These receptors are activated and gated open by $Ins(4,5)P_3$ following phospholipase C (PLC) activation which breaks down phosphatidylinositol 4,5-bisphosphate ($PtdIns(4,5)P_2$) into $Ins(4,5)P_3$ and diacylglycerol (DAG) (the mechanism of which will be discussed in more depth later). $Ins(4,5)P_3Rs$ are composed of several domains. The N-terminal tail of each subunit is composed of a suppressor domain, $Ins(4,5)P_3$ binding domain, TRPC coupling domain and regulatory domain which make up ~85% of the channel's total weight. The rest of the protein is made up of the C-terminal tail and a transmembrane domain which encompasses the pore region (Figure 1.2). $Ins(4,5)P_3$ is highly water soluble, allowing it to rapidly diffuse into the cytoplasm and bind to the $Ins(4,5)P_3$ binding domain of $Ins(4,5)P_3Rs$ on the ER. This binding causes a conformational change in the channel thereby opening it and allowing Ca^{2+} to move down its concentration gradient and enter the cytosol (Bootman et al., 2001a). There are three mammalian $Ins(4,5)P_3R$ subtypes (1, 2, and 3), which can form the subunits of heterotetrameric channel complexes. The channel opens upon $Ins(4,5)P_3$ binding to all subunits (Tu et al., 2004). For the most part $Ins(4,5)P_3R$ subtypes act similarly but have differences in their affinity for $Ins(4,5)P_3$, sensitivity to Ca^{2+}, and regulation by phosphorylation, ATP and associated proteins (Foskett et al., 2007). In humans, the three $Ins(4,5)P_3R$ subtypes possess a sequence homology of ~75% with the Ca^{2+} sensor and pore region remaining highly conserved between them (Kume et al., 1997).

Most mammalian cell types express all three subtypes however it has been reported that $Ins(4,5)P_3R$-1 is predominantly expressed in the brain while $Ins(4,5)P_3R$-2 and $Ins(4,5)P_3R$-3 are predominantly expressed in the heart and pancreas, respectively (Taylor et al., 1999). Ca^{2+} is an allosteric modulator of this receptor as it activates the channel and raises its open

probability at low ER Ca^{2+} concentrations (<300 nM) and inhibits channel opening at higher Ca^{2+} concentrations (Berridge, 2012, Finch et al., 1991). It is important to note however that Ca^{2+} only enhances the open probability of Ins(4,5)P_3Rs but cannot open them in the absence of Ins(4,5)P_3 (Finch et al., 1991). In addition, an increase in ER intraluminal Ca^{2+} level increases sensitivity of the Ins(4,5)P_3R to Ins(4,5)P_3 (Khachaturian, 1987). Certain kinases are able to phosphorylate and modulate Ins(4,5)P_3Rs such as Ca^{2+}/calmodulin (CaM)-dependent kinase-II (CaMKII) (Bare et al., 2005), cGMP-dependent protein kinase (PKG) (Stutzmann et al., 2006), protein kinase C (PKC), cAMP-dependent protein kinase A (Berridge et al., 2003) and tyrosine kinase Lyn (Yokoyama et al., 2002), some of which increase channel activity while others decrease it. Ins(4,5)P_3 itself is phosphorylated or dephosphorylated quickly by enzymes after it is produced which inhibits its Ca^{2+} releasing ability, making it a very short lived messenger with an half-life of only a few seconds (Bootman et al., 2001b). Phosphorylation of Ins(4,5)P_3 produces 1,3,4,5-tetrakisphosphate (Ins(3,4,5)P_4) which can also act as an intracellular messenger. Cullen et al. have shown that Ins(3,4,5)P_4 can bind to small (Ras) G-proteins and can further modulate Ca^{2+} release (Bootman et al., 2001b, Cullen et al., 1995).

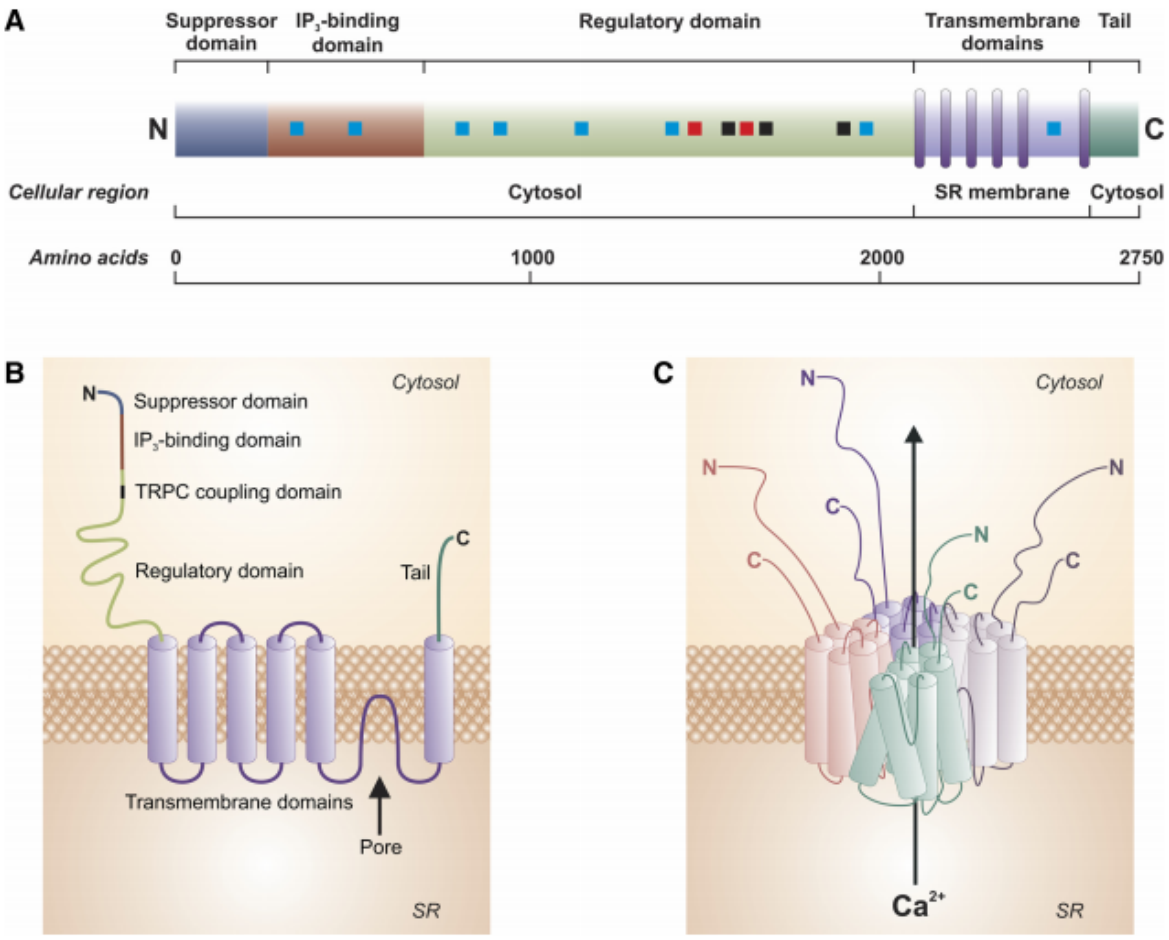

Figure 1.2: Molecular structure of Ins(4,5)P_3Rs. **A** schematic representation of Ins(4,5)P_3R domains. Blue squares=Ca^{2+} binding site, red squares=phosphorylation site, black squares=ATP binding site. **B** Representation of a single Ins(4,5)P_3R subunit showing distribution of domains in relation to the plasma membrane, SR and Cytosol. **C** Representation of a complete Ins(4,5)P_3R. The channel is made up of four subunits and can form heterotetramers composed of different Ins(4,5)P_3 subtypes, therefore a variety of Ins(4,5)P_3R isoforms can exist, implications of which are unclear. Abbreviations: SR, sarcoplasmic reticulum; N, NH2 terminus; C, COOH terminus. Image taken from Narayanan et al., 2012.

RyRs are named after their high affinity for the plant alkaloid ryanodine, which binds to RyRs when they are in their open state conformation. Ryanodine binding to the outside of the permeation pore is believed to have allosteric effects on the channel's Ca^{2+} permeability (Fessenden et al., 2001). This property has enabled researchers to use [^{3}H]-ryanodine as a means to study channel activation which has led to purification and subsequent characterisation of three RyR isoforms (Fleischer et al., 1985, Hawkes et al., 1992, Meissner and el-Hashem, 1992, Pessah et al., 1985). These three RYR subtypes (1, 2, and 3) exhibit approximately 70% amino acid sequence homology in mammals and form homotetrameric channels, with each subunit ~550 kDa in size (Marks et al., 1989, Masumiya et al., 2003, Nakai et al., 1990). RYRs

possess a protein structure similar to Ins(4,5)P_3Rs as they have a large cytoplasmic N terminal tail (containing phosphorylation and glycosylation sites as well as binding sites for nucleotides, Mg^{2+}, and calmodulin), a six transmembrane modulatory domain that forms the channel pore and a cytoplasmic C-terminal domain (that has binding sites for Ca^{2+}) (Bhat and Ma, 2002, Chen et al., 1992, Hakamata et al., 1992, Zorzato et al., 1990). RyRs are approximately 2 MDa in size and consist of abundant accessory proteins, making them the largest of the identified ion channels (Inui et al., 1987, Lai et al., 1988). They have twice the ion conductance of Ins(4,5)P_3Rs (Bootman et al., 2001b) and are activated by Ca^{2+} in a process termed Ca^{2+}-induced Ca^{2+} release (CICR). This process allows for Ca^{2+} entering the cell across the plasma membrane to act as a messenger, triggering further release of Ca^{2+} from internal stores (Berridge, 2012). RyRs are activated by Ca^{2+} in a similar manner to Ins(4,5)P_3Rs in that they are inactivated by low nM concentrations, activated by low μM concentrations, and inactivated by high mM concentrations. RyRs can also release Ca^{2+} in response to other factors including ATP, Mg^{2+}, protein kinase A (PKA), CaMKII and cyclic adenosine diphosphate ribose (cADPR), (Brillantes et al., 1994, Chen and MacLennan, 1994, Mery et al., 1996, Wang and Best, 1992).

A highly important role in which RyRs are involved in is contraction of cardiac muscles in a process called excitation contraction coupling (ECC, Cheng et al., 1996). In this process, action potentials (AP) travelling down a motor neuron induce opening of voltage operated Ca^{2+} channels (VOCCs) on the axon terminal which allow Ca^{2+} entry. This increased Ca^{2+} causes exocytosis of vesicles containing a neurotransmitter called acetylcholine (Ach) which traverses the synaptic cleft and binds to Ach receptors (AchRs) on muscle fibres. AchRs are ion channels that allow for ions to enter into skeletal muscle fibres. This initiates an AP in muscle fibres which travels across the entire sarcolema and is conducted swiftly into the muscle fibre interior by transverse tubules (t-tubules). This depolarisation of t-tubules in turn causes Ca^{2+} release from the SR by means of two receptors. Changes in membrane potential are detected by L-type Ca^{2+} channels that allow Ca^{2+} entry into cells, which subsequently activates type 2 RyRs on the SR. This leads to Ca^{2+} release from the SR by CICR. The resulting rise in Ca^{2+} levelsinduces contraction (Ebashi, 1991).

RyR-2 is therefore essential for ECC in cardiac muscles. RyRs however are also expressed in a number of other cell types. RyR1 is expressed in smooth muscle, stomach, kidney, thymus, adrenal gland, ovaries and testis (Giannini et al., 1995, Nakai et al., 1998, Neylon et al., 1995). Similarly, RyR2 is expressed in the stomach, kidneys, adrenal glands, lungs, thymus, and

ovaries (Giannini et al., 1995, Kuwajima et al., 1992), and RyR3 is expressed in lung, ileum, jejunum, stomach, spleen, kidney, bladder and oesophagus (Giannini et al., 1995, Hakamata et al., 1992, Ottini et al., 1996). All RyR subtypes are found in the brain, primarily within the soma of neurons (Kuwajima et al., 1992, Seymour-Laurent and Barish, 1995), as well as other regions, with the predominant isoform being RyR-2. It is highly expressed in cerebellar purkinje neurons, and throughout the cerebral cortex (Nakanishi et al., 1992). Cerebellar purkinje neurons also express RyR-1 (Nakanishi et al., 1992, Seymour-Laurent and Barish, 1995). RyR-3 is present in regions involved in learning and memory, namely the cerebral cortex and hippocampus (Berridge, 2011). Distributions of RyRs and Ins(4,5)P3Rs are generally similar but some interesting differences have been noted. For example, the spines of purkinje neurons possess Ins(4,5)P_3Rs but not RyRs (Walton et al., 1991), whereas RyRs are present more abundantly than Ins(4,5)P_3Rs in spines of hippocampal cells of the CA1 region (Sharp et al., 1993).

Both Ins(4,5)P_3Rs and RyRs allow for sufficient Ca^{2+} release from the ER. Following stimulation of cells, Ins(4,5)P_3Rs and RyRs open for a duration of <1 second, generate small Ca^{2+} discharges called 'blips' and 'quarks' respectively, and elevate cytosolic Ca^{2+} concentrations by ~50-600 nM with a small spatial spread of ~2-6 μm (Niggli, 1999, Thomas et al., 2000). Clusters of receptors can become activated upon arrival of a stronger stimulus, generating a stronger localised Ca^{2+} release called 'puffs' and 'sparks' from Ins(4,5)P_3Rs and RyRs respectively. These transient Ca^{2+} spikes stimulate the opening of neighbouring receptor clusters which can spread through the cell in a salutatory manner thereby creating a global Ca^{2+} wave throughout the cell (Berridge et al., 2000). Figure 1.3 shows this mechanism for Ins(4,5)P_3Rs. This Ca^{2+} wave can propagate to neighbouring cells as reported in endocrine cells (Fauquier et al., 2001), vertebrate gastrula (Wallingford et al., 2001) and intact perfused liver (Robb-Gaspers and Thomas, 1995). Such intracellular waves can also propagate between different cell types as reported between smooth muscle and endothelial cells (Yashiro and Duling, 2000) as well as neuronal and glial cells (Hassinger et al., 1995).

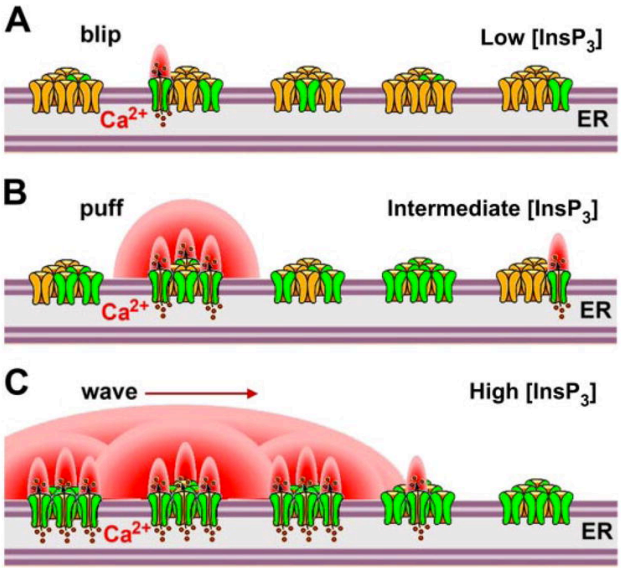

Figure 1.3: Propagating Ca^{2+} wave. Different amounts of Ca^{2+} is released from Ins(4,5)P_3Rs depending on the strength of agonist stimulation and therefore concentration of cytoplasmic Ins(4,5)P_3, forming blips at low concentrations (A), puffs at intermediate concentrations and Waves at high concentrations (C). Image taken from Foskett et al., 2007.

As with other cell types, neurons require intra- and extracellular Ca^{2+} to direct a diverse range of neuronal processes including excitability, associativity, neurotransmitter release, synaptic plasticity, and gene transcription (Berridge, 1998). Neurons have a continuous ER system that extends throughout the entire cell. The outer nuclear membrane of neurons is continuous with the ER which extends to their dendrites and axon (Broadwell and Cataldo, 1984). This vast network of ER running throughout the neuron suggests its important role as a Ca^{2+} store that allows for regulation of neuronal function.

1.1.2.2. Calcium release from mitochondria

In addition to their role as the cells energy producer in the form of ATP, mitochondria also serve as stores that can take up and release Ca^{2+}. Ca^{2+} release by mitochondria occurs through the Na^+/Ca^{2+} exchanger (NCX_{mito}) which functions similarly to its plasma membrane counterpart, albeit in the opposite direction as it conversely acts to increase cytosolic Ca^{2+} levels (Palty et al., 2010). Ca^{2+} release can also occur through the H^+/Ca^{2+} antiporter (HCA) which can function in either direction depending on the intra- or extra-mitochondrial Ca^{2+} concentration and pH (Jiang et al., 2009). In addition, certain conditions such as when mitochondria are overloaded with Ca^{2+} induce the formation of pores on their surface. These pores are called mitochondrial permeability transition pore (mPTP) and are composed of three proteins; voltage-dependent anion channel (VDAC) in the outer membrane, adenine nucleotide

translocase (ANT) in the inner membrane and cyclophilin D (CypD) in the cytosol. Formation of the mPTP can also be induced by oxidative stress as this causes oxidation of two essential thiol groups close to the adenine nucleotide binding site on the ANT proein, which prevents adenine binding and so increases sensitivity of the pore towards Ca^{2+} (McStay et al., 2002). This protein pore displays two states of activation. The first state is characterised by a low conductance and opens in a pH-dependent manner, expelling only small ions including Ca^{2+}. The second state is characterised by high conductance and causes the non-specific release of larger ions and metabolites weighing up to 1.5 kDa (Bernardi and Forte, 2007, Crompton et al., 1999). This second state is also associated with apoptosis (Ichas and Mazat, 1998). Furthermore, Rizzuto *et al*. reported that Ca^{2+} release from the ER through Ins(4,5)P_3Rs can be taken up by mitochondria immediately, showing that cross-talk exists between these organelles (Rizzuto et al., 1998).

1.1.2.3. Calcium release from other intracellular stores

Vesicles including endosomes, lysosomes and secretory vesicles are also able to store and release Ca^{2+}. Mitchell *et al.* reported the presence of RyRs on the membranes of secretory vesicles, making them capable of CICR. They also proposed that this CICR is capable of modulating exocytosis of these vesicles (Mitchell et al., 2001). In addition, the second messenger nicotinic acid adenine dinucleotide phosphate (NAADP) binds to and opens Ca^{2+} channels (recently identified as two pore channels) on endosomes, lysosomes and secretory vesicles (Churchill et al., 2002, Mitchell et al., 2003, Ruas et al., 2010) NAADP can also cause release of Ca^{2+} from nuclear envelope (NE) stores (Gerasimenko et al., 1995). RyRs and Ins(4,5)P_3Rs are also involved in Ca^{2+} release from the NE which is comprehensible as the NE is continuous with the ER (Erickson et al., 2004, Humbert et al., 1996). Several studies have also described the Golgi apparatus (GA) as a potential Ca^{2+} store mainly due to the presence of SERCA, Ins(4,5)P_3Rs and secretory pathway Ca^{2+} ATPase (SPCA), a distinctive Ca^{2+} ATPase present on GA membranes (Gunteski-Hamblin et al., 1992, Pinton et al., 1998, Taylor et al., 1997).

1.1.2.4. Ca^{2+} entry at the plasma membrane

During the ON reaction, a major source of Ca^{2+} is entry from the extracellular space. Because of the densely packed and hydrophobic fatty acid tails in the plasma membrane core, ions cannot simply pass through the plasma membrane and would otherwise require large amounts of energy to do so (Parsegian, 1969). In order to achieve this movement of Ca^{2+} from the

outside of the cell to the inside, cells have a series of mechanisms that enable this. These include various types of channels and exchangers, each possessing different properties, that participate in this process as summarised in Figure 1.4

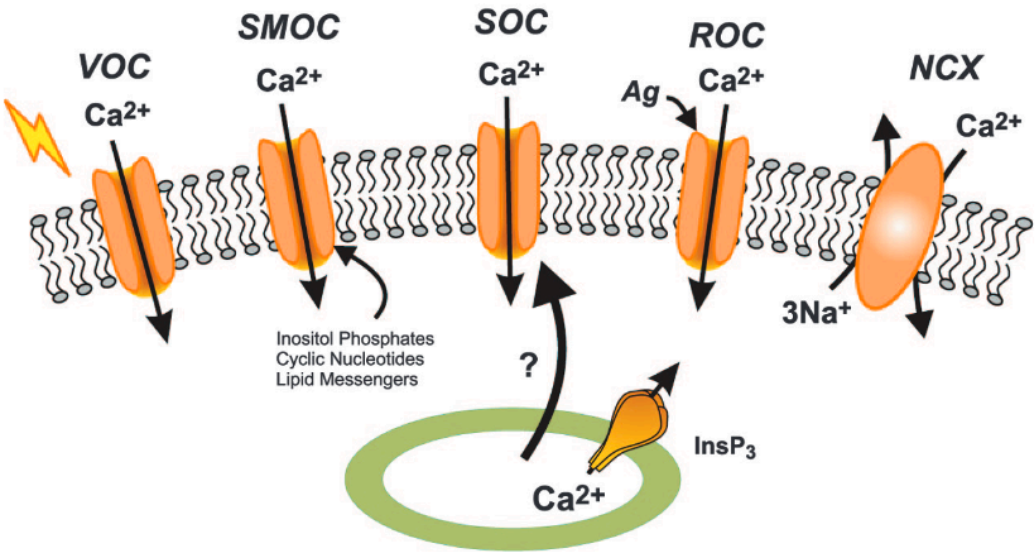

Figure 1.4: Different mechanisms that increase intracellular Ca^{2+} concentration at the plasma membrane. These include receptor-operated channels (ROCs) which are binding sites for agonists (Ag) such as the neurotransmitter glutamate, second messenger- operated channels (SMOCs) which are activated by second messengers including diacylglycerol (DAG) and cyclic AMP from the cytoplasmic side, voltage-operated channels (VOCs) that are activated by membrane depolarization, exchangers such as the sodium-calcium exchanger (NCX) and store operated channels (SOCs) that allow Ca^{2+} entry in response to ER Ca^{2+} levels. Image taken from Parekh and Putney, 2005.

1.1.2.4.1. Voltage operated channels (VOCs)

VOCs are multimeric transmembrane proteins found in excitable cells that create swift ion fluxes in response to changes in voltage across the membrane. Several types of VOCs exist with each one gating either Na^+, K^+, Cl^- or Ca^{2+} (VOCCs). VOCCs respond to changes in voltage through a region of the protein that possesses charged amino acids that act as a voltage sensor and reposition following changes in the membrane electric field. This repositioning causes a conformational change in the channel, causing it to open (Bezanilla, 2005). There is a large electrochemical gradient between the outside and inside of the cell that drives movement of Ca^{2+} into the cell once the channels are open. This rise in intracellular Ca^{2+} results in rapid onset of cellular processes including synaptic vesicle release for neurotransmission, and muscle contraction (Simon and Llinas, 1985, Szent-Gyorgyi, 1975). One cell can have multiple types of Ca^{2+} currents entering through several channels that possess different voltage-dependent

gating properties (Hagiwara et al., 1975). Upon characterisation, these channels were placed into the low voltage activity (LVA) group if they had a threshold of positive to -70 mV or the high voltage activity (HVA) group if they had a threshold of positive to -40 mV, as determined by patch clamp studies. During a sustained depolarization, LVA channels possess a smaller single channel conductance and faster inactivating whereas HVA channels exhibit larger single channel conductance and slower inactivating. Alternatively, LVA channels are called T-type Ca^{2+} channels. There are different forms of HVA channels which differ structurally and vary in their Ca^{2+} gating properties. These are called L-, N-. P/Q-, and R type VOCCs (Ertel et al., 2000). These are identified in the laboratory through their responses to different drugs that specifically inhibit them. For example, The L-type channels are also called dihydropyridine (DHP) receptors as they are blocked by DHP (Dunlap et al., 1995). Generally, mammalian VOCCs are composed of four subunits; α1, α2δ, β and γ which function to regulate channel gating. The principal subunit which is essential for channel functioning is the α_1 subunit because it forms the Ca^{2+} selective pore, a region that contains voltage-sensing machinery and the drug/toxin-binding sites. In total, ten α_1 subunits have been identified in human VOCCs and have been distinguished into 3 groups: Ca_V1, Ca_V2 and Ca_V3 (Catterall et al., 2005). Table 1 summarizes the classification of different VOCCs, their current type, their major tissue location, and the physiological functions they facilitate.

α1 subunit categorization	Ca^{2+} current type	Primary tissue location	Physiological functions
$Ca_v1.1$	L (HVA)	Skeletal muscle	Excitation-contraction coupling (ECC)
$Ca_v1.2$	L (HVA)	Cardiac muscle, Smooth muscle , neuronal	ECC, Regulation of enzyme activity, regulation of gene transcription
$Ca_v1.3$	L (HVA)	Pancreas, cardiac, neuronal, ear, adrenal medulla	Endocrine secretion, pacemaking, auditory transduction
$Ca_v1.4$	L (HVA)	Eye, immune system	Visual transduction, T-cell signalling/ homeostasis, neurotransmitter release
$Ca_v2.1$	P/Q (HVA)	Neuronal	Neurotransmitter release
$Ca_v2.2$	N (HVA)	Neuronal	Neurotransmitter release
$Ca_v2.3$	R (HVA)	Neuronal	Neurotransmitter release
$Ca_v3.1$	T (LVA)	Neuronal, cardiac	Pacemaking, repetitive firing
$Ca_v3.2$	T (LVA)	Neuronal, cardiac, kidney	Pacemaking, repetitive firing
$Ca_v3.3$	T (LVA)	Neuronal	-

Table 1.1: The categorisation and properties of VOCCs. Abbreviations: HVA, High voltage activated. LVA, Low voltage activated.

1.1.2.4.2. Receptor operated channels (ROCs)

Receptor operated channels (ROCs), also called ligand-gated ion channels open in response to chemical messengers and allow for ion movement following their activation. While VOCs commonly allow for gating of one ion, ROCs are less selective and allow two or more types of ions to pass through them. Many molecules including ATP, ADP, acetylcholine, histamine, vasopressin, neurokinin A and substance P act on these receptors and cause ion influx as shown in smooth muscle cells, hepatocytes, and platelets (Rosado and Sage, 2000). ROCs that gate Ca^{2+} (ROCCs) have been identified. ROCCs include the N-methyl-D-aspartate (NMDA) receptors, so called because of selective binding of the ligand NMDA, are also activated by co-binding of the neurotransmitters glutamate and glycine (or D-serine) (Kleckner and Dingledine, 1988). These receptors are highly Ca^{2+} permeable (Mayer and Westbrook, 1987) and have important roles in synaptic plasticity and memory formation (Dunlap et al., 1995). Glutamate can also bind to α-amino-3-hydroxyl-5-methyl-4-isoxazole-propionic acid receptors (AMPAR). Generally, AMPARs are permeable to Na^+ and K^+ but not Ca^{2+}. Subsets of AMPARs however have been identified that are permeable to Ca^{2+} such as in human neural progenitor cells, in which they are important for neurogenesis (Whitney et al., 2008). Furthermore, ion flow through AMPARs triggers a depolarization of the cell membrane that

removes Mg^{2+} which blocks Ca^{2+} flow through unstimulated NMDARs (Rao and Finkbeiner, 2007). Another example is nicotinic acetylcholine receptors (nAChR) which are present in neuromuscular junctions (Tsuneki et al., 1997), and in the brain at pre- and postsynaptic nerve terminals as well as extrasynaptic membranes (Horch and Sargent, 1995). Following activation of these receptors by nicotine or Ach at the presynaptic terminal, Ca^{2+} enters and allows for neurotransmitter release (Li et al., 1999). In contrast to other seretonin receptors which are GPCRs, type 3 seretonin receptors (5-HT_3) are also ligand-gated Ca^{2+} channels (Hargreaves et al., 1994), and are present in synapses in the hippocampus, amygdala, hypothalamus (Tecott et al., 1993), and at the parasympathetic synapses of the gut (Akasu et al., 1987).

1.1.2.4.3. Store operated calcium channels (SOCCs)

The ER has a range of Ca^{2+} dependent functions within the cell including, vesicle trafficking (Gorelick and Shugrue, 2001), stress signal release (Kaufman, 1999), regulation of cholesterol metabolism (Brown and Goldstein, 1999), apoptosis (Ferri and Kroemer, 2001), and correct folding of newly synthesised proteins by means of Ca^{2+}-dependent chaperone proteins, amongst others (Feske et al., 2001). As a consequence of prolonged depletion of Ca^{2+} in the ER, incorrect protein folding, ER stress responses and cell death can occur (Brown and Goldstein, 1999, Parekh and Putney, 2005). Therefore, following stimulation, cells must have mechanisms in place to replenish this important Ca^{2+} store and maintain its functional integrity. This is accomplished by SOCCs at the plasma membrane that are activated in response to a decrease in ER Ca^{2+} concentration. As such, store operated calcium entry, also called capacitative calcium entry, is the main source of Ca^{2+} entry in non-excitable cells (but can also occur in excitable cells) and can become active no matter what process empties the stores (Parekh and Penner, 1997). This concept was proposed in 1986 following experiments on parotid acinar cells to determine the relationship between Ca^{2+} store depletion and Ca^{2+} entry at the plasma membrane. The authors observed increased Ca^{2+} entry as stores emptied (Putney, 1986). Further evidence came from electrophysiological studies in mast cells that showed increased Ca^{2+} currents in response to store depletion. This non-voltage dependent, inward Ca^{2+} current was termed Ca^{2+} release activated Ca^{2+} current or I_{CRAC} (Hoth and Penner, 1992). An important feature of this process is that the emptying of stores and not the resulting rise in cytoplasmic Ca^{2+} level is responsible for activating channels (Parekh and Penner, 1997). The mechanism of channel opening can be explained by the interaction of proteins on the ER and plasma membrane. The interaction of stromal interaction molecules (STIMs) -1 and -2 on the

ER with the pore forming Orai proteins (-1, -2, and-3) on the plasma membrane result in channel opening upon depletion of ER Ca^{2+} (Prakriya et al., 2006).

1.1.2.4.4. Second messenger operated calcium channels (SMOCCs)

Second messenger operated channels (SMOCCs) are activated by intracellular messengers. Once activated, these receptors allow the movement of ions into the cell. The best known example is the arachidonic acid (AA) regulated Ca^{2+} channels (ARC). AA is a fatty acid produced mainly by activated phospholipase A2 which separates it from a bound phospholipid molecule (Murakami and Kudo, 2002) and can induce Ca^{2+} entry through these Ca^{2+} selective channels. AA is lipid soluble and thus able to easily cross the plasma membrane (Kamp et al., 1995). It was therefore unclear whether AA was acting at the intra- or extracellular surface. This was addressed by utilising an AA analogue, arachidonyl coenzyme A (ACoA) which possesses a large head group thereby preventing its movement through the plasma membrane. This resulted in channel activation only when applied intracellularly via a patch pipette (Mignen et al., 2003). Studies have shown currents that are similar to ARC channel activity in cell lines including COS, HeLa, HEK293 and SY5Y as well as primary parotid and pancreatic acinar cells (Li et al., 2008, Mignen et al., 2003). STIM and Orai proteins are important for ARC channel functioning as its activation is dependent on the STIM-1 pool that is present at cell membranes (Mignen et al., 2007). The channel itself is composed of Orai-1 and Orai-3 subunits (Mignen et al., 2008).

Other examples of SMOCCs include cyclic nucleotide gated channels that allow entry of Ca^{2+}, Na^{+} and K^{+}. These channels respond to binding of cyclic adenosine monophosphate (Nomikos et al.) and cyclic guanosine monophosphate (cGMP) which have implications in phototransduction (Fesenko et al., 1985). PKC has been shown to activate non-capacitative Ca^{2+} entry in platelets (Rosado and Sage, 2000). Some transient receptor potential channels (TRPC) are activated by DAG (Tu et al., 2009) which is important for sensory signal transduction, as occurs in nociception (Woo et al., 2008). Furthermore Lückhoff and Clapham also showed Ca^{2+} channel activation by Ca^{2+} itself and Ins(3,4,5)P4 in a class of Ca^{2+} channels that are specific to endothelial cells (Luckhoff and Clapham, 1992).

1.1.2.4.5. Plasma membrane calcium pumps and exchangers

As stated above, several channel types are available to allow Ca^{2+} entry into the cell, however only two are responsible for its removal: the high capacity, low affinity Na^{+}/ Ca^{2+} exchanger (NCX_{PM}) and the low capacity, high affinity plasma membrane Ca^{2+} ATPase (PMCA). The proportion of these two is different depending on the cell type with excitable cells such as cardiac and neuronal cells having a higher proportion of NCX_{PM} (Brini and Carafoli, 2011). The PMCA pump is a member of the P-type ATPases (named such because of attachment of an iorganic phosphate to an aspartate group upon activation) and operates by using energy from ATP to drive movement of Ca^{2+} across the plasma membrane. One Ca^{2+} is removed for every molecule of ATP hydrolyzed (Wetzker et al., 1987). PMCA functions by being directly activated by Ca^{2+} but many agents can also modulate it. CaM lowers the Kd of the pump for Ca^{2+} to 1 μM from 10-20 μM in its resting state (Brini and Carafoli, 2011). Acidic phospholipids also increase the Ca^{2+} binding affinity of the pump, although its significance is not yet known (Niggli et al., 1981). This pump may function to fine tune the levels of Ca^{2+} because of its high affinity for this ion (Brini and Carafoli, 2011). Even in excitable cells that have a larger proportion of NCX_{PM}, the PMCA could act as a fine tuner as it is functional at concentrations in which the low affinity NCX_{PM} is not very efficient (Brini and Carafoli, 2011).

The NCX_{PM} functions by using the electrochemical gradient of Na^{+} and for every three Na^{+} ions that enters the cell, one Ca^{2+} ion moves out against its electrochemical gradient (Blaustein and Lederer, 1999). Under resting membrane potential, the NCX_{PM} functions to remove Ca^{2+} from the cell but because the NCX_{PM} works by moving Na^{+} and Ca^{2+} across their electrochemical gradient, it can function entirely in reverse in certain conditions. For example during systole in the heart, the plasma membrane becomes depolarized, voltage operated Na^{2+} channels open and so intracellular Na^{+} levels increase. Under this condition the NCX_{PM} reverses its function to expel Na^{+} from the cytoplasm and thus results in Ca^{2+} influx into the cell (Haddock et al., 1997, Wetzel et al., 1995).

1.1.3. G-protein coupled receptors (GPCRs) and their effectors

Calcium is a modulator of many proteins including the ubiquitous Ca^{2+} binding protein calmodulin as well as kinases, phosphatases and transcription factors, many of which are regulated through activation of GPCRS. In this section, GPCRs and their mechanism of

activation will be described, followed by an overview of heterotrimeric G proteins and their effectors

1.1.3.1. G-protein coupled receptors

With more than 800 members grouped into five principal families; Rhodopsin, Secretin, Adhesion, Glutamate, and the Frizzled/Taste2 families as well as various subfamilies based on their amino acid sequence (Fredriksson et al., 2003), the GPCRs are the largest protein family in mammalian genomes (Lagerstrom and Schioth, 2008). In humans, the largest of these families is the Rhodopsin family with 701 members; the other families are not as large and include Frizzled/Taste2 family with 24 members, the Adhesion family with 24 members, the Glutamate family with 15 members, and the Secretin family, also with 15 members (Fredriksson et al., 2003). It is predicted that approximately 460 are olfactory receptors but no physiological function has been assigned to the majority of these receptors and they are referred to as orphan GPCRs (Fredriksson et al., 2003). The number of orphan receptors however is constantly declining because of the great interest pharmaceutical companies have in these receptors (Kobilka, 2007). They all have a common seven transmembrane (7-TM) structure with an intracellular carboxyl terminus and an extracellular amino terminus. Essentially, they function as mediators of external signals into internal cellular responses (Fredriksson et al., 2003).

In contrast to the similarity in structure of these receptors, the ligands that activate them are very diverse in structure, ranging from subatomic particles such as photons, ions (including Ca^{2+}) and small organic molecules which mostly bind within the 7TM segment, to peptides and proteins which bind to the amino terminus as well as TM domains (Ji et al., 1998). Many physiological processes including sight, smell, taste as well as neurological, cardiovascular, and reproductive functions require GPCR activity, making them major drug targets (Azzi et al., 2003, Luttrell and Lefkowitz, 2002) and approximately 30% of all pharmaceutical drugs target GPCRs (Hopkins and Groom, 2002). Despite the 7-TM topology they all possess, little sequence homology is shared between the five major families of human GPCRs (Fredriksson et al., 2003). They are however common in their ability to activate heterotrimeric G proteins which leads to the separation of the Gαβγ trimer into Gα and the Gβγ dimer, the roles of which will be discussed next.

1.1.3.2. Heterotrimeric G-proteins

Heterotrimeric guanine nucleotide binding proteins or G-proteins are intracellular partners of GPCRs. Many proteins within cells alter between active and inactive states to regulate intracellular signal pathways and G-proteins are one example, changing from a GDP bound off state and a GTP bound on state to regulate the duration and intensity of a signal. When the G-protein is in its inactive heterotrimeric form, Gα is bound to GDP. In this state, the association of Gβγ with Gα helps to localize the trimer to the plasma membrane (Evanko et al., 2001). Gβγ also slows down the spontaneous exchange of GDP for GTP by behaving as a guanine nucleotide dissociation inhibitor (GDI) for Gα (Brandt and Ross, 1985). When GPCRs are activated by agonists, they become guanine nucleotide exchange factors (GEFs) and help to release GDP from Gα. GTP is present at a much higher concentration than GDP, so the unbound Gα binds to GTP, resulting in a conformational change in Gα which subsequently dissociates from the Gβγ dimer subunit (Wall et al., 1998). Both of these subunits are then capable of interacting with downstream proteins and engaging different signalling pathways.

Eventually the gamma-phosphate moiety of GTP is hydrolysed by Gα to GDP through its intrinsic guanosine triphosphatase (GTPase) activity, inactivating the subunit and resulting back into an inactive G-protein with the Gβγ dimer, thereby turning off downstream signalling (Ford et al., 1998, Li et al., 1998). This reaction is amplified by GTPase-accelerating proteins (GAPs) such as the regulator of G-protein signalling proteins (RGS, Siderovski et al., 1996). Figure 1.5 shows this process.

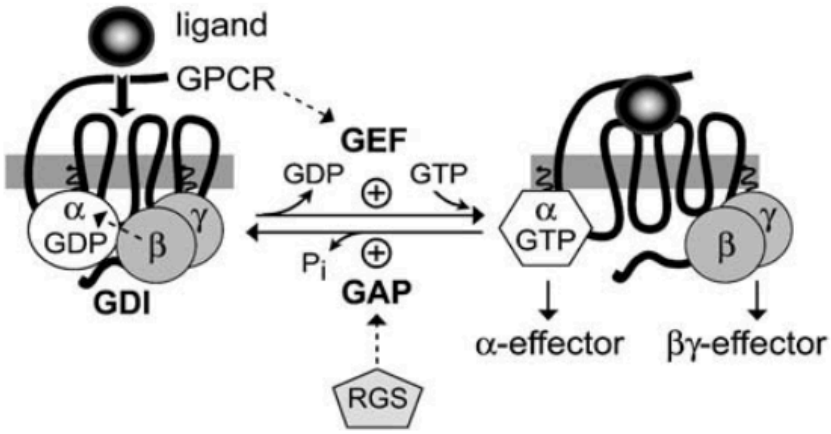

Figure 1.5: Schematic diagram of inactive and active G-proteins. In the absence of a ligand, Gα is bound to GDP and kept in an inactive state as a heterotrimer with Gβγ which also acts as a GDI that prevents spontaneous G-protein activation. This trimer is bound to the cytoplasmic loops of the 7TM domain of GPCRs. Upon binding of an agonist, GPCRs act as GEFs by producing a conformational change in Gα causing dissociation of GDP and subsequent binding of GTP. This causes detachment of the trimer into Gα and Gβγ, both of which are capable of modulating downstream effectors. The trimer reforms following exchange of GTP for GDP, a process that is augmented by GAPs such as RGS. Abbreviations: GAPs, GTPase-accelerating proteins. GDI, guanine nucleotide dissociation inhibitor. GPCRs, G protein coupled receptors. GEFs, guanine nucleotide exchange factors. RGS, Regulator of G-protein signalling. Image taken from McCudden et al., 2005.

1.1.3.3. Effectors of heterotrimeric G-proteins

G-protein classification is based on their Gα subunit. To date, there are 23 identified Gα proteins, ranging from 39 to 45 kDa (Nurnberg et al., 1995). They are encoded by 16 Gα genes in the human genome, with the higher number of proteins resulting from alternative gene splicing. This variety of Gα proteins is what gives GPCRs their diverse function. These proteins are grouped into four major classes based on the similarity of their amino acid sequence and include $G_{s/olf}$, $G_{i1/i2/i3/o/t\text{-}rod/t\text{-}cone/gust/z}$, $G_{q/11/14/16}$, and $G_{12/13}$ (Simon et al., 1991). They all act on different cellular targets: G_s stimulates adenylase cyclase (AC; Ross and Gilman, 1977), the first identified Gα effector (Sutherland and Rall, 1958), whereas G_i inhibits AC (Hsia et al., 1984). Recent evidence has also indicated regulation of membrane bound AC by Gβγ (Hanoune and Defer, 2001). G_{gust} and G_{olf} are involved in sensory transduction of taste and odour, respectively (Buck, 2000, Margolskee, 2002). G_t is involved in regulation of the cyclic GMP-gated Na^+/Ca^{2+} channel through its effector cGMP phosphodiesterase which is important in the GPCR-mediated phototransduction, required for vision (Arshavsky et al., 2002). G_q activates

PLC enzymes which are important in breaking down the membrane phospholipid PtdIns(4,5)P_2 into second messengers Ins(4,5)P_3 and DAG (Rhee, 2001), which have important functions in Ca^{2+} signalling and PKC activation, respectively. $G_{12/13}$ proteins regulate the small GTPase RhoA (Worthylake et al., 2000), PDZ-RhoGEF (Fukuhara et al., 1999, Longenecker et al., 2001), Ras GTPase activating protein, as well as PLCε, and PLD (Kurose, 2003).

Despite the initial belief that the Gβγ dimer only functioned to facilitate formation of the Gαβγ heterotrimer, it is now well established that Gβγ can activate many of its own effectors (Clapham and Neer, 1997), the first identified being the G-protein-regulated inward-rectifier K^+ channels (GIRK or $K_{ir}3$ channels), (Logothetis et al., 1987). Gβγ (as well as Gα) can also regulate N- and P/Q-type Ca^{2+} channels of neurons (Kammermeier et al., 2000). Overexpression of Gβγ in superior cervical ganglion neurons results in direct interaction of Gβγ with N-type Ca^{2+} channels and inhibits their activity, an effect that is prevented by Gβγ scavengers (Garcia et al., 1998, Herlitze et al., 1996). Kinases and small G-proteins are also regulated by Gβγ as stimulation of certain GPCRs activates ERK1/2, JNK and p38 mitogen activated protein kinases (MAPKs). Activation of these proteins is inhibited when using Gβγ sequestering agents (Yamauchi et al., 1997, Crespo et al., 1994). Amongst other identified roles of Gβγ within cells, is the direct interaction with an important signalling protein found in leukocytes called phosphoinositide 3-kinase-g (PI3Kg), (Stephens et al., 1997), the positive and negative regulation of AC (Tang et al., 1991), activation of PLC-β and PLC-ε, (Boyer et al., 1992, Wing et al., 2001), and localisation of G-protein coupled receptor kinases (GRK)-2 and -3 to the plasma membrane (Haga et al., 1994).

1.1.4. Aberrant calcium signalling in disease

Studies mentioned above reveal the importance of Ca^{2+} in many cellular processes so it is clear that aberrations in Ca^{2+} homeostasis will lead to defective signalling, which can give rise to disorders including hypertension, chronic kidney disease, colon cancer, premenstrual syndrome and osteoporosis amongst others (Power et al., 1999). For the scope of this project, interest lies in the Ca^{2+} dysregulation that may arise in Alzheimer's disease and during foetal development. This is due to the nature of the proteins of interest. PLCη2 is expressed in neurons, is activated by physiological Ca^{2+} levels and functions to release Ca^{2+} from intracellular stores. This released Ca^{2+} can feed back and re-activate PLCη2 thereby maintaining high Ca^{2+} levels. It is therefore possible that PLCη2 contributes to the "calciumopathy" that is associated with AD (This will be discussed and analysed in detail, in

Chapter 5). Interest in development is because of a recently identified mutation in PLCη1 in clinical cases of holoprosencephaly (HPE, personal communication with Dr Geoff Woods and Dr Mike Nahorski, University of Cambridge, UK), where the C-terminal tail of PLCη1 was found to be truncated. This mutant variant (N1075X) was created using site directed mutagenesis and compared with WT PLCη1 in relation to cellular localisation and effect on the Sonic hedgehog (Shh) pathway, as detailed in Chapter 6. It is unclear whether this is due to dominant or recessive inheritance. In this section several lines of evidence will be reviewed which shows the effects of hallmark features of AD on normal Ca^{2+} homeostasis followed by the essentiality of Ca^{2+} in embryonic development.

1.1.4.1. Alzheimer's disease (AD)

AD is a fatal neurodegenerative disorder with increased prevalence in older individuals. This disease is the most common type of dementia, gradually destroying neurons and cognitive abilities. It is classed into two categories; sporadic AD which has late detectable onset of ~65 years of age with an unknown aetiology and the less common familial AD which is an inherited form of the disorder and has an early onset of ~30-50 years of age (Blennow et al., 2006).

1.1.4.1.1. Perturbed calcium homeostasis

AD has several hallmark features such as amyloid plaque deposits (Aβ), neurofibrillary tangles, cell death and severe cognitive impairment which are all late stage markers of the disease. Strong evidence of Ca^{2+} dysregulation in the pathophysiology of AD comes from the fact that changes in Ca^{2+} signalling and alterations in neuronal excitability are observed throughout the lifetime of organisms and are evident long before plaque and tangle formation which are not detected until mid to late disease stage (Stutzmann et al., 2006).

It has been hypothesised that a persistent increase in Ca^{2+} level is likely to cause memory loss by enhancing the mechanism of long term depression (LTD) which effectively erases newly acquired memories. Normally, brief high concentration (~1000 nM) spikes of Ca^{2+} activate LTP and cause memory formations that are placed in a temporary memory store during the day. During certain phases of sleep at night, these memories are transferred to a permanent memory store. Short periods of Ca^{2+} elevation (~300 nM) then erase memories in the temporary memory store by activating LTD. In AD however, the permanent increased Ca^{2+} level may erase newly acquired memories from the temporary memory store before they can be transferred to the permanent memory store. In other words, up-regulation of intracellular Ca^{2+}

levels and the consequent persistent activation of LTD may increase the normal memory erasure mechanism and thus, leads to memory loss (Figure 1.6; Berridge, 2011). This indicates that memory loss (at least in the earlier stages of AD) is not necessarily due to neurodegeneration but that it results from altered Ca^{2+} signalling. Neurodegeneration may arise later as a result of further Ca^{2+} dysregulation that affects essential processes required for neuronal survival.

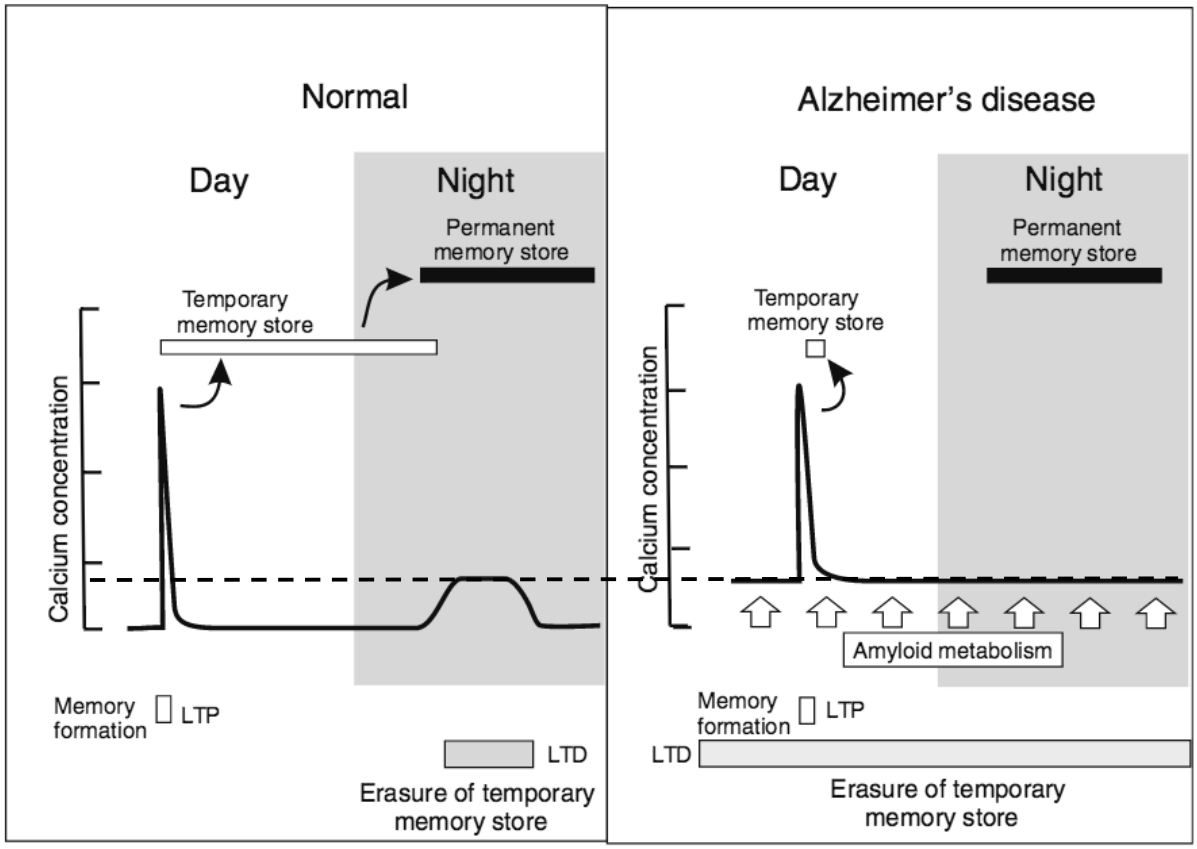

Figure 1.6: LTD and memory erasure in normal and AD states. Brief spikes of Ca^{2+} activate LTP,forming memories that are kept in a temporary memory store during the day and are transferred to a permanent memory store during sleep at night. Intermediate elevations of Ca^{2+} then activate LTD which erases memories in the temporary memory store. This process however is disturbed in AD due to the permanently increased Ca^{2+} levels resulting from amyloid metabolism. This level of Ca^{2+} keeps LTD persistently activated which results in erasure of memories in the temporary memory store before they can be transferred to the permanent memory store, thereby causing memory loss. Abbreviations: AD, Alzheimer's disease. LTD, long term depression. LTP, long term potentiation. Figure taken from Berridge, 2011. A dashed line is added to show the constantly raised basal level of Ca^{2+} in AD.

Brains of AD patients show a decrease in levels of calbindin-D28K and calmodulin in the temporal, parietal and frontal cortex. This decreased Ca^{2+} buffering can also be a contributing factor to neurodegenerative processes (McLachlan et al., 1987). Studies have also shown mitochondrial defects in fibroblasts taken from AD patients in that they have reduced ability to take up Ca^{2+} compared to normal mitochondria, and because mitochondria are important Ca^{2+} regulators, this can contribute towards neurodegeneration (Supnet and Bezprozvanny, 2010).

As described previously, maintaining a healthy level of intracellular Ca^{2+} is vital to cell function. In relation to neurons, this importance can be reflected by the fact that the ER extends through multiple neuronal compartments, extending from the soma to dendritic spine heads. So taking into account the concentration gradient between the ER lumen and the cytosol, and the vast ER networks throughout the neuron, it is clear why Ca^{2+} homeostasis must be kept under control (Berridge et al., 1998).

1.1.4.1.2. Amyloid beta (Aβ)

Several studies have shown a relationship between Aβ peptides, especially the oligomeric form (Demuro et al., 2005), and Ca^{2+} whereby Aβ production causes an increase in intracellular Ca^{2+} levels. Cultured neurons treated with Aβ peptides showed intracellular Ca^{2+} levels of 300-400 nM whereas neurons treated with a control peptide had levels of 120-140 nM (Mattson et al., 1992). It is not clear by what mechanism but this could be due to the formation of new Ca^{2+} pores or regulation of existing Ca^{2+} channels such as NMDA or AMPA receptors (Kelly and Ferreira, 2006). Such studies have shown that Aβ peptides causes formation of Ca^{2+} permeable channels in lipid bilayer preparations (Arispe et al., 1993), human fibroblasts and hypothalamic neurons (Zhu et al., 2000). This increased Ca^{2+} as a result of Aβ is thought to be a source of metabolic stress for the neuron (Mattson and Chan, 2003) and is sufficient for activating the release of vesicle containing neurotransmitters (Green and Peers, 2001).

There is also the possibility of Aβ causing increased release of Ca^{2+} from ER stores that can lead to over activation of Ca^{2+} dependent signalling pathways, activation of ER stress responses, activation of the unfolded protein response, mismetabolism of mitochondria energy and activation of metabolic pathways (Berridge et al., 1998). Increased RyR-3 expression also occurs upon Aβ 1-42 exposure (Arispe et al., 1993). Preclinical studies using the RyR inhibitor dantrolene showed that this drug, which is commonly used to prevent anaesthetic induced excessive opening of RyR-1 in patients with malignant hyperthermia, can protect neurons

against damage caused by Aβ in an in vitro model of AD (Berridge et al., 1998). On the other hand, increased Ca^{2+} levels can increase intracellular Aβ1-42 production, resulting in plaque formation (Pierrot et al., 2004). Such problems associated with neuronal Ca^{2+} dysregulations effect neuronal function by causing deficiencies in synaptic proteins, alterations in synaptic plasticity as well as reduction in the number of synapses and neuronal processes (Deshpande et al., 2006).

1.1.4.1.3. Neurofibrillary tangles

Neurofibrillary tangles are insoluble filaments composed of hyperphophorylated tau protein which form tangles within the brain of AD patients. Tau is a neuronal protein that is normally responsible for microtubule assembly, thus maintaining a cells structure and allowing axonal transport (Lindwall and Cole, 1984). These tangles are found 20 years prior to plaque formation which could mean that they contribute to the histopathology of AD rather than being an end result (Blennow et al., 2006). Following hyperphosphorylation of tau microtubules are broken down, axonal transport is weakened, and synaptic functions are decreased, all of which contribute towards neuronal death (Iqbal et al., 2005). Investigating the interaction between tau and Ca^{2+} revealed that Ca^{2+} increases the phosphorylation of tau and vice versa, as hyperphosphorylated tau can also raise Ca^{2+} levels inside the cell. This means that following hyperphosphorylation of tau, Ca^{2+} is released from internal stores which goes on to phosphorylate tau resulting in further release of Ca^{2+}, thereby forming a continuous cycle. Furthermore, increased Ca^{2+} levels are believed to trigger Ca^{2+} activated kinases including glycogen synthase kinase β, cyclin dependent kinase 5, and PKC which facilitate tau phosphorylation (Avila et al., 2004). So it may be possible that increased Ca^{2+} levels result in tangle formation through increases in kinase activity.
Collectively, these studies indicate that disruptions to normal intracellular Ca^{2+} levels results in the activation of mechanisms that can ultimately lead to the formation of hyperphosphorylated tau and Aβ1-42.

1.1.4.1.4. Genetic risk factors

Familial Alzheimer's disease (FAD) is linked to mutations in several genes of the amyloid pathway, namely the presenilin (PS1 and PS2) and amyloid precursor protein (APP) genes. APP is a transmembrane protein that is normally cleaved by α-secratase and γ-secratase to release soluble fragments. In the disease state however, APP is alternatively cleaved by β-

secratase and γ-secratase to form shorter fragments called amyloid-β. These hydrophobic fragments, which are mainly comprised of 40 and 42 amino acid residues, cluster together to form insoluble amyloid plaques that are thought to interfere with normal neuronal function (Hardy & Selkoe, 2002). APP mutations generally cause the same effect, either by causing increased cleavage by β-secratase or by modifying γ-secratase activity (Citron et al., 1992, Stenh et al., 2002). The catalytic component of γ-secratase is formed by presenilins (PSN) and mutations in both presenilin homologues, PSN1 and PSN2 alter the conformation of γ-secratase, which results in increased Aβ1-42 production (Borchelt et al., 1996). Therefore, these mutations mainly result in the formation of pathogenic Aβ1-42 and accumulation of Aβ plaques both inside and outside of the cell (Hutton et al., 1996). A number of studies have shown ER Ca^{2+} dysregulations in mutant PS1 transfected oocytes (Leissring et al., 1999), fibroblasts derived from FAD patients (Etcheberrigaray et al., 1998), and cultured neurons (Guo et al., 1996). Strutzmann *et al*. also showed Ca^{2+} signalling dysregulations in neurons obtained from young, adult, and aged mutant PS1 expressing mice which indicate the possibility of Ca^{2+} disruption being present throughout one's lifetime. These alterations have been reported to be specific to intracellular Ca^{2+} stores as they do not alter Ca^{2+} entry through the plasma membrane (Stutzmann et al., 2006). It is apparent from these results that presenilin mutations are targeting specific signalling pathways that may be linked to downstream manifestation of AD pathology. Studies have shown that mutated presenilin causes up-regulation of RyRs (Chan et al., 2000) and increases the open probability of $Ins(4,5)P_3Rs$ at low cytosolic $Ins(4,5)P_3$ levels (Kelly and Ferreira, 2006). This however can be a neuroprotective strategy as mutant presinilin prevents the ability of normal presenilin protein to serve as ER leak channels which normally operate in opposition to SERCA pumps thereby causing increased cytosolic Ca^{2+} levels (Tu et al., 2006).

Further evidence of calcium involvement in AD comes from apolipoprotein E4 (ApoE4) which is a gene, considered to be a risk factor in sporadic AD. ApoE functions in the brain, primarily as a cholesterol carrier and is involved in lipid transport and repair of injury. There are three alleles of APOE. APOE4 increases the risk of AD in comparison to APOE3, which is the most common allele, and APOE2 decreases the risk (Liu et al., 2013). APOE4 has been found to increase intracellular Ca^{2+} levels through different pathways. When physiological levels of ApoE4 were applied to cortical and hippocampal neurons, Ca^{2+} levels increased by 70% causing neurotoxicity and cell death (Veinbergs et al., 2002). By treating rat hippocampal neurons with ApoE4, Ohkubo *et al*. showed increased Ca^{2+} levels through APOE receptors,

NMDA receptors and L-type VOCCs as Ca^{2+} entry was inhibited by pre-treatment with their inhibitors; RAP, MK801, and nifedipine (Ohkubo et al., 2001). The RyR inhibitor dantrolene also prevented increased Ca^{2+} levels upon APOE4 treatment, all of which suggest that APOE4 initially stimulates Ca^{2+} entry through APOE receptors, NMDA receptors and L-type VOCCs which then activate RyRs that further increase intracellular Ca^{2+} by release from ER stores (Ohkubo et al., 2001). APOE4 however does not increase Ca^{2+} levels by entry through AMPA or kainite receptors (Tolar et al., 1999). In addition APOE4 produces long term effects by activating Ca^{2+} dependent transcription factors including phosphorylated (and therefore activated) cAMP response element binding protein (pCREB), cfos and Bcl-2 (Ohkubo et al., 2001, Rajadhyaksha et al., 1999). ApoE4 is also involved in slowing vesicular transport and reducing the number of transported vesicles, a process that is regulated by Ca^{2+} (Dekroon and Armati, 2002).

1.1.4.2. Developmental disorders

For normal development to occur, from fertilisation through to embryonic development and beyond, a strict sequence of irreversible events must take place in a timely manner, an overview of which will be discussed. Ca^{2+} is important in all stages of the development process and aberrations in its normal signalling at any point can cause developmental abnormalities such as foetal deformities.

1.1.4.2.1. Involvement of calcium during fertilisation and development

The role of Ca^{2+} begins at the very inception of the process as it is required for activation of the egg following sperm fertilisation (Steinhardt et al., 1977). This Ca^{2+} is derived from internal stores within the egg (Crossley et al., 1988). Microinjection of $Ins(4,5)P_3$ into the egg can trigger its activation (Whitaker and Irvine, 1984), which points towards involvement of a PLC in this process. Indeed the sperm specific PLCζ has been shown to generate Ca^{2+} oscillations upon gamete fusion (Saunders et al., 2002), producing a Ca^{2+} wave that propagates throughout the mammalian egg cell in a period of around 2 seconds (Deguchi et al., 2000). Ca^{2+} signals also control many aspect of the rapid cell division which follows fertilisation. This process fits into three stages: dissolution of the nuclear envelope, chromatin condensation and mitotic spindle formation; separation of chromosomes; and separation of daughter cells by formation of the cleavage furrow (CF). Phosphoinositide signalling is important in all of these stages as they can be blocked by addition of lithium, which blocks phosphoinositide synthesis by

preventing the formation of an essential component, *myo*-inositol, an effect that is reversed by *myo*-inositol treatment (Becchetti and Whitaker, 1997). In addition studies in sea urchins show that as sister chromatids separate, a sharp but brief calcium transient signal is produced. This process occurs even when embryos are placed in Ca^{2+} free sea water but blocked when using the Ins(4,5)P_3R antagonist heparin (Groigno and Whitaker, 1998), which provides further evidence of the involvement of Ca^{2+} from internal stores. Ca^{2+} signalling is also involved in formation of the CF as a slow propagating Ca^{2+} wave is observed along the CF arc as shown in frog and fish embryos (Fluck et al., 1999, Muto et al., 1996). Local rises in Ca^{2+} and activation of calmodulin around the CF is also observed in mammalian embryos (Torok et al., 1998). Furthermore, the ER is present in the CF of human early embryos (Goud et al., 1999). Breakdown of nuclear envelope also occurs following a Ca^{2+} spike but is blocked by heparin in starfish embryos (Stricker, 1995).

1.1.4.2.2. Involvement of calcium in developmental signalling pathways

During embryonic growth, Ca^{2+} signalling is imperative for a wide variety of processes including cell migration, mesoderm formation, proper axis development (anterior-posterior, dorso-ventral and left-right) and organogenesis (Webb and Miller, 2003). Mesoderm formation is dependent on the fibroblast growth factor (FGF) pathway which is downstream of FGFR1 (a class 1 RTK). Upon activation of this receptor in *Xenopus* embryos, PLCγ1 is phosphorylated and consequently activated, leading to Ca^{2+} release through Ins(4,5)P_3R activation (Muslin et al., 1994). Diaz *et al*. also witnessed periodic Ca^{2+} signals caused by FGF (Diaz et al., 2002).

Another important pathway that has been studied more widely is the Wnt signalling pathway. Wnt is a zygotic effect gene as it is expressed in early embryos. These genes are activated in the zygote and are transcribed from the zygote's DNA. They differ from maternal effect genes that are transcribed from the mother's DNA. Wnt proteins are secreted lipid modified glycoproteins that exist in several forms, measuring 350-400 amino acids in length (Cadigan and Nusse, 1997). Following the discovery of Wnt-1 in 1982, many more Wnt genes have been discovered across species and 19 Wnt genes have been identified in humans, many of which are conserved among vertebrates (Miller, 2002). Wnt signalling is involved in regulation of cells at the blastula stage, morphogenesis during gastrulation, and involvement in organogenesis (Cadigan and Nusse, 1997). There are three sets of characterised Wnt signalling cascades. The best characterised is the canonical Wnt/β-catenin pathway (Figure 1.7A) which

upon binding of wnt to its receptor Frizzled (Fzd) and its co-receptor low-density-lipoprotein-related protein5/6 (LRP5/6), initiates the signal transduction pathway. Initially, disheveld (Dsh) and axin are recruited to the plasma membrane, with Dsh binding to Fzd and axin binding to LRP5/6. This induces the release of β-catenin from a destruction complex made up of several proteins: axin, adenomatosis polyposis coli (APC), glycogen synthase kinase 3 (GSK3) and casein kinase 1α (CK1α). In the absence of Wnt, this complex phosphorylates and ubiquitinates β-catenin, allowing it to be degraded by proteasomes. By preventing β-catenin degradation, it builds-up in the cytoplasm and subsequently enters into the nucleus to initiate transcription by acting as a transcriptional co-activator of the lymphoid enhancing factor/ T-cell factor DNA-binding transcription factors (Clevers, 2006, Gordon and Nusse, 2006).

Another group of Wnt signalling pathways is the non-canonical planar cell polarity pathways, each serving to regulate different processes. These include: Wnt-RAP1 (Ras-related protein 1) which regulates gastrulation (Tsai et al., 2007), Wnt-Ror2 (tyrosine protein kinase transmembrane receptor) which is important for cell migration (Nishita et al., 2006), Wnt-PKA which is crucial for myogenesis (Chen et al., 2005), Wnt-RYK (related to receptor tyrosine kinase) which is important for neurite outgrowth and axon guidance and Wnt-mTOR (mechanistic target of rapamycin) which is required for cell growth (Choo et al., 2006, Inoki et al., 2006, Schmitt et al., 2006, Zou, 2004). These pathways have a significant degree of overlap among them. Disruptions to these Wnt signalling pathways can cause human disorders including a multitude of cancers and spina bifida which causes incomplete closure of the neural tube (Logan and Nusse, 2004).

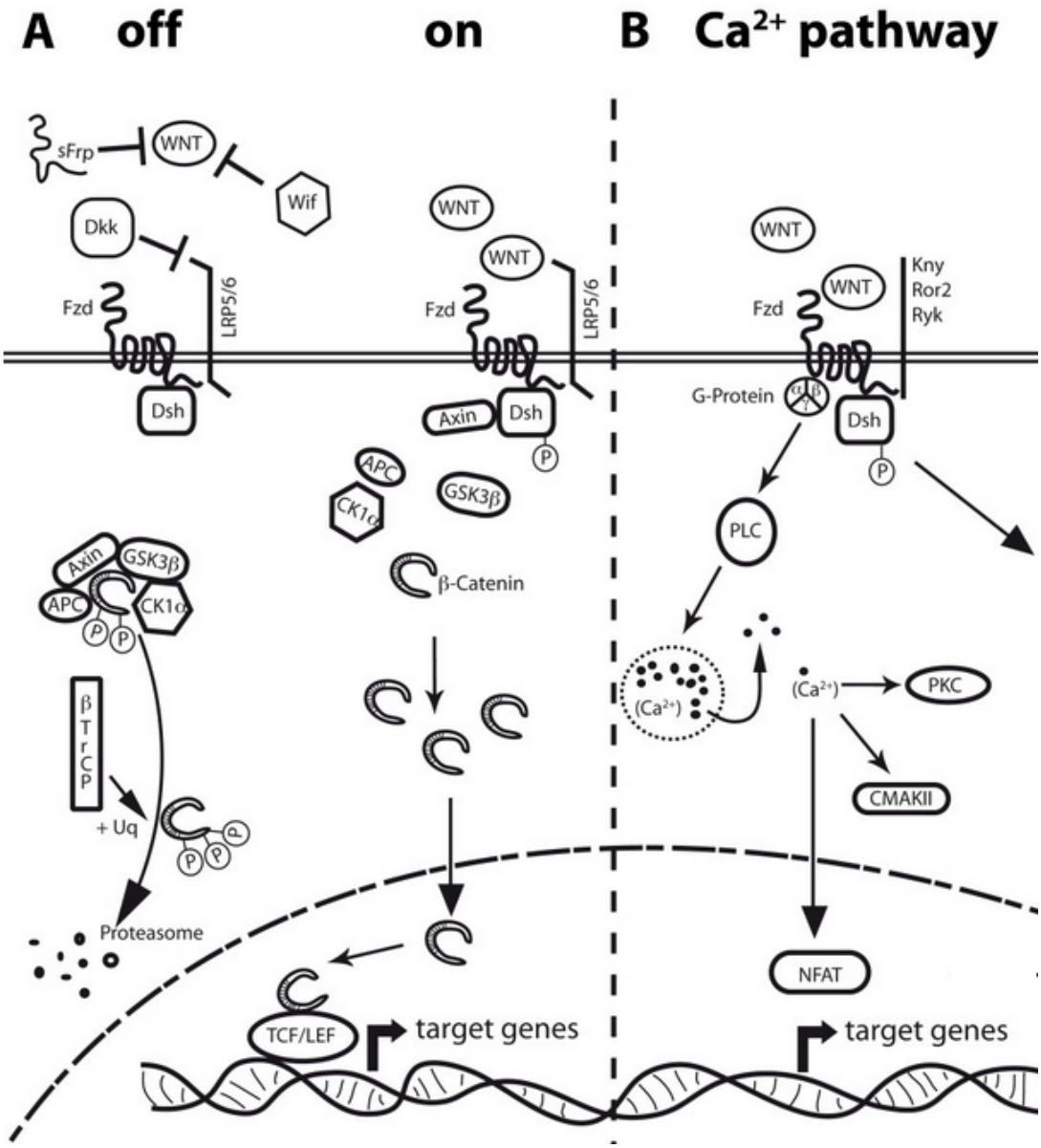

Figure 1.7: Canonical and non-canonical Wnt signalling pathways. **A** Canonical β-catenin pathway. In the "off state", Wnt protein is not present or is inhibited from binding to its receptor Fzd by factors including sFRP, DKK and Wif. The protein complex, APC-Axin-GSK3β- CK1α binds to and phosphorylates β-catenin which is then ubiquitinated by β TrCP and degraded in proteasomes. In the "On state" when Wnt binds to its receptor Fzd and its co-receptor LRP5/6, Dsh and Axin are recruited to Fzd, breaking apart the degradation complex. β -catenin is now free to enter the nucleus and allow transcription of genes by functioning as a transcription co-activator of TCF/LEF transcription factors. **B** Non-canonical Wnt/Ca^{2+} pathway. Binding of non-canonical Wnt proteins to Fzd receptors leads to activation of Dsh and heterotrimeric G-proteins which activate PLC enzymes and subsequently increase intracellular Ca^{2+} levels. As a result CAMKII, PKC and the transcription factor NFAT are activated. Abbreviations: APC, Adenomatosis polyposis coli. GSK3, glycogen synthase kinase 3. CK1α, casein kinase 1α. Dsh, disheveld. PKC, Fzd; Frizzled. Protein kinase C. CMAKII, Ca^{2+}/calmodulin-dependent protein kinase II .NFAT, Nuclear factor of activated T-cells. Figure taken from Liebner and Plate, 2010.

Ca^{2+} is important in Wnt signalling as there is also a non-canonical β-catenin independent Wnt/Ca^{2+} pathway (Figure 1.7B), also crucial in development. This pathway is especially important in regulation of dorsal axis formation, ventral cell fate, tissue separation, convergent extension movements during gastrulation and heart formation (Kohn and Moon, 2005, Slusarski and Pelegri, 2007). Wnt5a and Wnt11 are involved in the Wnt/Ca^{2+} pathway as they cause Ca^{2+} release without having an effect on β-catenin (Slusarski and Pelegri, 2007). This pathway is initiated following binding of Wnt to its receptor, Frizzled which is a GPCR (Koval and Katanaev, 2011). Activation of this receptor results in increased levels of DAG, Ins(4,5)P_3 and subsequently Ca^{2+}. This results in activation of CaMKII by calmodulin (Kuhl et al., 2000) and activation of PKC by DAG (Sheldahl et al., 1999). Both CaMKII and PKC activate nuclear transcription factors such as NFκB and CREB which leads to expression of necessary developmental genes. CaMKII also activates the transcription factor NFAT that is involved in ventral cell fate as shown in *Xenopus* embryos (Kuhl et al., 2000). Furthermore, PKC regulates the mechanism of tissue separation that occurs during gastrulation (Winklbauer et al., 2001). Genetic mutation of Wnt5a and Wnt11 prevents convergent extension movements (the lengthening and narrowing of a field of cells that structures embryonic tissues) during gastrulation, an effect that is partly recovered by expressing CaMKII in zebrafish embryos (Heisenberg et al., 2000, Kilian et al., 2003, Westfall et al., 2003). This pathway appears to be important in axon path finding as Wnt5a mediated signalling leads to axonal cone growth by cleaving the cytoskeleton protein spectrin via the Ca^{2+} dependent protease calpain (Yang et al., 2011). Yoshida *et al*. showed that inhibiting a Ca^{2+}/calmodulin dependent protein phosphatase, calcineurin which is involved in the Wnt/Ca^{2+} signalling pathway leads to abnormalities including formation of tumours in the heart, liver and kidney, as well as gut coiling defect and oedema during *Xenopus* development (Yoshida et al., 2004). Doi *et al*. also reported that cadmium induced omphalocele (a developmental disorder characterised by formation of intestines and liver in a sac outside the abdomen) occurs by disruption to the Wnt/Ca^{2+} pathway in the chick embryo (Doi et al., 2010). All of these studies reveal an important modulatory role for Ca^{2+} in many aspects of development.

1.2. The role of the plasma membrane in cell signalling

Eukaryotic membranes are essential for maintaining the internal environment of the cell and are crucial to cell survival in all species. Membranes are made up of a multitude of phospholipids which also serve as major components in signalling pathways. This section will provide an overview of plasma membrane phospholipids followed by a review of phospholipase C (PLC) enzymes that break down certain membrane phospholipids into essential secondary signalling messengers, with emphasis on their domain structure and regulation. For the scope of this project, involvement of PLCs in neuronal functioning and embryonic development will be discussed.

1.2.1. Overview of membrane phospholipids

The main components of plasma membranes are lipids, especially the glycerophospholipids, of which there are different types. The four primary phospholipids of eukaryotic cells are phosphatidylcholine (PtdCho), phosphatidylethanolamine (Ptdetn), phosphatidylserine (PtdSer), and sphingomyelin (SM). PtdCho accounts for 45-55%, Ptdetn accounts for 15-25%, SM accounts for 5-10%, and PtdSer accounts for 2-10% of total membrane lipids (Vance and Steenbergen, 2005). Phosphatidylinositol (PtdIns) and phosphatidic acid (PA) are also present in membranes but are less abundant in comparison, accounting for approximately 10% and 1-2% of membrane lipids respectively, with only trace amounts of phosphoinositides. PtdIns(4,5)P_2 is the most abundant of these and makes up approximately 0.5-1% of total membrane lipids (Suetsugu et al., 2014). PA is the acidic form of phosphatidate which is the substrate required for synthesis of the above mentioned lipids (Kent, 1995). PtdIns however is produced from cytidine diphosphate diglycerol (which is a derivative of PA) and *myo*-inositol by the enzyme PtdIns synthase (Paulus and Kennedy, 1960). PA is also a signalling molecule and facilitates many cellular processes including membrane binding of proteins, modulation of kinase activity (Delon et al., 2004, Rizzo et al., 1999), binding to signalling enzymes such as cAMP-specific phosphodiesterase and phosphatase-1 (Grange et al., 2000, Yang et al., 2005) as well as having structural effects on the plasma membrane by influencing membrane curvature (Wang et al., 2006).

Phospholipid bilayers are approximately 5 nm thick, possessing hydrophilic head groups on the outside and hydrophobic tails containing different lengths of saturated or cis-unsaturated fatty acyl chains on the inside. PtdCho along with SM are mainly localised to the outer

membrane of the lipid bilayer, while Ptdetn is mainly found in the inner membrane. This of course means that plasma membrane lipids have an asymmetric distribution in the inner and outer membranes. PtdSer, PtdIns, and phosphoinositides including PtdIns 4-phosphate (PtdIns(4)P), PtdIns(4,5)P_2, and PtdIns 3,4,5-trisphosphate (PtdIns(3,4,5)P_3) are present in the inner leaflet of the plasma membrane (Bohdanowicz and Grinstein, 2013, Di Paolo and De Camilli, 2006). The polar head groups in all of these phospholipids differ in size and charge which allows different lipid types to form different structures. Ptdetn head groups for example are smaller than head groups of PtdSer, PtdCho, and SM which in turn are smaller than the polar head groups of phosphoinositides, a property they have because of the phosphate-bearing inositol ring they possess (Janmey and Kinnunen, 2006) as seen in Figure 1.8. Plasma membranes consist of different lipids with differing structures that determine the membranes shape, electrostatic nature, and binding of different proteins (Suetsugu et al., 2014). The lipid packing of membranes is also dependent on the type of acyl chains. A kink in the acyl chain produced by the presence of a double bond can lead to altered lipid packing (Bigay and Antonny, 2012). The oleyl chain for example is comprised of 18 carbons and consists of one double bond. This takes up a larger volume in comparison to the 16 carbon palmitoyl chain with no double bond (Suetsugu et al., 2014). Therefore, the lipid packing of membranes is determined by the size of their polar head group and arrangement of their acyl chains. PtdIns and phosphoinositides are a good example because they contain polyunsaturated fatty acids which mainly comprise of 1-stealyl and 2-arachidonyl acyl chains. A sharp bend is produced in the acyl chain because the arachidonyl chain possesses four double bonds. This coupled with its large polar head group leads to disturbed lipid packing of membranes and often results in large spots of lipid packing abnormalities in areas of concentrated phosphoinositides (Randazzo et al., 2000). Such abnormalities however are of advantage to downstream signalling pathways as cytosolic proteins can electrostatically interact more easily with phosphoinositides in these regions in comparison to closely packed ones (Mattila et al., 2007).

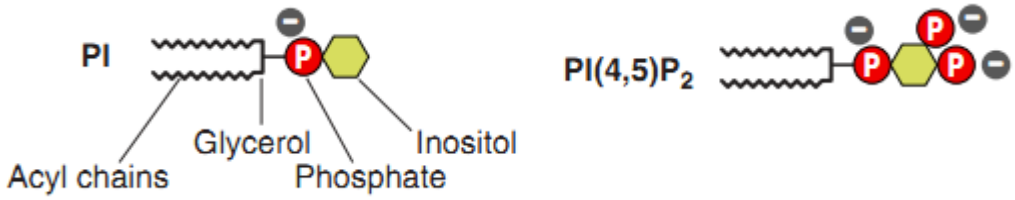

Figure 1.8: Schematic diagram of phosphatidylinositol (PI) showing its relative components and its phosphorylated derevative PI(4,5)P_2. Their polarity is due to the negative charges they possess as a result of phosphate binding to the inositol ring. Image taken from Suetsugu et al., 2014.

1.2.2. Types of phosphoinositides

Phosphoinositides are the phosphorylated derivatives of PtdIns (also written PI). As shown in Figure 1.8, different phosphoinositides are produced following phosphorylation of the hydroxyl group on the inositol ring at positions C-3, C-4, and C-5 in varying combinations and with increased phosphate groups, phosphoinositides carry a stronger negative charge thereby resulting in stronger electrostatic interactions with cytosolic proteins. However, the C-2 and C-6 positions are not phosphorylated (Suetsugu et al., 2014).

Mammalian cells consist of 7 types of phosphoinositides depending on the combination of phosphorylated C groups on the inositol ring, which comprise PtdIns 3-phosphate (PtdIns(3)P), PtdIns(4)P, PtdIns5-phosphate (PtdIns(5)P), PtdIns 3,4-bisphosphate (PtdIns(3,4)P_2), PtdIns 3,5-bisphosphate (PtdIns(3,5)P_2), PtdIns(4,5)P_2, and PtdIns(3,4,5)P_3 (Di Paolo and De Camilli, 2006). These phosphoinositides are metabolised by a multitude of kinases, phosphatases and phospholipases as shown in Figure 1.9.

Phosphoinositides have different membrane distributions as determined by the spatial localisation of their lipid kinases and phosphatases (Sasaki et al., 2009) which is important for localisation of different proteins to membranes of different organelles. PtdIns(4,5)P_2 is the major phosphoinositide present at the plasma membrane but PtdIns(3,4)P_2 and PtdIns(3,4,5)P_3 are also present less abundantly. PtdIns(4)P is localized at the golgi apparatus, PtdIns(3)P at endosomes and PtdIns(3,5)P_2 at multi vesicular bodies (Hammond et al., 2012). PtdIns(5)P, the least characterised phosphoinositide, localizes to the PM, nucleus and endosomes (Shisheva, 2013). Phosphoinositides however are not restricted to only one membrane. PtdIns(4,5)P_2 for example is also present at the nucleus where it serves to regulate essential processes such as regulation of gene expression (Mellman et al., 2008). Despite the low abundance of phosphoinositides, they are very important for signal transduction pathways

following receptor activation. Examples include the breakdown of PtdIns(4,5)P_2 into the second messengers Ins(4,5)P_3 and DAG (Berridge and Irvine, 1989) and involvement of PtdIns(3,4,5)P_3 in Wave2 induced lamellipodia formation and Dock180 signalling that activates small G proteins (Cote et al., 2005, Oikawa et al., 2004).

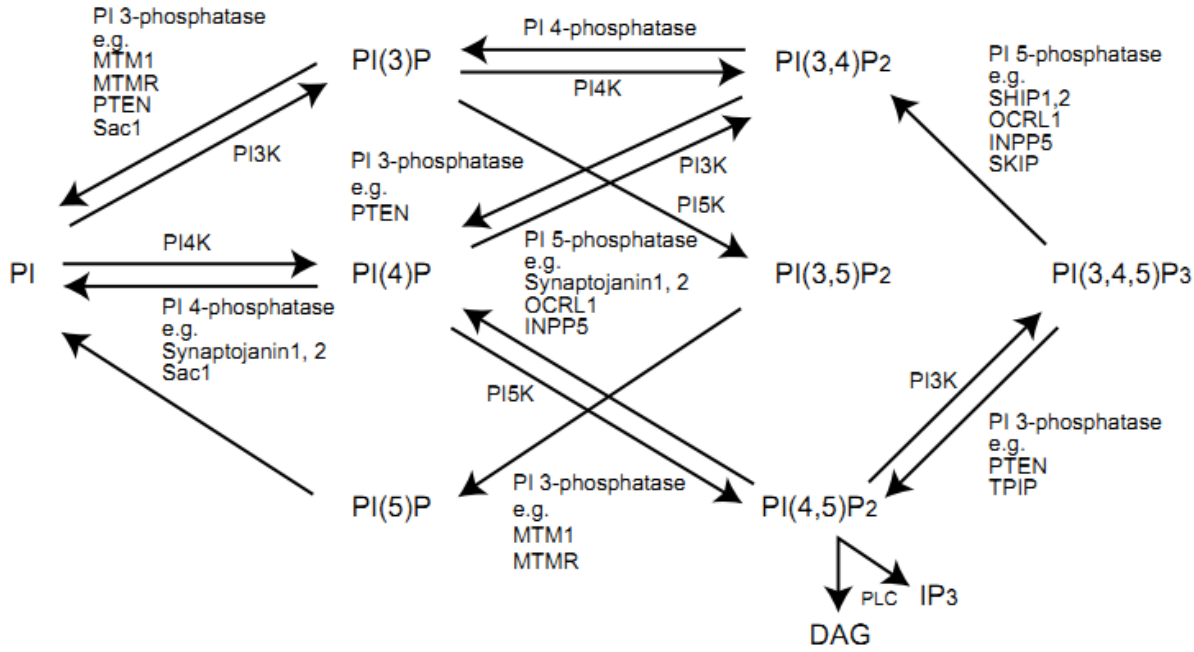

Figure 1.9: Variety of kinases and phosphatases that are involved in metabolism of the different phosphoinositides. Production of the most abundant of the phosphoinositides, PtdIns(4,5)P_2 begins by phosphorylation of PtdIns by PtdIns4-kinase to PtdIns(4)P which is further phosphorylated by PtdIns5K to PtdIns(4,5)P_2 which can then be broken down into Ins(4,5)P_3 and DAG. In reverse, phosphorylation of PtsIns(4,5)P_2 by PtdIns5-phosphatase produces PtdIns(4)P which is further dephosphorylated by PtdIns4-phosphatases to PtdIns. Abbreviations: MTM1, myotubularin1. MTMR, myotubularin related protein. PTEN, phosphatase and tensin homolog. SKIP, ski-interacting protein. Image taken from Suetsugu et al., 2014.

1.2.3. Overview of Phospholipase enzymes

Phospholipase enzymes are present in all cell types and act by hydrolysing specific ester bonds in phospholipids to bring about the physiological effects of numerous growth factors, hormones, and neurotransmitters. Based on the ester bond that is cleaved, phospholipases are categorised into two groups, the acyl hydrolases which constitute Phospholipase A1 (PLA_1), phospholipase A2 (PLA_2) and phospholipase B (PLB) and the phophodiesterases which constitute phospholipase C (PLC) and phospholipase D (PLD) as shown in Figure 1.10

(Richmond and Smith, 2011). Phospholipases possess very diverse properties but have the general function of serving as digestive enzymes, maintaining and remodelling the plasma membrane, and regulating essential cellular mechanisms by creating second messengers that are required for certain signal transduction pathways.

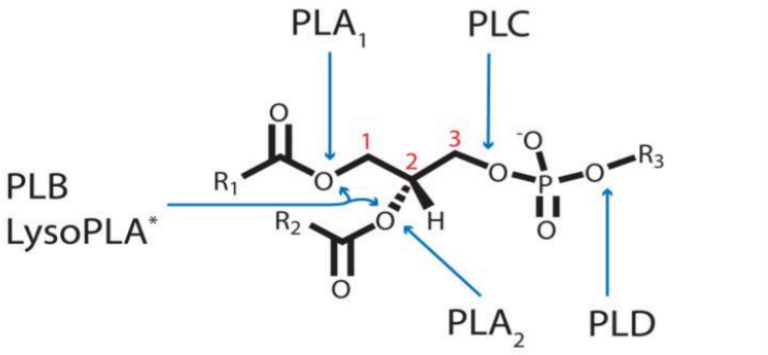

Figure 1.10: Specificity of phospholipases for different ester bonds. PLB hydrolyses ester bonds that emanate from the *sn*-1 and *sn*-2 carbon. PLA1, PLA2 and PLC cleave ester bonds on *sn*-1, *sn*-2 and *sn*-3 carbons, respectively and the remaining ester bond is hydrolysed by PLD. Image taken from Richmond and Smith, 2011.

The most widely studied phospholipase is PLC. These enzymes are soluble multi-domain proteins that range from 85-150 kDa in size and are conserved amongst species as they are present in yeasts, slime moulds, fungi and plants. PLC enzymes in such species bear closest resemblance to mammalian PLC delta (δ), (Kim et al., 1990). These enzymes catalyse the cleavage of the proximal phosphodiester bond of PtdIns(4,5)P_2 thereby producing Ins(4,5)P_3 and DAG (Fukami, 2002). This process is shown in Figure 1.11. DAG remains membrane bound where it acts primarily to activate PKC which in turn regulates several signalling pathways and Ins(4,5)P_3 diffuses into the cytoplasm where it binds to and opens Ins(4,5)P_3Rs on the ER, causing Ca^{2+} release. Therefore, these two secondary messengers can alter the activity of a diverse range of downstream targets including ion channels, enzyme sysytems, and structural proteins (Takai et al., 1979).

The first evidence of PLC activity came in 1953 through the studies of Hokin *et al.* who stimulated pigeon pancreas slices with cholinergic drugs and detected hydrolysis of phospholipids (Hokin and Hokin, 1953). Further evidence came in 1978 where two independent studies showed the breakdown on PtdIns(4,5)P_2, labelled with P^{32} following stimulation with norepinephrin in rabbit muscle cells (Abdel-Latif et al., 1978, Allan and

Michell, 1978). These findings led to several studies which showed increased Ins(4,5)P_3 levels resulting from PtdIns(4,5)P_2 breakdown (Berridge et al., 1983, Putney, 1982, Weiss et al., 1982), and in 1983 Sterb *et al*. reported an increase in intracellular Ca^{2+} levels resulting from Ins(4,5)P_3 generated from PtdIns(4,5)P_2 hydrolysis (Streb et al., 1983). Several studies in the 1980's revealed three different families of PLC enzymes based on size and immunoreactivity; PLCβ, PLCδ, and PLCγ. (Hofmann and Majerus, 1982, Ryu et al., 1986, Takenawa and Nagai, 1981). Three other PLC families were discovered in the following years including ε, ζ, and η (Harden and Sondek, 2006, Kelley et al., 2001, Stewart et al., 2005). PLC isozymes have been classified in this way based on their amino acid sequence, domain structure and mechanism of activation. With the exception of the sperm specific PLCζ, these PLCs can all function simultaneously within a cell and contribute towards its overall signalling.

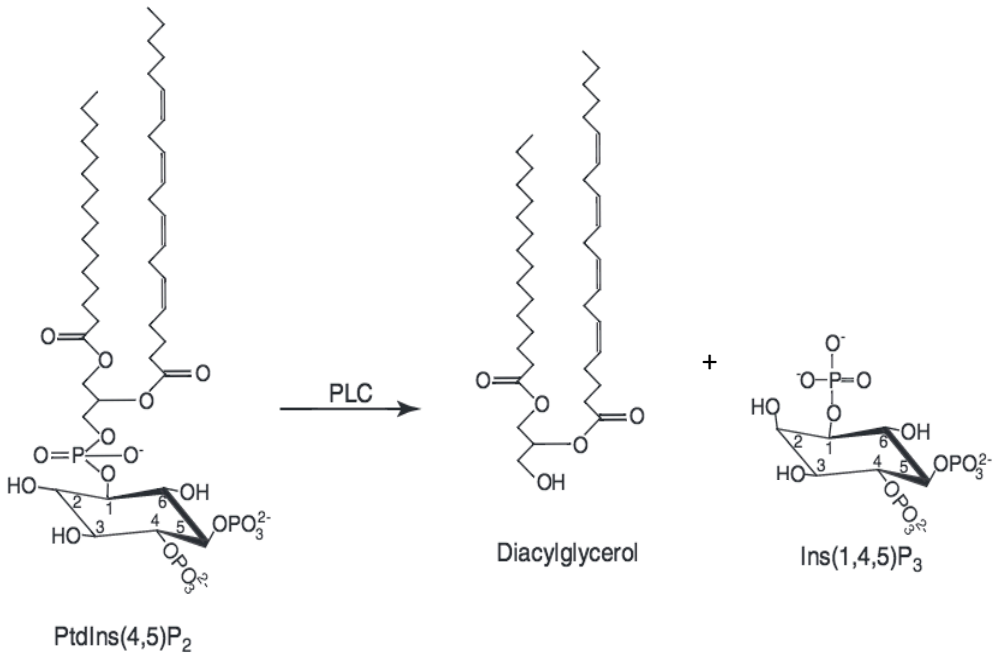

Figure 1.11: Chemical structure of PtdIns(4,5)P_2 and the two products diacyclglycerol and Ins(1,4,5)P_3 following breakdown by PLC. Image taken from Bunney and Katan, 2011.

PLD has specificity for the glycerolipid Phosphatidylcholine and hydrolyzes its *sn*-3 phosphodiester bond to generate phosphatidic acid (PA) and free choline (McDermott et al., 2004). Like PLCs, the mechanism of action and structural charecteristics of various PLDs have been well defined (McDermott et al., 2004). The other PLs have been studied less extensively, but several studies have given insight into their mechanism of action. PLA_1 cleaves phospholipids at the sn-1 position while PLA_2 cleaves at the sn-2 position, producing a free

fatty acid and lysophospholipids (Aoki et al., 2007, Burke and Dennis, 2009). Phosphatidic acid and phosphatidylserine are cleaved by PLA_1 to produce lysophosphatidic acid and lysophosphatidylserine respectively (Aoki et al., 2007). PLA_2 however acts primarily to initiate the arachidonic acid (AA) cycle (Gilroy et al., 2004). AA can then be converted into more than 150 eicosanoids including prostaglandins, thromboxanes, and leukotrienes which are powerful inflammatory mediators (Bogatcheva et al., 2005). PLB enzymes can hydrolyse phospholipases at sn-1 and sn-2 positions (Gassama-Diagne et al., 1992). They are essential for the digestion of dietary lipids in mammals and are involved in the molecular machinery of neutrophil immune response (Xu et al., 2009).

1.2.3.1. Phospholipase C (PLC) enzyme domain structure

PLC isozymes utilize a set of domains in order to regulate production of $Ins(4,5)P_3$ and DAG. Much of our understanding of the different domains in PLC isozymes comes from crystallographic studies that revealed the three dimensional structure of PLCδ1 (Essen et al., 1996, Ferguson et al., 1995). Many of these domains are conserved amongst PLC enzymes including the pleckstrin homology (PH) domain, EF-hand like domain, X and Y catalytic domains and the C2 domain, while others are isozyme specific such as the Src homology (SH) domains in PLCγ and Ras activation related domains in PLCε (Suh et al., 2008). Domain structures of all six PLC isozymes are shown in Figure 1.12 and the three dimensional structure of the rat PLCδ1 enzyme is shown in Figure 1.13.

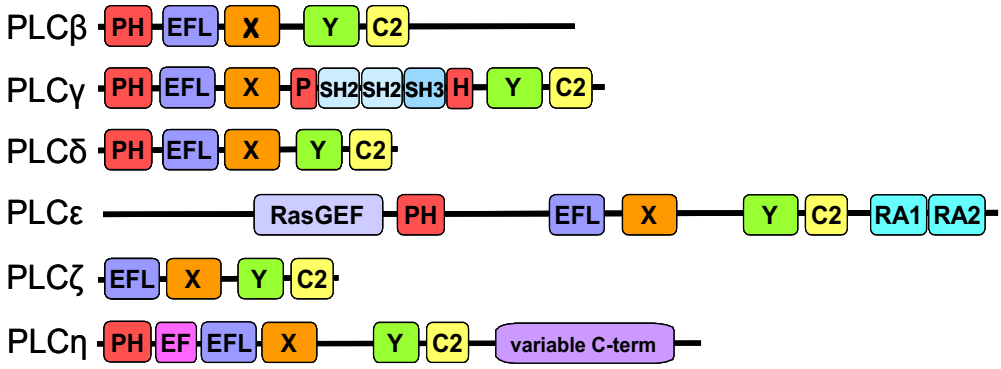

Figure 1.12: Domain structure of different PLC isozymes. As shown, many domains are conserved whereas others are isozyme specific. Abbreviations: PH: Pleckstrin homology domain, EF: EF-hand domain, EFL: EF hand-like domain, X: Catalytic X domain, Y: Catalytic Y domain, C2: C2 domain, SH2, SH3: SRC homology domains, RasGEF: guanine nucleotide exchange factor domain for Ras-like small GTPases, RA: Ras association domain, variable C-term: variable C-terminal domain. Figure was produced by Dr Alan Stewart (University of St Andrews, UK).

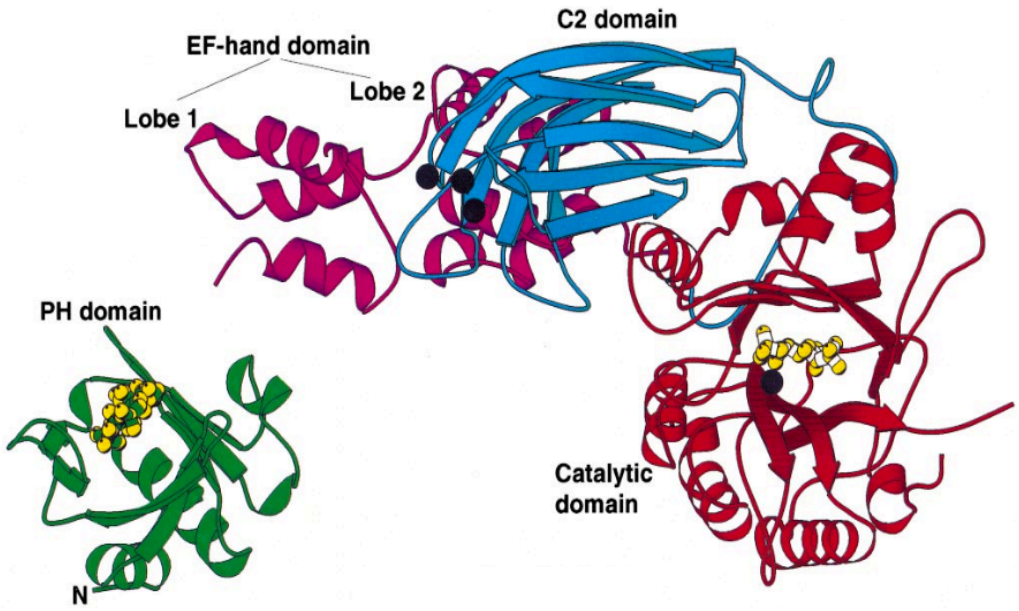

Figure 1.13: Three dimensional depiction of rat PLCδ1. Image shows the PH domain, EF-hand domain, C2 domain and catalytic domain showing binding sites of Ins(4,5)P_3 (yellow) and Ca^{2+} (black dots). PH domain is separate from the rest as it was characterised independently to the rest of the enzyme. Image taken from Williams, 1999.

1.2.3.1.1. Pleckstrin homology (PH) domain

With the exception of PLCζ, the N-terminal region of all PLC isozymes consists of a PH domain which is approximately 100-130 amino acid residues long. This domain was first identified in the protein pleckstrin but has since been reported in over 100 proteins (Yoon et al., 1994). In PLC enzymes, this domain is responsible for binding to phosphoinositides and therefore targets cell membranes. The crystal structure of PLCδ1 showed that the PH domain was disordered which is indicative of flexible attachment to the enzymes catalytic core (Essen et al., 1996). There are small differences in structure of this domain between different PLC isozymes which allows for specificity towards different phospholipids. PLCγ1 for example has high affinity for PtdIns(3,4,5)P_3 (Falasca et al., 1998). The SH2 domain of PLCγ1 also binds to PtdIns(3,4,5)P_3 with high affinity and this can contribute towards tighter binding to the membrane (Bae et al., 1998). PLCδ1 has high affinity for PtdIns(4,5)P_2 (Lomasney et al., 1996) and can also bind strongly to Ins(4,5)P_3 (Ferguson et al., 1995). PLCβ isozymes do not have high affinity for PtdIns(4,5)P_2 or PtdIns(3,4,5)P_3 (Tall et al., 1997) and are thought to bind to

some phospholipids non-specifically (McCullar et al., 2003). PLCβ1 and PLCβ2 have also been reported to bind strongly to PtdlCho (Wang et al., 1999). PH domains however are not always responsible for membrane binding as the PH domain is not a critical determinant for membrane binding of PLCδ4 (Lee et al., 2004). Furthermore, Kim *et al.* have reported that membrane binding of PLCβ isozymes may be directed by the C-terminal tail region, which also expresses a nuclear localisation sequence (Kim et al., 1996). PLCζ isozymes which are expressed exclusively in sperm are deficient of a PH domain but can still bind to phospholipids by their C2 domain (Kouchi et al., 2005). Not much is known about the lipid binding properties of PLCε PH domain but computer model analysis has predicted that it binds non-specifically to phospholipids (Singh and Murray, 2003).

1.2.3.1.2. EF-hand domain

This domain was named the EF-hand based on the mechanism by which the E- and F-helices move between open (haloprotein) and closed (apoprotein) conformations in parvalbumin (Kretsinger and Nockolds, 1973). An EF-hand is composed of a Ca^{2+}-binding loop in-between 2 α-helices. Following binding of Ca^{2+} to the loop, one of the helices moves away from the other and becomes perpendicular to it, thus altering the EF-hand from an apoprotein state to a holoprotein state (Lewit-Bentley and Rety, 2000). A typical EF-hand domain is comprised of four helix-loop-helix motifs that are arranged into two lobes, with each lobe containing two EF-hands (Essen et al., 1996). These two lobes are arranged in a face-to-face manner and are further stabilised by formation of an antiparellel β-sheet between the Ca^{2+}-binding loops of the two EF- hands (Grabarek, 2006).

Ca^{2+}-sensitive proteins such as calmodulin, neuronal calcium sensor-1and troponin C contain a homologous Ca^{2+}-binding EF-hand domain (Burgoyne et al., 2004, Parmacek and Leiden, 1991, Vetter and Leclerc, 2003). PLC enzymes possess an EF-hand domain which forms a flexible tether to the PH domain, but with the exception of PLCη which will be described later and PLCζ which is highly Ca^{2+} sensitive, and is accountable for Ca^{2+} oscillations in fertilized oocytes (Kouchi et al., 2005), other PLC isozymes have limited or no Ca^{2+} binding ability (Bairoch and Cox, 1990).

1.2.3.1.3. C2 Domain

The C terminal region of PLC enzymes contains a C2 domain composed of an eight stranded, anti-parallel β-sandwich consisting approximately 120 amino acid residues. (Williams, 1999)

This domain resembles the conserved second domain of PKC which was the first protein in which the C2 domain was determined (Xu et al., 1997). Subsequently, this domain was identified in synaptotagmin (Perin et al., 1990), Ras GTPase activating proteon (RasGAP), (Yamamoto et al., 1999), PtdIns 3-kinase (Hiles et al., 1992), cytosolic PLA_2 (Evans et al., 2004), PKCβ, PKCδ (Pappa et al., 1998) and PLCs (Rhee, 2001). C2 domains can possess two different topologies which are structurally very similar but are circular permutations of each other. The C2 domain of PLCδ1 matches that of PKCδ and cytoplasmic PLA_2 (Williams, 1999). Because there is a clear sequence similarity in the C2 domain of all PLCs (Williams, 1999), Other PLCs are likely to be identical to these. The C2 domain is usually found in proteins that interact with phospholipids. As such, this domain can function as a lipid membrane binding module upon binding Ca^{2+} (Nalefski and Falke, 1996) and is the second most common lipid binding domain after the PH domain (Cho and Stahelin, 2006). PLCζ lacks a PH domain and requires the C2 domain for membrane binding. Kouchi *et al*. showed that a PLCζ mutant, lacking a C2 domain was inactive which indicates that this domain is required for enzyme functioning (Kouchi et al., 2005). The crystal structure of PLCδ1 C2 domain revealed three metal binding sites between loops at one end of the β-sheets and solution studies are consistent with this as they show three Ca^{2+} binding sites in each domain (Grobler and Hurley, 1998). Other proteins however may bind 1, 2 or 3 Ca^{2+} ions depending on the C2 domain subtype they possess (Perisic et al., 1998, Sutton and Sprang, 1998). Binding of proteins to lipids via the C2 domain is dissimilar between some PLC isoforms. For example the C2 domain of PLCδ1 and PLCδ2 bind to phosphatidylserine in a Ca^{2+} dependent manner whereas PLCδ4 is less selective for lipid binding and can bind in a Ca^{2+} independent manner (Ananthanarayanan et al., 2002). Grobler *et al*. also proposed a stronger interaction between membranes and PLCδ1 following formation of a "Ca^{2+} bridge" which forms by phospholipids supplying Ca^{2+} ligands that interact with the C2 domain (Grobler et al., 1996).

1.2.3.1.4. Catalytic domain

The catalytic domain of PLC enzymes consists of α-helices and β-strands which form a structure that resembles the triosphosphate isomerise (TIM) β/α barrel and in the case of PLCδ1 is composed of a distorted $(\beta/\alpha)_8$ barrel (Williams, 1999). This domain consists of an X and Y region (147 and 118 residues, respectively in PLCδ1) that form the two halves of the β/α barrel with the X region showing most sequence similarity between PLC isozymes and across species (Tall et al., 1997). This domain is responsible for cleaving phosphoinositides and eukaryotic

PLCs have a preference for PtdIns(4,5)P_2 > PtdIns(4)P > PtdIns but not phosphoinositides phosphorylated at the "3-position" (Rebecchi and Pentyala, 2000). Preference for PtdIns(4,5)P_2 is due to the series of salt bridges and hydrogen bonds that form between the phosphorylated groups at 4- and 5-positions on the PtdIns(4,5)P_2 polar head group and basic residues on the catalytic domain, specifically Lys438 and Lys440 on the first half, and Ser522 and Arg549 on the second half of the β/α barrel of PLCδ1. This allows for ligation of PtdIns(4,5)P_2 at positions 4 and 5 (Cheng et al., 1995, Wang et al., 1996). Binding of a single Ca^{2+} to the active site of PLCδ1 (as coordinated by several residues, Asn312 Glu341 Glu341 Asp343 and Glu390) is essential for catalysis (Ellis et al., 1998, Essen et al., 1997a) and despite other domains having the ability to bind Ca^{2+}, the binding of Ca^{2+} to the catalytic domain appears to be the only essential one as mutating Ca^{2+} binding regions of the C2 domain still results in catalysis (Grobler and Hurley, 1998). The catalytic domain of PLCδ1 is surrounded by a hydrophobic ridge (composed of Leu320, Tyr358, Phe360, Leu529, and Trp555) which is believed to be involved in insertion of PLC enzymes into the membrane thus allowing for complete enzyme activity (Boguslavsky et al., 1994, Essen et al., 1996). Completing the catalytic domain is an XY- linker sequence (Z region) between the X and Y regions. This region is poorly conserved amongst PLC isozymes and is not required for catalysis (Bristol et al., 1988, Schnabel and Camps, 1998) indicating that this region may be involved in subtype specific regulation (Rebecchi and Pentyala, 2000). The X/Y-linker region of PLCγ is the most extensive, consisting of several adaptor proteins which include a PH domain encompassing two SH2 domains followed by an SH3 domain. The SH2 domains in this X/Y linker region are essential for enzyme activation by tyrosine kinases (Horstman et al., 1999).

1.2.3.2. Regulation of PLC enzymes

Extracellular stimuli activate PLCs by binding to cell surface receptors, mainly GPCRs and receptor tyrosine kinases (RTKs). It is also important to note that while second messengers account for the majority of signalling, important signalling is also carried out by inositol lipids. PtdIns(4,5)P_2 for example, binds to PH, FYVE, and PX domains of specific proteins (Lemmon, 2003) and modifies their activity or cellular localization thereby leading to a varietyof cellular responses including alterations in cell signalling, ion channel activity, actin assembly and remodelling as well as vesicle trafficking (Ling et al., 2006, Suh et al., 2008, Yin and Janmey, 2003). Furthermore, PtdIns(4,5)P_2 levels affect other signal transduction pathways such as the phosphoinositide 3-kinase pathway (Alessi, 2001).

There are 6 different classes of PLC isozymes, consisting of 13 different isoforms in humans. These are regulated differently and are activated mainly by tyrosine phosphorylation (Meisenhelder et al., 1989, Wahl et al., 1989) or by heterotrimeric and monomeric G-proteins (also called small G-proteins; Morris et al., 1990).

PLCβ is activated by heterotrimeric G-proteins, acting downstream of G protein coupled receptors (GPCRs) that belong to the rhodopsin superfamily of transmembrane receptors. Activation is carried out by Gα subunits of the G_q subfamily, specifically $G\alpha_q$ and $G\alpha_{11}$ (Smrcka et al., 1991, Taylor et al., 1991, Waldo et al., 1991). Rac GTPases have also been reported to activate PLCβ2 and PLCγ2 isoforms (Harden et al., 2009). All PLCγ isoforms however are activated following agonist stimulation of receptor tyrosine kinases (RTKs) (Kamat and Carpenter, 1997) which causes dimerisation and tyrosine autophosphorylation on its cytoplasmic side, resulting in tethering sites to which PLCγ can bind to through its SH2 domain (Hubbard and Till, 2000). These receptors in turn increase the catalytic activity of PLCγ1 by phosphorylating it at five residues: Tyr472, Tyr771, Tyr775, Tyr783, and Tyr1254 (Bae et al., 2009, Gresset et al., 2010). Rho and Ras family of small G-proteins are activated by Gα variants, $G\alpha_{12}$ and $G\alpha_{13}$ (or by other proteins) which in turn activate PLCε by binding directly to its catalytic Y domain (Harden and Sondek, 2006, Harden et al., 2009, Seifert et al., 2008). However while these GTPases stimulate PLCε transiently, Rap is accountable for its continuous activation (Song et al., 2002). Park *et al*. also showed that Gβγ dimers are able to activate PLC enzymes. In their study, these enzymes had different susceptibilities to Gβγ in the following order from strongest to weakest: PLCβ3, PLCβ2, PLCβ1, and PLCδ1. This difference in susceptibility of PLC activation by Gα and Gβγ shows that PLC isoforms are regulated differently in response to GPCR activating ligands (Park et al., 1993). By using scavenger molecules to block $G\alpha_q$ and Gβγ activity, it has been shown that $G\alpha_q$ produces long-lasting elevations in cytosolic Ca^{2+} signals whereas Gβγ produces short-lasting Ca^{2+} oscillations in pancreatic acinar cells, effects that are probably brought about through activations of different PLC isoforms (Zeng et al., 1996). Subsequent studies have shown that Gβγ functions by binding to the PH domains of PLCβ (Wang et al., 2000b). PLCε is also activated by the Gβγ dimer, although its mechanism of binding has not been established (Wing et al., 2001). Certain subtypes of PLCs can also be activated or deactivated by kinases. Whereas phosphorylation of PLCδ1 by PKC increases its enzymatic activity (Fujii et al., 2009), phosphorylation of PLCβ3 by PKA or PKC inhibits Gα and Gβγ stimulated activity (Yue et al., 1998, Yue et al., 2000). Another regulator of PLC activity is Ca^{2+} which can activate PLCδ

enzymes (Nakahara et al., 2005). It is also the only activator of PLCζ enzymes (Kouchi et al., 2005). Figure 1.14 summarises this complexity of PLC regulation.

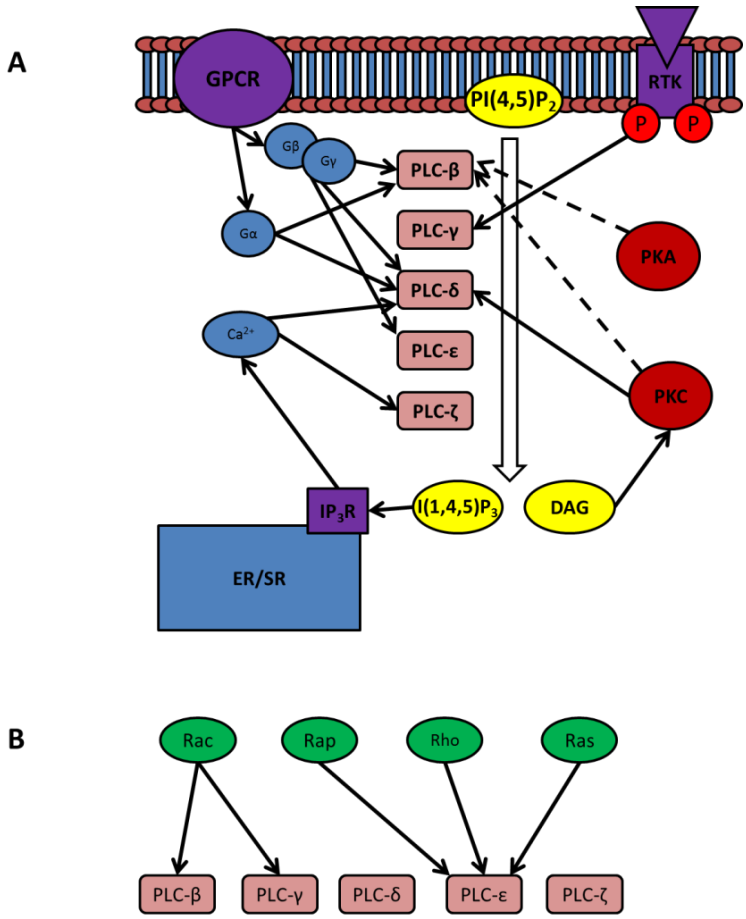

Figure 1.14: Mechanisms of activation of different PLC isoforms. **A** PLC activation following receptor stimulation. Activation of GPCRs by extracellular ligands breaks down the Gαβγ heterotrimer into Gα and Gβγ. Gα induces activation of PLCβ and PLCδ isozymes whereas Gβγ activates PLCβ, PLCδ and PLCε isozymes. RTK activation phosphorylates only the PLCγ isozymes. These activated PLCs breakdown PtdIns(4,5)P_2 into Ins(4,5)P_3 and DAG. Ins(4,5)P_3 binds to Ins(4,5)P_3Rs and causes release of Ca^{2+} from the ER which can contribute the Ca^{2+} activation of PLCδ and PLCζ. DAG activates PKC which activates PLCδ but negatively regulates PLCβ. PKA also has the same effect on PLCβ. **B** PLC activation by monomeric G-proteins. PLC-β, -γ and –ε are activated by small G-proteins. PLCβ and and PLCγ are activated by Rac whereas PLCε is activated by Rap, Rho and Ras. Abbreviations- GPCR: G protein-coupled receptor, PtdIns(4,5)P_2: phosphatidylinositol 4,5-bisphosphate, Ins(4,5)P_3: inositol 1,4,5-trisphosphate, DAG: diacylglycerol, PKC: protein kinase C, PKA: protein kinase A, Ins(4,5)P_3R: inositol 1,4,5-trisphosphate receptor, RTK: receptor tyrosine kinase, ER/SR: endo/sarcoplasmic reticulum. Image taken from Popovics, 2012.

1.2.3.3. Neuronal PLC enzymes

Numerous PLCs have been identified in the brain which implies that these enzymes play a role in neuronal physiology. Watanabe *et al*. showed that mRNA of all four PLCβ isoforms is

expressed in different brain regions. PLCβ1 is abundantly expressed in the cerebral cortex, hippocampus, amygdala and striatum. PLCβ2 is mainly expressed in white matter structures of the brain including corpus callosum, fimbria and medulla of the cerebellum. PLCβ3 is present specifically in cerebellar Purkinjee and granular cells and PLCβ4 is expressed in the olfactory bulb, thalamus, brainstem and cerebellum (Tanaka and Kondo, 1994, Watanabe et al., 1998). PLCγ enzymes have a low expression in the brain but PLCγ1 is expressed in the olfactory bulb, hippocampus, cerebellum, piriform and frontal cortex (Ross et al., 1989) while PLCγ2 is present in a small region of the cerebellum (Tanaka and Kondo, 1994). Similarly, PLCε isoforms are sparsely expressed in brain regions (Lopez et al., 2001). PLCδ on the other hand appears to be expressed in all brain regions (Lee et al., 1999). PLCδ3 is the predominant isoform in cerebellar granule cells and is expressed in the cerebellar cortex (Kouchi et al., 2011). PLCδ4, the most recently identified PLCδ isoform is also highly expressed in the brain but its specific distribution is yet to be determined (Lee and Rhee, 1996).

Temporal changes in PLC activity have also been detected within the brain. Studies have reported increased Ins(4,5)P_3 levels in the cerebellum, striatum and cortex (Igwe and Filla, 1997, Mundy et al., 1991) with increased age in rats. To determine age-related changes in protein levels, Shimohama *et al*., investigated the expression of PLCβ1, PLCγ1 and PLCδ1 in cytosolic and particulate fractions of the brain. They reported that PLCβ1 levels increased after birth, reached its upper limit at 4 months, and then declined gradually. Its distribution within the cell also appears to alter with age as PLCβ1 is primarily found in the cytosolic fraction up to 8 weeks of age, then becomes enriched in the particulate fraction. Consistent with PLCβ1, PLCδ1 levels increased with age however only declined at 18 months after birth whereas PLCγ1 levels decreased with age. Both of these PLC isozymes were found primarily in the cytosolic fraction (Shimohama et al., 1998). The diversity of PLC enzymes within the brain and localisation of different PLCs in different brain regions and cellular compartments may be a mechanism by which neurons in different brain regions are able to act differentially to a stimulus.

1.2.3.3.1. Neuronal PLC functions and their relation to brain disorders

Consistent with their expression in the brain, many neuronal processes are linked to PLC activity and dysregulation of PLC enzymes have been connected to a diverse range of brain related diseases. One such process is neuronal differentiation. Kouachi *et al*. reported the involvement of PLCδ3 in neurite outgrowth through the inhibition of Rho kinase signalling in cerebral and cerebellar neurons (Kouchi et al., 2011). PLCε1 is also likely to have a role in neuronal differentiation as its expression is up-regulated in neuronal precursor cells that are destined to become neurons (Wu et al., 2003). Not all PLC isozymes however aid differentiaion as overexpressed PLCγ1 causes an abnormal expression pattern of cell cycle regulators: CDK1, CDK2 and cyclin D1, thereby leading to inhibition of nerve growth factor induced differentiation of pheochromocytoma cells (Nguyen Tle et al., 2007).

Studies have reported the involvement of $Ins(4,5)P_3$ driven Ca^{2+} release in neuronal transduction and PLC activity has been linked to neurotransmitter receptors including serotonergic, adrenergic, histaminergic, muscarinic and cholinergic receptors (Wallace and Claro, 1990a, Xu and Chuang, 1987). PLCβ1 has been implicated in the modulation of muscarinic acetylcholine receptor signalling in hippocampal neurons, therefore it is involved in regulating synaptic plasticity and cortical development (Hannan et al., 1998, Spires et al., 2005). Transgenic PLCβ1 knock-out mice displayed epilepsy (Kim et al., 1997) and abnormal behaviour due to excessive hippocampal neurogenesis and uncharacteristic migration of adult-born neurons (Wallace and Claro, 1990b, Choi et al., 1989). Human patients exhibiting a loss of function mutation in PLCβ1 are also affected by early onset epileptic encephalopathy (Kurian et al., 2010). In addition, orbitofrontal cortex samples from schizophrenic and bipolar patients showed a deletion of the PLCβ1 gene (Lo Vasco et al., 2012, Lo Vasco et al., 2013). PLCβ4 is involved in the regulation of LTD in rostral purkinje cells of the cerebellum (Hirono et al., 2001) and signals mediated by mGluR1 in this brain region require PLCβ4 activation. As such, both mGluR1 and PLCβ4 knock-out mice display ataxia, a neurological problem that affects voluntary muscle movement (Kim et al., 1997, Park and Poo, 2013). Following activation of the receptor tyrosine kinase, TrkB by neurotrophic factors, PLCγ1 regulates synaptic plasticity, neurite outgrowth and neuronal migration (Minichiello, 2009, Park and Poo, 2013). PLCγ1 involvement has also been reported in depression, bipolar disorder, epilepsy, Huntington's disease and Alzheimer's disease (Jang et al., 2013). In addition, PLCγ1 signalling leads to activation of CREB which subsequently leads to elevated brain derived

neurotrophic factor (BDNF) which causes long term anti-depressant effects in the hippocampus (Minichiello et al., 2002, Yagasaki et al., 2006).

1.2.3.3.2. Involvement of PLC enzymes during embryonic brain development

Many studies have reported the association of the phosphoinositide signal transduction pathway with other signalling pathways and proteins that are involved in neural development and neurogenesis during brain development. PLCs of course are key enzymes in the phosphoinositide pathways and are likely to be involved in neurogenesis as they are believed to be responsible for the spontaneous calcium-transient activity observed in the multipotent neural crest cells (NCC). NCC that display such Ca^{2+} transient activity are able to generate neurons (Carey and Matsumoto, 1999). As discussed previously, an important signalling pathway during development is the Wnt signal transduction pathway (Poncet et al., 1996). This pathway regulates gene expression by way of three different signalling cascades, one of which is the Wnt/Ca^{2+} pathway that involves PLC activation to release organelle stored Ca^{2+}, thus further activating CaMKII and PKA, both of which can regulate expression of downstream developmental genes (Jung et al., 2009, Kuhl et al., 2000).

PLC enzymes interact with Ca^{2+} sensitive TRPC channels and may, to some extent regulate their roles in neural development, proliferation, cerebellar granule cell survival, neuronal morphogenesis, axon path finding and synaptogenesis (Suh et al., 2008, Venkatachalam et al., 2003). PLC enzymes are also implicated in signalling of other proteins that play a role in development including: Neurotrimin which is involved in the development of thalamo-cortical and pontocerebellar projections (Gil et al., 1998, Struyk et al., 1995), the pleiotropic neuropeptide pituitary adenylate cyclase-activating polypeptide (PACAP) which is involved in gliogenesis and neurogenesis (Dejda et al., 2006, Nicot and DiCicco-Bloom, 2001), papaverine which has neuroprotective activities (Itoh et al., 2011), and the axonal growth related molecules neurin-1 (Ledeen and Wu, 2004) and tenascin (Rigato et al., 2002). On top of these, PLC enzymes are involved in the cAMP-response element-binding protein/mitogen-activated protein kinase (CREB/MAPK) system, thereby regulating transcription during development (Belcheva et al., 2005). Furthermore, PLC enzymes are involved in signalling pathways of thyroid hormones (Smallridge et al., 1992), growth factors (Chun, 1999), and serotonin which is involved in craniofacial morphogenesis (Katan, 2005, Salles et al., 1993). PLC enzymes have

also been reported to interact with muscarinic receptors (Melliti et al., 1999) and metabotropic glutamate receptors in the human foetal brain (Hannan et al., 2001).

1.2.3.4. PLC-eta (η) enzymes

PLCη enzymes are the most recently identified class of PLC enzymes and are the primary focus of this project. Their expression within neurons coupled with their high sensitivity towards Ca^{2+} makes them probable regulators of many neuronal processes and possible candidates for drug treatment in certain diseases. This section will begin with a brief overview of their initial characterisation, followed by a review of their domains, a summary of the literature and possible cellular functions.

1.2.3.4.1. Characterisation of PLCη enzymes

In 2005, several groups (Cockcroft, 2006, Hwang et al., 2005, Nakahara et al., 2005, Stewart et al., 2005, Zhou et al., 2005) independently discovered PLCη which is the most recently identified class and consists of two isozymes, PLCη1 and PLCη2 with approximately 50% amino acid sequence homology between them. Genes encoding human PLCη1 and PLCη2 are respectively located on chr.3q25.31 and chr.1p36.32 with orthologous proteins also present in mice, rat, zebrafish, puffer fish and nematode worm (Stewart et al., 2005). Both isozymes have been proven to catalyse the hydrolysis of PtdIns(4,5)P_2 (Nakahara et al., 2005), meaning that this class of PLC like others is involved in DAG and Ins(4,5)P_3 production. PLCη enzymes have a domain structure that is most similar to the PLCβ enzymes but they are most closely related to the PLCδ enzymes which have the highest Ca^{2+} sensitivity in comparison to other PLC isozymes (with the exception of PLCζ). (Rhee, 2001, Stewart et al., 2005).

PLC enzymes consist of several homologous domains, also present in the majority of other PLC classes. These include the EF-hand domain, catalytic X/Y domains, PH domain and C2 domain. The latter two bind to phospholipids and in the case of the C2 domain, in a Ca^{2+} dependent manner. They are therefore accountable for membrane association (Ananthanarayanan et al., 2002, Essen et al., 1996). It has been reported that in cells transfected with endogenous PLCη2, only 6% of the protein is present at the cell surface following removal of the PH domain compared with 85% of native PLCη2 and 97% of FLAG-tagged PLCη2 constructs (Nakahara et al., 2005). Popovics *et al.* showed that a mutant form of the enzyme that was deficient of a PH domain did not show activation following treatment with the the Na^+/H^+ antiporter monensin or incubation with Ca^{2+} in transfected COS7 cells, presumably

because this mutant was unable to bind to membranes. A mutation in the C2 domain at the predicted Ca^{2+} binding site also resulted in a significant reduction in enzyme activity in response to monensin, suggesting an important regulatory role for this domain. This mutant however did not show altered sensitivity to Ca^{2+}, which implies that the C2 domain is not accountable for Ca^{2+} sensing (Popovics et al., 2011). In addition, a high degree of PLCη2 co-localisation was shown with PtdIns(3,4,5)P_3 in differentiated Neuro2A cells, which suggests that PLCη2 localisation is governed by PtdIns(3,4,5)P_3 (Popovics et al., 2013).

As mentioned previously, most PLC isozymes possess a non-functional EF-hand domain. Exceptions include PLCζ which utilises the EF-hand domain as a Ca^{2+} sensor, and PLCδ1 in which it appears to also be functionally important in regulating binding of the enzyme through its PH domain to PtdIns(4,5)P_2 in the plasma membrane (Yamamoto et al., 1999). Although its role is unclear in other PLC isozymes, the EF-hand seems to serve as a hinge-like link between the PH and the catalytic domains in these enzymes (Kanemaru et al., 2010). PLCη2 also has a functional EF-hand domain that operates as a Ca^{2+} sensor. PLCη2 possesses an EF-hand domain consisting of two EF-loops comprised of a canonical 12 residue loop (EF-loop 1) and a non-canonical 13 residue loop (EF-loop 2). Through mutation of EF-loop 1, a ~10 fold reduction in Ca^{2+} sensitivity was noted in response to monensin compared to wild type (WT) in transfected COS7 cells (Popovics et al., 2014). Mutation of various residues in EF-loop 2 however did not show any difference in response compared with wild-type, suggesting that the second loop is not involved in Ca^{2+} sensing.

The X and Y domains fold up to form a catalytic site and are both involved in substrate binding. Ca^{2+} also binds to the X domain which is necessary for catalysis (Essen et al., 1996). In comparison to PLCδ enzymes which are most closely related to PLCη enzymes, both PLCη isozymes contain an extended loop which is approximately 100 residues longer between the X and Y domains. In addition, PLCη enzymes contain an additional C-terminal region that is rich in serine and proline residues (Stewart et al., 2005). This domain may be of functional importance to PLCη enzymes as proline rich regions of proteins are often involved in protein-protein interactions and are present in many transcription factors which require activation by other proteins (Berridge, 2009, Stutzmann et al., 2006). In addition, some splice forms of PLCη enzymes possess a class II PDZ (post synaptic density protein, *Drosophila* disc large tumour suppressor, and zo-1 protein) conserved binding motif (PDZCBM) at their C-terminus. PLCβ enzymes also possess a PDZCBM and forms multi-protein complexes such as the inactivation-no-afterpotential D (inaD) complex that is required for photoreceptor assembly (Georgiev et

al., 2005, Huber et al., 1998). By possessing such a domain, PLCη enzymes may also form such protein complexes. As shown in Figure 1.15, different splice variants that differ in their C terminus region (length and consistence of PDZ domain) have been identified, three for PLCηl; a, b and c (with sizes: 1002, 1693 and 1035 amino acids in the human isoform) and five for PLCη2; 21a/23, 21a/22/23, 21b/23, 21b/22/23 and 21c/22/23 which are characterised based on the exon structure of the spliced forms (with sizes: 989, 1156, 1211, 1416 and 1583 amino acids in the human isoforms; Hwang et al., 2005, Zhou et al., 2005). All of the PLCη1 isozymes, but only two of the PLCη2 isozymes (21a/23 and 21b/23) contain a PDZCBM which suggests the possibility for different functions between the PLCη2 spliced forms (Stewart et al., 2007). Of the Five PLCη2 variants, two are expressed in the brain, namely the 21/b/22/23 and 21c/22/23 variants (Zhou et al., 2005).

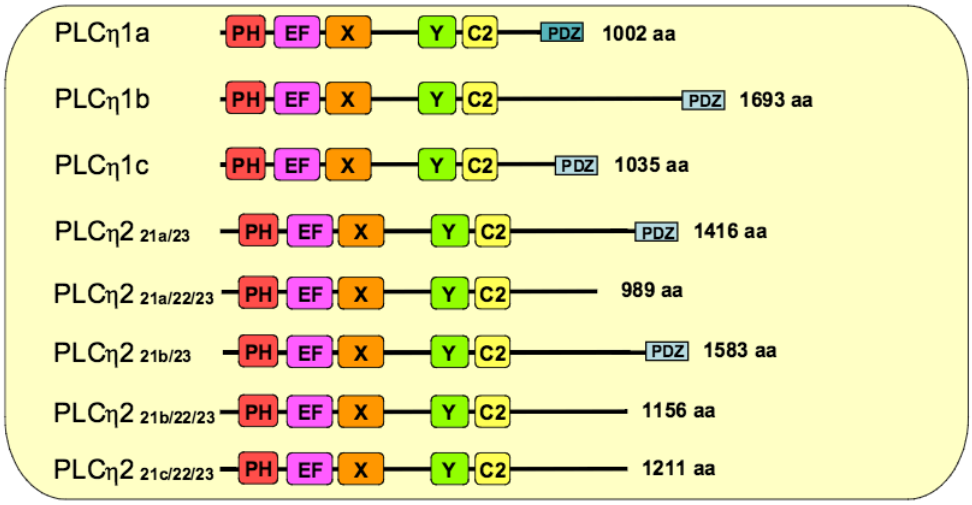

Figure 1.15: Domain structure of PLCη1 and 2 isozymes. Abbreviation: PH, Pleckstrin homology domain. EF, EF-hand domain. X, catalytic X domain. Y, catalytic Y domain. C2, C2 domain. PDZ, post synaptic density protein, Drosophila disc large tumor suppressor, and zo-1 protein C-terminal binding motif. Image taken from Stewart et al., 2007.

1.2.3.4.2. Expression and possible roles of PLCη enzymes

The role of PLCη enzymes is yet to be fully determined but studies have shown their abundance within several tissue types. Investigations using RT-PCR and primer pairs targeting a common area of PLCη1 variants showed high abundance within the brain and kidneys but also noted their presence in the lung, spleen, intestine, pancreas, and thymus (Hwang et al., 2005). The same study was performed for the PLCη1a variant and was found to be present only in the brain and lung (Hwang et al., 2005). Immunoblotting further showed the presence of this

variant in the cerebrum, cerebellum and spinal cord. High expression levels were also found in the olfactory bulb, hippocampus, cerebellum, cerebral cortex, zona incerta, habenular nuclei and hypothalamus using in situ hybridization (Hwang et al., 2005). With the exception of zona incerta, high levels of PLCη2 was also detected in these regions with most abundant expression in the olfacoty bulb, cerebral cortex and pyramidal cells of the hippocampus (Nakahara et al., 2005), all of which contribute to memory circuits. Because the cerebral cortex is involved in thinking, memory and language processes, PLCη2 may be involved in these processes. Kanemaru *et al*. also reported high expression in the habenula and retina, both of which are involved in regulating circadian rhythm (Kanemaru et al., 2010). A gradual increase in PLCη2 levels is also observed during postnatal development in the mouse brain and retina (Nakahara et al., 2005). In spite of previous claims that PLCη2 is neuron specific (Nakahara et al., 2005), more recent studies have shown its presence in the intestine of mice (Guo et al., 1996) as well as in cDNAs isolated from a range of nervous and non-nervous tissues such as anaplastic oligodendroglioma, epithelioid carcinoma, leukopherosis, lymph, nerve tumours, optic nerve, pancreatic islets, pituitary, and retinoblastoma (Stewart et al., 2005). Proposed roles for this enzyme include regulation of memory (Nakahara et al., 2005), circadian rhythm (Stewart et al., 2007), neurotransmitter and hormone release (Cockcroft, 2006, Stewart et al., 2007) and in neuronal tumourigenesis (Lo Vasco, 2011).

1.2.3.4.3. Biochemical and functional characterisation of PLCη enzymes

Several groups have addressed the Ca^{2+} sensitivity of PLCη enzymes and have confirmed the activation of purified PLCη enzymes by intracellular Ca^{2+}. Hwang *et al*. showed high sensitivity of PLCη1 towards Ca^{2+} at 0.1-1 μM with maximal activity at 10 μM Ca^{2+} (Hwang et al., 2005). Popovics *et al.* recently showed sensitivity of PLCη2 at 0.1-1 μM free Ca^{2+} with highest activation at 10 μM free Ca^{2+} and approximately 80% of its maximal activity at 1 μM free Ca^{2+} This is significant as 0.1-1 μM is the physiological range of free cytosolic Ca^{2+} (Popovics et al., 2011, Berridge et al., 2000). These studies show that both PLCη1 and PLCη2 have the same level of sensitivity towards Ca^{2+}. The highest activity of PLCη2 is also the same as that of PLCη1 but is reached at ten-fold lower Ca^{2+} concentration than PLCδ1 as Nakahara *et al.* showed the maximal activity of PLCδ1 at 100 μM Ca^{2+} (Nakahara et al., 2005).. Furthermore, treatment with monensin also resulted in a five fold increase in PLCη2 activity. This effect was inhibited by CPG-37157 which is a selective inhibitor of mitochondrial Na^{+}/Ca^{2+} exchange (Popovics et al., 2011), indicating that the observed increase in PLCη2

activity is at least to some extent due to mitochondrial Ca^{2+} release. To identify activators of PLCη2 enzymes, Zhou *et al.* co-expressed a variety of known PLC regulators with purified PLCη2 in COS7 cells then measured PtdIns(4,5)P_2 hydrolysis. They identified $G\beta_1\gamma_2$ as the only activator for PLCη2. This dimer however did not activate PLCη1 which highlights their different modes of activation (Zhou et al., 2008). The only known activator of PLCη1 is therefore Ca^{2+}. Kim *et al.* also reported increased activation of PLCβ upon activation of PLCη1 which suggests that PLCη1 can serve to amplify PLCβ activity (Kim et al., 2011). Table 1.2 summarises the domains present and current information on the Ca^{2+} sensitivity of different PLC isoforms. As can be seen, there is contradictory results in the data regarding Ca^{2+} sensitivity and maximal activation by Ca^{2+}.

PLC isoform	Functional domains	Ca^{2+} sensitivity (μM)	Maximum activity Ca^{2+} (μM)
PLCβ	PH, EFL, X, Y, C2	NA	NA
PLCγ	PH, EFL,X, Y, SH2, SH3, C2	NA	NA
PLCδ	PH, EFL,X, Y, C2	PLCδ1 0.1-1 (Hwang et al., 2005) 0.1-1 (Nakahara et al., 2005)	PLCδ1- 100 (Hwang et al., 2005, Nakahara et al, 2005) 10 (Nakahara et al., 2005)
PLCε	RasGEF, PH, EFL,X, Y, C2, RA1, RA2	NA	NA
PLCζ	EF, EFL, XY, C2	0.01-0.1 (Kouchi et al., 2005)	1 (Kouchi et al., 2005)
PLCη	PH,EF, EFL,XY, C2	PLCη1- 0.1-1 (Hwang et al., 2005) PLCη2- 0.01-0.1 (Popovics et al., 2011) PLCη2- 0.1-1 (Popovics et al., 2011)	PLCη1- 10 (Hwang et al., 2005) PLCη2- 10 (Popovics et al., 2011) PLCη2- 1 (Nakahara et al., 2005)

Table 1.2: Table showing a list of PLC isoforms, their functional domains, their sensitivity towards Ca^{2+} and the Ca^{2+} concentration at which they show highest activity. Abbreviations: PH: Pleckstrin homology domain, EF: EF-hand domain, EFL: EF hand-like domain, X: Catalytic X domain, Y: Catalytic Y domain, C2: C2 domain, SH2,SH3: SRC homology domains, RasGEF: guanine nucleotide exchange factor domain for Ras-like small GTPases, RA: Ras association domain, NA: not applicable.

PLCη2 has been shown to be involved in neuronal differentiation. Neuro2A cells exhibit development and growth of neurites following a four day treatment with retinoic acid (RA). Using this system, Popovics *et al.* reported an increase in PLCη2 expression levels as neurites develop, exhibiting low expression at day 0 and maximal expression at the final day 4 time point (Popovics et al., 2013). Through creation of a Neuro2A cell line stably expressing PLCη2-targetted shRNA plasmids (resulting cells expressed ~67% less PLCη2 at the protein level), it was shown that these PLCη2 knock-down cells displayed a significant decrease in differentiation as determined by the extent of neuritogenesis following a four day treatment with RA (Popovics et al., 2013). In accordance with this, Nakahara *et al*. reported an increase in PLCη2 expression levels in the brains of mice as they developed. They noted low expression at birth which increased as the mice developed (Popovics et al., 2013). Elevation of PLCη2 was also noted in the retina of developing mice, again showing increased expression from birth

(Kanemaru et al., 2010). Such expression patterns could stem from development and maturation of neurites.

In a study aimed at identifying an interaction partner for PLCη2, Popovics *et al.* identified LIMK-1 by conducting a bacterial two-hybrid screen (Popovics et al., 2013). LIMK-1 is a serine protein kinase that primarily functions downstream of Rho GTPases to phosphorylate cofilin. Therefore LIMK-1 is involved in neurite formation by phosphorylating and subsequently inactivating cofilin family proteins, which function to sever and depolymerise actin filaments (Endo et al., 2007, Yang et al., 1998). This protein co-localised with PLCη2 as determined by immunofluorescence in differentiated and undifferentiated Neuro2A cells. In addition, the above mentioned knock-down cells exhibited a significantly lower level of LIMK-1 phosphorylation following a 2 day treatment with RA, which suggests that PLCη2 may be directly or indirectly involved in phosphorylating LIMK1 (Popovics et al., 2013).

Recently, a new role has emerged for PLCη2 in exocytosis of peptide containing, dense core vesicles. This occurs partly due to regulation of two vesicle priming factors; CAPS and Munc13-2 following breakdown of the membrane phospholipids PtdIns(4,5)P_2 by PLCη2 (Kabachinski et al., 2014). The other factor is disassembly of F-actin filaments and subsequent up-regulation of dense core vesicles. This was noted following increased intracellular Ca^{2+} concentration by treatment of neuroendrocrine PC12 cells with high concentration (95 mM) KCL which raises intracellular Ca^{2+} concentration to 800 nM, an effect that was not achieved in PLCη2 KD cells (Yamaga et al., 2015). This finding along with the fact that PtdIns(4,5)P_2 is involved in F-actin assembly, through regulation of actin binding proteins (Saarikangas et al., 2010) suggests that dense core vesicle upregulation results from an increased breakdown of PtdIns(4,5)P_2 following activation of PLCη2. PtdIns(4,5)P_2 sequesters proteins such as cofilin and scinderin which are released upon its hydrolysis. Once released, these proteins can promote actin severing (Saarikangas et al., 2010). In accordance, the authors also noted co-localisation of PLCη2 with actin filaments (Yamaga et al., 2015). The presence of actin filaments physically prevents increased up-regulation of cytoplasmic dense core vesicles to the plasma membrane (Bittner and Holz, 2005), therefore breakdown of actin following increased PtdIns(4,5)P_2 hydrolysis removes this inhibition from the cell. Furthermore, treatment of PC12 cells with lower concentration (56 mM) KCL, which raises Ca^{2+} concentration to 400 nM did not result in upregulation of cytoplasmic dense core vesicles to the plasma membrane, suggesting that PLCη2 may be required for increased neuropeptide release under certain conditions (Yamaga et al., 2015).

1.2.3.5. Hypothesis and aims

The major hypothesis underlying this thesis is to gain a better understanding of how PLCη enzymes are activated, to understand more about the functional role of PLCη2 in relation to neuronal differentiation/neuritogenesis and to determine whether PLCη enzymes are involved in development and certain diseases.

The aims of this thesis are to

1) Determine the activation of PLCη1 and PLCη2 by Ca^{2+}.

2) Confirm the activation of PLCη2 by Gβ1γ2.

3) Determine the cellular localisation of PLCη1 and PLCη2.

4) Confirm the direct interaction of PLCη2 with LIMK-1 and examine whether their interaction plays a role in neuronal differentiation/neuritogenesis.

5) Confirm that PLCη2 is required for Neuro2A differentiation and examine whether this is dependent on the enzymes ability to become activated by Ca^{2+}.

6) Identify other proteins that may be involved in neuronal differentiation/neuritogenesis.

7) Investigate the relevance of PLCη2 to Alzheimer's disease.

8) Examine whether the mutant form of PLCη1 (N1075X) shows an altered cellular distribution and examine whether it has altered effects on the sonic hedgehog (Shh) pathway

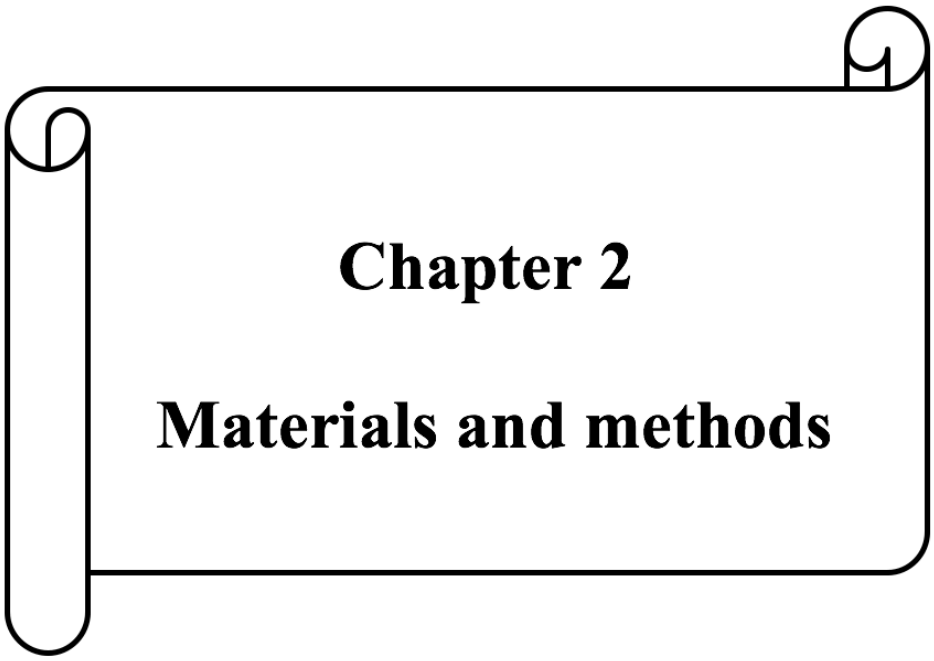

Chapter 2

Materials and methods

This chapter describes general methods used throughout the theses. Specific methods are described in the respective chapters.

2.1. Molecular biology methods

2.1.1. Measuring RNA and DNA concentration

In order to measure the concentration of RNA or DNA in a given solution, 2 µl of purified nucleic acid solution was applied to the NanoVue spectrophotometer (GE Healthcare) chamber to measure the concentration of RNA or DNA, at 260 nm. Contamination was tested with 260/280 nm ratio.

2.1.2. RNA extraction

Cells were grown in a six-well plate to 90% confluency, washed once with PBS then incubated for 5 mins with 1 ml of Trizol (Invitrogen, Waltham, MA, USA) to extract the RNA. Cells were then scraped using a cell scraper and collected in an eppendorf tube. Chloroform was then added (0.2 ml) and the sample mixed by shaking vigorously for 15 secs, followed by incubation at room temperature (RT) for 2 mins. This was followed by centrifugation at 12,000 × g for 15 mins at 4^{o}C which leads to a two-phase mixture. The colourless top layer containing RNA was added to a new eppendorf tube containing 0.5 ml of isopropanol, mixed by inversion and incubated for 10 mins at RT. Samples were then centrifuged at 12,000 × g for 15 mins at 4^{o}C to pellet the RNA. The supernatant was then removed and RNA pellet washed with 1 ml of 75% ethanol in DEPC water. This was centrifuged at 7,500 × g for 5 mins at 4^{o}C. Finally, the supernatant was removed; the RNA pellet was allowed to dry at RT then resuspended in 50 µl of DEPC treated water. To completely dissolve the pellet, samples were held in a water bath which was set at 55^{o}C for 2 mins. RNA was stored at -80^{o}C until required.

2.1.3. Complementary DNA (cDNA) synthesis

To synthesise cDNA, 2 µg of RNA was incubated with 2 µl DNAse (RQ1 RNase-Free DNase, Promega, Fitchburg, WI, USA), 1 µl DNAse buffer and water to make a 10 µl solution. This reaction was then incubated for 1 hour at 37^{o}C to remove DNA contamination. DNAse was terminated by addition of 1 µl DNAse stop solution (Promega), mixed and incubated for 10 mins at 65^{o}C. Half of this reaction was then used as template RNA. To this, 100 pmol oligo $(dT)_{18}$ (Thermo Fisher Scientific, Waltham, MA, USA), 5x reaction buffer, 20 units RNAse inhibitor (Promega), 0.5 mM dNTP mix (Sima-Aldrich, St. Louis, MO, USA), 200 units (1 µl)

RevertAid premium reverse transcriptase (Thermo Fisher Scientific) and DEPC treated water up to 20 µl was added. Reactions were then incubated for 60 mins at 42^{o}C and terminated by heating at 70^{o}C for 10 mins to create cDNA.

2.1.4. Conventional Polymerase Chain Reaction (PCR)

To amplify DNA, 1 µl of the synthesised cDNA was used for each PCR reaction. PCR reations were performed using the Phoenix 2 thermal cycler (Helena Biosciences, Tyne and Wear, UK). Three different systems based upon different polymerase enzymes were used during the project:

2.1.4.1. GoTaq polymerase

To the cDNA, 1.25 units GoTaq polymerase (Promega), 1x buffer, 1.5 mM $MgCl_2$, 0.2 mM dNTPs (Sigma-Aldrich, St-Louis, MO, USA), 250 nM forward and reverse primers, and sterile water were added to a final volume of 50 µl. Thermal cycling profile used: 95^{o}C for 15 secs, 30 cycles of 60^{o}C for 30 secs and 72^{o}C for 1 min, preceded by incubation at 95^{o}C for 2 mins to allow enzyme activation.

2.1.4.2. BIO-X-ACT short mix

To the cDNA, 25 µl of the mixture was added. This mixture is a ready to use 2x reaction mixture containing BIO-X-ACT short DNA polymerase, $MgCl_2$ and dNTPs. 250nM forward and reverse primers were also added and sterile water to a final volume of 50 µl (Bioline, London, UK). Thermal cycling profile used: 95^{o}C for 1 min, then 35 cycles of 95^{o}C for 30 secs 60^{o}C for 30 s and 68^{o}C for 30 secs. Finally reactions were heated to 72^{o}C for 1 min.

2.1.4.3. Expand long template kit

To the cDNA, 0.2 mM dNTPs, 250 nM forward and reverse primers, 5 µl 10x buffer 2, 1 µl (5 units) DNA polymerase (containing a mixture of thermostable Taq DNA polymerase and Tgo DNA polymerase, which has proof reading activity, Sigma-Aldrich). Thermal cycling profile used: 94^{o}C for 2 mins, the 30 cycles of 94 ^{o}C for 10 s, 60 ^{o}C for 30 s for 45 secs. The last step (elongation step) is increased by 20 secs in each cycle which ensures higher yield of PCR product.

2.1.5. Quantitative PCR (qPCR)

Quantitative PCR (qPCR) was used to measure the level of gene expression relative to levels of large ribosomal protein P0 (RPLP0) mRNA by using the PerfeCTa SYBR Green FastMix (Quanta biosciences, Gaithersburg, MD, USA). Each reaction mixture contained 1 µl of cDNA (which was synthesised as described earlier), 250 nM of forward and reverse primer, 10 µl of 2x reaction mixture and RNAse free ultrapure water to a final reaction volume of 20 µl. The ViiA 7 Real-time PCR system (Thermo Fisher Scientific) was used to perform PCR with the following parameters: 50^{o}C for 2 mins, 95 ^{o}C for 10 mins and 40 cycles of 95 ^{o}C for 10 mins and 60 ^{o}C for 40 secs. Gene expression levels were analysed by adding a melting curve to the end of the qPCR program. Expression levels were measured by the deltaCT method.

2.1.6. Agarose gel electrophoresis

Agarose gels were created using 1% (w/v) agarose (Sigma-Aldrich) which was melted in Tris-acetate/EDTA buffer (composed of 40 mM Tris acetate and 1mM ETDA). To this, 3µl of ethidium bromide (10 mg/ml) was added to enable detection of DNA/RNA bands. This mixture was poured into a gel tray and a comb was inserted to form gel wells. Once set, the gel tank (containing gel tray with gel) was filled with TAE buffer to a level that covers the entire gel. PCR samples were mixed with 6x loading dye and loaded into gel wells. Hyperladder I (Bioline, 200-10,000 bp) was loaded into one well to allow identification of DNA sizes. Gel was run at 150 V for 45 mins to allow separation of DNA/RNA bands. Bands were visualised in a Gel Doc XR+ Imager and analysed using the Image Lab 2.0 software (Bio-Rad Laboratories, Inc.).

2.1.7. Gel purification of DNA bands

Gel was placed on a Blue Light Transilluminator (Life Technologies) which uses UV light to allow visualisation of DNA bands. A sterile razor blade was used to excise blocks of gel containing DNA bands. QIAquick Gel Extraction Kit (Qiagen Venlo, Netherlands) was then used to purify DNA from the gel blocks, according to the manufacturers guidelines. Following purification, DNA was eluted in 30-50 µl of sterile water, depending on size of the initial band obtained.

2.1.8. Restriction endonuclease digestion

Restriction enzymes (obtained from New England Biolabs, NEB, Ipswich, MA, USA) were used to digest DNA to diagnostically confirm the presence of the correct DNA insert into the vector. A double digest was performed in some cases using a reaction buffer that was suitable for both restriction enzymes. For the reaction mixture, 1µg of DNA was mixed with 2 µg BSA, 2 units of enzyme and 1x buffer (different buffers were recommended for each restriction enzyme) and sterile water to a final volume of 20 µl. Reactions were incubated at 37^{o}C for 90 mins.

2.1.9. Transformation of vectors into competent *E. Coli*

For propogation of appropriate ligation products (and plasmid DNA), the respective plasmids were transformed into competent *E. coli* cells by a heat-shock method. For each transformation, 2 µl of ligation mixture or plasmid DNA was transformed by heat-shock into 25 µl of Alpha-select chemically competent cells (Bioline) according to the manufacturer's protocol. SOC medium (Bioline) was then added to the mixture and incubated for 1 hour at 37^{o}C. This was then spread onto previously prepared agar plates containing ampicillin (100 µg/ml) to allow only growth of colonies that contain the vector which contains an antibiotic resistance gene. Plates were then incubated at 37^{o}C overnight.

Formed colonies were chosen and placed into 50 ml falcon tubes containing 1 ml Luria broth (LB) media (Sigma Aldrich) and incubated overnight at 37^{o}C in a shaking incubator set at 1,900 RPM. This enables bacteria to multiply in numbers. Stocks were created by adding 500 µl of culture media and 500 µl of glycerol into a cryovial which was mixed by vortexing and stored at -80^{o}C. For diagnostic purposes, 100 µl of culture media was isolated using the Plasmid Miniprep Kit (Biomiga, San Diego, CA, USA), according to the manufacturer's protocol.

2.1.10. Isolating plasmid DNA

A small amount of glycerol stock of *E. coli* cells contining plasmid of interest was selected using a pipette tip and placed into 1 ml of LB media containing appropriate antibiotic for 6-8 hours. 200 ml of LB media containing antibiotic was placed into a shaking flask and 100 µl of culture media was added to it. This was incubated overnight at 37^{o}C in a shaking incubator set at 1,900 RPM. To prepare plasmids for transfection into mammalian cells,

plasmids were isolated using plasmid Maxiprep Kit (Qiagen), according to the manufacturers protocol and stored at -20^{o}C.

2.1.11. DNA precipitation

DNA precipitation was performed by placing 200 µl of DNA into a 1.5 ml eppendorf tube. To this, 20 µl (one tenth) of 3M sodium acetate, pH 5.2 was added. Then 440 µl (2 volumes) of cold 100% ethanol was added and the sample stored at -20^{o}C for 1 hour. This was then centrifuged for 15 mins at 12,000 rpm at 4^{o}C. The supernatant was removed and 250 µl of cold 70% ethanol was added. Centrifugation was then repeated at the same settings for 5 mins. The ethanol was again removed and the pellet placed in a water bath set at 37^{o}C to allow complete evaporation of ethanol. The pellet was then re-suspended in a smaller volume of sterile water.

2.1.12. Gene sequencing

The full length of cloned genes were sequences commercially by sending purified plasmid DNA samples as well as sequencing primers (obtained from Eurofins, Luxembourg) to Dundee Sequencing Services, Dundee, UK.

2.2. Cell culture methods

2.2.1. Cell line and their maintenance

Four cell lines were used throughout the thesis as stated in Table 2.1. All cells were maintained at 37^{o}C and 5% CO_2, using either Eagle's minimal essential medium (EMEM) or Dulbecco`s modified Eagle`s medium (DMEM). All media was acquired from Sigma-Aldrich. To continuously maintain cells, they were split twice a week into sterile T-75 (75 cm^2) flasks. This was done by washing cells with sterile PBS (Sigma-Aldrich), adding 2 ml of trypsin to dislodge cells and incubating at 37^{o}C for 2-3 mins. Following dislodging of cells by gentle tapping, 8 ml of media was added to flasks to inactivate the trypsin and 0.5 ml was transferred into a new T-75 flask containing 25 ml of complete media. COS7 cells were a gift from Prof. Robert P. Millar (Queen's Medical Research Institute, Edinburgh, UK), C3H10T1/2 cells were a gift from Prof. Andrew Riches (School of medicine, University of St Andrews, UK), N7 hypothalamic cells were a gift from Dr Javier Tello (School of medicine, University of St Andrews, UK) and Neuro2A cells were acquired from The European Collection of Cell Cultures (ECACC).

Cell type	Origin	Maintenance
Neuro2A	murine neuroblastoma cell line (Klebe and Ruddle 1969)	EMEM supplemented with 10% FBS, 2 mM L-glutamine, 50 units/ml of penicillin/streptomycin mixture (Invitrogen).
COS7	immortalised kidney cells from African green monkey (Gluzman 1981)	DMEM containing high glucose (4500mg/L) supplemented with 10% FBS, 2 mM L-glutamine and 50 units/ml of penicillin/streptomycin mixture.
C3H10T1/2	Mouse embryonic mesenchymal stem cells	EMEM, as above
N7	Mouse embryonic cells hypothalamus cell line	DMEM, as above

Table 2.1: Cell lines used, their origin, and their maintenance

2.2.2. Cryopreservation of cells

Cells were grown in T-75 flasks to near full confluency, and then dislodged by trypsinisation as described earlier. Cell suspensions were centrifuged at 800 rpm (for Neuro2A, C3H10T1/2 and N7 cells) or 1,500 rpm (for COS7 cells) for 3 mins. The cell pellet was resuspended in 3 ml of freezing media (FBS containing 10% BSA) and aliquoted into to 3 cryovials (Nunc, Thermo Fisher Scientific). Cell freezing was performed in stages. Cryovials were placed into a perspex box that was lined with cotton wool and stored at -20^{o}C for two hours, then stored at -80^{o}C for 24 hours. Cryovials were finally stored in a container filled with liquid nitrogen until required.

2.2.3. Thawing of cryopreserved cells

Frozen cells in cryovials were defrosted in a water bath set at 37^{o}C and added to a falcon tube containing 5 ml of growth medium. Tubes were centrifuged as above to remove the DMSO, resuspended in 5 ml of complete media then grown in a T-25 flask. When confluent, cells were transferred into a T-75 flask.

2.2.4. Transfection of cells by electroporation

Cells (Cos7, Neuro2A, C3H10T1/2 and N7 cells) were trypsinised and seeded in 14 cm dishes containing 25 ml complete the appropriate media until they reached full confluency. For each transfection, 1.5 x 10^7 cells were counted using the haemocytometer and placed into a 50 ml falcon tube. This was centrifuged at 1,500 rpm for 5 mins to pellet cells. The media was then removed and cells were resuspended in the same volume of Optimem I reduced-serum medium (Life technologies) to wash and remove the FBS which would otherwise decrease the efficiency of transfection. Centrifugation was repeated to form a cell pellet, the supernatant was removed and the cell pellet was resuspended in 700 µl of Optimem I. This was added to an electroporation cuvette and mixed with 15 µg of DNA. Where multiple transfections were required, they were performed in parallel. Electroporation was performed by placing the cuvette into a Bio-Rad Gene Pulser set at 230 V, 950 µF. Cuvettes were left at RT for 10 mins then added to 25 ml of complete growth medium, before being seeded onto appropriate cell culture dishes in experiments.

2.2.5. Chemical transfection of cells

2.2.5.1. Lipofectamine transfection

This method was used to transfect Neuro2A cells with EV, PLCη2, PLCη2+Gβ1γ2, and mut.PLCη2+Gβ1γ2 constructs (described in chapter 3). C3H10T1/2 and N7 cells were also transfected by this method using a GFP construct. Cells were seeded at low density (100/mm^2) into wells of a 12 well plate containing 1 ml of supplemented media but lacking antibiotics. After incubation of cells overnight, 1.6 µg of DNA and 4 µl of Lipofectamine (Invitrogen) were mixed separately, each in 100 µl of Optimem I. These were left at RT for 5 mins then mixed together and left at RT for 20 mins. This solution was then added to the well in a dropwise manner with constant swirling of the plate. Where multiple transfections were required, they were performed in parallel. The plate was then placed into the incubator and the solution changed to complete medium after 6 hours. This was returned to the incubator for 24 hours.

2.2.5.2. FuGene 6 transfection

This method was used to transfect C3H10T1/2 and N7 cells with a GFP construct. For each reaction, 2 x 10^4 cells were seeded into a well of a clear bottom 96 well plate in 100 µl of

complete media. The next day, 6 µl of FuGene 6 transfection reagent (Promega) was mixed with 2 µg of DNA and incubated at RT for 15 mins, then added to plated cells containing complete media to a final volume of 100 µl. Extent of transfection was determined by fluorescent microscopy.

2.3. Protein analysis methods

2.3.1. Protein extraction

Cells were grown in 6-well plates until fully confluent then washed twice with PBS. The plate was placed on ice and 100 µl of cold RIPA buffer (Roche, Burgess Hill, UK) was added and incubated for 2 mins. Cells were then scraped using a cells scraper and collected into 1.5 ml ependorf tubes. Cell lysates were centrifuged at 14,000 rpm at 4^{o}C to pellet cell debris and allow separation of the protein containing supernatant, which was added to a fresh ependorf tube. To measure protein concentration, the BCA protein assay kit (Thermo Fisher Scientific) was used according to the manufacturer's instructions.

2.3.2. Western blotting

Samples were prepared by placing 20 µg of protein into an ependorf tube, mixing with 4x NuPAGE LDS sample buffer (Thermo Fisher Scientific) and heating at 95^{o}C for 5 mins in a DB-3 heat block (Techne, Minneapolis, MN, USA). Samples were then loaded into wells of a NuPAGE precast polyacrylamide gel (4-12% BIS-Tris) that was placed into an Xcell SureLock electrophoresis system (Thermo Scientific) and filled with 1x NuPage running buffer (Life technologies). PageRuler pre-stained protein ladder (Thermo Fisher Scientific) was loaded into the first well. Samples were separated by electrophoresis at 150 V for 60-90 mins.

A semi-dry transfer method was used to transfer gel separated proteins onto a polyvinylidene difluoride (PVDF) membrane (Bio-Rad). The cut membrane was first placed in a container with 100% methanol for 30 secs then placed into a container containing sterile water and incubated at RT, with gentle rocking. Two blotting pads (Fisher, Scientific) were soaked in NuPage transfer buffer (Life Technologies, supplemented with 0.01% SDS and 11% methanol). The PVDF membrane was positioned between the two blotting pads and placed into the transfer apparatus (Trans-Blot SD semidry transfer cell, Biorad, Hercules, CA, USA). A glass tube was then rolled across the surface of the blotting pad to remove trapped air bubbles. Transfer was performed at 18 V for 30 mins. The membrane was next placed into a

milk solution (5% non-fat milk in TBS) and incubated at RT with shaking for 1 hour to block the membrane and prevent unspecific binding of antibodies.

The membrane was then placed into a container with 10 ml antibody solution (1% non-fat milk with 0.5% Tween-20 in TBS) containing the required primary antibody and incubated at 4^{o}C with gentle rocking. Primary antibodies used in different experiments were: goat polyclonal anti-PLCη2 antibody (1:250 dilution; Santa Cruz Biotechnology, Heidelberg, Germany), mouse monoclonal anti-β-actin antibody (1:10,000 dilution; Sigma-Aldrich) and Mouse polyclonal anti-phospho-c-Jun (Ser73) antibody.

The membrane was washed 3 times with TBST (TBS containing 0.5% tween), 15 mins each time then incubated in antibody solution containing horseradish peroxidise-conjugated antibodies (1:10,000 dilution, Thermo Fisher Scientific) for 90 mins. This was followed by 3 washes with TBST, 15 mins each time. The SuperSignal West Dura chemiliminescent substrate (Thermo Fisher Scientific) was then used to detect binding of antibodies using the LAS-3000 phosphpoimager (Fujifilm, Düsseldorf, Germany)

2.4. Statistical analysis

All experiments were performed in triplicates and data was presented as mean values ± standard deviation or in some cases standard error of mean (SEM). To determine statistical significance, aeither an unpaired T-test (with applied Bonferroni's correction in the case of figure 4.13) or a one way analysis of variance (ANOVA) using Tukey's honest significance test was performed using Prism 6 software. P-values were indicated on charts as such: *, $P<0.05$; **, $P<0.01$; ***, $P<0.001$ and ****, $P<0.0001$.

Chapter 3

Mechanisms of PLCη activation

3.1. Introduction

PLC enzymes can be activated by heterotrimeric G-proteins and by small GTPases. In humans, six different classes of PLC enzymes have been identified which consist of 13 different isoforms that are regulated by different mechanisms. The G proteins, $G\alpha_q$ and $G\alpha_{11}$ are for example, activators of PLCβ (Smrcka et al., 1991, Taylor et al., 1991, Waldo et al., 1991), different forms of Gβγ dimers have been reported to activate PLCβ (1, 2 and 3) and PLCδ1 (Park et al., 1993) and Rac GTPases have been identified as activators of PLCβ2 and PLCγ2 (Harden et al., 2009). The activation of PLCη enzymes have also been addressed; to identify G-proteins that can activate PLCη enzymes, Zhou *et al.* investigated the rate of PtdIns(4,5)P_2 hydrolysis by measuring Ins(4,5)P_3 accumulation following transfection of PLCη2 and a variety of previously identified PLC activators into COS7 cells. Their studies did not identify any Gα subunits of heterotrimeric G-proteins or GTPases as activators of PLCη2 but revealed activation by the $G\beta_1\gamma_2$ heterodimer (Zhou et al., 2005). To confirm that this increase in activity was due to $G\beta_1\gamma_2$ dimer activation of the enzyme and not a result of increased PLCη2 expression, PLCη2 protein expression levels were compared between control and $G\beta_1\gamma_2$ transfected cells, showing no difference between them (Zhou et al., 2005). Subsequent studies by the same group, comparing a variety of Gβγ dimers showed that activation of PLCη2 is achieved to a small extent by $G\beta_2\gamma_2$ and $G\beta_4\gamma_2$ but highly by $G\beta_1\gamma_2$. $G\beta_3\gamma_2$ and $G\beta_5\gamma_2$ on the other hand did not result in any activation. Because of the sequence similarity of both PLCη isozymes they also investigated PLCη1 activation by $G\beta_1\gamma_2$; however their results revealed that $G\beta_1\gamma_2$ does not activate PLCη1 which indicates that these two isozymes possess different modes of activation (Zhou et al., 2008). The activation of PLCη enzymes by Gβγ heterodimers may serve an important role during development, which is believed to be a process in which PLCη enzymes are involved in, as discussed in chapters 4 and 6. Expression of Gβ1/2/4/5, and Gγ2/3/5/7 have been noted with differential expression in all stages of development as observed in oocytes, eggs and preimplantation embryos (Williams et al. 1996). GPB-1 (a Gβ subunit) has been shown to have a role in adjusting proper mitotic spindle positioning in C.*elegans* embryos, a process that is required for asymmetric cell division, which gives rise to daughter cells with different fates. GPB-1 is a negative regulator of spindle fibre force generators (a complex comprised of two Gα proteins, LIN-5 and GPR-1/2), with increased presence in the anterior side. GPB-1 depletion results in altered distribution of GPR-1/2 thereby leading to altered pulling forces and therefore, affecting asymmetric cell division. Likewise, proper

asymmetric division of *Drosophila* neuroblasts does not occur upon mutation of the Gγ subunit (Izumi et al., 2004). These studies suggest that the Gβ and Gγ subunits plays a role in regulating spindle fibre orientation and centrosome separation (Thyagarajan et al., 2011).

Because of a functional EF-hand domain that operates as a Ca^{2+} sensor, certain PLC enzymes can also be activated by Ca^{2+} as has been reported for PLCζ and PLCδ (Kouchi et al., 2005, Nakahara et al., 2005). PLCη enzymes also possess a functional EF-hand domain and are activated by Ca^{2+} (Popovics et al., 2014). Kim *et al.* previously showed that the Ins(4,5)P_3 receptor inhibitor 2-APB caused a decrease in lysophosphatidic acid (LPA, a GPCR activator) stimulated PLC activity in control Neuro2A cells which shows the importance of ER Ca^{2+} release in PLC activity. 2-APB however did not have a further inhibitory effect in PLCη1 KD cells upon addition of LPA which suggests that PLCη1 is activated by Ca^{2+} release from the ER. They also showed a lower level of Ins(4,5)P_3 following treatment of PLCη1 KD cells with the Ca^{2+} ionophore, ionomycin (Kim et al., 2011). In accordance, the activation of PLCη1 and PLCη2 by Ca^{2+} has been addressed. Hwang *et al.* reported that PLCη1 is sensitive to 0.1-1 μM Ca^{2+} and is maximally activated at 10 μM Ca^{2+} (Hwang et al., 2005). Popovics *et al.* determined that the sensitivity and activation of PLCη2 by Ca^{2+} is the same as that of PLCη1, as reported by Hwang *et al.*, but their results differed from that of Nakahara *et al.* who reported the sensitivity of PLCη2 to 0.01-0.1 μM Ca^{2+} and maximum activation at 1μM (Popovics et al., 2011, Nakahara et al., 2005, Hwang et al., 2005). These results are slightly conflicting but both show that PLCη enzymes are highly sensitive to Ca^{2+} which suggests that they are activated by small rises in intracellular Ca^{2+}.

The aims of this chapter are to confirm the activation mechanisms of PLCη enzymes beginning with a study into the activation of PLCη2 by $G\beta_1\gamma_2$ using a mechanism which utilises bacterial 2A sequences. These sequences are used by viruses to produce more than one protein from one transcript by assembling multiple protein coding sequences in a single open reading frame (discussed in more detail later). This method is utilised to incorporate all three genes (PLCη2, Gβ1 and Gγ2) into one vector thereby allowing for a more efficient method for expressing 3 proteins into cells. This study will also determine whether the 2A co-expression system is a good method for determining activation of proteins by different Gβγ combinations. The activation of both PLCη1 and PLCη2 by Ca^{2+} is also exmined in a cellular context by transfecting COS7 cells with plasmids engineered to express either PLCη1 or PLCη2 then permeabilising the cells and incubating them with different concentrations of Ca^{2+}. Using this

approach, it will be possible to identify the concentration of intracellular Ca^{2+} required to activate each PLCη enzyme.

3.2. Materials and methods

3.2.1. Preparation of vectors for transfection

For the experiments detailed, the 21b/22/23 splice variant of murine PLCη2 was used; it is one of the variants known to be expressed within the brain (Zhou et al., 2005). This will be referred to as PLCη2 throughout the thesis unless otherwise indicated. The coding sequence of this variant of mouse PLCη2 (residues 75-1238) cloned into pcDNA3.1 was a gift from Prof. Kiyoko Fukami (Tokyo University of Pharmacy and Life Science, Japan).

A synthetic gene in pBluescriptII vector containing the fused coding sequences of murine $G\beta_1$ and murine $G\gamma_2$ each preceded by 2A sequences from thosea asigna virus (TaV) and equine rhinitis A virus (ERAV), respectively ($2A\beta_1 2A\gamma_2$) was purchased from Eurofins Scientific (Luxembourg). To create a vector that expresses the PLCη2 coding sequence as well as $2A\beta_1 2A\gamma_2$, the pcDNA3.1 was digested using xbaI which is a restriction site immediately downstream of the PLCη2 coding sequence. A PCR reaction was then performed using the BIO-X-ACT short mix PCR kit (Bioline) as described in chapter 2, to isolate the $2A\beta_1 2A\gamma_2$ sequence. Both of these were run on a 1 % agarose gel and gel purified as described in chapter 2. Primers used were: forward: 5'-TCCACCGTTAGGGATAGAG CCGAGGGCAGGGGAAG-'3 and reverse: 5'-AAACGGGCCCTCTAGAGGGGCGCCTT TAAAGGATGGCG-3'. These primers consist of 15 base pair overhangs that are complimentary to the cut region of pcDNA3.1 which allows insertion of $2A\beta_1 2A\gamma_2$ into the pcDNA3.1 by recombination. To achieve this, the in-fusion HD cloning kit (Clontech, Saint-Germain-en-Laye, France), was used according to the manufacturers instrutions. A pcDNA3.1 vector containing a mutated form of PLCη2 had previously been created by Dr Petra Popovics using site directed mutagenesis where a key amino acid residue, histidine, in the enzymes active site at residue 460 was replaced with glutamine (H460Q). The $2A\beta_1 2A\gamma_2$ sequence was inserted into this vector using the same protocol as mentioned above (mut.PLCη2-$G\beta_1\gamma_2$). The other two controls used in the experiment were pcDNA3.1 containing the PLCη2 coding sequence (PLCη2) and pcDNA3.1 with no inserted sequence (EV).

3.2.2. Inositol phosphate release assay

To assess inositol phosphate release, COS7 cells (1.5 x 10^7 cells) were transfected with 15 µg of the appropriate plasmid DNA (EV, PLCη2, PLCη2-G$\beta_1\gamma_2$ or PLCη2(H460Q)-G$\beta_1\gamma_2$) by electroporation as described in Chapter 2. Transfection mixture was then mixed with 25 ml of complete DMEM and 1 ml was added to wells of a 12 well plate. The following day medium was changed to serum- and inositol-free DMEM (MP Biomedicals, Illkirch, France) containing 1 µCi/ml myo-D-[^{3}H]inositol (GE Healthcare) and incubated for 24 hours. Cells were then treated with 10 mM LiCl in HEPES buffered DMEM which inhibits inositol monophosphatases and allows for accumulation of inositol phosphates. 1 ml of 10 mM formic acid was then added to each well and incubated at 4^{o}C for 30 mins. 0.5 ml Dowex AG 1-X8 resin (Bio-Rad Laboratories, Inc., Hemel Hempstead, UK) containing 1:1 mixture of resin and water was placed into a small 10 ml tube. The formic acid containing ^{3}H-labelled inositol phosphates was added to this and vortexed for 10 secs. The tubes were left until the resin settled then the supernatant was aspirated. To wash the resin 1 ml of water was added, vortexed and aspirated. The same was performed with 60 mM ammonium formate/5 mM sodium tetraborate (PH 8.6) to further wash the resin. To elute inositol phosphates 1 ml of 1 M ammonium formate/0.1 M formic acid (PH 4.6) was added to the resin and vortexed. Resin was allowed to settle and 800 µl of the supernatant was added to scintillation tubes containing 2.5 ml Optiphase Hisafe 3 (Perkin Elmer) and mixed thoroughly. The amount of ^{3}H-labelled inositol phosphates was then measured via a MicroBeta^2 scintillation counter (PerkinElmer, Waltham, MA, USA).

3.2.3. Permeabilisation of COS7 cells to calcium

The transfected COS7 cells were added to 25 ml of complete DMEM and seeded onto dishes measuring 14 cm in diameter then incubated for 48 hours. The medium was then changed to serum- and inositol-free DMEM as described previously and incubated overnight. Cells were then trypsinised, centrifuged at 1,500 rpm for 3 mins and washed in 50 ml Buffer A, consisting of 145 mM NaCl, 5.6 mM KCl, 5.6 mM glucose, 15 mM HEPES, 0.1 % BSA (pH 7.4). Cells were again subjected to centrifugation and resuspended in 50 ml Buffer B consisting of 20 mM PIPES (K^+ salt), 129 mM glutamate (K^+ salt), 5 mM glucose, 5 mM ATP, 5.31 mM $MgCl_2$, 5 mM EGTA, 10 mM LiCl, 0.1% BSA (pH 6.6). Cells were then counted, centrifuged and resuspended in Buffer B to achieve equal cell density in each group. A custom made device (Guild, 1991) was used to permeabilise 1ml of each cell suspension by subjecting them to 5 electrical discharges of 3 kV/cm^3 at both +ve and –ve polarities. The permeabilised cell suspension (40µl) was then added to 960 µl of Buffer B, consisting of different Ca^{2+}

concentrations as shown in Table 3.1. These were then incubated at 37°C for 2 hours. This was followed by addition of 10 mM formic acid and centrifuged at 5,000 rpm for 3 mins. 800 µl was then added to Dowex AG 1-X8 resin and [^{3}H]inositol phosphate concentration assessed as described previously.

[$CaCl_2$] (mM)	**[$MgCl_2$] (mM)**	**Free [Ca^{2+}] (logM)**
0	5.31	-9
0.020	5.30	-8
0.197	5.30	-7
1.460	5.29	-6
4.050	5.25	-5
5.159	5.10	-4
7.340	4.11	-3

Table 3.1: Concentrations of $CaCl_2$ and $MgCl_2$ used to produce different concentrations of free Ca^{2+} in equilibrium with 5 mM EGTA. Solutions created in accordance with Popovics *et al.* (Popovics et al, 2011)

3.3. Results

3.3.1. $G\beta_1\gamma_2$ activates PLCη2

Studying the interaction of multiple proteins is usually complicated by the requirement to simultaneously transfect multiple expression constructs into cells. Due to the different sizes of genes (and thus vectors) some constructs may be transfected more efficiently than others thereby affecting the result of assays. Viruses use 2A peptide sequences to produce more than one protein from one transcript. Members of the picornavirus family share 18 conserved amino acid residues that cause cleavage between the C-terminal glycine of this 2A sequence and the N-terminal proline of a downstream 2B sequence (de Felipe et al., 2006). Based on this, Professor Martin Ryan (School of Biology, University of St Andrews) developed a co-expression system that makes use of these 2A signal peptides, which allows for expression of multiple genes by transfecting only one vector into cells. Two 2A-like sequences were created to separate gene sequences: RAEGRGSLLTCGDVEENPGP, derived from TaV and QCTNYALLKLAGDVESNPGP derived from ERAV (Donnelly et al., 2001a, Szymczak et al., 2004).

The 2A peptide sequences allow cleavage of the nascent poly-protein into its constituting proteins by causing a pause in translation when the ribosome comes in contact with the 2A sequence. This system is utilised here to create an expression construct that contains DNA corresponding to PLCη2, $G\beta_1$ and $G\gamma_2$ which are connected together by 2A sequences, a schematic diagram of which can be seen in Figure 3.1. All of this assembles into a single open reading frame thereby allowing transcription from a single promoter, which is translated into three protein products that will be expressed in equal quantities (de Felipe et al., 2006). This expression construct was then transfected into COS7 cells which are immortalised kidney cells derived from African green monkey (Gluzman, 1981). These cells are often used in expression studies because of their high transfection rate (Parham et al., 1998). Another advantage of using these cells is that they do not endogenously express PLCη enzymes, making them ideal for identifying effects caused by PLCη enzymes (Stewart et al., 2005). Following transfection by electroporation and consequent expression into these cells, this polyprotein is cleaved into its constituent parts. PLC activity was assessed by ^{3}H-inositol phosphate accumulation. For control purposes an EV (empty vector) construct was used, as well as a construct expressing

only PLCη2 and a construct co-expressing $G\beta_1$, $G\gamma_2$ and a catalytically inactive PLCη2 mutant, separated by the aforementioned 2A sequences (mut.PLCη2+Gβ1γ2).

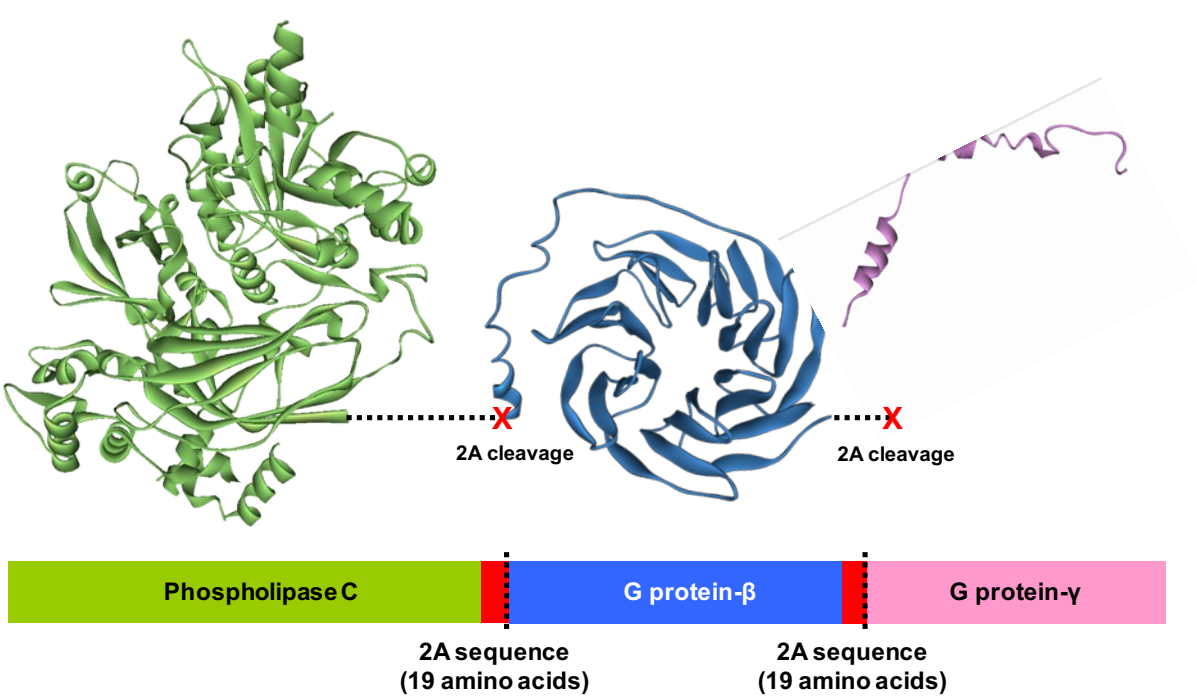

Figure 3.1: Schematic diagram of the 2A co-expression system. Image shows the 3D representation of a PLC enzyme, Gβ and Gγ with relative positions of 2A sequences. Amino acid sequence of the first 2A sequence from TaV: RAEGRGSLLTCGDVEENPG-P (N-terminal proline of the proceeding protein is required for cleavage). Amino acid sequence of the second 2A sequence from ERAV: QCTNYALLKLAGDVESNPG-P. Image produced by Dr Alan Stewart (University of St Andrews, UK).

Figure 3.2 shows results of the inositol phosphate release assay. A signal is seen in the empty vector group, presumably due to the activity of other endogenous PLC isozymes. The PLCη2 group also shows a signal but is not significantly different from the EV group suggesting that the over-expressed PLCη2 is not being activated. This is also the case for the mut.PLCη2+ $G\beta_1\gamma_2$ group which makes sense as this mutant is catalytically inactive since a histidine residue at the catalytic site (residue 460) which is conserved in PLC isozymes was mutated into a glutamine residue using a site directed mutagenesis kit, forming an inactive enzyme. The PLCη2+$G\beta_1\gamma_2$ group however showed a significantly higher inositol phosphate count compared to the other three groups.

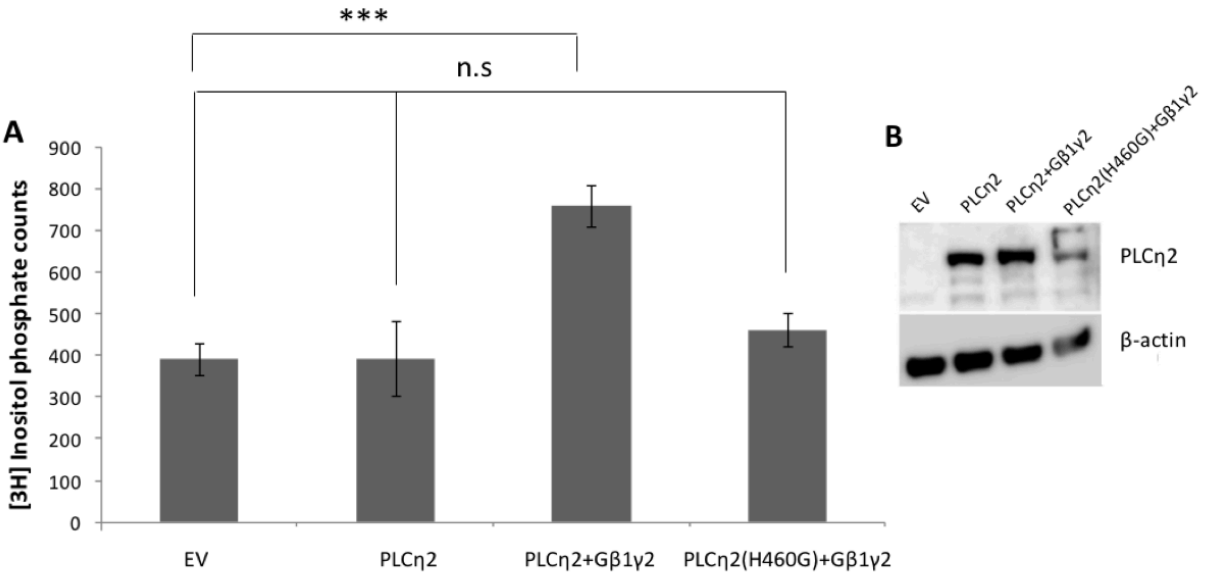

Figure 3.2: A PtdIns(4,5)P_2 hydrolysis following overexpression by electroporation of $G\beta_1\gamma_2$ in Cos7 cells. Endogenous activity of PLCs was assessed by empty vector transfected cells. Cells transfected with PLCη2 and PLCη2(H460G)+$G\beta_1\gamma_2$ showed a similar inositol phosphate count to the EV group. However, cells transfected with PLCη2+ $G\beta_1\gamma_2$ show a significant rise in inositol phosphate turnover. **B** Western blot analysis shows presence of protein in all but the EV transfected group. Band sizes: PLCη2=119 kDa, β-actin= 45 kDa. Other bands are non specific as they also occur in the EV group. The statistical significance between EV and PLCη2+$G\beta_1\gamma_2$ groups is indicated as ***, *P*=0.001. Difference between the other three groups was non-significant (n.s). Statistical analysis is determined by one-way ANOVA. n=3.

In the above experiment, a relatively high degree of cell death occurred due to electroporation of cells and so counts had to be normalised using the number of viable cells for each group. To bypass this cell death and achieve higher counts, the same experiment was conducted but this time transfection was carried out chemically, by lipofectamine (described in section 2). As can be seen from Figure 3.3, higher counts are noted for all groups but the general trend is similar. One difference however is the higher inositol phosphate count observed in the PLCη2(H460G)+$G\beta_1\gamma_2$ group. This may be due to the more efficient overexpression of Gβ1 and Gγ2 which can activate other PLC isozymes.

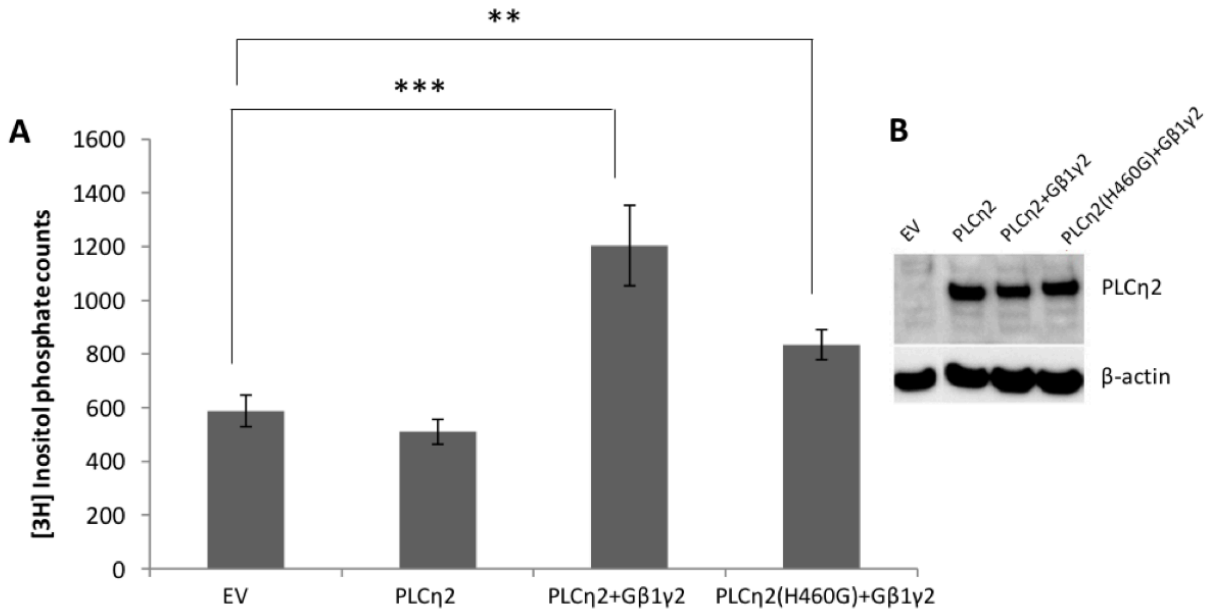

Figure 3.3: PtdIns(4,5)P_2 hydrolysis following overexpression by lipofectamine of Gβ1γ2 in Cos7 cells. Endogenous activity of PLCs was assessed by empty vector transfected cells. Cells transfected with PLCη2 showed a similar inositol phosphate count to the EV with no significant difference between them. Cells transfected with PLCη2+ $G\beta_1\gamma_2$ and PLCη2(H460G)+$G\beta_1\gamma_2$ show a significant rise in inositol phosphate turnover compared to EV. **B** Western blot analysis shows presence of protein in all but EV transfected group. Band sizes: PLCη2=119 kDa, β-actin= 45 kDa. Other bands are non specific as they also occur in the EV group. The statistical significance between EV and PLCη2+Gβ1γ2 groups and EV and PLCη2(H460G)+$G\beta_1\gamma_2$ groupsis indicated as ***, *P*=0.001. and **, P=0.01 respectively. No significant difference was observed between the EV and PLCη2 groups. Statistical analysis is determined by one-way ANOVA. n=3.

These results show that the co-expression system has worked successfully and is a good model for studying activation of proteins by Gβγ dimers. There is an increase in ^{3}H-labelled inositol phosphate turnover in the PLCη2+$G\beta_1\gamma_2$ group which suggests that the overexpressed PLCη2 is being activated by overexpressed $G\beta_1$ and $G\gamma_2$. This is indicative of higher PtdIns(4,5)P_2 hydrolysis in cells transfected with PLCη2, $G\beta_1$ and $G\gamma_2$ as compared to the other groups, suggesting a higher level of PLC activity in this group. These results are in agreement with Zhou *et al.* who have shown that PLCη2 is activated by Gβ1γ2 (Zhou et al., 2005), however the method which has been utilised here to achieve these results is a more efficient one as it bypasses the problem of equally transfecting all three genes into cells.

3.3.2. PLCη1 and PLCη2 are activated by physiological ranges of calcium

As mentioned previously, Hwang *et al.* investigated the sensitivity and activity of PLCη1 towards Ca^{2+} and reported the enzyme's sensitivity between 0.1-1 μM free Ca^{2+} (as indicated by the highest increase in enzyme activity) with maximum activation at 10 μM. This was done by purifying PLCη1 and investigating its activity in buffers containing different concentrations of Ca^{2+} (Hwang et al., 2005). Nakahara *et al.* showed sensitivity of PLCη2 between 0.01-0.1 μM free Ca^{2+} and maximum activity at 1 μM (Nakahara et al., 2005). Popovics *et al.* also investigated the level of PtdIns(4,5)P_2 hydrolysis caused by PLCη2 in the presence of different Ca^{2+} concentrations, showing sensitivity of PLCη2 between 0.1-1 μM free Ca^{2+} with maximum activation at 10 μM (Popovics et al., 2011). These results are not in agreement but it seems that the experimental conditions used by Popovics *et al.* is a better approach since they carried out their experiments in a cellular environment whereas Nakahara *et al.* conducted their experiments on purified recombinant protein *in vitro*. Experiments here were therefore performed according to the method of Popovics *et al*. to investigate Ca^{2+} induced activation of PLCη1 in permeabilised transfected COS7 cells. PLCη2 activation by Ca^{2+} was also investigated as a positive control.

In this experiment, expression vectors containing PLCη1 or PLCη2 were transfected into COS7 cells by electroporation. These cells were subsequently permeabilised and incubated with different concentrations of Ca^{2+} (10-fold dilutions from 10^{-3} to 10^{-9} M Ca^{2+}) for two hours. An inositol phosphate release assay was then performed by measuring [^{3}H]inositol phosphate accumulation in cells. For experimental control, EV transfected cells were used. Results from the Figure 3.4 shows a very similar activation pattern for PLCη1 and PLCη2 as both are sensitive to, and show highest rise in activity between 0.1-1 μM free Ca^{2+} with both exhibiting maximum activation at 10 μM free Ca^{2+}. Despite the similar trend in activation towards different Ca^{2+} concentrations, a noticeable difference is the higher maximal activation of PLCη2 compared to PLCη1. This however could be due to more efficient transfection and therefore higher expression of PLCη2. For enzyme activity, these results are in accordance with Hwang et al. and Popovics *et al.* (Hwang et al., 2005, Popovics et al., 2011) but differ from that of Nakahara *et al.* (Nakahara et al., 2005) as results here show a maximum activation at 10 μM for both PLCη1 and PLCη2 whereas they reported maximal activation at 1 μM for PLCη2. Another difference is that sensitivity of both PLCη isozymes is between 0.1-1 μM free Ca^{2+} whereas they noted PLCη2 sensitivity to lower concentrations, between 0.01-0.1 μM. From the graph in Figure 3.4, it can also be seen that as Ca^{2+} levels rise beyond 10 μM, enzyme activity

starts to decrease. This could suggest an important inhibitory mechanism which prevents the enzyme from continuous activation. It is worth mentioning however that from previous experiments carried out by Popovics *et al.*, the EV group (which is a measure of endogenous PLC activity) usually shows a rise in activity at 10 μM free Ca^{2+} but here, this rise is noted at 1 μM. Attempts at repeating the experiment however failed because of equipment malfunction.

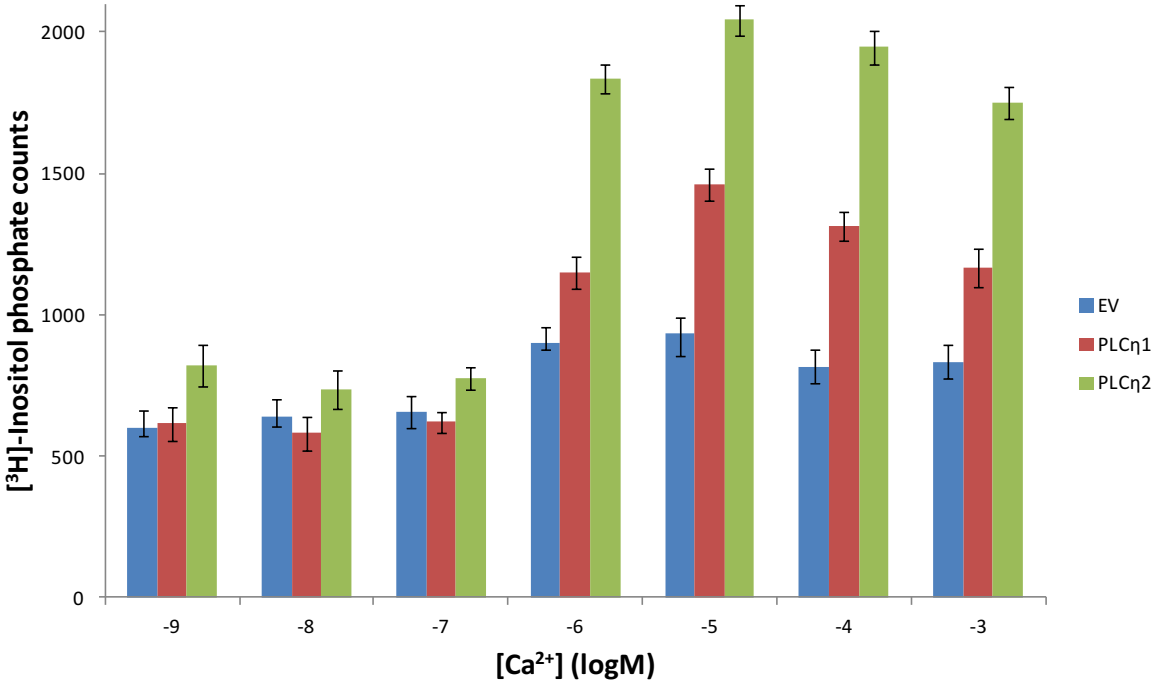

Figure 3.4: PLCη1 and PLCη2 activity at various Ca^{2+} concentrations, in relation to empty vector. Maximum activation for both PLCη1 and PLCη2 isozymes is at 10 μM free Ca^{2+}. n=3.

3.4. Discussion

3.4.1. PLCη2 is activated by $G\beta_1\gamma_2$ as determined by the 2A co-expression system

The main aim of this chapter was to further determine the activation mechanisms for PLCη1 and PLCη2 by improving previous research and experimental models, beginning with the investigation of PLCη2 activation by the $G\beta_1\gamma_2$ heterodimer. This was performed based on the results of Zhou *et al.* who screened a variety of known PLC activators including all heterotrimeric Gα subunits, $G\beta_1\gamma_2$ and small G proteins belonging to the Ras superfamily. Their results showed activation of PLCη2 only by $G\beta_1\gamma_2$ (Zhou et al., 2005). In a subsequent study they co-transfected PLCη2 with a variety of Gβγ heterodimers and noted highest rate of activation following co-transfection of this enzyme with $G\beta_1\gamma_2$ (Zhou et al., 2008). The efficient transfection of multiple genes into cells is crucial to such studies and different

approaches have been used in the past including the use of multiple promoters (Baron et al., 1995), co-infection using multiple viral vectors (Mastakov et al., 2002) and internal ribosomal entry site elements (IRES), (Spires et al.). These methods however often led to unreliable protein expression (Mastakov et al., 2002). For example, IRES elements are nucleotide sequences in mRNA that are often isolated from poliovirus and encephalomyocarditis virus to create constructs that enable initiation of translation in regions other than the 5' end, allowing for more than one ribosome to attach to the mRNA and produce more than one protein from a single mRNA. The problem with this system is that upstream sequences in the open reading frame are transcribed more efficiently than IRES-controlled downstream ones, leading to imbalanced protein expression (Hennecke et al., 2001). IRES elements are large, ~165 amino acids whereas 2A sequences are shorter, ~18 amino acids (de Felipe et al., 2006). Viruses use 2A sequences which are self processing peptide bridges that work by a "skipping" mechanism, resulting in a pause in translation (Donnelly et al., 2001b), thereby producing more than one protein from one transcript by assembling multiple protein coding sequences in a single open reading frame (Ryan et al., 1991). The 2A sequences essentially change the normal translational process of the cell by causing the ribosome to skip the synthesis of a peptide bond thereby preventing continuation of the peptide backbone and so releasing the translated product. Peptide bond formation is skipped between the last amino acid of the 2A sequence and a proline residue, producing an upstream protein that possesess an 18 amino acid tail. After release of the first protein, the ribosome can continue translation, producing a downstream protein that possesses an N-terminal proline. This technique is called CHYSEL (*cis*-acting hydrolase element; Ryan et al., 1999, Donnelly et al., 2001b). By utilising fluorescent reporters and viral 2A sequences, de Felipe *et al.* showed equal quantities of protein following expression into HeLa cells. Furthermore, addition of a post-translational signal peptide which targets one of the fluorescent reporters, enhanced cyan fluorescent protein (ECFP) to the mitochondria resulted in accumulation of ECFP at the mitochondria, addition of a co-translational signal sequence resulted in ECFP translocation to the ER whereas enhanced yellow fluorescent protein (EYFP) containing no post-translational signal sequence remained cytosolic (de Felipe et al., 2006). In accordance, Lorens *et al.* created a polyprotein consisting of two proteins; P21 and Lyt2 that were connected together by a 2A sequence. Because P21 possesses a nuclear localisation signal, it was detected to be present and functional in the nucleus of transfected cells (Lorens et al., 2004). This shows that the poly-protein is cleaved into its separate constituent proteins and that the resulting proteins function independently of one another based on the different signal sequences they possess.

The findings of Zhou *et al.* that $G\beta_1\gamma_2$ can activate PLCη2 (Zhou et al., 2005) were consistent with results here, although this study was performed using a 2A co-expression strategy that utilised 2A cleavage signal peptides. The use of the 2A sequence approach by-passed the requirement of purifying or transfecting multiple proteins with high efficiency. Therefore this method offered an advantage over the method used by Zhou *et al.* who transfected three different constructs simultaneously. Following transfection of appropriate expression vectors by either electroporation or through use of lipofectamine into COS7 cells, an inositol phosphate release assay was performed to measure the rate of PtdIns(4,5)P_2 hydrolysis and therefore activation of PLCη2 by $G\beta_1\gamma_2$. In agreement with Zhou *et al.* results here show activation of PLCη2 by $G\beta_1\gamma_2$. This experiment consisted of three control groups including cells transfected with empty vector to measure the activity of endogenous PLCs, cells transfected with PLCη2 to measure activity of over-expressed PLCη2 and cells transfected with a vector expressing $G\beta_1$, $G\gamma_2$ and a mutated form of PLCη2 that possesses an single amino acid substitution at a key conserved catalytic site residue (histidine to glutamine change at position 460, H460Q) that renders the enzyme inactive (Heinz et al., 1998). By mutating the corresponding His residue in PLCδ1 (His356), Stallings *et al.* showed that this mutation prevents PLCδ1 activity (Stallings et al., 2005). All control groups had similar levels of activation that was approximately 2 folds less than the experimental group. The PLCη2(H460G)+$G\beta_1\gamma_2$ group displayed a slightly higher level of activation in the lipofectamine transfected experiment but this could be due to the more efficient expression of $G\beta_1\gamma_2$ that can activate other PLC isozymes. Several studies have indeed reported activation of PLCβ (1,2 and 3), PLCδ1 and PLCε by $G\beta_1\gamma_2$ (Zhou et al., 2008, Zhou et al., 2005, Wing et al., 2001, Park et al., 1993). Results here are in agreement with studies of Zhou *et al.* and confirm that the 2A co-expression system is a good model for analysing the activation of different proteins by Gβγ dimers. This system can be utilised to investigate activation/interaction of a variety of proteins and a similar system has been used to co-express proteins in cultured cell lines (Lengler et al., 2005), embryonic stem cells (Hasegawa et al., 2007) and neurons (Furler et al., 2001, Tang et al., 2009) as well as in systems neuroscience to determine neural circuits in genetic mouse models by targeting neuronal subtypes using fluorescent proteins (Tang et al., 2009).

3.4.2. PLCη1 and PLCη2 are activated by small rises in intracellular calcium

Another mechanism by which PLCη enzymes may be activated is directly through binding of Ca^{2+}. It is well established that the sperm specific PLCζ is activated by Ca^{2+} as it can sense Ca^{2+} via its functional EF hand domain (Nomikos et al., 2005). Kouchi *et al.* showed the sensitivity of PLCζ between 0.01-0.1 μM free Ca^{2+}, with maximal activity at 1 μM free Ca^{2+}, and 80% of its maximal activity at 0.1 μM free Ca^{2+} (Kouchi et al., 2005). The EF hand domain of PLCδ also has functional importance as it regulates the binding of the enzyme via its PH domain to PtdIns(4,5)P_2 in the plasma membrane. It has also been shown that PLCδ1 is activated by capacitative Ca^{2+} entry (Yamamoto et al., 1999, Allen et al., 1997, Murthy et al., 2004). Nakahara *et al.* revealed that PLCδ1 can be activated between 0.1-1 μM Ca^{2+} and displays maximal activation at 10 μM Ca^{2+}. Nomikos et al. also investigated the Ca^{2+} activation for PLCδ and PLCζ using an in vitro PLC activity assay. Their results were in agreement with that of Kouchi *et al.* and Nakahara *et al.* (Nomikos et al., 2005). To date the only known activators of PLCη2 are $G\beta_1\gamma_2$ and Ca^{2+}, whereas PLCη1 only appears to be activated by Ca^{2+} (Zhou et al., 2008, Kim et al., 2011). Nakahara *et al.* reported that PLCη2 was sensitive to 0.01-0.1 μM free Ca^{2+} and is maximally activated by 1 μM free Ca^{2+} (Nakahara et al., 2005). In their experiment they used immunoprecipitates of PLC enzymes derived from brain lysates to determine PLC activity in a reaction mixture containing [^{3}H]PtdIns(4,5)P_2. Here, experiments were conducted in accordance to those performed by Popovics *et al.* who used a cellular model where COS7 cells were transfected with PLCη constructs, permeabilised and stored in a buffer that mimicked the physiological environment of cells but with different free concentrations of Ca^{2+}. Activity of PLCη1 and PLCη2 was then determined by counting [^{3}H]inositol phosphates using a scintillation counter. This experiment showed a very similar pattern of activation by Ca^{2+} for both PLCη1 and PLCη2. Both of these enzymes showed greatest increase in activity between 0.1-1 μM Ca^{2+} with maximal activation at 10 μM Ca^{2+}. These results are in agreement with results obtained by Hwang et al. and Popovics et al. who respectively reported PLCη1 and PLCη2 sensitivity to 0.1 μM Ca^{2+} with maximal activation at 10 μM (Nakahara et al., 2005, Popovics et al., 2011). These results therefore differ from results of Nakahara et al. (Nakahara et al., 2005) but this could be due to the inefficiency of their results which had a high level of variance. The physiological range of Ca^{2+} within cells is 0.1 μM at rest and up to 1 μM upon activation (Berridge et al., 2003). At the upper limit of this physiological range of cellular Ca^{2+} concentration, PLCη enzymes show a high level of activity which is approximately 70% compared to their maximal activation at 10 μM. The greatest rise in PLCη activity is between

0.1 and 1 μM Ca^{2+} in comparison to PLCδ1, which shows the greatest rise between 1 and 10 μM (as determined by Nomikos *et al.*). This means that PLCη enzymes are ~10-fold more sensitive to Ca^{2+} than PLCδ1. Based on the work of Kouchi *et al.* and Nomikos *et al.* the greatest rise in PLCζ activity was between 0.01 μM and 0.1 μM Ca^{2+} making PLCη enzymes 10-fold less sensitive to Ca^{2+} than PLCζ. PLCζ is 100-fold more sensitive to Ca^{2+} compared with PLCδ1 which is due to its functional EF hand domain (Nomikos et al., 2005). PLCη enzymes however also have a functional EF hand domain but appear to be 10-fold less sensitive to Ca^{2+} (Popovics et al., 2014), reasons for which, are still unknown

This high Ca^{2+} sensitivity of PLCζ is crucial to early embryonic development as it induces crucial Ca^{2+} oscillations that are essential for this process (Swann and Lawrence, 1996, Jones, 1998). It has been established that this rise in Ca^{2+} that occurs as gametes fuse is due to Ca^{2+} release from the ER and occurs mainly through Ins(4,5)P_3Rs. Furthermore, inhibition of PLCζ activity in sperm extracts results in prevention of Ca^{2+} oscillations (Miyazaki et al., 1993). It is therefore clear why PLCζ has such a high Ca^{2+} sensitivity. The high Ca^{2+} sensitivity of PLCη enzymes is also likely to serve essential processes. Results here show that PLCη enzymes have the second highest sensitivity towards Ca^{2+} and because they are found in neuronal cells, there is a strong indication that these enzymes are involved in neuronal Ca^{2+} regulated processes. The greatest rise in activation for PLCη enzymes is between 0.1 μM and 1 μM which is the physiological level of Ca^{2+} within cells. This suggests that PLCη enzymes can become active following small rises in intracellular Ca^{2+} and may even be functional when the cell is at rest. This high sensitivity to Ca^{2+} and punctate distribution in cells led Popovics *et al*. to hypothesise that PLCη2 may be the primarily reacting PLC (Popovics and Stewart, 2012b), meaning that PLCη2 activation may result in activation of other PLC enzymes. This is in accordance with a study performed by Kim *et al.* who showed that PLCη1 amplifies Ca^{2+} signalling and lowers the threshold for PLCβ1 activation by strengthening responses to external stimuli (Kim et al., 2011).

By functioning over the physiological range of Ca^{2+}, PLCη enzymes may be involved in many neuronal processes. One such process is LTP which induces learning at the cellular level. This has two phases; early LTP (E-LTP) which is short lasting and late LTP (L-LTP) which is long lasting and involves gene transcription and protein synthesis. Long term memories are produced when short term alterations in synaptic plasticity (as occurs in E-LTP) are consolidated by gene transcription and protein synthesis into more permanent changes (L-LTP). For this to occur, stimulated synapses must relay information into the cell's nucleus.

This is an unsolved predicament in neuroscience but certain possibilities exist. Signalling molecules that are generated at synapses may diffuse into the nucleus. Examples include translocation of protein kinase A and MAP kinase (that are intermediates of the cAMP pathway and Ras pathway, respectively) into the nucleus following neuronal activity (Bacskai et al., 1993, Martin et al., 1997). Another mechanism is transmission of information into the nucleus by transcription factors (Meberg et al., 1996). However because of the long distances between the dendrites and the nucleus, this process will occur in a long timeframe and it is likely that the messengers will be altered as they travel for long distances (Berridge, 1998). It is therefore likely that another mechanism exists to transfer information into the nucleus. Taking into account the vast ER network that spans throughout neuronal cells, one possibility is that this information is relayed to the nucleus in the form of Ca^{2+} waves along the ER. This takes place in a saltatory manner by Ca^{2+} release through RyRs or $InsP_3Rs$. PLCη enzymes may be a contributing factor in this process by causing rises in $Ins(4,5)P_3$ levels as Ca^{2+} wave propagates along the ER. Popovics *et al.* have previously shown by immuno-labelling, the localisation of PLCη2 in neurites and in the nucleus of differentiated Neuro2A cells (Popovics et al., 2013). It is therefore possible that this enzyme functions throughout the cell, to assist in creating a propagating Ca^{2+} wave throughout the ER system from dendritic spines to the nuclear envelope and is further activated in the nucleus where it aids in essential processes such as activation of transcription factors that are required for LTP. Support for this comes from the Allen Brain Atlas that shows the presence of PLCη2 in the CA1-CA3 region of the hippocampus which are regions of the brain that are related to memory formation and learning.

3.5. Conclusion

An effective method for transfecting multiple genes into cells by utilising viral 2A sequences has been shown here. By using this method the activation of PLCη2 by $G\beta_1\gamma_2$ has been confirmed. This method is therefore useful for investigating activation of proteins by different Gβγ combinations. As performed here, inclusion of mutated/non-functional proteins will be a suitable control for experiments. Furthermore, this system may prove useful in creating transgenic "knock-in" animals that express specific Gβγ combinations and in identifying Gβγ binding partners using 2-hybrid screens since both Gβγ subunits are governed by a single promoter.

It was also shown here that both PLCη1 and PLCη2 are activated by Ca^{2+}, possess the same sensitivity towards Ca^{2+} and are both active within the physiological range of cellular Ca^{2+}

concentration. Activation of these enzymes by nanomolar Ca^{2+} concentrations allows amplification of intracellular Ca^{2+} levels by inducing release through ER stores via $Ins(4,5)P_3Rs$. The released Ca^{2+} can then feed back and further activate PLCη enzymes, creating a continuous loop that increases intracellular Ca^{2+} concentrations which can reduce the threshold for activating other PLC enzymes. Such rises in intracellular Ca^{2+} levels may also regulate many other Ca^{2+} dependent processes. Because PLCη enzymes are expressed in neuronal cells, it is likely that this enzyme is involved in essential Ca^{2+} related neuronal processes such as LTP.

Chapter 4

Localisation of PLCη enzymes and involvement of PLCη2 in neuronal differentiation

4.1. Introduction

Because eukaryotic cells are highly compartmentalised, the localisation of a protein is commonly linked to its function within the cell, therefore identifying the cellular localisation of a protein can aid in understanding its functional role. Until now, the precise cellular localisation of PLCη2 has not been determined. Popovics *et al.* reported a punctuate distribution of green fluorescent protein (GFP)-tagged PLCη2 throughout the cytosol following transfection into heterologous COS7 cells (Popovics et al., 2011) and Nakahara *et al.* reported localisation to the plasma membrane following transfection of full length PLCη2 into HelaS3 cells (Nakahara et al., 2005). This altered distribution is likely to be due to the difference in membrane phospholipid composition of these cells. To achieve a clearer picture of PLCη2 localisation in neuronal cells, Popovics *et al.* used immuno-labelling to determine the localisation of endogenous PLCη2 in Neuro2A cells which is a mouse neuroblastoma cell line derived from mouse neural crest tumour cells (Klebe and Ruddle, 1969). They noted its localisation mainly in the nucleus of these cells (Popovics et al., 2013). A major aim of this chapter is to confirm the nuclear localisation of PLCη2 in neuronal like cells, identify other cell compartments to which it localises and determine its cellular function.

As described in Chapter 1, the PH domains of PLC enzymes are crucial for the cellular localisation and those from different PLCs exhibit different specificities towards different phospholipids (Singh and Murray, 2003). Popovics *et al.* previously addressed the specificity of PLCη enzymes towards phosphoinositides. This was done by purifying glutathione S-transferase (GST)-tagged PH domains from both PLCη1 and PLCη2, which were then subjected to a Förster resonance energy transfer (FRET) assay. In this assay, GST-PH domains bind to anti-GST antibody (that is labelled with Eu chelate) and to its favoured biotinylated phospholipid. Biotinylated phospholipids also bind to streptavidin-tagged allophycocyanin (APC), a light-sensitive protein derived from algae. Following excitation (at 340 nm) the PH domain bound Eu-chelate and the APC come in close proximity of each other, thus producing a FRET signal. The ability of non-labelled phosphoinositides to disrupt the FRET complex was also examined and used to assess the phosphoinositide-binding specificity of PH domain. Those examined were PtdIns(3,4,5)P_3, PtdIns(4,5)P_2, PtdIns(3,4)P_2, PtdIns(3)P and PtdIns(4)P. Collectively, these experiments revealed that the PH domains from both PLCη1 and PLCη2 bound PtdIns(3,4,5)P_3 with highest affinity and to a lesser extent, PtdIns(4,5)P_2 (Gray et al., 2003, Popovics et a., 2011). This suggests that the cellular localisation of PLCη enzymes and their cellular functioning may be governed by the presence of PtdIns(3,4,5)P_3 in

cellular compartments. As PLCη2 is expressed in neurons (Nakahara et al., 2005) its localisation, and therefore function may be governed by PtdIns(3,4,5)P_3 in these cells.

It is well established that PLCη2 is expressed in neuronal cells and is activated by small rises in intracellular Ca^{2+} (Nakahara et al., 2005). This property indicates that PLCη2 regulates certain processes within neurons. Nakahara *et al.* showed a correlation between PLCη2 levels and postnatal development. They reported an increase in PLCη2 expression as the mouse brain develops, with low expression at birth but a gradual increase and maximum expression at week four (Nakahara et al., 2005). Elevation in PLCη2 expression levels during intrauterine development have not been addressed but it is quite likely that this is also the case in prenatal development. These results point towards a functional role for PLCη2 in neuronal differentiation or maturation.

Neuro2A cells have been shown to be a suitable model for studying differentiation, whereby neurite growth may be stimulated by the addition of retinoic acid (RA). RA is a derivative of vitamin A required for neuronal formation and normal embryonic development by regulating gene expression following binding to the nuclear receptor, retinoic acid receptor (RAR). Upon activation, RAR heterodimerises with retinoid X receptor (RXR), thereby allowing binding to promoters (Lane and Bailey, 2005). Popovics *et al.* revealed that PLCη2 expression gradually increases in Neuro2A cells over a 4-day period following stimulation with RA (Popovics et al., 2013). Using an shRNA-mediated approach, a knock-down cell line was created that exhibited a 67% reduction in PLCη2 expression at the protein level (PLCη2 KD cells). Following treatment with RA, these cells displayed a 60% reduction in neurite growth compared non-targetted shRNA to control cells (ShRNA control, Popovics et al., 2013), thereby demonstrating the requirement of PLCη2 in the differentiation process.

To gain a better understanding as to the mechanism by which PLCη2 may influence neurite outgrowth, Popovics *et al.* carried out a bacterial two-hybrid screen, a technique that allows for identification of protein-protein interactions. The C-terminal domain of PLCη2 consists of many proline residues and is believed to be a site of interaction for other proteins (Stewart et al., 2005). They cloned the C-terminal region of PLCη2 and a pancreas cDNA library into "bait" and "target" plasmids respectively, which were then co-transfected into E-coli reporter cells. Upon interaction of the C-terminal domain with proteins encoded by the "target" vector, His3 and Aad3 genes are expressed in reporter E-coli cells that allow colonies to form on agar plates containing 3-aminotriazole and streptomycin. Upon sequencing of "target" vectors in

growing colonies, one was found to encode residues 519-647 of LIMK-1 which corresponds to its C-terminal region (Popovics et al., 2013). PLCη2 and LIMK-1 are present in growing neurites and nucleus of Neuro2A cells, showing a high degree of co-localisation as determined by immuno-labelling (Popovics et al., 2013). In this study, the authors also showed phosphorylation of LIMK-1 after a two day differentiation period with RA.

LIMK-1 is a serine protein kinase that primarily functions downstream of Rho GTPases to phosphorylate cofilin family proteins which include cofilin-1, cofilin-2 and destrin. These proteins encourage actin depolymerisation and severing of actin filaments in outgrowing neurites. Following phosphorylation, cofilin family proteins are inactivated thereby allowing actin assembly and formation of elongated neurites (Endo et al., 2007, Yang et al., 1998). Although LIMK-1 is a known player in neuronal differentiation and that it was identified in the aforementioned two-hybrid screen as a putative binding partner of PLCη2, direct interaction of the two proteins within a cellular context has yet to be confirmed.

The aims of this chapter are to confirm the binding specificity of GFP-tagged PLCη2 PH domain to PtdIns(3,4,5)P_3 in a cellular environment. In addition, the precise subcellular localisation of PLCη2 will be determined using immuno-electron microscopy and the intracellular localisation of PLCη1 will be determined by immuno-cytochemistry. Interaction of PLCη2 with LIMK-1 will be assessed in differentiated Neuro2A cells using bimolecular fluorescence complementation and through use of a proximity ligand assay. Other proteins potentially involved in neuronal differentiation will be identified using 2D-gel electrophoresis. This will provide a clearer understanding of the signalling pathways that are involved in neuronal differentiation/neuritogenesis. Finally, it will be determined whether the high Ca^{2+} sensing ability of PLCη2 contributes to its role in neurite growth.

4.2. Materials and methods

4.2.1. Molecular cloning: creating GFP-tagged PLCη2 PH domains and pBiFC vectors

All PCR protocols are mentioned in Chapter 2. Primers relating to this chapter are listed in Table 4.1. DNA sequence corresponding to the PH domain of PLCη2 was initially amplified by Taq polymerase. This was done using the TA cloning method. Taq polymerase has terminal transferase activity which enables it to add a single deoxyadenosine to the 3' end of a double stranded PCR product. The resulting DNA was then run on an agarose gel, excised using a

clean blade and gel purified as described previously. The purified PH domain DNA sequence was then inserted by ligation into pcDNA3.1/NT-GFP-TOPO vector (Life Technologies) which consists of overhanging 3′ deoxythymidine residues. Purified DNA (1 µl) was mixed with the ligation mixture (containing 1 µl salt solution, 1 µl vector (10 ng) and 2 µl sterile water) and incubated for 30 mins at RT. This enables incorporation of PCR products into the vector by joining to the overhanging 3′ deoxythymidine residues. PLCδ1 PH domain which was conjugated to mCherry using the pmCherry-C1 vector (Clonetech, Saint-Germain-en-Laye, France) was kindly supplied by Dr. Alexander Gray (College of Life Sciences, University of Dundee, UK).

pBiFC-VC155 and pBiFC-VN173 vectors were acquired from Addgene (Cambridge MA, USA). These vectors contain partial sequences of a yellow fluorescent protein (YFP) called Venus: residues 155-238 and 1-172, respectively. Both vectors were transformed into competent E-coli cells then isolated using Isolate plasmid Miniprep kit (Bioline, London, UK), as described previously.

pcDNA3.1 expressing the coding sequence of mouse PLCη2 (residue 75-1238) was used as a template for amplification of PLCη2. A vector containing the complete coding sequence of human LIMK-1 was used as a template for LIMK-1 amplification. This was obtained from Prof. Michael Olson (Beatson Institute, Glasgow, UK). The expand long template PCR system (Roche, Burgess Hill, UK) was used to amplify the sequence corresponding to PLCη2 and LIMK-1 which were then run on an agarose gel, excised and gel purified. pBiFC-VC155 and pBiFC-VN173 vectors were digested near the cloning site with SalI and HindIII, respectively. To allow for insertion into pBiFC vectors via In-Fusion HD cloning kit (clontech), forward and reverse primers were designed to have 18 base pair overhanging DNA ends to allow insertion via recombination, according to the manufacturer's instructions. For experimental control, PLCη2 was also inserted into pBiFC-VC155. To identify interaction, 2 µg of pBiFC-VC155-LIMK-1 and pBiFC-VC155-PLCη2 were transfected into Neuro2A cells by electroporation as described in Chapter 2 and seeded onto glass coverslips that were placed into a 6 well plate. The following day, cells were fixed, labelled with Dapi (to label the nucleus) and mounted onto glass slides according to section 4.2.3.

A multiphoton confocal microscope (TCP SP2 system, Leica Microsystems GmbH, Wetzlar, Germany) was used to take images of labelled cells This microscope consisted of a Leica DM

IRE2 inverted microscope and HeNe (633 nm), HeNe (594 nm), Arg (488 nm) and diode (405 nm) excitation lasers.

PLCη2 PH-F	5'-GTAGTGGAGCGATGCATGAGTGC-3'
PLCη2 PH-R	5'-TTAGGCTAGGCTGTCTTCATCGCTG-3'
VN173_PLCη2-F	5'-ACAAAGACGATGACGACAAGCTTATGCCTGGTCCCCAGCGCTC-3'
VN173_PLCη2-R	5'-AATTCGCGGCCGCAAGCTTATCCCTAACGGTGGAGAACATGGG-3'
VC155_LIMK-1-F	5'-ATGGAGGCCCGAATTCGGTCGACATGGGAGAGGAAGGAAGCGAGTTG-3'
VC155_LIMK-1-R	5'-TCGAGAGATCTCGGTCGACGTCGGGGACCTCAGGGTGG-3'
VC155_PLCη2-F	5'-ATGGAGGCCCGAATTCGGTCGACATGCCTGGTCCCCAGCCGTC-3'
VC155_PLCη2 –F	5'-TCGAGAGATCTCGGTCGACATCCCTAACGGTGGAGAACATGGG-3'

Table 4.1: Primer sequences used in PCR reactions in Chapter 4. F: forward, R: reverse

4.2.2. Immuno-electron microscopy (EM)

ShRNA control and PLCη2 KD Neuro2A cells were previously created by Popovics *et al.* by transfecting Neuro2A cells with a vector encoding a non-target shRNA and a vector encoding shRNA that targeted PLCη2 expression, respectively (Popovics et al., 2013). These cells were grown in a T-75 flask and left to grow to full confluency. Cells were then fixed with a mixture of 4% *p*-formaldehyde, 0.05% glutaraldehyde, 0.2 M PIPES, pH 7.2 for 15 mins at room temperature. Following incubation, cells were scraped using a cell scraper and collected in a 1.5 ml eppendorf tube. Tubes were then centrifuged at 1,000 x g for 5 mins, leading to formation of a cell pellet which was incubated in 2.3 M sucrose in PBS (cryoprotectant) and incubated at 4°C overnight. Small blocks were cut from the pellet and placed onto nails which were plunge frozen in liquid N_2. A cryomicrotome (Leica EM FC7; Vienna, Austria) was then used to cut a ribbon of cell sections with 80 nm thickness at -100°C. These ribbons were then picked up using a 1:1 mixture of 2.1 M sucrose:2% (w/v) methyl cellulose and placed onto pioloform-coated EM copper grids (Agar Scientific, Stansted, UK), then stored at 4°C overnight. Grids were washed three times for 5 mins by pipetting drops of ice-Cold PBS then once for 1 min with PBS at RT. Grids were then incubated in 0.5% fish skin gelatin (FSG, Sigma Aldrich) in PBS for 10 mins. Antibody labelling was performed by incubating a custom polyclonal rabbit antibody raised commercially against a short peptide of PLCη2

(SKVEEDVEAGEDSGVSRQN; EZBiolab, Westfield, IN, USA, 1:400 dilution) for 30 mins at RT. Three PBS washes were then carried out for 5 mins at RT. Next, grids were incubated with 10 nM protein A-gold in FSG (1:50 mixture) for 20 mins, followed by Six PBS washes for 5 mins at RT. Ten, 1 min washes were carried out using ddH_2O at RT to remove any salts and Finally, grids were incubated for 10 mins using ice-cold mixture of 2% (w/v) methylcellulose:3% (w/v) uranyl acetate for contrasting. For quantification, labelled sections were visualised at a nominal magnification of 5,000 x using a JEOL 1200 EX transmission electron microscope, operated at 80 KV. Images were taken with an Orius 200 digital camera (Gatan, Abingdon, UK) and analysed by a systematic uniform random (SUR) sampling method. Sections of ShRNA control and PLCη2 KD Neuro2A cells were always prepared in parallel.

4.2.3. Immunocytochemistry-PLCη1 localisation in Neuro2A cells

Neuro2A Cells were grown overnight on coverslips that were placed in a 6 well plate. The following day, cells were fixed with 4% *p*-formaldehyde in PBS for 10 mins, followed by three, 5 min washes with PBS. Cells were then blocked using 10% FBS in PBS for 1 hour and permeabilised with 0.2% Triton-X. PLCη1 antibody (purchased from Abcam, Cambridge, UK, 1:50 dilution) was diluted in antibody diluent made up of 5% FBS in PBS and used to label endogenous PLCη1. Cells were incubated with this primary antibody for 1 hour, followed by three PBS washes. Cells were then incubated with secondary antibody (anti-rabbit Dylight 488, Jackson, West Grove, PA, USA) which was diluted in the antibody diluent (1:300) for 1 hour, followed by three PBS washes. This was followed by incubation with 2.1% citrate buffer containing 0.5% Tween-20 in PBS for 5 mins. Finally cells were incubated with 11.8% citrate in PBS containing DAPI (1:1000) for 5 mins. Glass slides were then mounted onto coverslips using moviol. Images were taken using the TCP SP2 confocal system.

4.2.4. Establishment of stable cell lines

To create stable cell lines, transfection by electroporation was performed as described in Chapter 2. Cells were then transfected with constructs expressing EV, PLCη2, an EF-hand mutant (D256A) and a catalytically inactive mutant (H460Q, all created by Dr Petra Popovics). Following transfection, cells were seeded onto 5 cm dishes and incubated for 48 hours. The media was then replaced with complete EMEM containing 500 μg/ml G418 (Thermo fisher scientific) and replaced every other day until separate colonies formed. Cloning rings (Sigma-

Aldrich) were used to isolate colonies which were trypsinised and transferred into wells of a 6 well plate, then into T-75. Transfection efficiency was determined by qPCR as described in Chapter 2.

4.2.5. Duolink proximity ligand assay (PLA)

Ligand proximity assays were performed using the Duolink proximity ligand assay system (Sigma-Aldrich). Two sets of experiments were performed; the first with ShRNA control and PLCη2 KD Neuro2A cells and the second, with differentiated and undifferentiated Neuro2A cells grown for 4 days in the presence and absence of 20 μM retinoic acid, respectively. Cells were seeded onto coverslips at a low density (100 cells/mm^2) and left to grow overnight in a 6 well plate. Coverslips were then glued onto glass slides for easier handling. Cells were fixed using 4% *p*-formaldehyde in PBS for 10 min followed by three washes with PBS (all washes performed in coplin staining jar). Samples were then incubated with the provided blocking solution for 30 min (all incubations performed in a preheated humidity chamber at 37^{o}C). For specific visualisation of the PLCη2-LIMK-1 interaction in cells, samples were incubated for 1 hour with a custom rabbit anti-PLCη2 antibody (as described above; 1:100 dilution) and a mouse polyclonal anti-LIMK-1 antibody (Abcam, Cambridge, UK; 1:100 dilution in provided antibody diluent), both of which were diluted in the provided antibody diluent. This was followed by two, five minute wash periods using the provided wash buffer A. Samples were then incubated for 1 hour with PLA probes that recognise rabbit and mouse antibodies then followed by two, 5 min wash periods using wash buffer A. Cells were incubated with the provided ligase (1:5 dilution) for 30 mins which resulted in fusion of PLA probes. Two, 2 min washes were then performed with wash buffer A and finally, cells were incubated with the provided polymerase for 100 min which resulted in amplification of the fluorescent signal, allowing visualisation. Following two, 10 min washes with wash buffer B, samples were mounted with cover slips using the provided mounting media with DAPI. Samples were then analysed using the Leica TCS SP8 confocal microscope with a 63 x objective (Leica Microsystems, Heidelberg, Germany).

4.2.6. 2D-gel electrophoresis

2D-gel electrophoresis was performed using the ZOOM IPGRunner system (Life-technologies, Carlsbad, CA, USA). Two sets of experiments were performed: the first set comparing

differentiated (4 day RA-treated) and undifferentiated Neuro2A cells and the second set comparing differentiated ShRNA control and PLCη2 KD cells (created by Popovics et. al., 2013). Cells were grown to full confluency in a T-75 flask then scraped using a cell scraper and collected in 1 ml of rehydration buffer (8 M urea, 2% detergent, 20 mM DTT, 0.2% ampholytes). The collected protein was homogenised by pipetting then sonicated six times (20 s each time with 60 s cooling down period in between) with a QSonica sonicator (Qsonica LLC, Newton, MA, USA), at an amplitude of 60%. Samples were centrifuged at 12,000 x g for 30 min, the supernatant was placed into new tubes and centrifugation was repeated to remove residual cell debris. ZOOM immobilised pH gradient (IPG) strips (pH range: 3-10) were placed into a ZOOM IPGRunner cassette then incubated with 140 µl of each protein sample for 1 hour. ZOOM IPGRunner cassette was then placed into the ZOOM IPGRunner. Isoelectric focusing was performed using 250 V for one hour, then 500 V for 1 hour, followed by 1,200 V for 48 hours. The cassette was then loaded with 5 ml of NuPAGE LDS sample buffer containing 5% DTT and incubated at RT for 15 minutes on a rotary shaker. LDS sample buffer was decanted and replaced with 125 mM alkylating solution (23.2 mg of iodoacetamide/ 1 ml 1× NuPAGE LDS sample buffer) then incubated at RT for 15 mins on a rotary shaker. ZOOM strips were then removed from the cassette and placed into a NuPAGE Novex 4-12% Bis-Tris ZOOM gel to perform the second dimensions of separation. This was performed using sodium dodecyl sulphate-polyacrylamide gel electrophoresis (SDS-PAGE) at 200 V for 1 hour. Protein spots were visualised using coomassie blue and bands were identified by mass spectrometry.

4.2.7. Mass spectrometry

Bands of interest were excised from an SDS-PAGE gel and sent to the St-Andrews mass spectrometry unit where gel bands were cut into $1mm^3$ fragments then subjected to digestion, using a ProGest Investigator in-gel digestion robot (Genomic Solutions). Briefly, gel pieces were subjected to de-staining and washing with acetonitrile. Gel pieces were then reduced and alkalylated to irreversibly break up disulphide bonds resulting in an unfolded protein which was then digested with thermolysin at 55^oC to obtain short fragments of the protein. Formic acid (10%) was used to extract peptides. Nano-scale liquid chromatographic tandem mass spectrometry (nLC-MS/MS) was used to identify proteins. Solution containing digested peptides (0.5 µl) was subjected to matrix-assisted laser desorption/ionization mass spectrometry (nLC-MALDI-MS/MS) by using a 4800 MALDI time of flight (TOF) Analyzer

(ABSciex) equipped with a Nd:YAG355 nm laser (calibrated using a mixture of peptides). MS/MS data was analysed using GPS explorer (ABSciex) to interface with the Mascot 2.4 search engine (Matrix science). Parameters selected were: no species restriction, trypsin as the cleavage enzyme and carbamidomethyl modification of cysteines.

Protein spots that could not be identified by nLC-MALDI-MS/MS were subjected to electrospray ionisation mass spectrometry (nLC-ESI-MS/MS). Briefly, proteins were concentrated using SpeedVac (ThermoSavant) and separated on a C18 column (ThermoFisher Scientific). Peptides were then eluted using acetonitrile containing 0.1% formic acid. This was then subjected to a TripleTOF 5600 electrospray tandem mass spectrometer (ABSciex). MS/MS data was analysed using the Mascot algorithm (Matrix Science) against the NCBInr database (Aug 2013). Parameters selected were: no species restriction, trypsin as the cleavage enzyme, carbamidomethyl modification of cycteins, methionine oxidation, deamination of glutamines and aspargines

4.3. Results

4.3.1. PH-PLCη2 localisation relative to PtdIns(3,4,5)P_3 and PtdIns(4,5)P_2 distribution

As mentioned previously, Popovics *et al.* reported binding of PH-PLCη2 to only two phospholipids based on their FRET analysis, showing highest binding affinity of PH-PLCη2 to PtdIns(3,4,5)P_3, and to a lower extent, PtdIns(4,5)P_2 with EC_{50} value 0.7611 pmol and 3.1131 pmol, respectively (Popovics et al., 2013). This however was performed in an artificially created environment. To confirm the PtdIns(3,4,5)P_3 specificity of PH-PLCη2, the PH domain of PLCη2 was expressed into a GFP tagged expression vector (GFP-PH-PLCη2), which was then transfected into Neuro2A cells to enable identification of PLCη2 interaction with membrane phospholipids. For a clearer understanding of its relative localisation, the PH domain of PLCδ1 (mCherry-PH-PLCδ1) which is tagged with the mCherry fluorophore and is specific for PtdIns(4,5)P_2 (Watt et al., 2002) was co-transfected into Neuro2A cells. Anti-PtdIns(3,4,5)P_3 antibody was also used to identify the PtdIns(3,4,5)P_3 distribution in these cells.

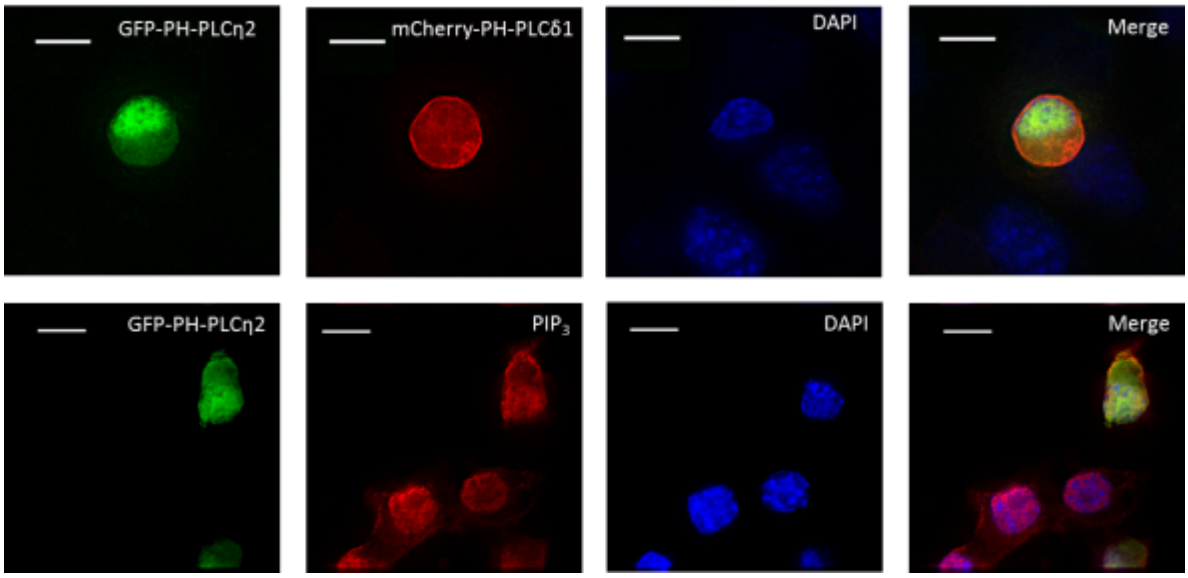

Figure 4.1 Co-localisation of GFP-PH-PLCη2 with PtdIns(4,5)P_2 and PtdIns(3,4,5)P_3 in Neuro2A cells. No co-localisation occurs in cells that were co-transfected with GFP-PH-PLCη2 and mCherry-PH-PLCδ1 (red, 0.0953, S.E.M.=0.033555, n=2, Pearson coefficient). Cells transfected with GFP-PH-PLCη2 and labelled with PtdIns(3,4,5)P3 antibody (red) however showed a high degree of co-localisation in the nucleus (0.7475, S.E.M=0.0355, n=2, Pearson coefficient). Images are representative and were taken from a deconvoluted Z-stack. Scale bars measure 10 µm. GFP tagged PLCη2 PH domain construct was created by the author of the thesis and experiment performed by Dr Petra Popovics. Image taken from Popovics et al., 2013.

Results from Figure 4.1 show a nuclear localisation for the PH-PLCη2. PtdIns(3,4,5)P_3 is also predominantly present in the nucleus and has a high degree of co-localisation with PH- PLCη2 (Pearson coefficient: 0.7475, S.E.M=0.0355, n=2). PH-PLCδ1 on the other hand is highly abundant in the plasma membrane and does not show co-locaisation with PH-PLCη2 (Pearson coefficient: 0.0953, S.E.M.=0.033555, n=2). These results are in agreement with FRET data carried out by Popovics *et al.* (Popovics et al., 2013). Whereas they showed the high binding specificity of PLCη2 with PtdIns(3,4,5)P_3 in an artificial setting, these results show co-localisation in a cellular context.

4.3.2. The subcellular localisation of PLCη2 is predominantly nuclear

To determine the precise subcelllular localisation of PLCη2, immuno-electron microscopy was utilised which allows visualisation with high resolution, the binding of an antibody to its antigen across all of the cell's organelles and compartments, thereby giving a clear understanding of a protein's localisation within the cell. PLCη2 KD cells were used as

experimental control because they expressed approximately 67% lower PLCη2 expression. Because specific binding will be lower in these cells, a comparison can be made between the signal in ShRNA control cells and PLCη2 KD cells to determine specific labelling. Thin (80 nm) sections of non-targeted shRNA control and PLCη2KD Neuro2A cells were prepared and labelled as described in the methods section, then analysed using a systematic uniform random (SUR) sampling method where the whole ribbon of cut cells was scanned in a random manner. Results are shown in Figure 4.2A. Raw gold counts however represent a mixture of specific and unspecific binding. Following quantification of gold particles, a series of calculations were performed to assess specific binding according to calculations of Lucocq *et al*. to correct for unspecific binding (Lucocq and Gawden-Bone, 2010), as shown in Figure 4.2B.

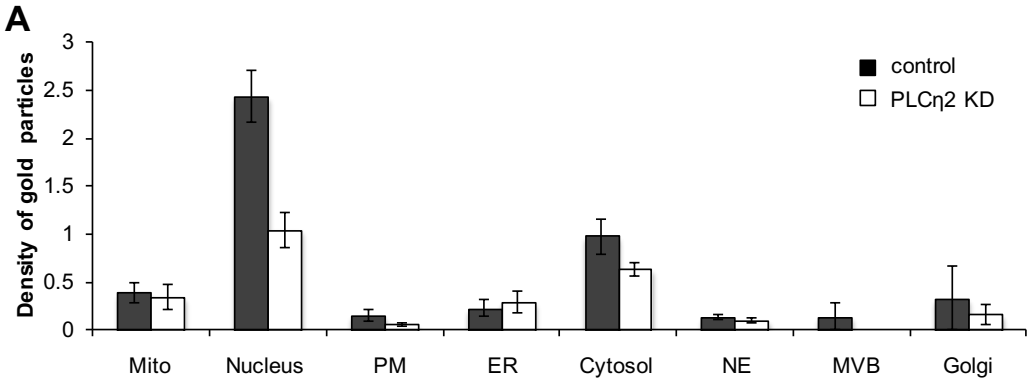

B

	Specific density (SD)	Fraction Specific (FS)	Total raw gold	Specific gold (SG)	% Specific
Mitochondria	0.16	0.48	25.33	9.59	8.82
Nucleus	1.74	0.72	102.00	71.60	54.38
PM	0.12	0.75	9.67	7.15	5.47
ER	0.04	0.21	19.67	1.23	1.71
Cytosol	0.56	0.57	62.67	35.77	27.38
NE	0.07	0.53	5.00	2.29	2.25
MVB	0.14	0.33	1.00	0.00	0.00
Golgi	0.22	0.22	0.33	0.00	0.00

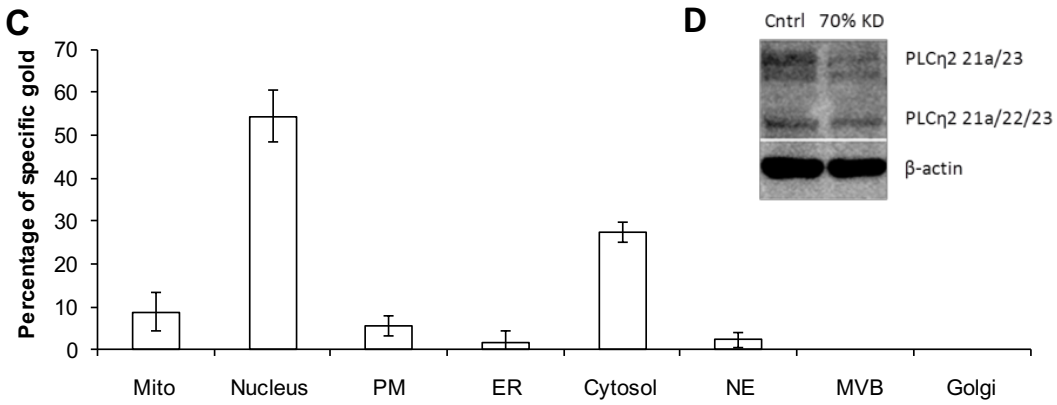

Figure 4.2: Precise localisation of PLCη2 as determined by immune-EM. **A** Density of gold particles across organelles in control and KD cells. A set reference point was used to scan the entire ribbon of cut cells. The total number of gold particles per organelle was then divided by the number of times the organelle was intercepted by the reference point. **B** Table of calculations used to achieve specific distribution of gold particles in each organelle. Results are expressed as average values across 3 experiments. The average density of each organelle in KD cells was subtracted from that of the control cells to attain the Specific density (SD). This was then divided by the average density in control cells (as calculated in graph 1A) to obtain the fraction. FS was then multiplied by total number of gold particles counted in each organelle of control cells to obtain the specific gold (SG). This was then divided by the total SG across all organelles and multiplied by 100 to establish the specific percentage of gold particles, representing PLCη2 across organelles. **C** Graph showing percentage of specific gold in all organelles as determined in table 1B. **D** Western blot showing expression of PLCη2 variants in control and KD cells (top band= 164.3 kDa and bottom band= 119.2 kDa. B-actin= 45 kDa). Abbreviations: ER, Endoplasmic reticulum. Golgi, golgi apparatus. Mito, mitochondria. MVB, multi-vesicular body. PM, plasma membrane. NE, nuclear envelope.

As shown in the representative micrographs in Figure 4.3, the greatest proportion of gold particles, representing PLCη2 localisation, were found in the nucleus (54.4±6.1%). This is in accordance with the localisation of the GFP-PH-PLCη2 (as shown in Figure 4.1) and immuno-labelling of endogenous PLCη2 as performed by Popovics *et al.* (Popovics et al., 2013). A high level of labelling was also observed in the cytosol (27.4±2.4%). Other cellular compartments where the presence of PLCη2 was identified, albeit at much lower levels, are the mitochondria (8.8±4.6%), plasma membrane (5.5±2.3%) and nuclear envelope (2.2±1.7%). The ER (1.7±2.6%) also showed localisation but this was only the case in one out of three independent experiments. Generally however, both control and PLCη2KD cells showed a similar level of localisation in the ER. The Golgi apparatus and multi-vesicular bodies failed to show any nuclear staining. An interesting finding from this experiment is the presence of PLCη2 in darker regions of the nucleus which suggests that it binds to heterochromatin rich areas.

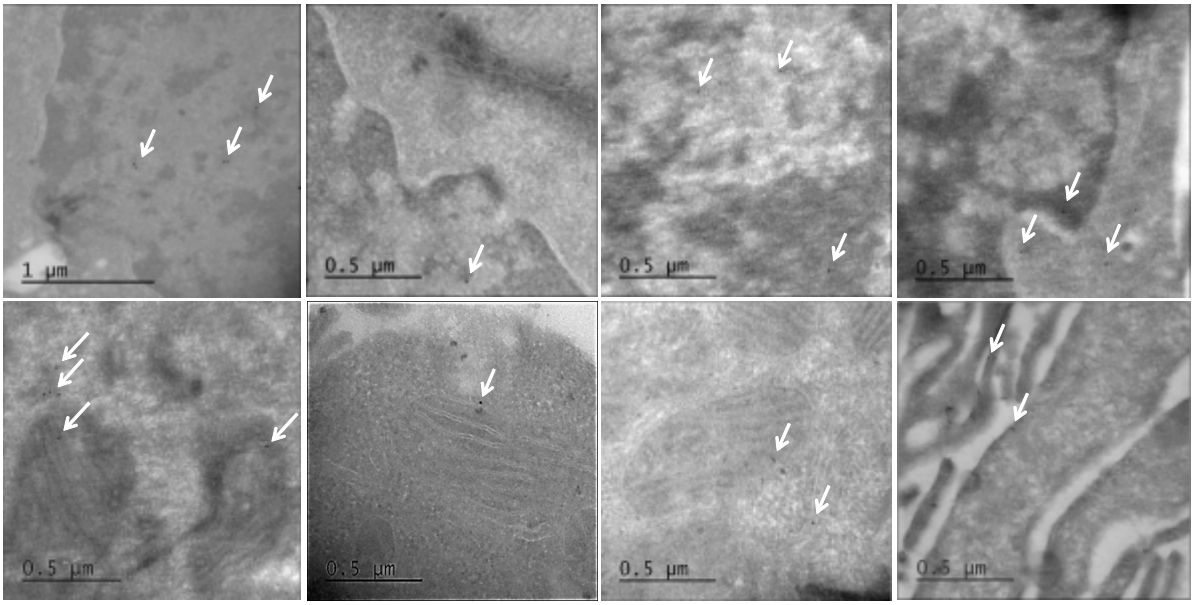

Figure 4.3: Representative immuno-EM images of PLCη2 localisation in scrambled control Neuro2A cells. Image **A**, **B** and **C** show the localisation of PLCη2 within the nucleus. This localisation is mainly at the darker regions of the nucleus which shows that PLCη2 localises to heterochromatin rich areas. Image **D** shows localisation at the nucleus, nuclear envelope and MVB. Localisation at the mitochondria was seen in all regions; the inner and outer membranes as well as the cristae as shown in Image **E**, **F**, and **G**. Image **G** also shows localisation in the ER but this signal was very low following quantification as the ER signal was very high in 70%KD cells as well. Image **H** shows localisation at the plasma membrane. Arrows point towards protein A gold particles. Images taken using JEOL 1200 EX transmission electron microscope.

4.3.3. PLCη1 localisation differs from PLCη2

As mentioned in the introduction section, FRET analysis studies performed by Popovics *et al.* using GST-labelled PH domains of PLCη1 and PLCη2 showed highest binding affinity towards PtdIns(3,4,5)P_3. Both PLCη1 and PLCη2 PH domains also bound well to PtdIns(4,5)P_2 but exhibited a 3 to 4-fold reduction in affinity relative to PtdIns(3,4,5)P_3 (Popovics et al., 2013). PLCη1 and PLCη2 distribution throughout cells was therefore expected to be similar. In addition to immuno-EM data, previous immuno-labelling studies performed by Popovics *et al.* confirmed a predominantly nuclear localisation for PLCη2, using anti-PLCη2 antibody (Popovics et al., 2013). Here, localisation studies aimed to determine the cellular localisation of PLCη1 in Neuro2A cells to establish whether PLCη1 and PLCη2 are located in the same cellular compartments. In this experiment, Neuro2A cells were seeded onto glass slides, fixed and labelled with anti-PLCη1 antibody, then counterstained with the nuclear marker DAPI.

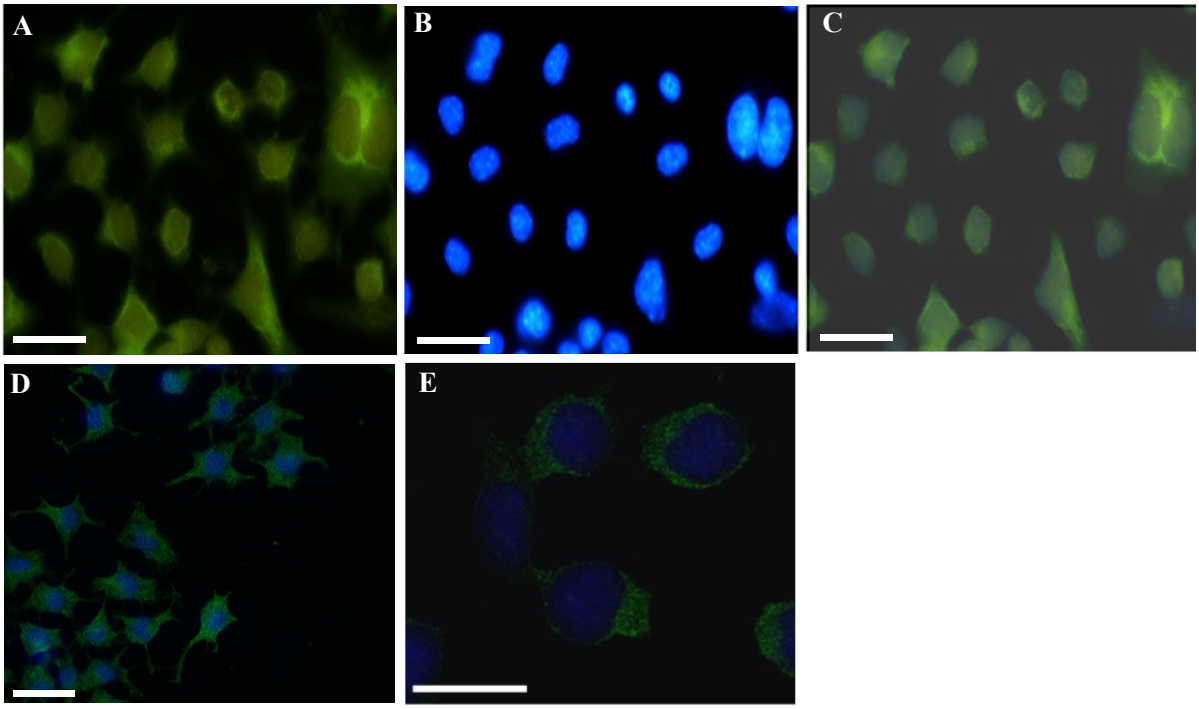

Figure 4.4: Neuro2A cells immunostained with anti-PLCη1 antibody (green) and DAPI (blue). **A**, **B** and **C** show labelling with anti-PLCη1 antibody, DAPI, and merged images respectively, showing a cytoplasmic distribution for PLCη1. Images taken at ×60 magnification. Image **D** and **E** show merged images of the same cells at ×40 and ×100 magnification respectively, again showing PLCη1 localisation in the cytoplasm. Images acquired via Leica confocal microscope (TCP SP2). Scale bars represent 10 µM.

Figure 4.4 shows the localisation of PLCη1 in cytoplasmic regions of these cells. This differs from PLCη2 which is localised in the nucleus of Neuro2A cells where it highly co-localises

with PtdIns(3,4,5)P_3. This result may either indicate that contrary to PH domain FRET data, full length PLCη1 enzyme binds preferentially to other phosphoinositides or that PLCη1 localisation is predominantly controlled by factors other than the binding specificity of the PH domain.

4.3.4. Analysis of PH and C2 domain sequences of PLCη enzymes

The altered distribution between full length PLCη1 and PLCη2 may be due to differences in their PH and C2 domains, both of which aid in membrane binding (Ferguson et al., 1995, Nalefski and Falke, 1996). The C2 domain is the second most common lipid binding domain after the PH domain (Cho and Stahelin, 2006) and the C2 domain of different PLCs have different binding preferences towards different lipids (Ananthanarayanan et al., 2002). Because PLCζ does not possess a PH domain, the C2 domain is required for binding to the plasma membrane (Kouchiet al., 2005). The amino acid sequence of both domains was compared for PLCη1 and PLCη2 to determine the extent of homology between them as shown in Figure 4.5. To identify domain boundaries, the NCBI conserved domain search tool was used. Sequence alignment was then established using the EMBOSS needle sequence alignment tool which aligns sequences using the Needleman-Wunsch algorithm. Results show a high level of sequence homology between PLCη1 and PLCη2 for both PH (86.8%) and C2 (92.8%) domains. Because these two domains are the most important domains in determining membrane binding, this high degree of sequence homology implies that both PLCη isozymes may possess similar phospholipid binding properties and so their altered localisation cannot be explained in terms of PH or C2 domain structure. Ananthanarayanan *et al.* showed that a mutation in the aspartic acid residue at position 861 of the C2 domain (D861N), changes the lipid binding specificity of this domain (Ananthanarayanan et al., 2002). Upon comparison of both sequences, it can be seen that this residue is conserved in both isozymes (Fig. 4.5B). However, other residues yet to be identified are likely to also control lipid-binding specificity in this domain.

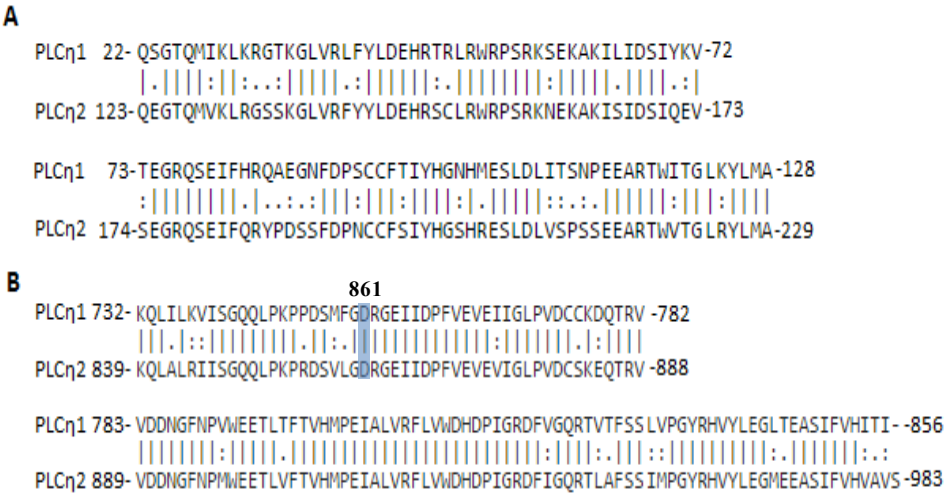

Figure 4.5: Amino acid sequence alignment of PLCη1 and PLCη2 PH and C2 domains. **A** Amino acid sequence comparison of PLCη1 and PLCη2 PH domains showing 86.8% similarity **B** Amino acid sequence comparison of PLCη1 and PLCη2 C2 domains showing 92.8% similarity. The high degree of sequence alignment for both domains indicates that the two PLCη isozymes possess similar phospholipid-binding properties. These domains are conserved across all PLCη isozymes. The biggest variation between PLCη1 and PLCη2 lies in their C-terminal tail region which varies greatly in amino acid composition and length as can be seen from their sequences as shown in Appendix I. Symbols used to express the rate of similarity: "|" identical, ":" high similarity, "." weak similarity. Residue D861 is conserved in both isozymes.

4.3.5. PLCη2 interacts directly with LIMK-1

As previously discussed, Popovics *et al.* identified LIMK-1 as an interaction partner of PLCη2 using a bacterial two-hybrid screen (Popovics et al., 2013). To confirm whether PLCη2 and LIMK-1 interact directly, a biomolecular fluorescence complementation (BiFC) assay was utilised where sequences encoding PLCη2 and LIMK-1 were inserted by recombination into pBiFC-VN173 and pBiFC-VC155 vectors, respectively. These vectors possess partial sequences of a yellow fluorescent protein. Following transfection into COS7 and Neuro2A cells, they were analysed by fluorescent microscopy where fluorescence was expected upon interaction of the two vectors. Cells were transfected with varying amounts of DNA (2 µg, 10 µg and 15 µg) but demonstrated optimal fluorescence complementation using 2 µg.

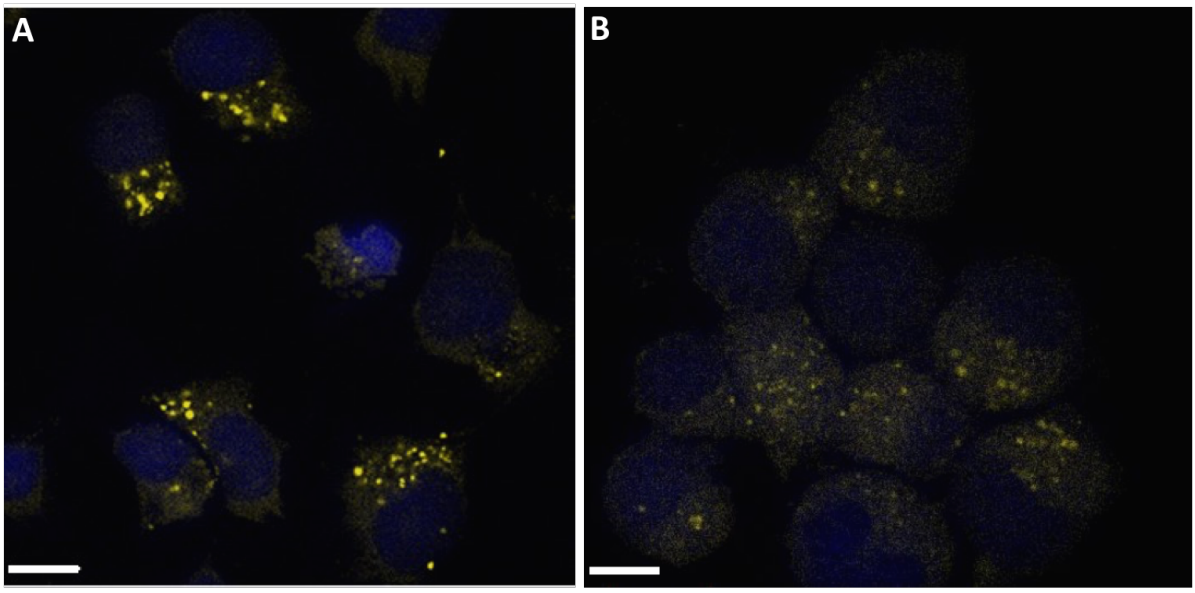

Figure 4.6: PLCη2 and LIMK-1 interaction by BiFC assay. Images showing **A** Cos7 cells and **B** Neuro2A cells following transfection with 2 μg pBiFC-VC155-PLCη2 and pBiFC-VN173-LIMK-1. Yellow fluorescent particles correspond to potential PLCη2-LIMK-1 interactions, nucleus is stained with DAPI and appears blue. Images were taken using a Leica confocal microscope (TCP SP2) at 20 x magnification. Scalebars correspond to 10 μm.

The results (as shown in Figure 4.6) revealed fluorescent spots mainly within the cytoplasmic region of COS7 and Neuro2A cells which indicates potential interaction between PLCη2 and LIMK-1 in this region. As an experimental control, pBiFC-VC155-LIMK-1 and pBiFC-VC155- PLCη2 were transfected into Neuro2A and COS7 cells. Association of these vectors should not give a fluorescent signal because the full sequence required to achieve fluorescence would not be available (half of which is provided by pBiFC-VN173- vector). Fluorescent spots however were also present in these control cells (data not shown) and so this system was not a reliable one for determining PLCη2/ LIMK-1 interaction.

4.3.6. PLCη2 interacts with LIMK-1 primarily in the cytoplasm and growing neurites of differentiated Neuro2A cells

The duolink proximity ligand assay (PLA) system allows for identification of endogenous protein interactions, providing a much better system to determine interaction of two proteins. This system also allows for inclusion of suitable experimental controls in the form of PLCη2 KD and undifferentiated Neuro2A cells. Figure 4.7 shows the principle of how this assay works.

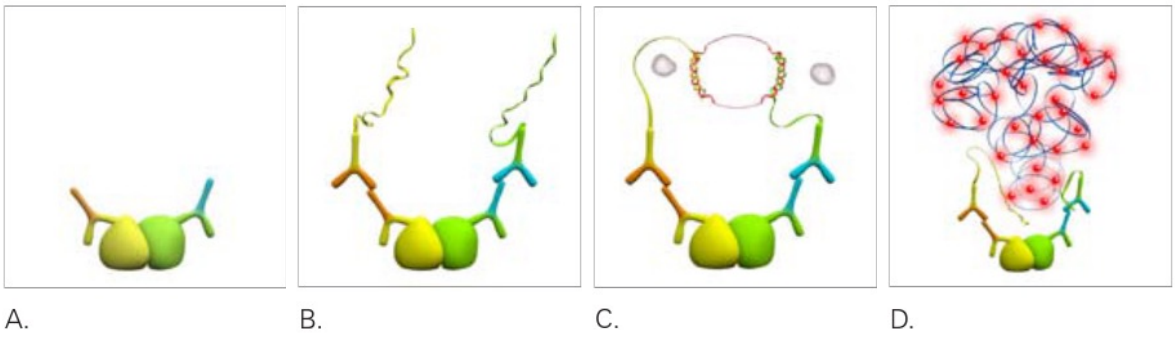

Figure 4.7: Stepwise identification of interacting proteins using the Duolink PLA system. **A** Fixed cells are labelled with primary antibodies that bind to the proteins of interest. **B** Cells are incubated with secondary antibodies that are conjugated with PLA PLUS and MINUS probes (oligonucleotides). **C** Ligation solution consisting of oligonucleotides (depicted in red) is added and if the proteins of interest are in close proximity, oligonucleotides will hybridize to both PLA probes and form a ligated circle. **D** Amplification solution is added consisting of nucleotides, fluorescent oligonucleotides and polymerase. The oligonucleotide bound to one of the PLA probes acts as a primer, allowing for rolling circle amplification using the ligated circle as a template, thus generating a repeat sequence product. Fluorescent oligonucleotides will then hybridize to this product which produces a fluorescent signal. Image obtained from Duolink user manual (www.olnk.com/products/duolink/download/duolink-manuals-and-guidlines on 10/08/2015).

The PLA assay was initially performed with ShRNA control and PLCη2 KD cells to determine the efficiency of the assay. The results of this are shown in Figure 4.8. As can be seen, fluorescent particles are present in both groups but are much more abundant in ShRNA control cells compared to PLCη2 KD cells with the vast majority of particles present in the cytoplasm. Following quantification, an approximately 8-fold higher level was noted in control cells in comparison to 67% KD cells, indicating that the majority of fluorescence is specific.

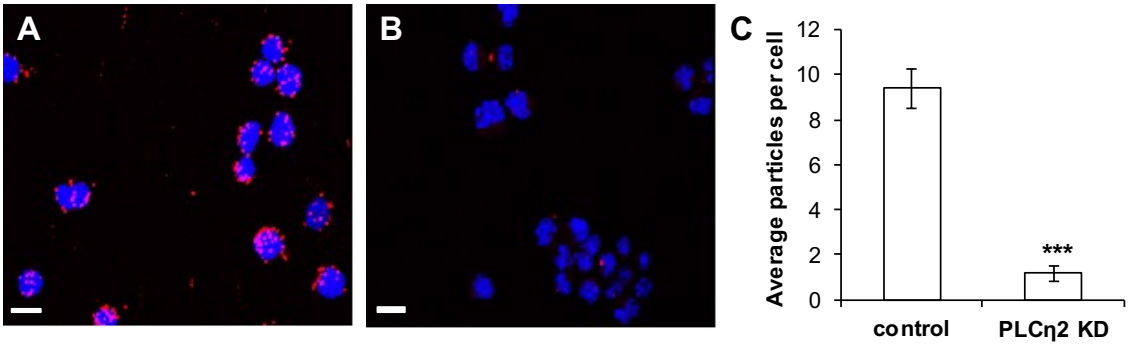

Figure 4.8: PLCη2 and LIMK-1 interacion determined by Duolink PLA assay. **A** and **B** Representative fluorescent images of ShRNA control and PLCη2 KD Neuro2A cells. Red fluorescent particles correspond to PLCη2-LIMK-1 interaction. DAPI-staining of nuclei is shown in blue. **C** Graph showing the average number of fluorescent particles in each cell for control and 67% KD groups. Five micrographs were taken at random for each group. Nuclei and fluorescent particles were counted according to a randomised counting method. Error bars represent coefficient of error between five micrographs. The statistical significance (as determined by unpaired T-test) is indicated as **, $P<0.001$. Scale bars correspond to 15µm. Images taken using the Leica TCS SP8 confocal microscope with a 63× objective.

This experiment confirms the efficiency of the assay and was therefore repeated in non-transfected differentiated and undifferentiated Neuro2A cells to determine whether or not this interaction occurs more often as Neuro2A cells differentiate.

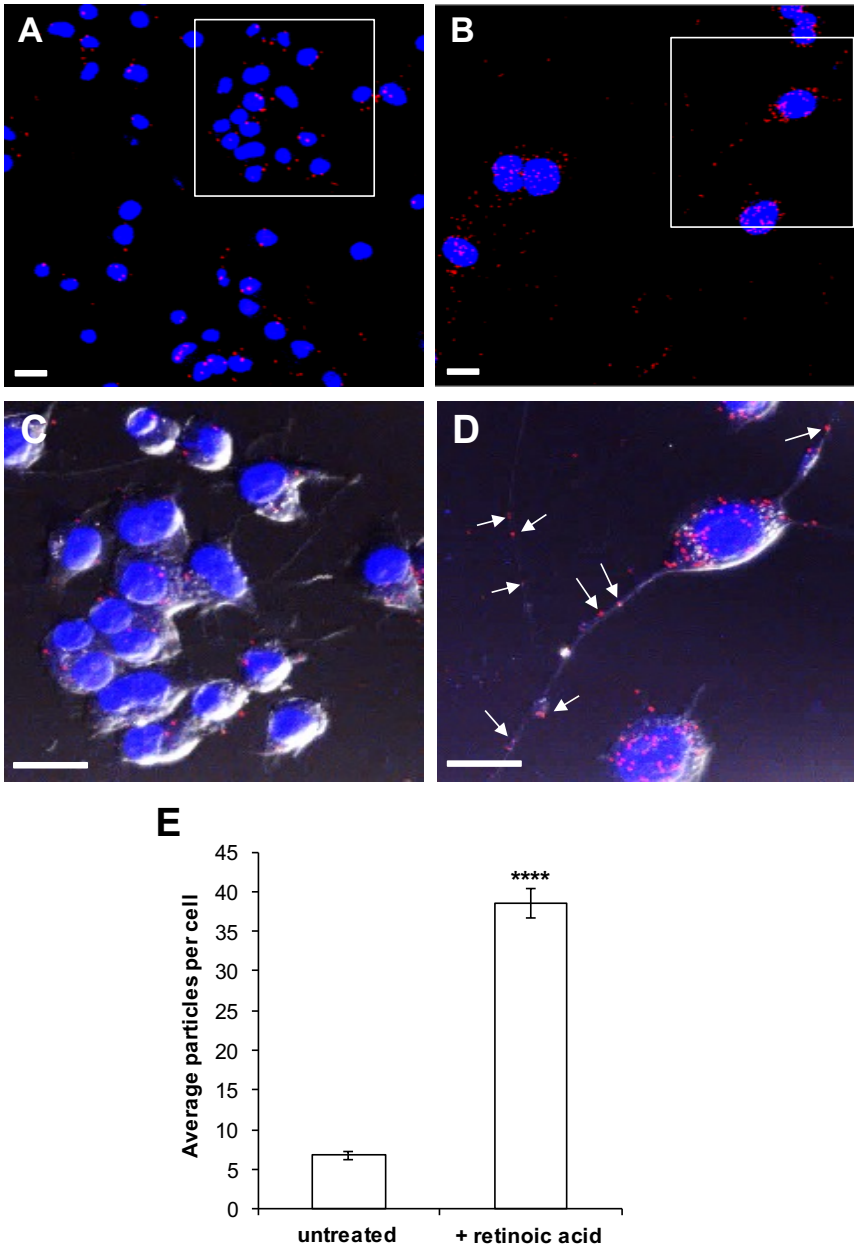

Figure 4.9: Increased interaction of PLCη2 and LIMK-1 in differentiated Neuro2A cells. **A** and **B** Representative fluorescent images of untreated and four day RA-treated Neuro2A cells, respectively. Red fluorescent particles correspond to PLCη2-LIMK-1 interaction, DAPI-staining of nuclei is shown in blue. **C** and **D** Respective "close-up" images of cells in **A** and **B** that are combined with bright field images taken simultaneously in order to view growing neurites. The arrows point to fluorescent particles in neurites. **E** Graph showing the average number of fluorescent particles in untreated and four day RA treated Neuro2A cells. Five micrographs were taken at random for each group. Nuclei and fluorescent particles were counted according to a randomised counting method. Error bars represent coefficient of error between five micrographs. The statistical significance (as determined by unpaired T-test) is indicated as ****, $P<0.0001$. Scale bars correspond to 15 µm. Images taken using the Leica TCS SP8 confocal microscope with a ×63 objective.

The results from the proximity ligand assay, as shown in Figure 4.9, reveal that differentiated Neuro2A cells exhibit a much greater number of fluorescent particles compared with undifferentiated control cells. In the experiments, an approximately 5 to 8-fold greater number of fluorescent particles per cell was observed in the differentiated group compared with undifferentiated control cells. Fluorescent particles were observed mainly within the cytoplasm, growing neurites and to a lesser degree in the nucleus. This rise in the number of fluorescent particles strongly indicates that PLCη2 and LIMK-1 interact within cells and that this interaction is significantly increased in RA-mediated Neuro2A cell differentiation.

4.3.7. Identification of proteomic changes upon RA induced differentiation

Many signalling cascades are active during neuronal development and by identifying proteins that are present in differentiated cells, a clearer understanding can be achieved of the signalling pathways that are involved in this process. With this in mind, two dimensional (2D)-gel electrophoresis was performed on proteins extracted from differentiated and non- differentiated Neuro2A cells as well as RA treated ShRNA control and PLCη2 KD cells in order to determine proteomic changes that take place upon RA induced differentiation of Neuro2A cells. 2D-gel electrophoresis is a useful technique which separates proteins firstly based on their isoelectric point and then by their mass, allowing for effective separation of proteins. Following separation on an SDS-PAGE gel, the respective protein spots were picked and subjected to trypsin digestion and mass spectrometric identification.

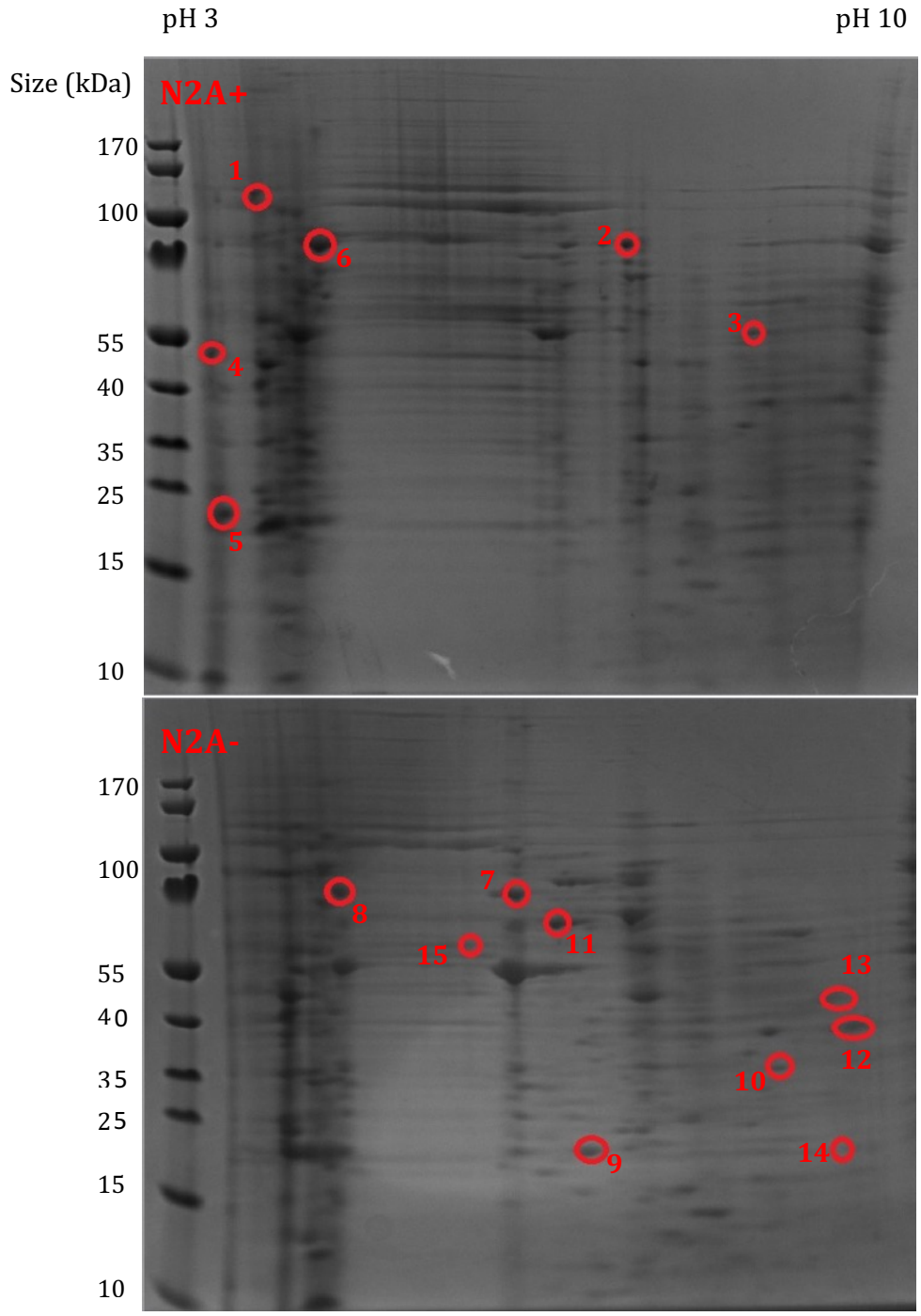

Figure 4.10: Differential protein expression in RA treated (N2A+) and untreated (N2A-) Nero2A cells. Protein samples were separated horizontally based on their isoelectric point which increases from left to right, then vertically based on their mass which decreases from top to bottom. Proteins bands were visualised using coomassie blue and those that were present in one group and absent from the other were analysed. Numbers correspond to spots that were picked and analysed.

Band	Protein name	Gene Name	Protein Function	Up/Down Regulated
1	Splicing factor, proline and glutamine rich	SFPQ	Regulates signal induced alternative splicing	Up
2	Heat shock protein 8	HSPA8	Chaperone protein and cytokine	Up
3	Enolase 1B, retrotransposed	ENO1B	Reversible conversion of 2-phosphoglycerate to phosphoenol-pyruvate	Up
4	Fructose-bisphosphate aldolase A	ALDOA	Key role in glycolysis and gluconeogenesis	Up
5	Peptidyl-prolyl cis-trans isomerase A alternative name-cyclophilin A	PPIA	Accelerates folding of proteins, Cis-trans isomerization of proline residues	Up
6	Bovine serine albumin (potentially a false positive derived from cell culture media)	ALB	Plasma transport protein	Up
7	Stress-induced phosphopeptide 1	STIP1	Mediates association of molecular chaperones HSC70 and HSP90	Down
8	Stress induced phosphoprotein 1	STIP1	Mediates association of molecular chaperones HSC70 and HSP90	Down
9	Stathmin	STMN1	Prevents assembly and promotes disassembly of microtubules	Down
10	Tyrosine 3-monooxygenase/ tryptophan 5-monooxygenase activation protein zeta polypeptide	YWHAZ	Adapter protein involved in regulation of signaling pathways	Down
11	Protein disulphide isomerase associated 3	PDIA3	Forming/ breaking/isomer-isation of disulphide bonds	Down

Band	Protein Name	Gene Name	Protein Function	Up/Down Regulated
12	Vimentin	VIM	Class 3 Intermediate filaments	Down
13	Serine/arginine-rich splicing factor 7	SRSF7	Required for pre-mRNA splicing	Down
14	Serine/arginine-rich splicing factor 7	SRSF7	Required for pre-mRNA splicing	Down
15	D-3-phosphoglycerate dehydrogenase	PHGDH	Catalyses transition of 3-phosphoglycerate into 3-phosphohydroxypyruvate	Down

Table 4.2: Table showing the name of proteins corresponding to cut bands from Figure 4.10, corresponding gene name, protein function (derived from www.string-db.org) and states whether they are up or down regulated in response to RA treatment.

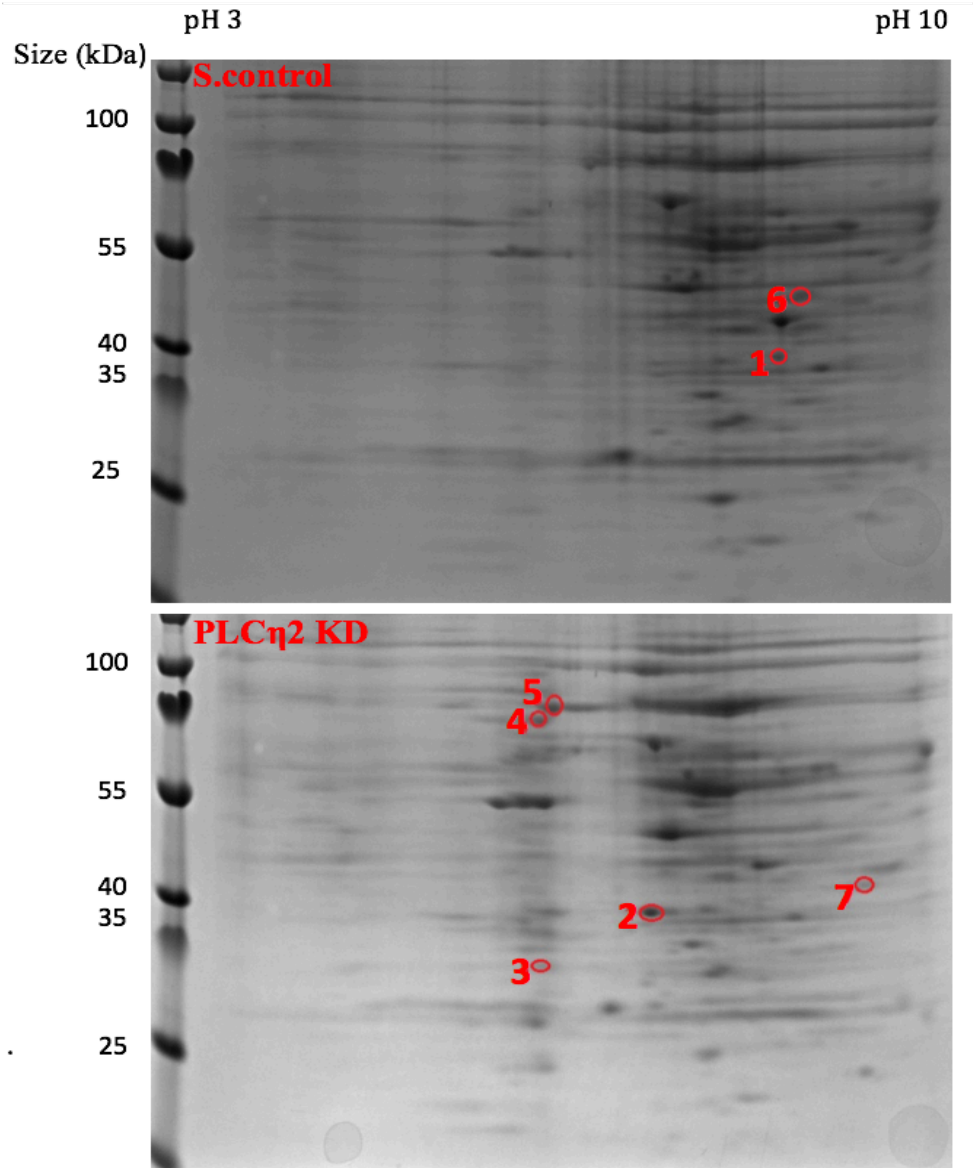

Figure 4.11: Differential protein expression in RA treated control and PLCη2 KD Nero2A cells. Protein samples were separated horizontally based on their isoelectric point which increases from left to right, then vertically based on their mass which decreases from top to bottom. Proteins bands were visualised using coomassie blue and those that were present in one group and absent from the other were analysed. Numbers correspond to spots that were picked and analysed.

Band No.	Protein name	Gene name	Protein function	Up/down regulated
1	Tropomyosin 4	TPM4	Binds to actin filaments, involved in muscle contraction and stabilization of cytoskeleton actin filaments in non-muscle cells	Up
2	Prohibitin	PHB	Inhibits DNA synthesis	Down
3	Parkinson disease protein 7	PARK7	Protects cells against oxidative stress and cell death	Down
4	Stress-induced phosphoprotein 1	STIP1	Mediates association of molecular chaperones HSC70 and HSP90	Down
5	Bovine serine albumin (false positive most likely derived from cell culture media)	ALB	Plasma transport protein	Up
6	Reticulocalbin-1	RCN1	Regulates calcium dependent activities in the ER	Up
7	Annexin A5	ANXA5	Anticoagulant protein that inhibits proteins involved in blood coagulation cascade	Down

Table 4.3: Table showing the name of proteins corresponding to cut bands from Figure 4.11, their gene name, protein function (derived from www.string-db.org) and states whether they are up or down regulated in response to RA treatment.

To provide further evidence that identified proteins are involved in RA-induced Neuro2A differentiation, several proteins were chosen and their mRNA expression levels were analysed by quantitative polymerase chain reaction (qPCR). This is a technique used to quantify the level of expressed genes. These results however, as displayed in Figure 4.12, do not necessarily correlate with those of the proteomics studies above. For example unexpressed proteins in non-differentiated Neuro2A cells such as PPIA show a similar mRNA expression level to expressed proteins in the differentiated Neuro2A cells. This suggests that the amount of mRNA does not necessarily reflect the relative protein expression in the cells.

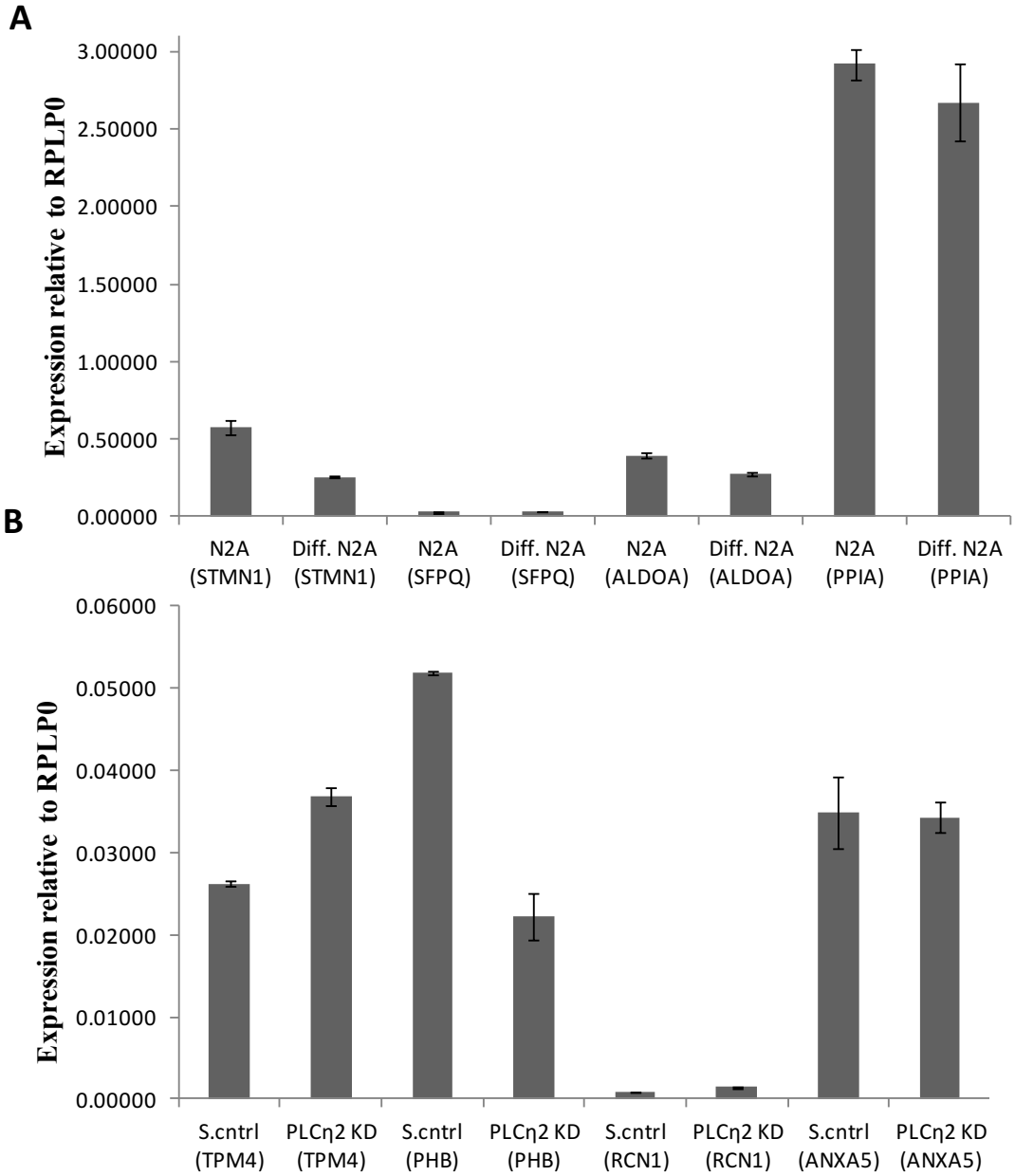

Figure 4.12: mRNA expression levels (relative to RPLP0) of interesting proteins from 2D-gel electrophoresis performed on **A** differentiated and undifferentiated Neuro2A cells and **B** Control and 67% KD Neuro2A cells.

4.3.8. Calcium induced activation of PLCη2 is not essential to its role in Neuro2A differentiation

The EF-hand domain of PLCη2 gives this enzyme its characteristic ability of becoming activated by intracellular elevations in Ca^{2+} (Popovics et al., 2013). To understand whether the sensitivity of PLCη2 towards Ca^{2+} is involved in differentiation of Neuro2A cells, a mutated form of the enzyme was utilised with a mutation in a key amino acid residue within loop one of the EF-hand domain where aspartic acid was replaced with alanine at position 256 (D256A).

Popovics *et al.* noted a 10-fold decrease in the enzymes sensitivity to Ca^{2+} with this mutant (Popovics et al., 2014). To further confirm that PLCη2 activity is required for neurite outgrowth, a mutated form of the enzyme was utilised where a key amino acid residue, histidine, in the enzymes active site at residue 460 was replaced with glutamine (H460Q). This residue is essential for enzyme activity and is conserved among PLC isozymes. Stable Neuro2A cell lines were created that over expressed an EV construct, wild type PLCη2, the EF-hand domain mutant (D256A) and the active site mutant (H460Q). These cells were then subjected to a four day treatment with 20 μM RA and differentiation was determined by the length of outgrowing neurites.

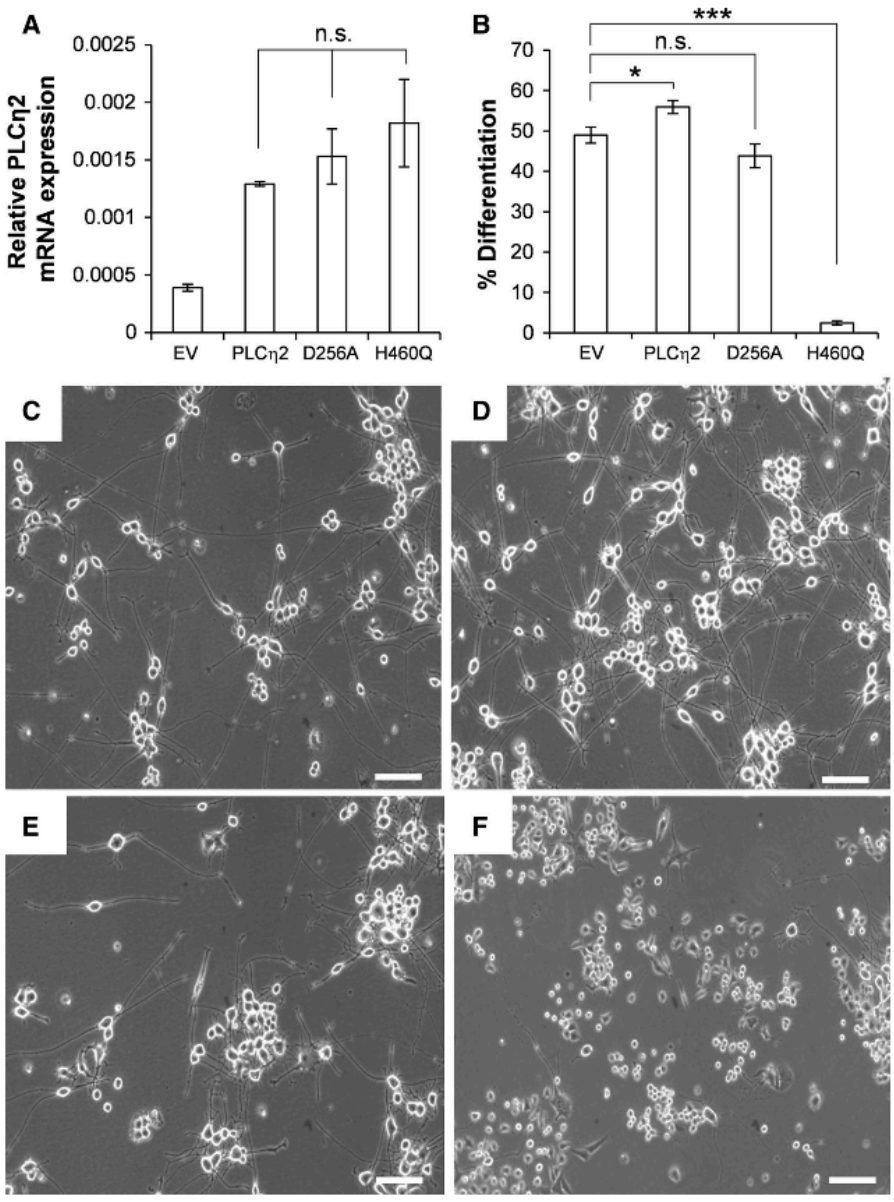

Figure 4.13: PLCη2 activity is necessary for RA induced differentiation, but its high calcium sensitivity is not involved. **A** Graph showing PLCη2 mRNA levels in relation to RPLP0 in stably transfected Neuro2A cell lines. The statistical significance was established by one-way ANOVA using Tukey's honest significance test. **B** Graph showing percentage of differentiation in different stable cell lines following four days of treatment with RA. The statistical significance was determined by unpaired T-test with applied Bonferroni's correction. **C**, **D**, **E** and **F** Show representative brightfield micrographs taken from stable cells expressing empty vector (EV), wild-type PLCη2 (PLCη2), D256A and H460Q mutants, respectively following four days of treatment with RA. There were no significant differences in PLCη2 mRNA expression levels between cell lines stably expressing PLCη2 variants as indicated by n.s; where $P>0.001$, as determined by one way ANOVA. The statistical significance (as determined by unpaired T-test) is indicated as ***, $P<0.001$ and *, $P<0.05$. Scale bars correspond to 10 μm. Bright field images taken by Zeiss Axiovert 40 CFL microscope with a 10× objective (Carl Zeiss Ltd., Cambridge, UK). n=3

Results from Figure 4.13 show a slight but significant rise in the number of differentiated cells over-expressing PLCη2 (55.9±1.6%) compared with the EV control group (49.0±2%), providing support for the involvement of PLCη2 in neurite outgrowth. Further support is provided by the catalytically inactive variant (H460Q) which showed a very significant decrease in growing neurites (2.4±0.5%) which proves that PLCη2 activity is required for neurite growth. In the bright field micrographs it can also be seen that in addition to the lack of neurites in H460Q cells, the size of cell bodies is also much smaller compared to other cell lines. The EF-hand mutant (D256A) however did not show any significant difference in the number differentiated cells (43.8±2.9%) which shows that the Ca^{2+} sensing ability of the enzyme is not responsible for its role in Neuro2A differentiation.

4.4. Discussion

4.4.1. PLCη enzyme localisation

4.4.1.1. PLCη2 has a primarily nuclear localisation whereas PLCη1 is cytoplasmic

A major focus of this chapter was to determine the cellular localisation of PLCη enzymes. Normally, PLC enzymes are distributed throughout the cytosol but bind to membrane phospholipids upon stimulation (Suh et al., 1988). However the punctate distribution of GFP tagged-PLCη2 has been shown in unstimulated COS7 cells (Popovics, 2012), suggesting that this enzyme binds to membranes even in its inactive form. The PH domain is an essential part of PLC enzymes (with exception to PLCζ) as it governs their binding to membrane phospholipids, thereby allowing these enzymes to carry out the essential function of catalysing the hydrolysis of PtdIns(4,5)P_2. Popovics *et al.* previously reported the importance of this domain by creating a PLCη2 mutant that lacks the PH domain. Following transfection into COS7 cells it was noted that this mutant, in contrast to its WT form was not activated following treatment with the Na^+/H^+ antiporter monensin or when incubated with different concentrations of Ca^{2+} (Popovics et al., 2011). Transfection of this GFP-tagged mutant into COS7 cells resulted in a diffuse distribution throughout the cytosol, indicating its inability to bind to membranes. Furthermore, western blotting analysis of membrane fractions collected from COS7 cells following transfection with the PH domain mutant showed a ~75% lower expression compared to WT, which confirms membrane binding of WT PLCη2 in heterologous COS7 cells (Popovics et al., 2011).

As mentioned previously, FRET analysis performed by Popovics *et al.* revealed the highest binding affinity of PH-PLCη1 and PH-PLCη2 to PtdIns(3,4,5)P_3, followed by PtdIns(3,4,5)P_2 (Popovics et al., 2013). This has been confirmed by using lipid absorbed membranes which revealed strong binding of PH-PLCη1 and PH-PLCη2 to PtdIns(3,4,5)P_3 (Popovics, 2012). The PH domains of different PLC isozymes have binding preferences for different phosphoinositides. PLCγ1 PH domain for example has high binding affinity for PtdIns(3,4,5)P_3 (Falasca et al., 1998) whereas PLCδ1 PH domain specifically binds to PtdIns(3,4,5)P_2 (Watt et al., 2002). This enabled the use of mCherry tagged-PLCδ1 PH domain as a tool for determining PtdIns(3,4,5)P_2 distribution. By creating a GFP-tagged PLCη2 PH domain and transfecting it into Neuro2A cells, a high degree of co-localisation was observed for this construct with PtdIns(3,4,5)P_3 antibody in the nucleus. There was however no co-localisation with co-transfected mCherry-PLCδ1 PH domain, which was present predominantly on the plasma membrane, suggesting that PLCη2 does not bind preferentially to PtdIns(3,4,5)P_2 in Neuro2A cells. These results are in agreement with previous studies that showed nuclear localisation of endogenous PLCη2 by immunostaining in undifferentiated and differentiated Neuro2A cells (Popovics et al., 2013). All of this indicates that the cellular localisation of PLCη2 is governed by PtdIns(3,4,5)P_3.

To confirm the nuclear localisation of PLCη2 and identify other organelles to which it is localised, quantitative immuno-electron microscopy was performed. Results from this experiment verified the nuclear localisation of PLCη2 in Neuro2A cells which opens up a path to explore why a highly Ca^{2+} sensitive PLC is present in the nucleus of neuronal cells. Nuclear Ca^{2+} is believed to be involved in a number of cellular processes including cell division, gene transcription and apoptosis (Berridge, 2001). This Ca^{2+} can be mobilised by several mechanisms: diffusion of Ca^{2+} waves into the nucleosome through nuclear pores (Power and Sah, 2002), release from the nuclear lumen into the nucleoplasm (Gerasimenko et al., 1995, Humbert et al., 1996) or release from invaginations of the nuclear envelope (nucleoplasmic reticulum) into the nucleoplasm (Alonso et al., 2006). In support of the last mechanism, $InsP_3$Rs and RyRs are present on the nucleoplasmic reticulum (Gerasimenko et al., 1995, Humbert et al., 1996, Echevarria et al., 2003, Gerasimenko et al., 2003, Quesada and Verdugo, 2005, Marchenko and Thomas, 2006). It is not entirely clear how these receptors are activated but this could be due to translocation of Ins(4,5)P_3 into the nucleus from the cytoplasm (Marchenko et al., 2005). $InsP_3$ and RyR agonists such as cyclic ADP-ribose and nicotinic acid adenine dinucleotide phosphate (NAADP) are also present within the nucleus; therefore

activation may occur from the nuclear side (Gerasimenko et al., 2003, Irvine, 2003, Adebanjo et al., 1999). This however remains controversial as NAADP is now considered to target two pore channels, which is located on acidic lysosomal-like Ca^{2+} stores (Patel et al. 2010).

Immuno-EM also revealed a high degree of localisation at the cytosol which suggests that this enzyme is not always bound to membranes. It is also present to a lower extent at the plasma membrane which is expected because of the PtdIns(4,5)P_2 hydrolysing activity of PLCη2. Another organelle where PLCη2 was identified was the mitochondria. In a recent study aimed to investigate the Ca^{2+} sensitivity of PLCη2, various Ca^{2+} mobilising agents were used including ionomycin, A23187, thapsigargin, bafilomycin and monensin. Only the latter was able to cause a significant rise on PLCη2 activity. A five-fold increase in PLCη2 activity was noted in response to the Na^+/H^+ antiporter, monensin. This response was prevented by CPG-37157, a selective inhibitor of mitochondrial Na^+/Ca^{2+} exchange which suggests that PLCη2 activity was increased, at least in part by mitochondrial Ca^{2+} efflux (Popovics et al., 2011)). The presence of PLCη2 at the mitochondria of course makes sense because it can respond to the Ca^{2+} being expelled from this organelle, which can contribute to the rise in PLCη2 activity. A high degree of co-localisation has previously been shown between PLCη2 and mitochondria in PLCη2 transfected COS7 cells that were labelled with mitoTracker (Popovics, 2012). A final identified compartment was the NE which had a small degree of localisation. This is expected if nuclear PLCη2, like its cytoplasmic counterpart functions (at least in part) by hydrolysing membrane phospholipids.

4.4.1.2. Mechanisms governing PLCη2 localisation

There is a high degree of sequence homology between the PH domains of both PLCη isozymes. This coupled with findings from the FRET analysis (Popovics et al., 2011) points towards a similar mechanism of binding to phospholipids and therefore similar distribution within cells. Immunostaining of endogenous PLCη1 and PLCη2 enzymes in Neuro2A cells however showed different localisation. Whereas PLCη2 immunolabelling confirmed its nuclear localisation in agreement with GFP-tagged PLCη2 PH domain, PLCη1 immunolabelling revealed a cytoplasmic distribution in Neuro2A cells. This suggests that the PH domain is not the only factor in determining phosphoinositide specificity.

The C2 domain also has membrane binding capability. The C2 domain of PLCδ enzymes for example are selective for PtdSer and target membranes composed of this phospholipid

(Ananthanarayanan et al, 2002). By conducting X-ray crystallography on PLCδ1 and using Ca^{2+} in the crystallography buffer, Essen *et al.* reported that two or three Ca^{2+} ions can associate with the C2 domain. This can then result in formation of bridges between the bound Ca^{2+} and the phospholipid head-groups. Alternatively, bound Ca^{2+} may modify the electrostatic properties of the protein and increase membrane association in this way (Essen et al., 1997b). This domain also has a role in PLCη2 activation. Following mutation of a residue (D861N) that is conserved in PLCη1, PLCη2, PLCδ1 and synaptotagmin 1, a ~55% decrease in enzyme activity and ~78% reduction in activation by 10 μM Ca^{2+} was noted in transfected COS7 cells that were treated with monensin. Despite the altered activity, sensitivity of this mutant towards Ca^{2+} did not change, which indicates that this domain is not involved in Ca^{2+} sensing but for PtdIns(4,5)P_2 to be hydrolysed effectively, the C2 domain must bind to the plasma membrane (Popovics et al., 2011). Analysis of the amino acid sequence of the C2 domain of both isozymes however, revealed a very high degree of sequence homology (~92%) and the D861 residue which is important for membrane binding is conserved in both isozymes. Therefore, this difference in localisation is unlikely to be explained in terms of different PH and C2 domains.

The C-terminal tail region of PLC enzymes also has implications for membrane binding. Kim *et al.* reported that PLCβ1 has a nuclear localisation sequence in its long C-terminal region (~400 amino acids), which allows its translocation to the nucleus (Rhee and Choi, 1992). By truncating this C-terminal, they showed that the enzyme no longer localises to the nucleus or associates with membrane fractions and is no longer activated by $G\alpha_q$ (Kim et al., 1996). It is therefore likely that the cellular localisation of PLCβ1 is mediated by the PH domain, C2 domain and its C-terminal region. The biggest variability in PLCη1 and PLCη2 isozymes is in their C-terminal tail region and this could be the reason for their different localisation. Three nuclear localisation sequences have been identified in PLCβ1 (Kim et al., 1996), none of which showed homology with amino acid sequences from the different PLCη2 variants (data not shown). PLCη2 may possess its own specific nuclear localisation sequence but further analysis is required to identify potential nuclear localisation sequences. The C-terminal tail of PLCβ has also been reported to form dimers which may affect its cellular distribution (Singer et al., 2002). Further studies are required to confirm whether or not PLCη isozymes also form such dimers. Immuno-electron microscopy will also give a better indication of PLCη1 localisation across cell compartments.

4.4.1.3. PLCη2 and nuclear phospholipid signalling

The presence of nuclear phospholipids in eukaryotic cells has also been well established in the last 30 years. Initial studies showed that cellular fractionation followed by digestion and removal the NE still leaves significant amounts of lipid (Irvine, 2003). Others have confirmed the presence of a nuclear phospholipid pool and it is now clear that these are distinct from their cytoplasmic counterparts in terms of regulation, synthesis, and function. Direct evidence emerged from mouse erythroleukemis (MEL) cells which possessed nuclear pools of PtdIns(4)P and PtdIns(4,5)P_2 that were metabolized differently to cytoplasmic lipids (Cocco et al., 1987) and Swiss 3T3 fibroblasts which showed regulation of nuclear phosphoinositol lipid metabolism in response to insulin-like growth factor-1 (Cocco et al., 1988, Divecha et al., 1991). Such studies showed an increase in nuclear DAG following a decrease in nuclear PtdIns(4)P and PtdIns(4,5)P_2, which was accompanied by translocation of PKC, an effector of DAG, to the nucleus (Cocco et al., 1988, Divecha et al., 1991, Martelli et al., 1991). The plasma membrane GPCR activating peptide Bombesin however only stimulated the plasma membrane inositol lipid cycle and did not affect nuclear pools (Divecha et al., 1991). These studies indicate the presence of a PLC cycle in the nucleus which leads to PKC translocation and therefore phosphorylation of nuclear proteins. Accordingly, there is evidence for nuclear localisation of PLCγ1 and PLCδ4 (Ye et al., 2002, Liu et al., 1996). However PLCβ1 is the best established PLC within the nucleus (Martelli et al., 1992, Divecha et al., 1993, Matteucci et al., 1998) and removing its lysine-rich nuclear localisation sequence renders it cytosolic following transfection into Rat-2 cells (Kim et al., 1996).

In the cytoplasm $G\alpha_q$ and $G\alpha_{11}$ proteins activate PLC enzymes which result in Ins(4,5)P_3 synthesis (Milligan and Kostenis, 2006). $G\alpha_i$ and $G\alpha_o$ associating with GPCRs are also able to activate PLC enzymes through dissociation of Gβγ heterodimers (Exton, 1996, Neves et al., 2002). These processes may also occur in the nucleus as several heterotrimeric G proteins including $G\alpha_i$, $G\alpha_s$, and $G\alpha_o$ are known to exist in the nucleus of neuronal and non-neuronal cells, such as S49 lymphoma cells (Crouch, 1991, Saffitz et al., 1994, Anis et al., 1999). GPCRs such as prostaglandin EP receptor 1 and lysophosphatidic acid receptors which couple to $G\alpha_q$ and $G\alpha_{11}$ proteins are present on the nuclear envelope of endothelial cells (Zhu et al., 2006). Kumar *et al.* showed the presence of group 1 metabotropic receptors (mGluR1 and mGluR5), that link to $G\alpha_q$ and $G\alpha_{11}$ proteins, on the inner nuclear membranes of cortical and striatal neurons. By expressing GFP-tagged $G\alpha_q$ in HEK cells, they also revealed the localisation of

$G\alpha_q$ to the nuclear membrane and further showed co-localisation of $G\alpha_q$ protein with mGluR5 and with lamin B_2 which is present on the inner nuclear membrane. Furthermore they showed coupling of nuclear mGluR5 receptors to $G\alpha_q$ and $G\alpha_{11}$ which leads to activation of PLC and $Ins(4,5)P_3$ mediated Ca^{2+} release in HEK cells and in striatal neurons (Kumar et al., 2008).

Activation of PLCη2 may however occur by another mechanism which is independent of GPCRs. Cocco *et al*. have reported the phosphorylation of PLCβ1 by extracellular signal-regulated kinase (ERK)/mitogen-activated protein kinase (MAPK) 1 or 2 following immunoprecipitation of PLCβ1 from nuclear fractions of cells treated with IGF-1 and noted phosphorylation at serine 982. This was prevented by the MAPK and ERK kinase inhibitor, PD98059. The significance of this phosphorylation has not been fully understood but evidence points towards its involvement in the growth response to IGF-1(Xu et al., 2001).

Nuclear PLC enzymes are likely to be involved in regulating essential processes within cells. There is evidence to show that nuclear PLC enzymes can lead to cellular differentiation. Treatment with DMSO induces differentiation in MEL cells; however it appears that this differentiation is consistent with a reduction in nuclear PLCβ1 activity (Divecha et al., 1995). Nevertheless the presence of this PLC within the nucleus seems to be essential as transfection of PLCβ1 lacking its nuclear localisation sequence attenuates differentiation of leukemia cells (Matteucci et al., 1998). This is consistent with a reduced expression of the transcription factor p45/NF-E2, a regulator of β-globin gene expression which is an indicator of differentiation (Faenza et al., 2002). Mouse oocytes show translocation of PLCβ1 to the nucleus as meiosis progresses and injection of an anti-PLCβ1 antibody into the nucleus results in the inhibition of germinal-vesicle breakdown which is a part of meiosis (Avazeri et al., 2000). In addition, it has been reported that PLCβ3 deficient mouse embryos fail to progress past the four cells stage (Wang et al., 1998a) so its expression could be involved in regulating cell proliferation. These studies provide further evidence for the necessity of nuclear phospholipases in growth and development, highlighting the importance of phospholipases in the nucleus. An interesting observation here was the presence of immuno-gold particles in darker regions of the nucleus which indicates binding to the more densely packed heterochromatin. Wang *et al*. have previously reported the localisation of PLCβ3 in nuclear heterochromatin of mouse neurons as determined by immune-EM (Wang et al., 1998b). They also showed that PLCβ2 and PLCβ3 are localised to nuclear heterochromatin areas of chief, mucous, parietal and enterochromaffin-like cells. PLCβ3 is also expressed in the nuclear heterochromatin of pancreatic cells including α-cells, β-cells, δ-cells, PP cells and acinar cells (Wang et al., 2000a). Heterochromatin areas

however prevent transcription of DNA due to their tight packing with histone proteins (Marcand et al., 1996). This binding of PLCs to heterochromatin needs to be investigated further to determine the precise role of nuclear PLCs.

4.4.2. PLCη2 involvement in Neuro2A differentiation

4.4.2.1. PLCη2 interacts directly with LIMK-1

The neuronal expression of PLCη2 has been well established (Nakahara et al., 2005). What remained to be determined was its functional role within neurons. Following reports that PLCη2 expression increases with age in mice after birth (Nakahara et al., 2005), its role in neurite growth and maturation was investigated (Popovics *et. al.*, 2013). A good model for such studies are Neuro2A cells which form a neuron-like morphology by forming an enlarged cell body and long, outward extending neurites following four days of treatment with RA (Zeng and Zhou, 2008). Popovics *et al.* showed that PLCη2 protein expression increases with differentiation, showing significant increases after only four hours of RA treatment and gradual increase throughout the four day process. At the final four day stage, PLCη2 expression was approximately 10-fold more than PLCη2 expression in untreated cells (Popovics *et. al.*, 2013). Furthermore, they created shRNA targeted PLCη2 KD neuro2A cells (~67% lower expression) of which only 8% of cells differentiated following the four day RA treatment, which is significantly lower compared to 73% in non-targeted shRNA transfected stable control cells (Popovics *et. al.*, 2013). These studies strongly indicate the involvement of PLCη2 in neuritogenesis.

They next identified LIMK-1 as an interaction partner of PLCη2 via a bacterial-two hybrid screen and showed by immuno-labelling, their co-localisation throughout differentiated neuro2A cells, mainly within the nucleus and growing neurites (Popovics *et. al.*, 2013). To attempt to confirm this interaction, a BiFC assay was performed which showed interaction of PLCη2 and LIMK-1 in the cytoplasm of COS7 and Neuro2A cells. This assay however was unreliable as fluorescence was observed in negative control groups. To achieve better resolution and investigate the interaction of endogenous proteins, a proximity ligand assay was utilised which showed direct interaction of the two proteins mainly in the cytoplasm, growing neurites and to a lower degree in the nucleus of differentiated Neuro2A cells. Popovics *et al.* showed (via western blotting) phosphorylation of LIMK-1 after two days of RA treatment. Expression of phosphorylated LIMK-1 (at Thr508) was several folds higher in comparison with RA-treated PLCη2 KD cells, strongly suggesting that PLCη2 is required upstream prior

to LIMK-1 activation (Popovics *et. al.*, 2013). Phosphorylation of LIMK-1 is significant to neurite outgrowth since activated LIMK-1 phosphorylates cofilin family proteins, inactivating them and thus allowing F-actin assembly which is the filamentous, polymerised form of actin that is required for neurite formation and extension of growth cones (Endo et al., 2007, Yang et al., 1998). In accordance, Popovics *et al*. showed by immuno-labelling with anti-β-actin antibody, the disruption of actin dynamics in PLCη2 KD cells (Popovics et al., 2013). Also Endo *et al*. reported the inhibition of neurite outgrowth following down-regulation of LIMK-1 levels using SiRNA (Endo et al., 2007).

The transcription factor, cAMP responsive element binding protein (CREB) is activated following phosphorylation by the cAMP pathway (Montminy and Bilezikjian, 1987). CREB is also directly activated by LIMK-1 in differentiating neurons, prompting transcription of genes that are required for neurite outgrowth (Yang et al., 2004). In accordance, phosphorylation of CREB (at ser133) was observed via western blotting following RA treatment which had approximately 40% more expression in comparison to RA treated PLCη2 KD cells (Popovics *et. al.*, 2013). Increased intracellular Ca^{2+} levels, to which PLCη2 can contribute, can activate Ca^{2+}/Calmodulin-dependent protein kinase IV (CaMKIV), which can subsequently activate LIMK-1 and CREB (Matthews et al., 1994, Takemura et al., 2009). Here, the proximity ligand assay has shown direct interaction of the two proteins with high occurrence in outgrowing neurites, indicating direct association of LIMK-1 with PLCη2 as neurites develop. Collectively, these studies have provided a clearer picture of the signalling pathways involved in neuronal differentiation as shown in Fig. 4.14.

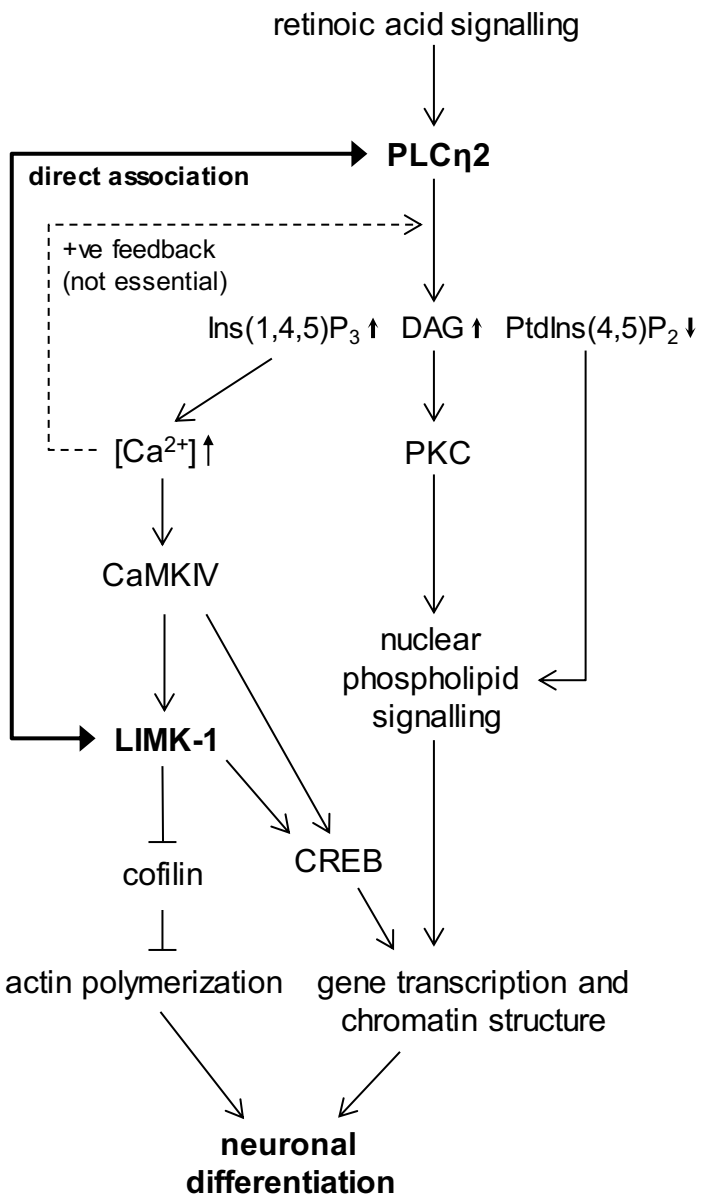

Figure 4.14: Schematic diagram showing potential pathways by which PLCη2 regulates neuronal differentiation. Following activation of PLCη2, breakdown of PtdIns(4,5)P_2 results in decrease in this phospholipid and subsequent increase in the level of Ins(4,5)P_3 and DAG. Ins(4,5)P_3 binds to its receptor on the ER and triggers Ca^{2+} release from this organelle resulting in activation of LIMK-1 and subsequently, CREB through activation of CaMKIV. PLCη2 can directly associate with LIMK-1 to potentially regulate its activity. Activated CREB initiates gene transcription. Activated LIMK-1 inhibits actin depolymerisation resulting in the assembly of actin filaments required for neuronal differentiation. Transcriptional activity may also be influenced by changes in the nuclear DAG and PtdIns(4,5)P_2 levels. Image created by Dr Alan Stewart (University of St Andrews, UK).

4.4.2.2. Identification of proteins involved in Neuro2A differentiation

Following four days of treatment with RA, Neuro2A cells undergo a clear change in morphology, developing an enlarged cell body and forming long outward-extending neurites. This occurrence is mainly due to altered dynamics of the actin cytoskeleton which occurs in differentiating neurons. Therefore identification of proteins that regulate the actin cytoskeleton during neuronal differentiation is of interest. Results from 2D gel electrophoresis performed on differentiated ShRNA control and PLCη2 KD cells as well as on differentiated and undifferentiated Neuro2A cells revealed differences in their proteomic profiles, which allowed for identification of several proteins that are potentially involved in neuronal differentiation. A variety of proteins were identified that alter protein & cytoskeletal structure, metabolism, and RNA splicing. The most interesting up-regulated proteins include:

Splicing factor, proline and glutamine rich (SFPQ) which is abundantly expressed in the brain and is reportedly required for neuronal survival and differentiation in zebrafish as zebrafish expressing a mutant form of SFPQ showed abnormal brain development (Lowery et al., 2007). SFPQ also effects mRNA splicing and proteins dervived from differentially spliced mRNAs will have a different amino acid composition, which can affect the proteins function. Therefore, altered regulation of genes that code for splicing proteins is important for the regulation of biological processes. Enolase 1B (Eno1b) has not been previously implicated in differentiation but is involved in glycolysis and gluconeogenesis, reversibly converting 2-phosphoglycerate to phosphoenolpyruvate. When coupled to ATP hydrolysis, gluconeogenesis becomes exergonic, thus providing energy for the cell (Sims et al., 2006). Eno1b may therefore contribute towards the increased energy required by the cell to drive cellular processes that are required for differentiation which may be the reason for its up-regulation. Fructose-bisphosphate aldolase A (AldoA) is also involved in glycolysis, gluconeogenesis and fructose metabolism by catalysing the reversible conversion of fructose-bisphosphate to glyceraldehyde-3-phosphate and dehydroxyacetone phosphate. In a more direct role, AldoA also enhances localisation of Wiskott-Aldrich Syndrome protein (WASP) to lamellipodia and filopodia thereby affecting actin dynamics (Ritterson Lew and Tolan, 2013) which may be contributing towards growing neurites in differentiating Neuro2A cells. The up-regulation of cyclophilin A is also interesting as Song *et al.* showed that is highly expressed in neurons and is essential for RA induced differentiation of p19 embryonic carcinoma cells. By performing a rescue study, they also showed that re-introducing cyclophilin A into cyclophilin A knock-down cells again induced neurite outgrowth (Song et al., 2004).

Other interesting proteins that were up-regulated in differentiated ShRNA control cells but not in differentiated knock-down cells are tropomyosin-4 and reticulocalbin-1 (RCN1). Tropomyosins are a large family of proteins that are important components of actin filaments as they regulate actin filaments in muscle and non-muscle cells (Helfman et al., 1986). These proteins have been strongly implicated in neurite outgrowth. Curthoys *et al.* noted that tropomyosin promotes neurite outgrowth in B35 neuroblastoma cells and also regulates neurite branching which shows that tropomyosins are important regulators of the actin cytoskeleton during neuritogenesis (Curthoys et al., 2014). In addition it has been reported that brain specific tropomyosin-1 and -3 mRNA levels increase in PC12 cells that are subjected to treatment with nerve growth factor, which induces differentiation. Tropomyosin-1 and -3 mRNA levels also rise during the most rapid phases of neurite outgrowth in developing rat cerebellum (Weinberger et al., 1993, Stamm et al., 1993). RCN1 is a Ca^{2+} binding protein with six EF-hand domains, two of which (the second and sixth domains) do not bind Ca^{2+} (Ozawa and Muramatsu, 1992). No known function has been determined for RCN1, but its presence in the lumen of the ER suggests a potential role in synthesis, modification and transport of proteins, which are believed to be Ca^{2+} regulated processes (Brostrom and Brostrom, 1990). Its upregulation in RA treated ShRNA control cells but not in RA treated PLCη2 KD cells may suggest a role in synthesis/transport of proteins that are required for neurite formation. PLCη2 may be involved in regulating RCN1 by increasing cellular, and therefore ER Ca^{2+} levels.

Some proteins that have implications in neuronal differentiation however were down-regulated following differentiation of Neuro2A cells: Stress-induced phosphopeptide 1 (Stip1) has been implicated in neuroprotection and neuritogenesis. It has been shown to mediate neurite outgrowth following interaction with Rnd1 (a Rho family GTAPase) in PC12 cells derived from Rat adrenal gland. Rnd1 alters the cells cytoskeleton and contributes to neurite outgrowth. This interaction was further confirmed in mouse brain extracts (Lopes et al., 2005, de Souza et al., 2014). Stathmin is a microtubule destabilisation protein with implications in neuronal growth (Grenningloh et al., 2004). Szpara *et al.* have reported increased gene expression of stathmin following neurite outgrowth and regeneration in mouse embryonic tissue (Szpara et al., 2007). Tyrosine 3-monooxygenase/tryptophan 5- monooxygenase activation protein zeta (YWHAZ) is also highly expressed in the brain (Fu et al., 2000). Rasmer *et al.* showed that YWHAZ binds directly to cell adhesion molecule L1 which is an essential protein in development of the mammalian nervous system. By binding to L1, YWHAZ promotes its

phosphorylation by casein kinase II thereby resulting in L1 induced neurite outgrowth in rat hippocampal neurons (Ramser et al., 2010).

It is clear that these proteins have proposed roles in differentiation and neurite outgrowth so their down-regulation in differentiated Neuro2A cells is unexpected. This however indicates that pathways that are engaged during differentiation differ depending on the cell type and stimulus which is applied. Multiple pathways are therefore believed to be engaged in neurite formation but these pathways may well be cell type dependent.

It is worth mentioning that the qPCR data did not correlate with the proteomic results, which suggests that the amount of mRNA does not necessarily reflect its relative protein expression. By using mass spectrometry based methods to quantify protein levels and microarrays to measure mRNA levels of a variety of cultured cells (including differentiated MPRO, mouse fibroblast, and human medulloblastoma cells), it has been determined that only 40% of proteins show good correlations with mRNA levels suggesting that in most cases protein concentrations are disproportional to mRNA levels (Tian et al., 2004, Vogel et al., 2010, Lundberg et al., 2010). Vogel *et al.* have stated that several important processes are involved in determining final protein concentrations including transcription, mRNA decay, translation and degradation of proteins (Vogel et al., 2010). The human genome consists of over one thousand genes encoding microRNAs which can repress translation by inhibiting mRNA translation into proteins. The human genome also consists of ubiquitin ligases and proteases that can degrade proteins. Protein degradation is further affected by presence of endosomes and lysosomes, therefore the level of mRNA cannot be a definite indicator of final protein concentration (Bartel, 2009, Moore, 2013). Furthermore, Schwanhausser *et al.* concluded that housekeeping genes such as ribosomal proteins have good correlation with their mRNA levels whereas poor correlation occurs for proteins involved in transcription, signalling, chromatin modification and cell cycle processes. Therefore proteins involved in cell differentiation are not expected to show a good level of correlation with their mRNA levels (Schwanhausser et al., 2011).

4.4.2.3. PLCη2 involvement in Neuro2A differentiation is independent of its Ca^{2+} sensing ability

PLCη2 is highly expressed in neuronal cells and has the second highest Ca^{2+} sensing ability between all of the PLC isozymes, the first being the sperm specific PLCζ (Nakahara et al., 2005). Because of such properties, PLCη2 is likely to be involved in many neuronal processes. It has been shown here that this enzyme is involved in the differentiation of Neuro2A cells since stable transfection of a catalytically inactive mutant variant only resulted in less than 5% of cells being differentiated in comparison to approximately 50% in stable control cells expressing EV. This is in agreement with previous studies which showed that PLCη2 KD cells created by stable expression of PLCη2 targeted shRNA, only led to approximately 8% cell differentiation (Popovics et al., 2013). Further evidence comes from stable cells over-expressing PLCη2 which showed approximately 10% more cellular differentiation compared to EV control cells. The role of PLCη2 in Neuro2A differentiation however is irrespective of its high Ca^{2+} sensing ability as stable cells over-expressing a non-functional EF-hand domain variant of PLCη2 showed a similar level of differentiation to control cells. It therefore seems likely that the involvement of PLCη2 is due to its interaction with other proteins and its involvement in certain signalling cascades that are necessary for neuritogenesis and neuronal differentiation.

4.5. Conclusion

This chapter has given us an insight into the cellular localisation of PLCη enzymes. Results here have shown a high degree of PH-PLCη2 co-localisation with PtdIns(3,4,5)P_3 in the nucleus of Neuro2A cells which is in agreement with previous studies that showed co-localisation of endogenous PLCη2 with PtdIns(3,4,5)P_3 in the nucleus of differentiated Neuro2A cells (Popovics, 2012), suggesting that PtdIns(3,4,5)P_3 is likely to be the principal phospholipid to which PLCη2 binds and therefore, the primary factor governing PLCη2 localisation in neuronal cells. Immuno-EM analysis confirmed the primarily nuclear localisation of this enzyme suggesting that PLCη2 is distributed mainly in the nucleus of neuronal cells where this PLC isozyme may predominantly serve to regulate nuclear processes rather than serving the typical role of PLC enzymes, in hydrolysing the plasma membrane phospholipid PtdIns(4,5)P_2. PLCη2 however may still be involved in this process as immune-EM also revealed its localisation in the cytoplasm with lower levels detected in the mitochondria, plasma membrane and nuclear envelope. The other variant, PLCη1 is determined

to be localised in the cytoplasm of Neuro2A cells, showing altered distribution in comparison to PLCη2 which could be indicative of a different functional role within cells. This altered localisation may be explained in terms of their different C-terminal tail regions since a high degree of homology was observed between their PH and C2 domains that are known to be involved in membrane binding.

The direct association of PLCη2 with LIMK-1 was confirmed. This interaction occurred mainly in the cytoplasm and in growing neurites where it likely regulates actin dynamics, most likely by promoting F-actin assembly which is essential for neuritogenesis. Several proteins that are involved in neurite formation were also identified to be up-regulated following differentiation of Neuro2A cells. The necessity of these proteins for Neuro2A differentiation must be confirmed to allow for better understanding of pathways that are required for neuronal differentiation. Finally, it was established that the role of PLCη2 in neuritogenesis is essential but is independent of its high Ca^{2+} sensing ability which indicates that the role of PLCη2 in this process is through its interaction with other proteins and involvement in certain signalling cascades. Collectively, these experiments contribute towards understanding of the molecular machinery that regulates the actin cytoskeleton during neuritogenesis. The significance of which is most notable in the development of therapeutics that could potentially assist in promoting neuritogenesis following nerve injury and in the repair of degenerating neurites in the CNS.

Chapter 5

Relevance of PLCη2 to Alzheimer's disease

5.1. Introduction

Alzheimer's disease (AD) is a neurodegenerative disorder that causes memory impairment and cognitive decline in affected individuals. AD has several pathological features including neurofibrillary tangles composed of hyperphosphorylated tau proteins, fibrous amyloid plaques created by formation of abnormal amyloid-β (Aβ) peptides and neuronal death (Masters et al., 1985). These however, appear to be late stage markers of AD and so could be secondary factors in the disease process. Therefore the root cause of AD has not yet been established.

Another mechanism which can lead to neuronal death is the increase in intracellular Ca^{2+} concentration which can alter normal neuronal functioning; a process referred to as "calciumopathy" because of the toxic effects it can have on neurons (Stutzmann, 2007). Studies have shown an increase in Ca^{2+} release from ER stores in neurons treated with Aβ and neurons obtained from AD model mice (Ferreiro et al., 2004, Stutzmann et al., 2006). It has been reported that neurons derived from young, adult and elder mice carrying mutations in the Presenilin 1 gene (which leads to formation of pathogenic Aβ1-42) show alterations in Ca^{2+} homeostasis which suggests that Ca^{2+} dysregulation may be occurring throughout a person's life (Stutzmann et al., 2006). Mutations in presenilins have been shown to increase activation of $Ins(4,5)P_3$ and RyRs (Cheung et al., 2010, Chan et al., 2000). Addition of Aβ peptides to primary neurons and neurons obtained from AD model mice have revealed an elevation in intracellular Ca^{2+} concentration from ~100 nM to ~300 nM. This affects synaptic plasticity which is the process of strengthening/weakening synaptic connections, thereby impacting memory processes (Kuchibhotla et al., 2008, Mattson et al., 1992). Consequently, alterations to normal Ca^{2+} homeostasis can lead to changes in the activity of many proteins and signalling pathways which can alter normal neuronal physiology. The exact mechanisms which lead to this altered Ca^{2+} homeostasis however remain elusive.

PLC enzymes may be involved in this process because they function by cleaving the membrane phospholipid $PtdIns(4,5)P_2$ into $Ins(4,5)P_3$ and DAG. $Ins(4,5)P_3$ binds to $Ins(4,5)P_3$Rs on the ER causing them to open and release Ca^{2+} into the cytosol. This property makes PLC enzymes key proteins in regulating Ca^{2+} dynamics. It has been established that PLCη2 is present in brain regions that are associated with memory and cognition (Nakahara et al., 2005) and is activated by small elevations in intracellular Ca^{2+} concentration (as discussed in Chapter 3). As mentioned, Ca^{2+} levels rise in AD affected neurons, most likely through the increased activation and/or expression of Ca^{2+} channels. A case study of over 3300 AD patients identified

a mutation in the neuronal Ca^{2+} channel CALHM1. This mutation results in an increased level of Ca^{2+} entry through the channel and subsequently results in an increased level of intracellular Aβ. Further studies indicated a relationship between this mutation and the rise in activity of γ-secretase which along with β-secretase cuts amyloid precursor protein to produce a 42 amino acid long peptide called amyloid β, the primary component of amyloid plaques (Green and LaFerla, 2008, Demuro et al., 2010). The increased intracellular Ca^{2+} resulting from overactive Ca^{2+} channels can activate Ins(4,5)P_3Rs and RyRs as well as Ca^{2+} sensitive PLC enzymes (Ferreiro et al., 2004, Stutzmann et al., 2006). Furthermore, production of DAG following activation of PLCη2 can activate PKC which can activate NMDA channels, further contributing to the rise in intracellular Ca^{2+} level (Lin et al., 2010). Such studies led Popovics *et al*. to hypothesise that PLCη2 may contribute to the "calciumopathy" that is associated with AD (Popovics and Stewart, 2012a). Therefore it is possible that PLCη2 plays a role in AD by increasing intracellular Ca^{2+} via release from ER stores or by potentiating its entry from the extracellular space. Figure 4.1 shows a pathway which Popovics and Stewart have proposed for the involvement of PLCη2 in AD.

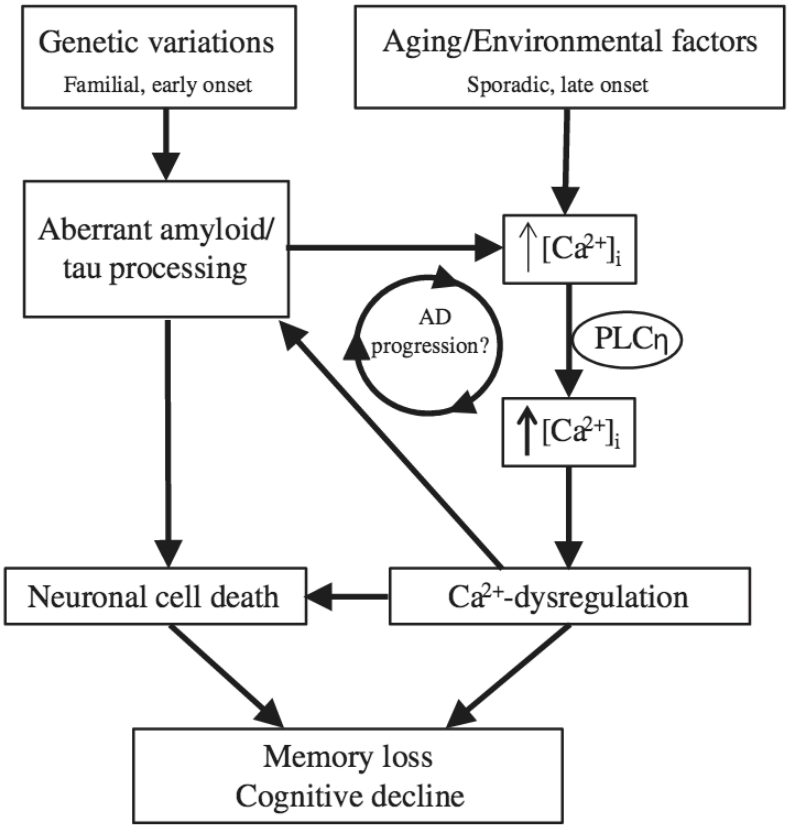

Figure 5.1: Proposed pathway for PLCη2 involvement in AD. Genetic variations that lead to abnormal amyloid and tau processing as well as environmental factors and ageing can raise physiological Ca^{2+} levels which can activate PLCη enzymes, thereby further raising the intracellular level of Ca^{2+}. This altered Ca^{2+} homeostasis can lead to abnormal amyloid and tau processing which can cause neuronal death, or can directly lead to neuronal death or loss of memory and cognitive impairment. It is possible that PLCη2 is being continuously activated in this process thereby leading to AD progression. Image taken from Popovics and Stewart, 2012a.

The aim of this chapter is to gain a better understanding of the involvement of PLCη2 in AD. This is done firstly by determining if oligomeric Aβ1-42 treatment of differentiated Neuro2A cells that express a neuronal like morphology (enlarged cell body with outgrowing neurites) is a good model for studying AD, by assessing toxicity via an MTT (3-(4,5-dimethylthiazol-2-yl)-2,5-diphenyltetrazolium bromide) assay . Next the expression of PLCη2 is compared at different time points following treatment of differentiated Neuro2A cells with oligomeric Aβ1-42 which will give an indication of whether PLCη2 is more or less functional in AD. As such, Yang *et al.* used this model to show the protective function of Sphingosine kinase-1 upon treatment with Aβ 25-35 (Yang et al., 2014). Finally, differentiated Neuro2A cells are treated with oligomeric Aβ1-42 and PLCη2 localisation determined by immuno-labelling at different time points to understand more about where it is functioning in the disease state.

5.2. Materials and methods

5.2.1. Preparation of oligomeric Aβ

Aβ 1-42 was obtained from Biopeptide co., LLC (Roselle, SD, USA) and 1 mg was dissolved in 1 ml of hexafluoro-isopropanol (HFIP) on ice, then incubated at RT for 1 hour. This was aliquoted into eppendorff tubes, each consisting of 0.05 mg Aβ 1-42. Tubes were left at RT overnight to allow HFIP to evaporate. The following day, tubes were placed in a vacuum for 1 hour to ensure complete drying and stored at -20^{o}C. When required, each aliquot was dissolved in 0.5 ml of differentiation media and added to cells.

5.2.2. MTT assay

Neuro2A cells were seeded at low density into wells of a 12 well plate and differentiated as described previously. Aliquots (0.05 mg) of oligomerised Aβ 1-42 was then added to wells. In control wells, differentiation media was added. MTT assay (Sigma-Aldrich) was performed according to the manufacturer's instructions. Briefly, 50 µl (10% of volume of culture media) was added to each well and incubated for 2 hours. At this stage, purple crystals formed. Culture media was removed and 600 µl of MTT solvent was added. A pipette was used to mix the contents of the well which were then added to an eppendorf tube. 200 µl was added to three wells of a 96 well plate and optical density recorded at 570 nm.

5.3. Results

5.3.1. Validating the experimental model

Large, insoluble aggregates of Aβ 1-42 are seen in brains of AD patients, yet there is no direct correlation between the number of plaques and dementia. Aβ 1-42 is however still believed to play a major role in AD pathogenesis as a hallmark feature of AD is the excessive production of Aβ 1-42 (Walsh and Selkoe, 2007, Walsh et al., 2002). Several lines of evidence gathered from neurons treated with Aβ peptides, transgenic mice overexpressing amyloid precursor protein and brains of AD patients reveal that aggregation of Aβ 1-42 monomers into the toxic and still soluble oligomeric form of the peptide is required for neuronal impairment (Lambert et al., 1998, Lesne et al., 2006, Shankar et al., 2008). Small Aβ 1-42 oligomers called dimers have been isolated from AD brains and Shankar *et al*. have shown that these dimers can disrupt synaptic plasticity in hippocampal slices derived from mice. Their results revealed that these

dimers cause inhibition of LTP, enhancement of LTD and reduction in density of dendritic synapses (Shankar et al., 2008). Insoluble amyloid plaques did not have an effect on LTP until they were solubilised to form Aβ dimers. This gives rise to the possibility that these plaques are composed of accumulated neurotoxic oligomeric Aβ peptides. They conclude that these dimers are the smallest synaptotoxic form of Aβ (Shankar et al., 2008). Based on such results, experiments here were performed using the oligomeric form of Aβ 1-42 and differentiated Neuro2A cells, as the neuronal model.

Initially, Neuro2A cells were seeded into wells of a 12 well plate and differentiated by a four day treatment with RA. Following this, cells were either treated with oligomeric Aβ 1-42 for 24 hours or left untreated. An MTT assay was then performed to determine the number of viable cells. This assay works by measuring the amount of formazan which is formed following reduction of MTT by metabolically active cells. This is done by mitochondrial dehydrogenase enzyme cleavage of the tetrazolium ring, forming a purple coloured solution. Following solubilisation by MTT solvent, its level can be measured by a spectrophotometer. Normal functioning cells will lead to higher counts in this assay.

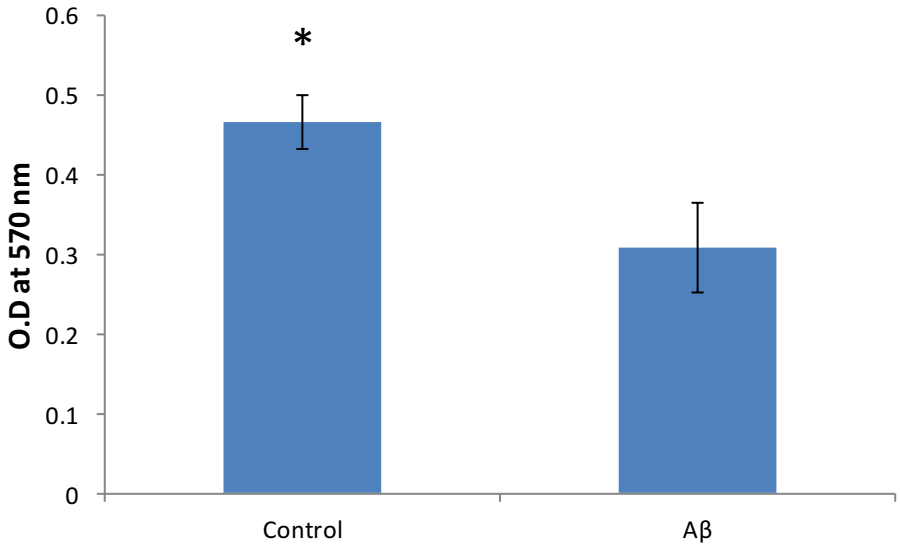

Figure 5.2: MTT assay showing mitochondrial death in the Aβ group. Error bars represent S.E.M. The statistical significance (as determined by unpaired T-test) is indicated as *, $P<0.05$.

The graph in Figure 5.2 shows a significantly higher number of viable cells in the control group compared with the Aβ treated group. This test has portrayed that a number of mitochondria in the Aβ group have ceased to function. This could be because of cell death or mitochondrial

dysfunction as a result of the Aβ peptide. In accordance Shoji *et al.* reported that Aβ peptides activate the JNK pathway which leads to neurotoxicity in primary cortical neurons (Shoji et al., 2000). These results show that the oligomeric form of Aβ 1-42 is having a toxic effect on differentiated Neuro2A cells, thereby validating this model for pursuing studies involving Aβ.

5.3.2. PLCη2 expression is unaffected by oligomeric Aβ 1-42

By looking at the amount of a certain protein that is produced in a disease state, a better understanding can be gained of that proteins involvement in the disease. As such, many proteins have been reported to have increased expression in AD. One example is Alpha-1-antichymotrypsin (ACT), a serine protease inhibitor. The amount of ACT in the cerebrospinal fluid and plasma of AD patients shows a positive correlation with disease progression. ACT is also a component of amyloid plaques and is overexpressed in astrocytes that are in close proximity to amyloid plaques (Abraham et al., 1990). Expression studies have therefore identified this protein as a potential player in AD which then prompted further studies to determine whether or not it is a suitable therapeutic target. Subsequent studies showed that ACT increases the rate of Aβ polymerisation in both in vitro and in vivo models of AD and that its increased expression in neuronal cells results in neurite loss, followed by apoptosis (Padmanabhan et al., 2006).

To identify whether the amount of PLCη2 is altered in AD, the validated model was used. Neuro2A cells were differentiated, then treated with the oligomeric form of Aβ 1-42 for 4, 8 or 24 hours. This was followed by analysis of PLCη2 expression via western blotting. Proteins were then transferred onto a membrane and the amount of expressed protein is analysed by using antibodies specific for the protein of interest. As a control, the level of phosphorylated c-jun was analysed. C-jun is a transcription factor known to be activated through the c-Jun N-terminal kinases (JNK) pathway following treatment with Aβ oligomers (Ma et al., 2009). β-actin expression levels were also determined as a loading control.

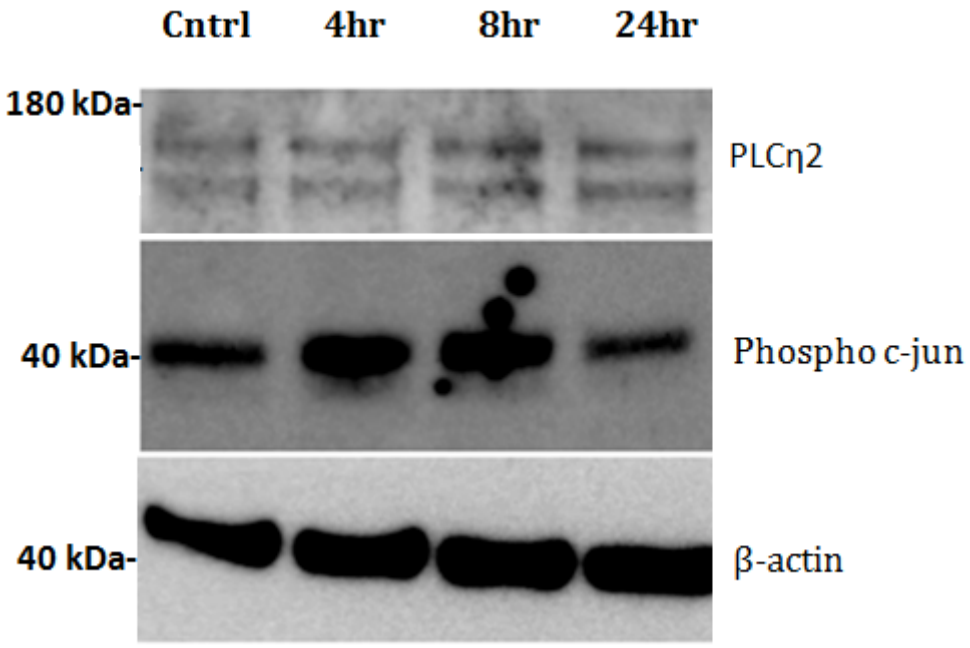

Figure 5.3: Western blot analysis showing the level of expressed PLCη2 following treatment with oligomeric Aβ 1-42. For experimental control and loading control, the expression levels of phosphorylated c-jun and β-actin were determined, respectively. PLCη2 (21a/23 variant-164.3 kDa), phospho c-jun= 48 kDa, β-actin= 45 kDa. Experiment repeated twice, the bottom half stained for phospho c-jun in one experiment and for β-actin in the other as both of these proteins have a similar weight.

Figure 3.2 shows that the experimental method used here is a suitable one as we see an increase in the amount of phosphorylated c-jun following treatment with oligomeric Aβ 1-42. This occurs following 4-8 hours of treatment with Aβ 1-42. Expression levels however fall at 24 hours post-treatment which implies that the JNK pathway is no longer activated at this point and c-jun becomes dephosphorylated. PLCη2 expression however remains the same, showing no increase or decrease in expression level. This experiment shows that pathogenic Aβ1-42 does not affect the expression of PLCη2 in differentiated Neuro2A cells which suggests that PLCη2 levels may also be unaltered in AD affected neurons. This however does not mean that PLCη2 is not involved in the associated "calciumopathy", as the rise in Ca^{2+} may be increasing the activity of PLCη2.

5.3.3. PLCη2 localisation is altered by oligomeric Aβ 1-42

As mentioned previously, cells have a compartmentalised nature, meaning that different compartments are segregated by lipid membranes. A protein's localisation is therefore a useful indicator of its function. If a protein's localisation is altered, its physiological function will also change and this can contribute to disease pathogenesis (Hung and Link, 2011). Certain proteins

have been identified to have altered localisation in AD. Chalmers and Love for example showed an altered localisation of phosphorylated SMAD3 in AD brains. Whereas it's normal physiological localisation is nuclear, their studies identified that SMAD3 binds to phosphorylated tau and attains a cytoplasmic localisation in AD affected neurons (Chalmers and Love, 2007).

The validated model was used here to determine the localisation of PLCη2 upon treatment with oligomeric Aβ 1-42. As with the previous western blot experiment, localisation was investigated in untreated control cells at 4, 8 and 24 hours post treatment via immuno-labelling (as described in Chapter 4), by using PLCη2 antibody.

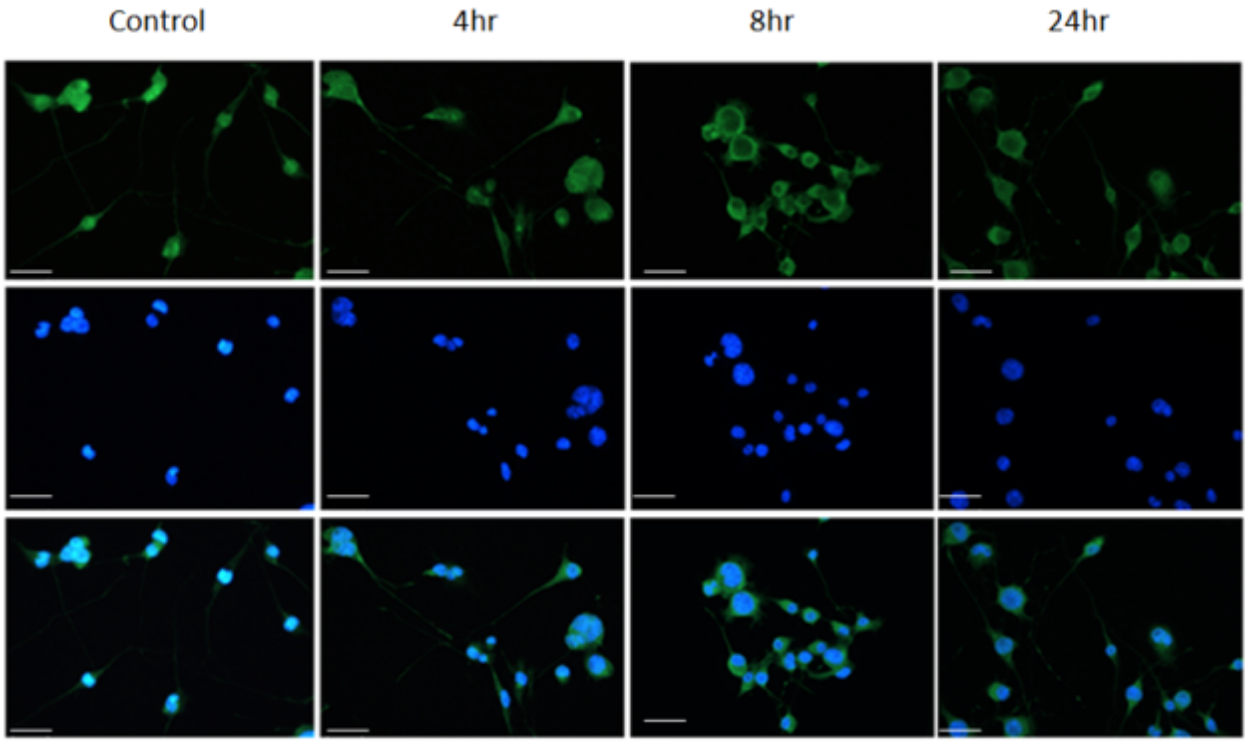

Figure. 5.4: Immuno-labelling showing the localisation of PLCη2 in differentiated Neuro2A cells. Staining can be seen throughout the cell in control cells. Upon Aβ treatment, staining is much less in nuclear regions, especially in the 8 and 24 hour treated groups. Scale bars represent 10 µm. Images taken using Leica DFC3000 fluorescence microscope, with a 20 x objective.

A

Group	No. of cells with nuclear staining	No. of cells without nuclear staining
Untreated	0	31
4 hour treated	3	47
8 hour treated	39	8
24 hour treated	23	6

B

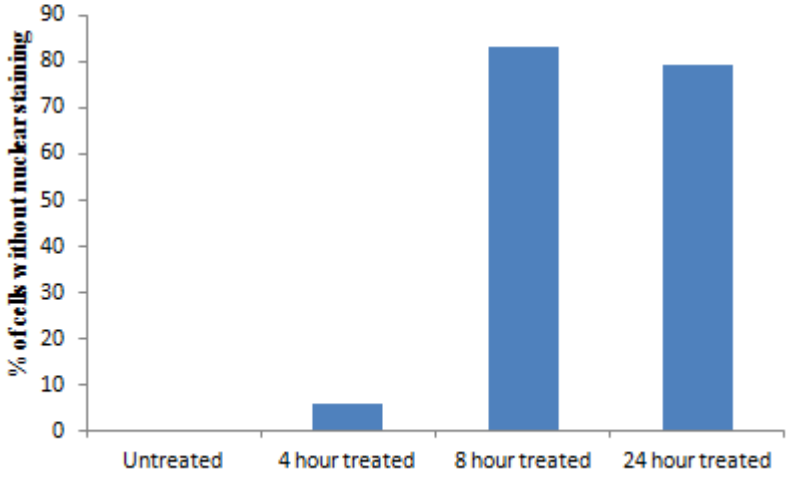

Figure 5.5: Percentage of differentiated Neuro2A cells without nuclear staining. Four micrographs were taken at random following treatment with RA at various time points. Quantification was performed by counting the number of cells with and without nuclear staining as shown in table A. This data was used to calculate the percentage of cells without nuclear staining as shown in graph B.

From Figure 5.5 it can be seen that PLCη2 labelling is present throughout differentiated Neuro2A cells. This staining is present in the cell body and growing neurites. This is also the case for cells treated with oligomerised Aβ 1-42 peptide for 4 hours. Following treatment with Aβ 1-42 for 8 and 24 hours however, the localisation of PLCη2 is altered. It is still present in the cell body and neurites but is no longer present in the nucleus. Figure 3.4 shows that a very high number of cells lack nuclear staining following RA treatment for 8 hours (83%) and 24 hours (79%). Very few cells lacked nuclear staining in the 4 hour treated group (4%), while all cells showed nuclear staining in the untreated group. This experiment therefore indicates that PLCη2 localisation is altered in AD affected neurons.

5.4. Discussion

The aim of this chapter was to gain an insight into the role of PLCη2 in AD. Popovics and Stewart proposed that PLCη2 is a potential contributing factor to AD pathogenesis as it is highly sensitive to Ca^{2+} and because it is expressed in neuronal cells within brain regions associated with memory (Popovics and Stewart, 2012a, Nakahara et al., 2005). Ca^{2+} has

ubiquitous roles within all cells and so disruption to its normal homeostasis can lead to disorders including neurodegenerative diseases. The proposed role is that PLCη2 can become activated by the rise in Ca^{2+} which may occur by increased entry from the extracellular space or by increased release from intracellular stores. As such there is evidence for both occurrences as a result of Aβ peptides (Ferreiro et al., 2004, Green and LaFerla, 2008). This rise in intracellular Ca^{2+} can activate PLCη2 which will result in increased breakdown of the membrane phospholipid PtdIns(4,5)P_2, thereby generating Ins(4,5)P_3 and DAG, leading to further increase in intracellular Ca^{2+}. Activation of PKC by DAG can then open NMDA channels (Tyszkiewicz and Yan, 2005) and Ins(4,5)P_3 causes Ca^{2+} release from the ER by binding to Ins(4,5)P_3Rs on this organelle (Tyszkiewicz and Yan, 2005, Popovics and Stewart, 2012a). As such, Ins(4,5)P_3 levels have been shown to increase with age (Igwe and Filla, 1997). PLCη2 may be responsible for this as the expression of PLCη2 also increases in brains of developing mice for the first few months following birth. It may also be possible that PLCη2 expression also continues to increase with age (Nakahara et al., 2005). Because AD symptoms become prevalent with age, increased levels of proteins that affect cellular Ca^{2+} dynamics may be the root cause of AD. Altered Ca^{2+} homeostasis can lead to changes in various signalling pathways which can increase the rate of Aβ production. Therefore it seems likely that Ca^{2+} and Aβ are involved in a feed-forward pathway.

In these experiments, the oligomeric form of Aβ 1-42 was used as previous studies have shown that this form of Aβ causes disruptions to normal Ca^{2+} homeostasis and results in neurodegeneration (Shankar et al., 2008). A model for use in AD studies was first validated using the MTT assay which showed that differentiated Neuro2A cells (that attain a neuronal like morphology) are adversely affected by the addition of oligomeric Aβ 1-42. Expression studies were then performed using this model which showed a constant level of PLCη2 upon treatment with oligomeric Aβ 1-42 for 4, 8 and 24 hours. The most interesting result obtained in this chapter was the altered localisation of PLCη2 following Aβ treatment. In untreated cells PLCη2 was present throughout all of the differentiated Neuro2A cells, showing clear nuclear staining but in a high number of the 8 hour (83%) and 24 hour (79%) Aβ1-42 treated groups, it was no longer present in the nucleus.

Translation of mRNA into Protein takes place in the cytosol of cells and half of the proteins that a cell produces must pass at least one biological membrane to reach its desired cellular destination (Chacinska et al., 2009). Movement of proteins to their requisite cellular destination arises from certain sequences within the protein and occurs via co-translational or post-

translational translocation (Rapoport, 2007, Schnell and Hebert, 2003, Wickner and Schekman, 2005). Some proteins are post-translationally translocated (ie. translocated after their translation is complete) including those targeted to peroxisomes, mitochondria and nucleus while others are co-translationaly translocated (ie. enter the ER before their translation is complete). These proteins include those that are intended to be targeted to the plasma membrane, lysosomes, ER, Golgi apparatus or those that will be secreted from the cells (Schmidt et al., 2010, Suntharalingam and Wente, 2003, Terry et al., 2007, Wickner and Schekman, 2005). Signal sequences that are present on some proteins are identified by specific receptors on the surface of organelles, some proteins mainly those that traffic to the mitochondria, require chaperone proteins (Rapoport, 2007; Schmidt et al., 2010-PLOC) while others gain access via membrane pores, as occurs in the nucleus. Small proteins (20-40 kDa) gain entry into the nucleus by diffusion through membrane pores whereas larger proteins (40 kDa-10 MD) gain entry by facilitated transport (Strambio-De-Castillia et al., 2010, Suntharalingam and Wente, 2003, Terry et al., 2007).

It is important for proteins to function within their physiological subcellular locations because it affects the protein's interaction with other proteins that may not be present in the altered location and thus prevent it from functioning in essential signalling cascades. This can alter the movement of information and material within the cell. Furthermore such mislocalisation can cause activity at the wrong place which can be damaging to the cell (Hung and Link, 2011). The altered localisation of proteins, as observed here may arise as a result of mutations or post-translational modifications that cause protein miss-folding, alterations to chaperone proteins/transport receptors and changes to nuclear localisation sequences (NLS). Because PLCη2 is a relatively large protein, the smallest isoform being 119 kDa, it requires a NLS to gain entry into the nucleus by facilitative transport via importins. It is therefore possible that an alteration to the NLS of PLCη2 is causing its mislocalisation.

5.5. Conclusion

This chapter has provided some insight into the role of PLCη2 in AD. The experiments were performed using a validated model in which differentiated Neuro2A cells were treated with the oligomeric form of Aβ1-42 peptide. Results suggest that PLCη2 has a similar level of expression in normal and Alzheimer's affected neurons, so it is unlikely that a rise in the amount of PLCη2 protein is occurring in the disease state. However, PLCη2 expression levels

did not decrease which means that it may still be involved in the disease process. As mentioned, several lines of evidence show a rise in intracellular Ca^{2+} levels in AD affected neurons, by extracellular Ca^{2+} entry and by release from intracellular stores. The initial cause of increased Ca^{2+} is not completely understood but due to the high sensitivity of PLCη2 to Ca^{2+}, this rise in Ca^{2+} concentration is able to increase the activity of PLCη2, subsequently increasing intracellular Ca^{2+} levels and thereby contributing to the "calciumopathy". A useful experiment therefore would be to investigate PLCη2 activity following treatment of cells with Aβ 1-42. The localisation of PLCη2 however appears to alter in Alzheimer's affected neurons. The altered localisation of proteins has been noted in a variety of diseases but further studies are required to establish that the altered localisation of PLCη2 is indeed occurring in AD affected neurons and whether it is a contributing factor towards AD. If this is the case, identifying and rectifying the mechanisms of PLCη2 mislocalisation may prove useful as a therapeutic strategy. The fact that PLCη2 is no longer present in the nucleus of differentiated Neuro2A cells is suggestive of a mechanism that prevents identification of its nuclear localisation sequence by specific nuclear receptors. One possibility is that PLCη2 is unable to enter the nucleus, another possibility is that it is being moved out of the nucleus. The absence of nuclear localisation after 8 hours may also suggest that the protein has a short half-life. Regardless of the mechanism, PLCη2 can build up in the cytoplasm where its increased activity in this region may affect Ca^{2+} regulated cell processes, thereby contributing to neuronal death.

Chapter 6

Relevance of PLCη1 to embryonic development

6.1. Introduction

Embryonic patterning and development relies on one group of cells to change the behaviour of another group of cells by releasing ligands that will initiate developmental signalling cascades, which will ultimately change the shape, mitotic rate and fate of cell groups (Mauch and Schoenwolf, 2001). Surprisingly, only a few developmental signalling pathways are known to exist and are named after the ligand that initiates signalling or based on the involved signal transducers. These include Notch, Hippo, Wnt, fibroblast growth factor (FGF), Epidermal growth factor (EGF), Hedgehog, transforming growth factor β (TGFβ)/bone morphogenic proteins (BMPs), cytokine, jun kinase (JNK), NF-κB and retinoic acid receptor. All of these rely on ligands that diffuse from one cell to another (paracrine signalling) except for Notch and Hippo which depend on direct cell-cell contact because of their ligands, which are anchored to the plasma membrane (juxtacrine signalling). These pathways ultimately result in regulation of transcription factors and therefore expression of different proteins that control cytoskeletal reorganisation, adhesion, cell migration, cell polarity, cell proliferation and cell fate. Because there are few signalling pathways, a specific pathway or ligand cannot be assigned to each cell type. Instead, cell fate is determined by duration/intensity of the signal, cell stage at which pathways become active, interaction of pathways and expression of transcription factors (Perrimon et al., 2012). Table 6.1 summarises findings relating to developmental signalling pathways.

The focus of this chapter is on the hedgehog signalling pathway which is involved in embryonic patterning and cranial development (Chiang et al., 1996). The interest in this pathway comes from studies of Professor Geoff Woods and Dr Michael Nahorski (University of Cambridge, UK) who identified a point mutation in PLCη1 that causes truncation at amino acid 1075 in newborns with holoprosencephaly (HPE), which is an embryonic developmental disorder. HPE has a prevelance of 1 in 16,000 live births (Cohen, 1989) and can result from abnormal chromosome structure or number in 25-50% of cases, copy number variations (which are duplication or deletion of DNA sections) in 10-20% of cases and gene mutations in 18-25% of cases. In some cases, the brain develops normally and deformities are mild such as abnormal development of lips, nose and distance between eyes. In more severe cases the forebrain fails to develop into two distinct hemispheres causing death before birth, in a form of HPE called cyclopia which is characterised by the failure of eyes to separate into two separate cavities (Raam et al., 2011, Solomon et al., 1993). Figure 6.1 shows the different degrees of HPE

severity. Abnormalities in the Shh pathway appears to be the main cause of HPE as 30-40% of HPE in patients who have normal chromosome numbers, results from a mutation in the Shh gene (Roessler et al., 1996, Solomon et al., 1993).

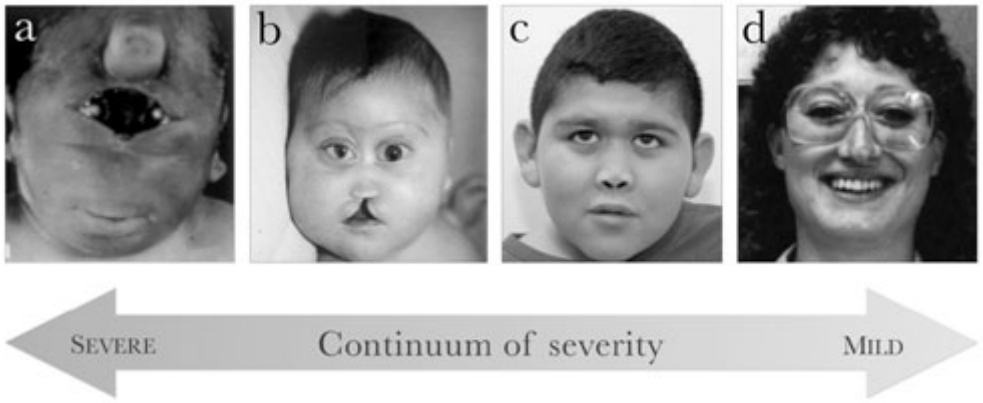

Figure 6.1: Different degrees of HPE severity. **a** Patient with severe abolar HPE showing cyclopia **b** patient with abolar HPE showing failure of eyes to separate completely, flat nasal bridge and cleft lip **c** patient with lobar HPE showing flat nasal bridge and partially separated nostrils. **d** individual with a mild form of HPE possessing a sharp nasal bridge and only one central incisor. Image taken from (Raam et al., 2011).

Signaling pathway	Receptor	Ligand	Transcriptional effector	Output
Wnt/Wg	Frizzled, dFrizzled2	Wg/Wnt	Armadillo/β-catenin with TCF/LEF	Patterning, growth, PCP (β-catenin independent)
Hh	Patched	Hh	Ci/Gli	Patterning, growth
TGFβ	Thickveins	Dpp/TGFβ	Smad (Mad/Medea)	Patterning, growth
RTK	EGFR	Spitz, Gurken, Keren, Vein	Pointed/Yan	Patterning, morphogenesis
	FGFR (Breathless, Heartless)	Branchless, Thisbe, Pyramus	Pointed/Yan	Patterning, morphogenesis, migration
	InR	dIlp1-dIlp7	Pointed/Yan, Foxo	Growth, metabolism, aging
	PDGF/VEGF receptor (PVR)	Pvf1-3	Pointed/Yan	Morphogenesis, migration
	Torso	Trunk, PTTH	Pointed/Yan	Patterning, metamorphosis
	dALK	Jelly belly	Pointed/Yan	Growth on starvation (CNS)
	Sevenless	Boss	Pointed/Yan	Patterning, cell-fate specification
Notch	Notch	Delta, Serrate	NICD with Su(H)	Patterning, lateral inhibition, cell-fate specification
Hippo	Fat	Dachsous	Yorkie with Scalloped	Growth, PCP
NF-κB	Toll	Spatzle	Dorsal/Dif	Patterning, innate immunity
JAK/STAT	Domeless	Unpaired1-3	STAT92E	Patterning, innate immunity
JNK	Eiger/TNF	Wengen	Jun and Fos	Migration, patterning, innate immunity
Nuclear receptors	EcRA, EcRB	Ecdysone	EcRA, EcRB with USP	Patterning, growth, metabolism

Table 6.1: Table showing the key pathways involved in development along with their respective receptors, ligands, transcription factors and functional output. Mutations in the Hh, TGFβ and RTK signalling pathways can lead to HPE. Specifically, Patched, Gli, FGFR and Smad have been linked to HPE. Abbreviations: TCF, T-cell factor; LEF, lymphoid enhancer-binding factor; PCP, planar cell polarity; TGF, transforming growth factor; RTK, receptor-tyrosine kinase; EGFR, epidermal growth factor receptor; FGFR, fibroblast growth factor receptor; PVDF, polyvinylidene difluoride; VEGFR, vascular endothelial growth factor; PTTH, prothoracicotropic hormone; CNS, central nervous system; NICD, Notch intracellular domain; STAT, signal transducer and activator of transcription; JNK, JUN kinase; TNF, tumor necrosis factor; USP, ubiquitin-specific protease. Table taken from Perrimon et al., 2012.

The hh gene was initially discovered in *Drosophila* where Nusslein-Volhard and Wieschaus identified that a mutation in a certain gene resulted in a smaller larval body that lacked the naked cuticle and was covered with small pointy projections called dendicles (almost twice as many as in WT). Because of this phenotype, this gene was named hh (Nusslein-Volhard and Wieschaus, 1980). Whereas *Drosophila* have only one hh ligand, there are three classes of closely related hh ligands in vertebrates called Desert hh, Indian hh and Sonic hh (Shh) which is the most broadly expressed and best studied of the three (Echelard et al., 1993). Shh is expressed in the notochord, floorplate, zone of polarizing activity (that instructs development of limb buds) and the neural tube (Odent et al., 1999). Prior studies had shown the importance of signals from the floorplate and notochord in patterning the neural tube (Placzek et al., 1993) and because Shh is a secreted ligand from these regions, there was a strong indication that it is involved in patterning of embryonic tissue (Riddle et al., 1993, Chang et al., 1994, Echelard et al., 1993, Krauss et al., 1993). It is now well established that Shh is imperative to growth, patterning and morphogenesis of embryonic tissue and almost all aspects of vertebrate body plan development are influenced in some way by hh signalling (Ingham and McMahon, 2001).

To initiate the Shh pathway, the Shh ligand must bind to its cell surface receptor, patched (Ptch). In the absence of Shh, Ptch inhibits expression of hh target genes (Ingham, 1998). This suggests that Shh binding to Ptch inhibits its activity which may be occurring by internalisation and degradation of Ptch (Incardona et al., 2000). A third protein called Smoothened (Smo) is essential in this pathway (Chen et al., 2001). This is a seven transmembrane GPCR that is confined to a vesicle in the cytosol and in the absence of Shh, it is inhibited from upregulating to the plasma membrane by Ptch, the mechanism of which is still not fully understood (Quirk et al., 1997). Once Ptch becomes inactive by binding of Shh, Smo inhibition is removed and it can translocate to the cell surface where it allows activation of the Shh pathway (Rohatgi et al., 2009). Smo is first phosphorylated by adrenergic receptor kinase beta 1 (Adrbk1, formerly called GRK2), allowing it to interact with a protein called β-arrestin2 thereby causing internalisation by endocytosis (Chen et al., 2004, Meloni et al., 2006). A complex is then formed, likely with KIF7 (a motor protein belonging to the kinesin 2 family), which allows translocation of Smo to the tip of the primary cilium (Liem et al., 2009). Once here, Smo can activate the transcription factors in this pathway, called Gli which can activate or repress target genes (Kim et al., 2009). Mechanisms of Gli transcription factor activation are also poorly understood but results suggest that activated Smo suppresses a protein called Sufu which when active, prevents nuclear translocation of Gli by sequestering it in the cytoplasm (Jia et al., 2009, Svard et al., 2006). This pathway is summarised in Figure 6.2. There are three mammalian Gli isoforms; Gli1, Gli2 and Gli3 which are present in different tissues and in different combinations. For example in the limb, effects are apparently produced by Gli3 as only a mutation in Gli3 results in abnormal number of digits (Hui and Joyner, 1993). Therefore patterning of different tissues may be under the control of different Gli transcription factors. Furthermore, Gli1 and Gli3 recognise the same sequence on target gene promoters (GACCACCCA) whereas Gli2 recognises a slightly different sequence (GAACCACCCA), (Kinzler and Vogelstein, 1990, Tanimura et al., 1998).

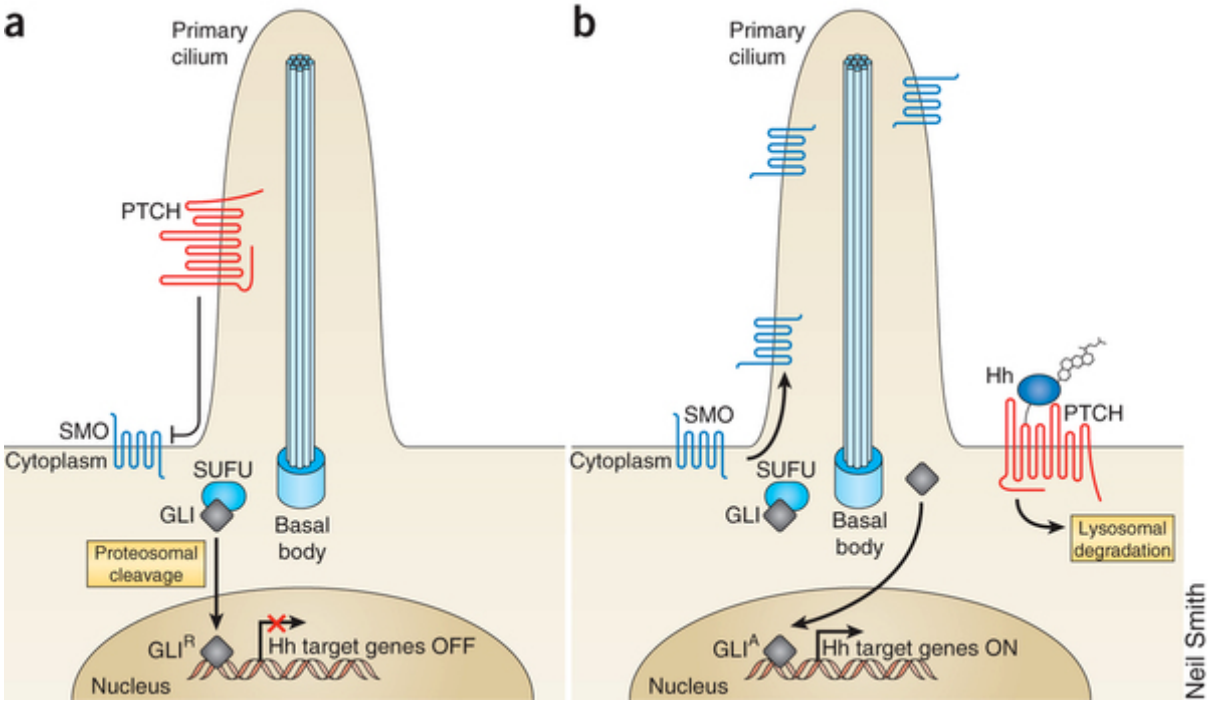

Figure 6.2: Figure showing the Shh pathway in the **a** inactive and **b** active state. **a** In the absence of Shh ligand, Smo is suppressed by Ptch and is unable to translocate to the plasma membrane. SUFU inhibits GLI translocation to the nucleus by sequestering it in the cytoplasm. This can then result in GLI proteasomal cleavage to form a C-terminal fragment of GLI that represses nuclear transcription. **b** Binding of SHH to its receptor PTCH prevents its inhibition of SMO activity. Once active, SMO translocates to the primary cilia and suppresses SUFU which allows translocation of GLI transcription factors into the nucleus, thus leading to transcription of GLI target genes. Image taken from Amakye et al., 2013.

The aim of this chapter is to determine whether a mutant form of PLCη1 (identified by Professor Geoff Woods and Dr Michael Nahorski, personal communication) has different effects on the Shh pathway in comparison to wild type PLCη1. The identified mutation was a point mutation that results in the creation of a premature STOP codon which causes truncation of the protein by 615 amino acid residues in the longest isoform (isoform 1) of human PLCη1; thereby resulting in a version of this isoform of PLCη1 that lacks most of its C-terminal domain. To examine the effect that this mutation has on the cellular function of PLCη1, a similar mutation was created in the corresponding mouse variant (variant N1075X) of PLCη1 since suitable cell lines for experiments were derived from mouse. Figure 6.3 shows alignment of mouse and human PLCη1 amino acid sequences. Initially, cellular localisation was investigated via immunolabelling following transfection of both variants into COS7 cells to gain an understanding of whether the mutant form functions at a different cellular region. Next, suitable cell lines that express Shh pathway genes were identified as a cellular model for planned

studies. Two cell lines were ultimately chosen including an embryonic mouse mesenchymal cell line called C3H10T1/2 which was chosen based on the studies of Murone *et al*. who showed Gli activation following Shh treatment of these cells (Murone et al., 2000), and an embryonic mouse hypothalamus cell line called N7 which was chosen after confirming the presence of Shh pathway genes, namely Smo, Ptch and Neogenin1 (Neo1) which is a cell surface receptor that has previously been implicated in Shh pathway regulation (Hong et al., 2012). These cell lines were subjected to a variety of transfection methods to identify the most efficient means of transfection. The cellular distribution of PLCη1 was then investigated in these cells. The Shh pathway functions in the primary cilium of cells, which is an organelle that is required for receiving signals that activate developmental pathways (Goetz et al., 2009, Goetz and Anderson, 2010). To determine whether endogenous PLCη1 localises to the primary cilia in C3H10T1/2 and N7 cells, these cells were co-stained with antibodies specific to PLCη1 and acetylated tubulin. Finally, the level of expressed Shh genes (Smo, Ptch and Neo1) was investigated by qPCR following transfection of mutant and wild type PLCη1 into N7 cells to determine whether the HPE associated mutant form of PLCη1 is having a different effect on the expression of Shh pathway genes.

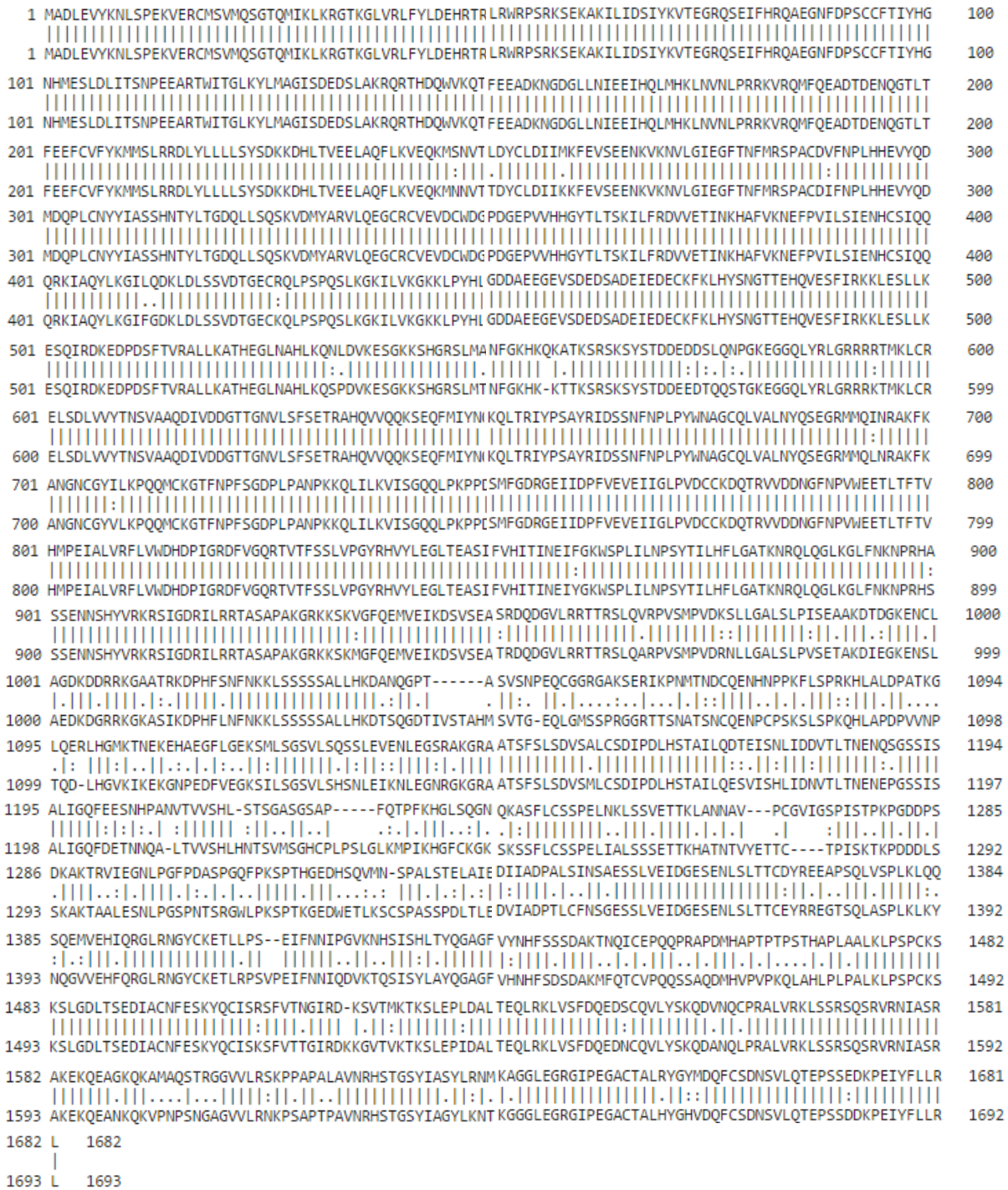

Figure 6.3: Sequence alignment of mouse and human PLCη1. Sequence alignment established using the EMBOSS needle sequence alignment tool. Top and bottom lines show sequence for mouse (PLCη1, variant 1) and human (PLCη1, variant a), respectively. Sequences show 89.5% homology. Symbols used to express the rate of similarity: "|" identical, ":" high similarity, "." weak similarity.

6.2. Materials and methods

6.2.1. Molecular cloning of PLCη1

The entire mouse PLCη1 gene was amplified by PCR using an image clone containing the coding sequence of PLCη1, variant 1, obtained from Source Bioscience (Nottingham, UK) and the Long Template PCR System (Roche, Penzberg, Germany) as described in Chapter 2. Primers used in the PCR reaction were: Forward, 5'-ATGCATGAGTGTAATGCAGTC-3'; Reverse, 5'-TCAAAGCCTCAAAAGAAAAGAAATTTCGGG-3'. The PLCη1 coding sequence was then inserted into the pcDNA3.1 expression vector using the In-Fusion HD cloning Kit (Clonetech) according to the manufacturer's instructions. Following confirmation of successful cloning by digesting the vector with restriction enzymes (as described in Chapter 2), the inserted gene was sequenced to make sure there were no single nucleotide polymorphisms (SNPs).

6.2.2. Site directed mutagenesis

The QuickChange II XL site directed mutagenesis Kit (Agilent technologies) was used to create an asparagine-Stop codon mutation at amino acid residue 1075 in the longest isoform (variant 1) of PLCη1, according to the manufacturer's guidelines. This mutation resulted in a variant that lacked a large portion of its C-terminal domain. Primers containing the required mutation were used for creating the mutant plasmid in PCR cycles. The kit also contained 1x buffer and PfuTurbo which is a proofreading DNA polymerase. Following amplification, DNA was digested by the restriction enzyme, DpnI which targets methylated DNA. The samples were prepared for sequencing to confirm the mutation.

6.2.3. Immuno-labelling

Transfection of Cos7 cells by electroporation, and immuno-labelling of COS7, C3H10T1/2 and N7 cells were performed in accordance to protocols described in Chapter 2. Primary antibodies used were: PLCη1 (Abcam, dilution 1:50, Cambridge, UK), alpha Tubulin (Abcam, dilution 1:100), β-actin (Abcam, dilution 1:100), and Acetylated Tubulin (Abca,, dilution 1:50).

6.2.4. Nucleofection

C3H10T1/2 or N7 cells were cultured in 15 cm dishes until they were 80% confluent, dislodged by trypsinisation and counted using the hemocytometer as described in Chapter 2. 5 million cells were used for each transfection. Cells were centrifuged at 90 x g to remove culture media and washed by re-suspension in Optimem (Life-technologies), in the same volume of media that was removed. Centrifugation was repeated and Optimum was removed. Cell pellet was then re-suspended in 100 µl of nucleofector solution V (Lonza, Basel, Switzerland) and mixed with 2 µg of a GFP expressing vector (gift from Dr Javier Tello, University of St Andrews, UK). This mixture was then placed into electroporation cuvettes and nucleofection was performed using amaxa nucleofector 1 (Lonza, Basel, Switzerland) and program T-030. Cells were immediately placed into 500 µl of complete culture media and seeded into 6-well plates. Following 48 hour incubation, transfection efficiency was determined by the number of fluorescent cells using the Zeiss Axiovert 40 CFL microscope with a 10× objective (Carl Zeiss Ltd., Cambridge, UK).

The same method was used to transfect EV, PLCη1 and mut.PLCη1 plasmids into N7 cells. RNA extraction, cDNA synthesis and qPCR analysis were performed according to protocols mentioned in Chapter 2.

6.2.5. Shh-N preparation

Shh-N was purchased from (R&D systems, MN, USA). This was reconstituted in sterile PBS containing 0.1% bovine serum albumin (0.1% BSA). A 0.45 µm syringe filter (Sartorius, Gottingen, Germany) was then used to sterilise the solution. Each well was treated with 0.5 µg of Shh-N. In control wells, 0.1% BSA was added. Review of the literature revealed that a concentration of 0.5 µg/ml is sufficient to elicit a response. As shown in Figure 6.4, this concentration will displace ~80% of immunolglobulin-labelled Shh (Shh-Ig) from its receptor, Patched (Pepinsky et al., 1998). Therefore, 0.5 µg/ml of Shh-N was used in experiments.

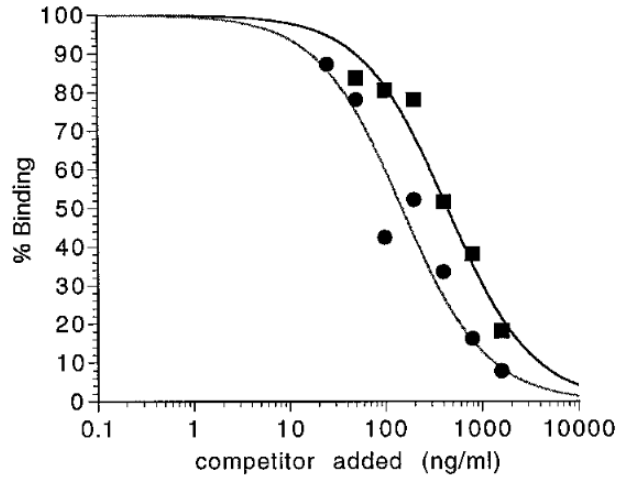

Figure 6.4: Binding affinity of Shh-N at different concentrations. EBNA-293 cells were transfected with Ptch then incubated with 5 nM Shh-Ig and serial dilutions of competitor Shh ligand, with (■) and without (●) the palmitoylation modification. Binding of Shh-Ig was then determined by Fluorescence activated cell sorting (FACS) analysis. Binding of both palmitoylated and unpalmitoylated Shh increases in a dose dependent manner. Image taken from Pepinsky et al., 1998.

6.2.6. Primers

Conventional and quantitative PCR was performed according to the methods in Chapter 2. Primer pair sequences used in this chapter are listed in Table 6.2.

Primer	Nucleotide sequence	Size of band (base pairs)
PLCη1, variant1-F	5'-CTGTCTGGCAGGAGACAAGG-3'	377
PLCη1, variant1-R	5'-CCAGGTTCTCTACCTCCAGAG-3'	
PLCη1, variant 2-F	5'-CTGTCTGGATCTGAATAGGAAGC-3'	265
PLCη1, variant 2-R	5'-CTTCGTTGCAGGATCCAGAGC-3'	
PLCη1, variant 3-F	5'-CTGCTTGGTACAGATCTGAATAGG-3'	253
PLCη1, variant 3-R	5'-CATTCCATGCAGTCTCTCTTG-3'	
PTCH-F	5'-CCTCAACTCATGATACAGACTCC-3'	250
PTCH-R	5'-CTTCTCCTATCTTCTGACGGG-3'	
SMO-F	5'-GCTGTGTGCTGTCTACATGC-3'	283
SMO-R	5'-GCTGTGCATGTCCTGGTGC-3'	
NEO1-F	5'-CTATCAGTGTGTAGCCACTGTGG-3'	249
NEO1-R	5'-CAACAATGCAGCGGTAGAGTC-3'	
β -ACTIN-F	5'-GACAGACTACCTCATGAAGATCC-3'	264
β –ACTIN-R	5'-GTCAACGTCACACTTCATGATGG-3'	
RPLP0-F	5'-AGATTCGGGATATGCTGTTGGC-3'	65
RPLP0-R	5'-TCGGGTCCTAGACCAGTGTTC-3'	
PLCη1 mutation primer- F	CCAAATATGACAAATGATTGCCAGGAAAACCAC TAGCCCCCGAAATTCCTTTC	-
PLCη1 mutation primer- R	GAAAGGAATTTCGGGGGCTAGTGGTTTTCCTGGC AATCATTTGTCATATTTGG	

Table 6.2: List of primers used in conventional and quantitative PCR in this chapter

6.3. Results

6.3.1. The mutated form of PLCη1 has altered localisation in transfected Cos7 cells

As mentioned previously, due to the compartmentalised nature of cells, the localisation of a protein can provide some clues as to its functional role. In order to identify whether the mutated form of PLCη1 has altered function due to different cellular localisation, Cos7 cells were transfected with the mutant and WT form of PLCη1, then labelled with an antibody specific to

PLCη1. Cos7 cells were chosen as they do not express endogenous PLCη1 (Stewart et al. 2007) and so the PLCη1 antibody will only show exogenously expressed PLCη1.

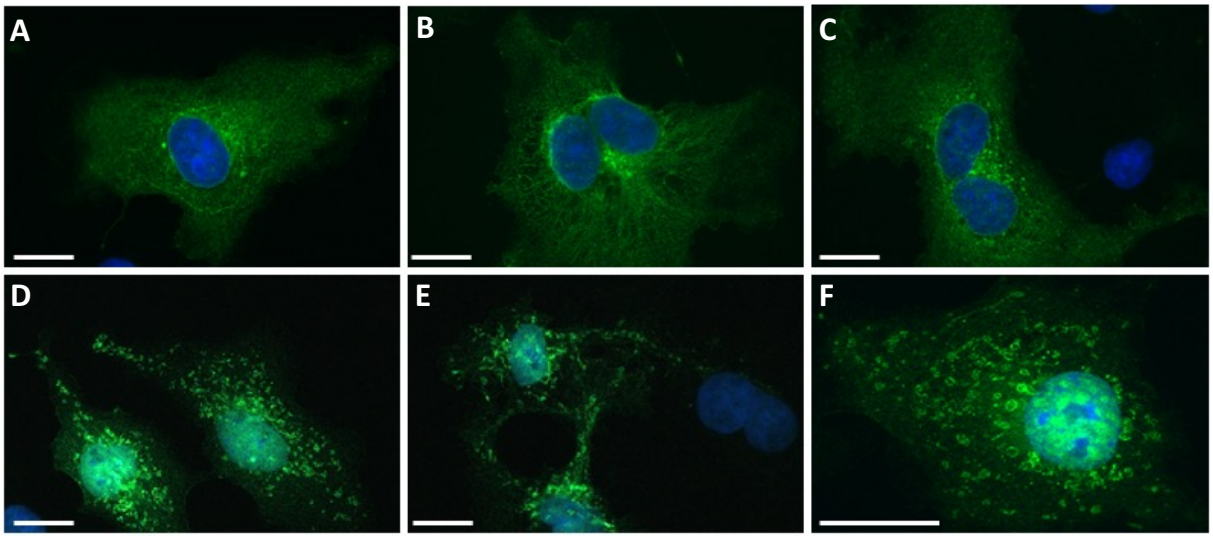

Figure 6.5: Merged images of Cos7 cells overexpressing WT and mutated PLCη1 (both in green). **A**, **B** and **C** show distribution of overexpressed PLCη1throughout the cytoplasm. **D**, **E** and **F** show localisation of mutated PLCη1 in the nucleus and throughout the cytoplasm. Cells were counterstained with DAPI (blue) to show the nucleus. Images were taken using Leica DFC3000 fluorescence microscope at x20 and x40 magnification (Leica Microsystems GmbH, Wetzlar, Germany). Scale bars represent 20 µm.

Immunolabelling of exogenously expressed PLCη1 as shown in Figure 6.5 reveals that it is distributed throughout the cytoplasm of Cos7 cells, mainly around the nucleus and appears to be cytoskeletal. The mutated variant however has a completely different localisation and is mainly present in the nucleus and throughout the cytoplasm. At a higher magnification (Figure 6.5F) it can be seen that the mutated form of PLCη1 is localised in vesicle-like structures throughout the cell.

6.3.2. Identifying cell lines with active Shh signalling and efficiently transfecting them

To establish the role of PLCη1 in the Shh pathway it was important to use a cellular model that endogenously expresses the protein components of the Shh pathway. Two cell lines were chosen for experiments; an embryonic mesenchymal stem cell line called C3H10T1/2, which has been utilised by others to study the Shh pathway (Shea et al., 2003, Zehentner et al., 2000)

and an embryonic hypothalamic cell line called N7. The latter were chosen because they are obtained from mouse embryonic tissue (between days 14-17) and it seemed possible that they would express Shh pathway genes. The suitability of these cell lines for studying the Shh pathway was determined by confirming the expression of Shh pathway genes, Smo, Ptch and Neo1 via RT-PCR as shown in Figure 6.6.

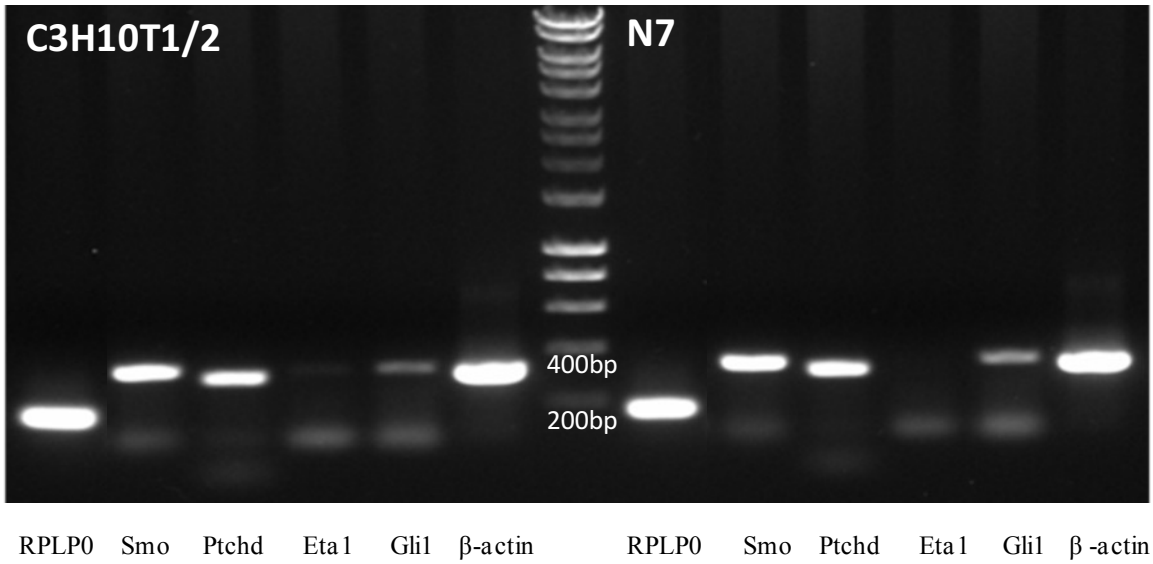

Figure 6.6: Gel showing the presence of Shh pathway genes in C3H10T1/2 and N7 cells. RPLP0 and β-actin were used as positive control. Abbreviations: Smo, Smoothened; Ptchd, Patched; Eta1, PLCη1. Hyperladder I used as DNA ladder.

The identified mutation was in human PLCη1 variant 1 (the longest isoform) and does not affect other variants. This is because the mutation is in the final large exon of variant 1. Variant 2 and 3 are spliced to form a shorter overall protein that lacks a large C-terminus, so they will be unaffected by the mutation. This is also the case for mouse PLCη1. Figure 6.7 shows the differences in exon composition between all three PLCη1 mouse variants. Mouse PLCη1 variant 1 shows 89.5% sequence homology with the human variant, as determined by the Emboss Needle alignment tool (data not shown), so it will be affected in a similar way. Expression of all three PLCη1 variants was also determined in both cell lines. As shown in Figure 6.8, PLCη1 is expressed in both cell lines.

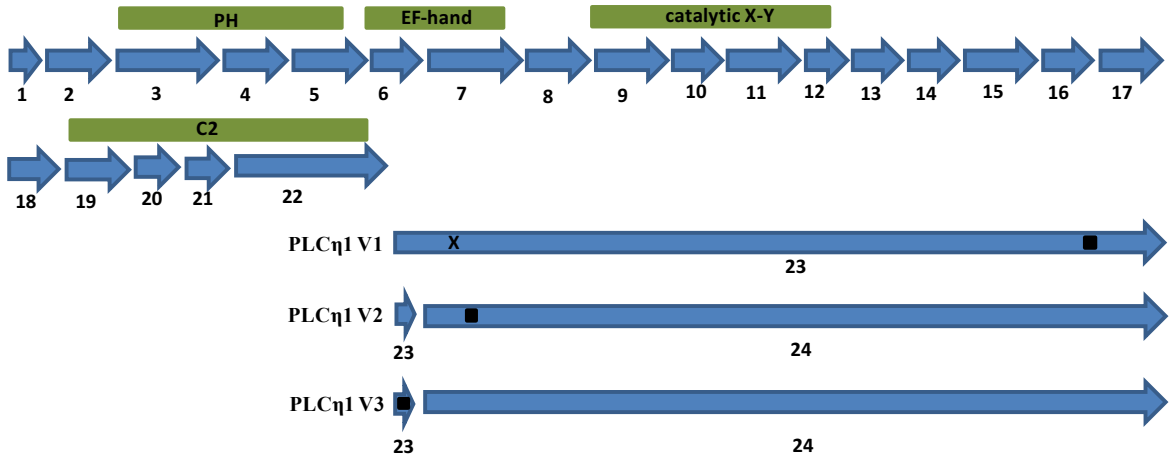

Figure 6.7: Differences in exon composition between the three splice variants (V) of mouse PLCη1. The arrows represent different exons and length of arrows represents their relative size. All three variants possess the same sequence from exon 1 until exon 22. V1 and V2 are spliced to form a short exon 23 (23 bp and 28 bp, respectively). Relative positions of stop codons are indicated by ■. The created mutation is marked with **X** (224 bp into exon 23) which truncates a large portion of PLCη1V1 C-terminus (by 1855 bp). Green bars represent relative location of PH, EF-hand, catalytic X-Y and C2 domains in relation to different exons. Image produced by author of this thesis

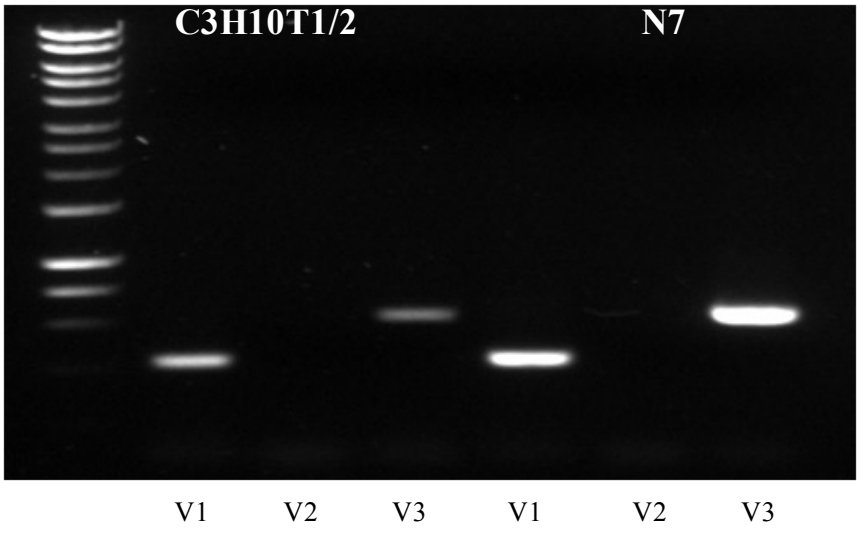

Figure 6.8: Expression of PLCη1 variants in C3H10T1/2 (lanes 2-4) and N7 cells (lanes 5-7). Both cell lines express variants 1 and 3 but not variant 2.

Having identified C3H10T1/2 and N7 cells as suitable cell lines for studying the Shh pathway, a variety of methods namely chemical transfection (via lipofectamine and FuGENE 6 tranfection reagents), electroporation and nucleofection were utilised to establish a method that would lead to the successful transfection of these cells. This is essential as later planned experiments require efficient transfection of cells. This was determined by transfecting a GFP

expressing construct into cells. Chemical transfection and electroporation of cells did not result in efficient transfection (data not shown). Nucleofection however resulted in good expression of genes. As can be seen in Figure 6.9, this resulted in transfection of approximately 50% of C3H10T1/2 cells and approximately 85% of N7 cells, which was determined by counting the number of fluorescent cells in relation to total cells in three randomly selected regions in the micrographs. As can be seen from image 6.4, both cell lines were transfected but the N7 cell line was transfected more efficiently.

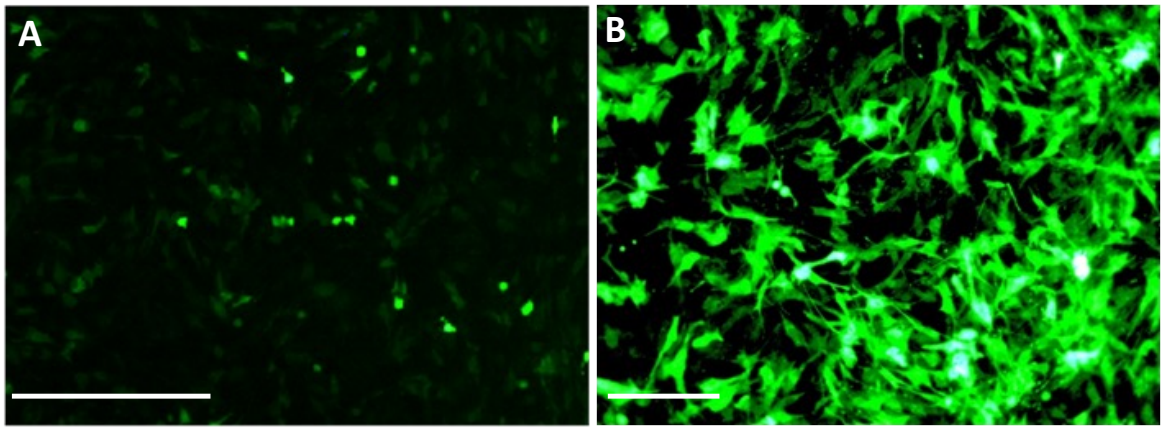

Figure 6.9: Transfection efficiency of **A** C3H10T1/2 and **B** N7 cells by a GFP expressing construct. The micrographs show a much higher level of transfection in N7 cells (~50%) compared to C3H10T1/2 cells (~85%). Dishes were fully confluent. Image's taken using Leica DFC3000 fluorescence microscope using 10 x and 20 x objective lenses. Scale bars represent 100 μm.

6.3.3. Localisation of PLCη1 in C3H10T1/2 cells

As shown previously, exogenously expressed PLCη1 in Cos7 cells revealed a cytoskeletal-like localisation. To determine whether this is the case for endogenously expressed PLCη1, C3H10T1/2 cells were labelled with an antibody specific to PLCη1 to identify the localisation of endogenous PLCη1 in cells containing the Shh pathway.

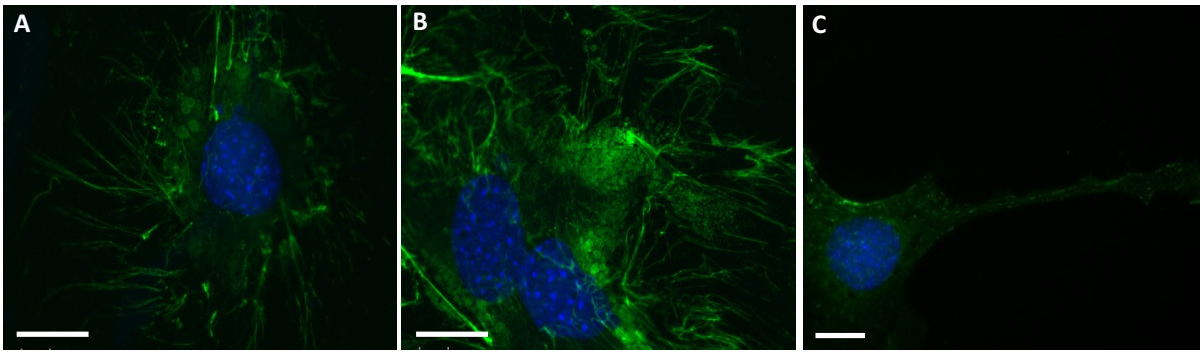

Figure 6.10: Localisation of endogenous PLCη1 in C3H10T1/2cells**. A**, **B** and **C** shows the localisation of PLCη1 in C3H10T1/2 cells. **C** shows a punctuate distribution within cell processes. Image's taken using Leica DFC3000 fluorescence microscope using 20 x and 40 x objective lenses. Scale bars represent 100 μm.

Immunolocalisation of PLCη1 in C3H10T1/2 cells as shown in Figure 6.10 reveals that PLCη1 is localised throughout the cell in linear structures, in a distribution that resembles that of the cytoskeleton. The cytoskeleton of eukaryotes is composed of microtubules made up of tubulin, microfilaments made up of actin and intermediate filaments made up of a multitude of proteins (Huber et al., 2013). Therefore, to further investigate the cytoskeletal localisation of PLCη1, C3H10T1/2 cells were dual stained for PLCη1 and tubulin as shown in Figure 6.11, and dual stained for PLCη1 and β-actin as shown in Figure 6.12. Both Figures suggest that there is some degree of co-localisation between PLCη1 and microtubules and PLCη1 and actin filaments.

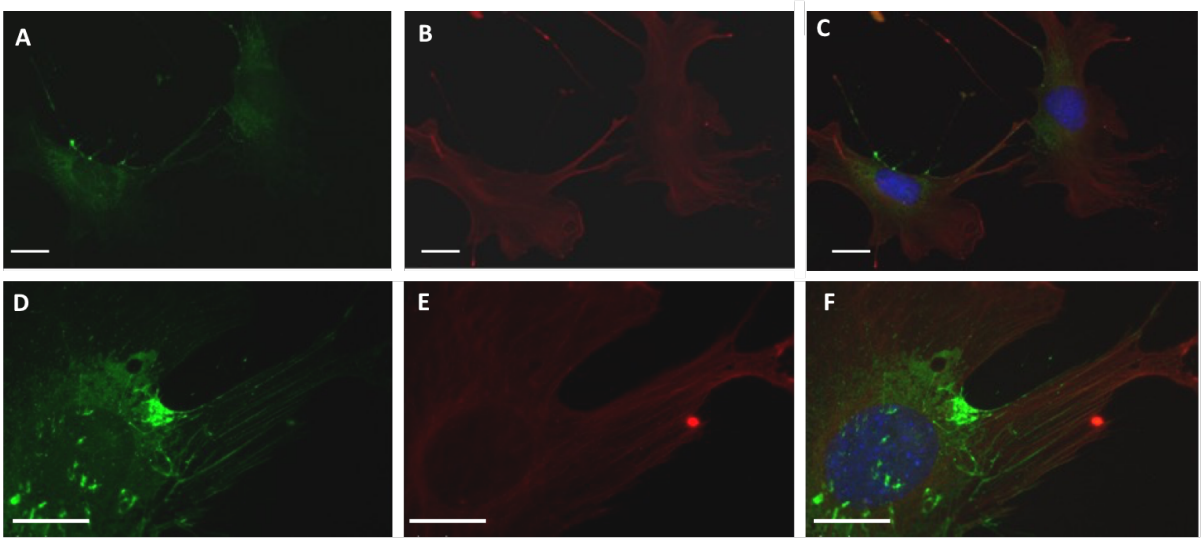

Figure 6.11: Co-localisation of PLCη1 and tubulin in C3H10T1/2 cells. Figure shows the localisation of PLCη1 (**A** and **D**), tubulin (**B** and **E**) and both merged with Dapi (**C** and **F**). Visually, a good degree of co-localisation is observed between PLCη1 and tubulin. Image's taken using Leica DFC3000 fluorescence microscope at 20 x and 40 x magnification. Scale bars represent 100 μm.

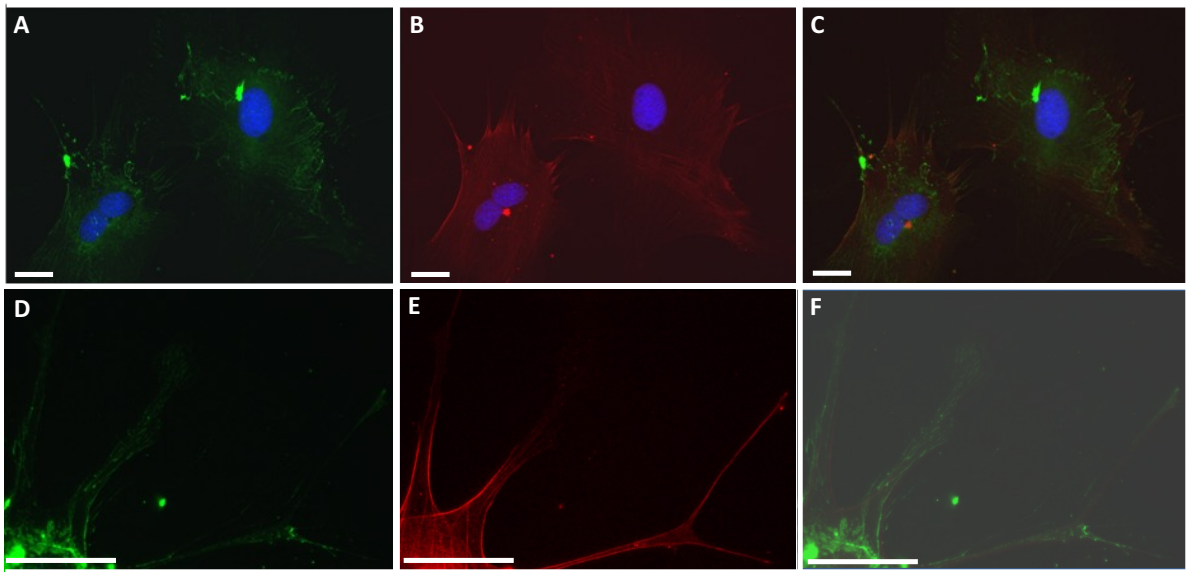

Figure 6.12: Co-localisation of PLCη1 and β-actin in C3H10T1/2 cells. Figure shows the localisation of PLCη1 (**A** and **D**), β-actin(**B** and **E**) and both merged with Dapi (**C** and **F**). Visually, a good degree of co-localisation is observed between PLCη1 and β-actin. Image's taken using Leica DFC3000 fluorescence microscope at 20 x and 63 x magnification. Scale bars represent 100 μm.

The Shh pathway occurs primarily at the primary cilium of cells (Goetz and Anderson, 2010), it was therefore investigated whether PLCη1 is present within the primary cilia by dual staining N7 and C3H10T1/2 cells with PLCη1 antibody and acetylated tubulin which labels primary cilia. As shown in Figure 6.13, PLCη1 is not present within primary cilia. As mentioned previously, some components of the Shh pathway such as Smo and Gli2 are absent from the primary cilia but are transported into this organelle upon Shh pathway activation. To understand whether PLCη1 is functioning within the primary cilia when the pathway is active, N7 and C3H10T1/2 cells were treated with Shh-N for 24 and 48 hours, then co-labelled with PLCη1 and acetylated tubulin. This however also resulted in no co-localisation (data not shown).

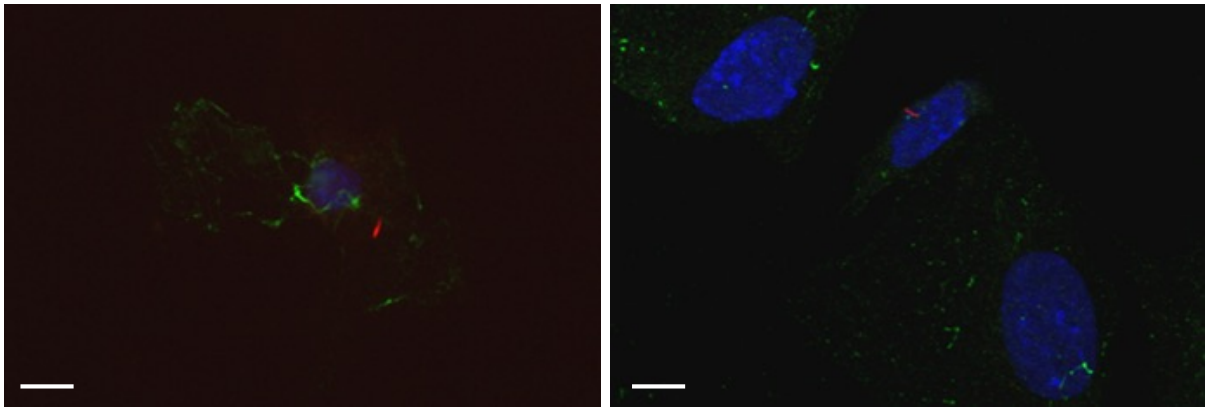

Figure 6.13: PLCη1 does not co-localise with primary cilia. Merged images showing the localisation of PLCη1 (green), primary cilia and nucleus (blue) in **A** N7 and **B** C3H10T1/2 cells. No co-localisation is observed between PLCη1 and primary cilia. Image's taken using Leica DFC3000 fluorescence microscope at 10 x magnification. Scale bars represent 10 μm.

6.3.4. The HPE associated form of PLCη1 has altered effects on Shh pathway gene expression

Because a PLCη1 mutation was identified in patients with HPE, it seemed likely that the mutant form (mut.PLCη1) of the enzyme is altering the functioning of the Shh pathway. To determine this, the expression levels of three Shh pathway genes; Smo, Ptch and Neo1 were analysed by qPCR in cells overexpressing WT and mutant form of PLCη1. Activation of the pathway leads to Gli transcription factor activation which allows transcription of Shh pathway genes, so the level of expressed genes will be a reflection of Shh pathway activity.

To allow initiation of the Shh signalling pathway, the Shh ligand must be processed in a particular way, by cleavage into an N-terminal form. Therefore Shh-N was used for this experiment. The processing steps of Hh polyproteins is shown in Figure 6.14.

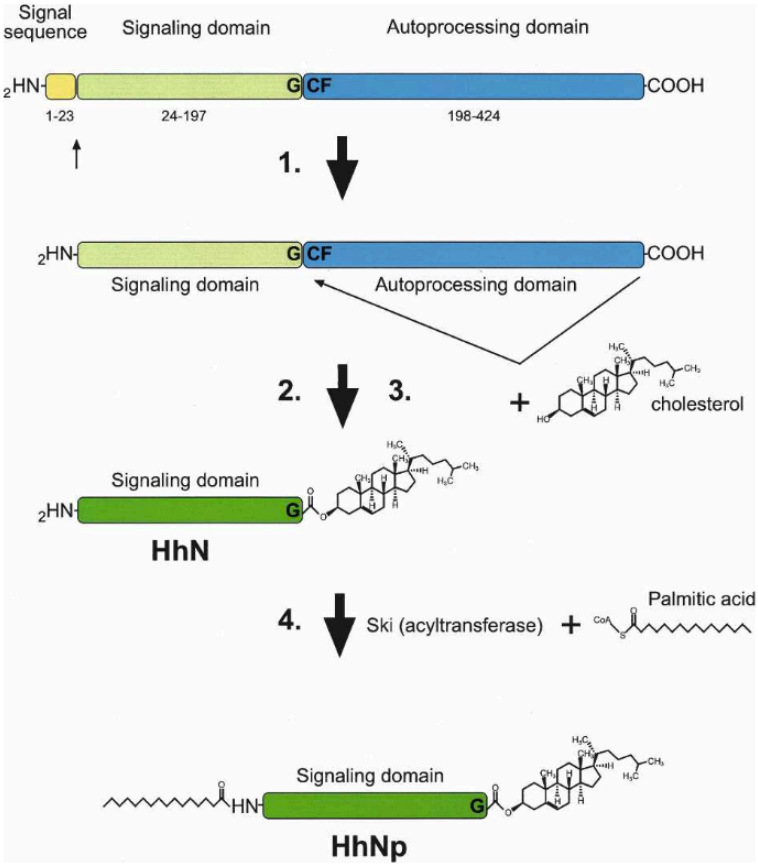

Figure 6.14: Processing steps of hedgehog proteins. Hh proteins are translated as large polypeptides, which must be processed in a particular way to carry out its function. These modifications are required to produce an active form of Shh and to allow Shh release from the cells in which it is produced. **1** The signal sequence is initially cleaved; **2** further cleavage occurs between the glycine and cystein residues and **3** cholesterol is added. Steps **2** and **3** are catalyzed by the C-terminal domain which results in formation of a C-terminal (which is rapidly degraded) and an N-terminal domain (HhN, ~19 kDa) with a bound cholesterol moiety. In this form HhN can bind to membranes, enabling addition of palimitic acid by Skinny hedgehog (an acetyl transferase) to the N terminus which forms the final product HhNp. This product can then be released from producing cells through the receptor; Dispatched (Disp) where it can bind to receiving cells. Image taken from Varjosalo and Taipale, 2008.

Before performing the planned qPCR assay, a suitable activating concentration of Shh-N was determined. This was chosen based on the studies of Pepinsky *et al*. who performed a binding assay to establish the concentration of Shh that is required for binding to its receptor Ptch, in EBNA-293 cells. As shown in Figure 6.4, 0.5 µg/ml Shh is sufficient to displace ~80% of Shh-Ig from ptch, following preincubation of ptch-transfected EBNA-293 cells with 5 nM Ig-Shh (Pepinsky et al., 1998) Yuasa *et al.* further showed this concentration to be sufficient for stimulating alkaline phosphatase activity, which is a marker of Shh pathway activity (Yuasa et al., 2002). This concentration was therefore used to treat N7 cells for 48 hours. The level of

Shh pathway genes were then analysed by RT-PCR to determine the amount of gene expression before and after treatment. Three genes were analyzed, Smo, Ptch and Neo1. As can be seen in Figure 6.15, the levels of all three genes increase upon treatment with Shh so this concentration and time point will be used to initiate the Shh pathway in planned assays.

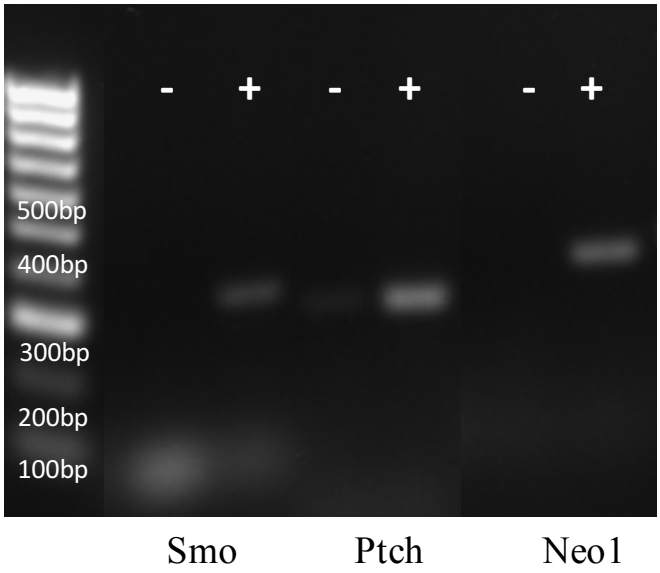

Figure 6.15: Expression of genes involved in the Shh pathway in cells treated (+) and untreated (-) with Shh for 48 hours. Expression levels of all genes were noted to increase upon Shh treatment.

Using qPCR, the expression levels of Shh pathway genes; Smo, Ptch and Neo1 were analysed in N7 cells that were transfected with EV, PLCη1, and mut.PLCη1, then treated with Shh-N or vehicle as a control. Expression levels of two genes, Smo and Ptch that are directly involved and are essential in the Shh pathway was analysed. Expression of Neo1 which is believed to regulate Shh pathway activity indirectly was also analysed. Results are shown in Figure 6.16.

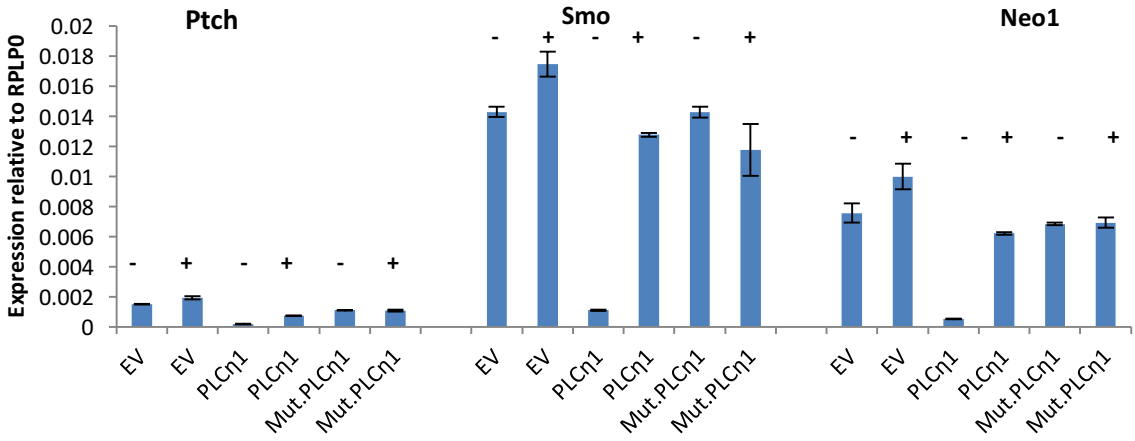

Figure 6.16: qPCR results showing expression levels of Ptch, Smo and Neo1 following treatment with Shh-N (+) and vehicle (-) in transfected N7 cells. n=3.

Gene expression results from Figure 6.16 reveal a similar trend for all three genes. Ptch (1.3-fold), Smo (1.2- fold) and Neo1 (1.3-fold) gene expression increases following Shh-N treatment in the EV control transfected cells. In PLCη1 transfected cells, expression levels are much lower for Ptch (6.3-fold), Smo (13.1-fold) and Neo1 (13.4-fold) compared to mut.PLCη1 transfected cells. However expression levels of Ptch (4.1-fold), Smo (11.7-fold) and Neo1 (12.2-fold) increased greatly following Shh-N treatment of PLCη1 transfected cells. This however results in partial rescue as levels of Ptch (2.1-fold), Smo (1.1-fold), and Neo1 (1.2-fold) are still higher in untreated EV transfected cells. Mut.PLCη1 transfected cells also show higher levels of Ptch (1.5-fold), Smo (1.1-fold) and Neo1 (1.1-fold) gene expression in comparison to Shh-N treated PLCη1 transfected cells. In the mut.PLCη1 transfected cells, expression levels are very similar to control EV transfected cells, but this group appears to be unresponsive to Shh treatment, as evident from the inability of Shh-N to cause a change in the level of Ptch, Smo or Neo1 in these cels.

6.4. Discussion

The aim of this chapter was to establish the role that PLCη1 may play during embryonic development, through localisation studies and by examining its influence upon Shh signalling. The mouse PLCη1 gene was cloned into an expression vector and mutated based on the findings of Prof. Geoff Woods and Dr Mike Nahorski (University of Cambridge, UK). In their studies, they identified a mutation in PLCη1 in children born with HPE (unpublished data). The identified mutation was in isoform 1, the longest isoform and results in a STOP in the sequence, which truncates the protein by 615 amino acid residues thereby producing a protein

that lacks a large portion of its C-terminal tail region. The mouse variant will be indicative of the human variant as they possess 89.5% homology. Most of this variation is in the C-terminal domain and there is a 98.2% sequence homology preceding the mutation.

6.4.1. Localisation of PLCη1 in embryonic cells

Following overexpression of the appropriate WT and mutated PLCη1 isoforms into COS7 cells (which do not endogenously express PLCη1), two very different localisations was observed. WT PLCη1 was present throughout the cytoplasm, in a cytoskeletal-like distribution. Mutant PLCη1 on the other hand was present in the nucleus as well as in round vesicle-like structures. It is likely that the C-terminus is a major determinant of subcellular localisation and without it; localisation is most-likely under the control of the PH and/or C2 domains, both of which are still present in the mutated form. The C-terminal tail therefore appears to be important in determining the localisation of PLCη1. As discussed in Chapter 4 and 5, localisation sequences present on the C-terminal tail are a major determinant of a proteins cellular localisation as these sequences allow entry into different cell compartments, the lack of which could explain the altered cellular localisation of mutated PLCη1. PLCη1 also contains a PDZ binding motif at the C-terminus which is a short sequence (usually 5 residues) that is recognised by the PDZ domain of other proteins, thereby allowing interaction with proteins that contain a PDZ domain (Lee and Zheng, 2010, Saras and Heldin, 1996). The PDZ domain is named as such based on the first three proteins in which it was identified; post synaptic density-95 (PSD-95), *Drosophila melanogaster* (DLG) and zonula occludens (Zo-1) (Harris and Lim, 2001). PDZ domains consist of 80-100 residues, comprised of six β-strands (βA-F) and two α-helices, one short (αA) and one long (αB) (Fanning and Anderson, 1996, Lee et al., 2009a, Lee et al., 2009b). Many PDZ domains have been identified in multiple proteins and thus far, 928 PDZ domains have been identified in 328 mouse proteins (Spaller, 2006). Such a diverse range of PDZ domains is indicative of their importance within cells. The most prevalent function of PDZ domains is recognition of PDZ binding sequences on other proteins. Following recognition, the two proteins join by addition of a β-strand from the partner protein to the groove between the βB and αB in the PDZ domain, a process referred to as β-strand addition (Doyle et al., 1996). By allowing such protein-protein interactions, this domain is important for creating multi-protein machines as well as influencing the transport and localisation of proteins (Lee and Zheng, 2010). Therefore without its C-terminal tail, PDZ domain containing proteins cannot bind to PLCη1 as the PDZ binding motif is no longer available, and this can

influence its cellular localisation. PLCβ for example can be regulated by PDZ domain containing proteins (Hwang et al., 2000, Tang et al., 2000). PLCβ isoforms have been implicated in the process of phototransduction by binding to PDZ domains of an important protein in the *Drosophila* phototransduction pathway called INAD (Tsunoda et al., 1997). Mammalian PLCβ1 and PLCβ2 isoforms also interact with the PDZ domain of a protein called NHERF which binds to TRP4 Ca^{2+} channels (Tang et al., 2000). NHERF also contains a C-terminal region called the FERM domain which interacts with the cytoskeletal protein, ezrin (Reczek et al., 1997). This interaction can therefore enable linkage of PLCβ1 and PLCβ2 to the cytoskeleton. The C-terminal of PLCγ1 is also required for its binding to the cytoskeleton by attaching to actin filaments, although this occurs by direct binding via its SH2 domain (Pei et al., 1996).

Similar events may be involved in the attachment of PLCη1 to the cytoskeleton as immuno-labelling experiments in this chapter show a cytoskeletal-like distribution in COS7 cells that exogenously express PLCη1. In C3H10T1/2 cells, endogenous PLCη1 also shows a cytoskeletal-like distribution which co-localises to some degree with actin and tubulin which are components of the cytoskeleton. In accordance, Yamaga *et al.* showed co-localisation of PLCη2 with actin filaments in PC12 cells (Yamaga et a., 2015). Further studies are required to understand how and why PLCη1 is binding to the cytoskeleton. One possibility is association with motor proteins that travel along the cytoskeleton. These include kinesin and dynein that move their cargo (proteins, vesicles, organelles) in opposite directions along microtubule filaments by sensing the polarity of microtubules. Kinesin travels retrogradely, away from the nucleus (+ end of microtubules) whereas dynein travels anterogradely, towards the nucleus (- end of microtubules) (Hirokawa et al., 1998, Vale, 2003), as shown in Figure 6.17. This is also the case for myosin V and VI that travel in opposite directions on actin filaments (Wells et al., 1999). Indeed, Gli transcription factor must enter into the nucleus to activate transcription. May *et al.* reported impairment of Gli activity in a mutant mouse with dysfunctional dynein 2 protein. Kim *et al.* further showed a punctuate cytoplasmic distribution for Gli2 and reported inhibition of Shh pathway activation following disruption of microtubules (by vinbastine) in NIH 3T3 cells (Kim et al., 2009). By being in close proximity to motor proteins, PLCη1 may be involved in creating the necessary Ca^{2+} signals that are required for proper motor protein function. Ca^{2+} dependent calmodulin for example, is important for maintaining the structural integrity of motor proteins and regulating their function. Kinesin-like calmodulin-binding protein (KCBP) which is a member of the kinesin motor protein family is disrupted by binding

of calmodulin, resulting in its dissociation from microtubules (Casey et al., 2003, Espindola et al., 2000, Song et al., 1997). The significance of such an event is not fully understood but dissociation may help certain motor proteins to skip others by manoeuvring over them or dissociating, then re-binding to adjacent microtubules in order to bypass motor protein "traffic" along microtubules.

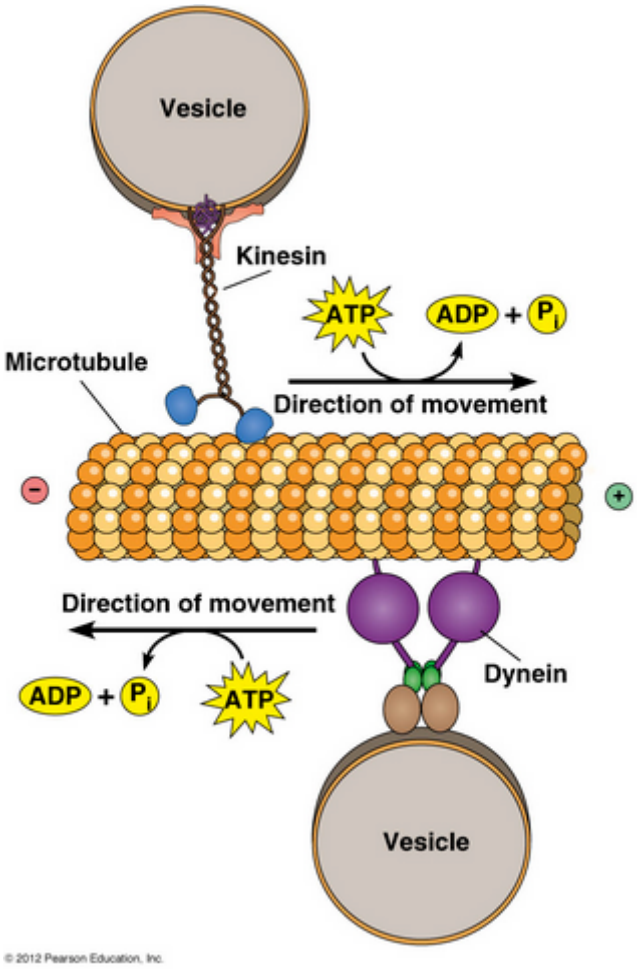

Figure 6.17: Diagramatic representation of kinesin and dynein motor proteins. Kinesisns hydrolyse ATP, allowing them to "walk" in a step by step manner along microtubules towards the plus end. Dyneins move their cargo towards the minus end by the same process. Image taken from Harden et al., 2012.

6.4.2. Relevance of PLCη1 to the Shh pathway

By analysing the expression levels of Shh pathway genes (Ptch, Smo and Neo1) in N7 cells overexpressing PLCη1 and comparing it to N7 cells overexpressing the HPE associated mutant form (mut.PLCη1), an insight into the effects of mut.PLCη1 on the Shh pathway was attained. Two interesting results were obtained from the performed qPCR assay. The first one is the significantly lower mRNA levels of Ptch, Smo and Neo1 in PLCη1 transfected N7 cells

compared to mut.PLCη1 transfected cells. This indicates that overexpression of PLCη1 is causing repression of the pathway which may be occurring as a result of altered Ca^{2+} dynamics in the cell, resulting from increased PLCη1 activity. Shh ligand release from producing cells through the receptor Dispatched, or Shh processing to form the N-terminally modified active form may be Ca^{2+} regulated processes. Such events may explain why Ptch, Smo and Neo1 gene activity is low in PLCη1 transfected N7 cells but increases following Shh-N treatment. Further experiments are however required to determine the components of the Shh pathway that are influenced by Ca^{2+}. The other intriguing finding was the inability of Shh-N to alter the expression of Ptch, Smo and Neo1 in cells that were transfected with mut.PLCη1. Therefore, it appears that Shh-N is not having an effect on these cells. This is in contrast to EV transfected control cells which did show a rise in Ptch, Smo and Neo1 gene expression upon Shh-N treatment. One possibility for this is that the transcriptional machinery is engaged in creating the mutant form of PLCη1 and therefore may not be responding efficiently to Shh-N treatment.

In general, qPCR results revealed different levels of Shh pathway gene expression in cells overexpressing PLCη1 and mut.PLCη1. It therefore appears that the mutant form is influencing the Shh pathway but in mechanisms occurring outside of the primary cilium of cells as it was established that PLCη1 is not present in the primary cilium of N7 or C3H10T1/2 cells. This was unexpected because the Shh pathway functions in the primary cilium of cells (Goetz et al., 2009, Goetz and Anderson, 2010) and inactivity of the Shh pathway is known to result in the developmental midline defect, HPE (Roessler et al., 1996). As mentioned previously, a mutation in PLCη1 was observed in children born with HPE but because PLCη1 is not present in the primary cilium, it may not be functioning directly in the Shh pathway, at least not in mechanisms within the primary cilium. One possibility is that PLCη1 is involved in dissociation of Gli from its suppressor Sufu which may be a Ca^{2+} dependent process. Another possibility is its involvement in regulating the expression or activity of Smo. Physiological Smo activity is essential for Shh pathway activity as its loss, and sometimes gain of function results in embryonic lethality in mice (Dey et al., 2012, Zhang et al., 2001). Smo functions by activating Gli transcription factors after entering into the primary cilium. In order to do so, Smo must first be up-regulated to the plasma membrane which occurs after removal of its inhibition by Ptch, following Shh ligand binding. It may be possible that PLCη1 is involved in the Shh pathway by assisting in upregulation of Smo to the plasma membrane or regulating its translocation into the primary cilium. This could explain why it is having an effect on the Shh pathway genes despite its absence in primary cilia. Smo is a seven-transmembrane GPCR and

is able to activate the $G\alpha_i$ (but not any other) family of G-proteins. Ogden *et al.* have reported activity of $G\alpha_i$ immediately downstream of Smo in *Drosophila* (Ogden et al., 2008). Also, zebrafish embryos treated with pertussis toxin (PTX), which uncouples $G\alpha_i$ from Smo, result in inhibition of muscle development (Hammerschmidt and McMahon, 1998). PTX also results in inhibition of Gli following Shh treatment of fibroblasts, but not in fibroblasts expressing constitutively active $G\alpha_i$ (Riobo et al., 2006).

$G\alpha_i$ activity in cilia suggests that heterotromeric $G\beta\gamma$ can function to activate PLC enzymes in this organelle. However Zhou *et al*. have reported the inability of $G\beta\gamma$ heterodimers to activate PLCη1 (Zhou et al., 2008), therefore other PLC isozymes may be activated. Belgacem *et al*. have addressed the possibility of PLC activation in the Shh pathway and have proposed a pathway as shown in Figure 6.18. This was based on their investigation into the relationship between the Shh pathway and Ca^{2+} dynamics in embryonic cells. Early Ca^{2+} spike activity, like Shh activity, is an embryonic developmental cue that is required for neuronal migration, differentiation and proliferation (Hanson and Landmesser, 2004, Komuro and Rakic, 1996, Manent et al., 2005). They showed via Ca^{2+} imaging, a higher Ca^{2+} spike duration and frequency in ventral embryonic spinal cord cells compared to lateral ones, in a graded manner (Belgacem and Borodinsky, 2011). Such a gradient also occurs for Shh in the embryonic spinal cord (Chamberlain et al., 2008, Echelard et al., 1993). They further showed that Shh-N causes an increase in Ca^{2+} spike activity in *Xenopous* embryonic spinal cells, in a dose dependent manner. The same result was achieved by overexpressing an active form of Smo (SmoM2) and by the Smo agonist SAG but inhibited by cyclopamine, a Smo antagonist (Belgacem and Borodinsky, 2011). Further investigation using a mixture of neuronal and notochord explant cells revealed higher Ca^{2+} spiking activity in neurons that were in close proximity to the notochord cells, an effect that was prevented by using cyclopamine. This indicates that Shh release from the notochord is responsible for raising Ca^{2+} spike activity in neurons. After showing the necessity of extracellular Ca^{2+} and voltage gated Ca^{2+} channels for Shh induced Ca^{2+} spike activity, the authors investigated whether intracellular Ca^{2+} is also required in this process. By blocking PLCs and in a separate experiment, $Ins(4,5)P_3Rs$, Ca^{2+} spike activity was prevented following Shh-N treatment in both cases, which indicates the importance of Ca^{2+} release from internal stores (Belgacem and Borodinsky, 2011). As discussed in Chapter 3, the only known activator of PLCη1 is Ca^{2+}. PLCη1 may therefore be functioning downstream in the pathway, after the initial activated PLC isozyme raises intracellular Ca^{2+} levels, which can

be a contributing factor to the rise in Ca^{2+} spike activity that is required for embryonic development.

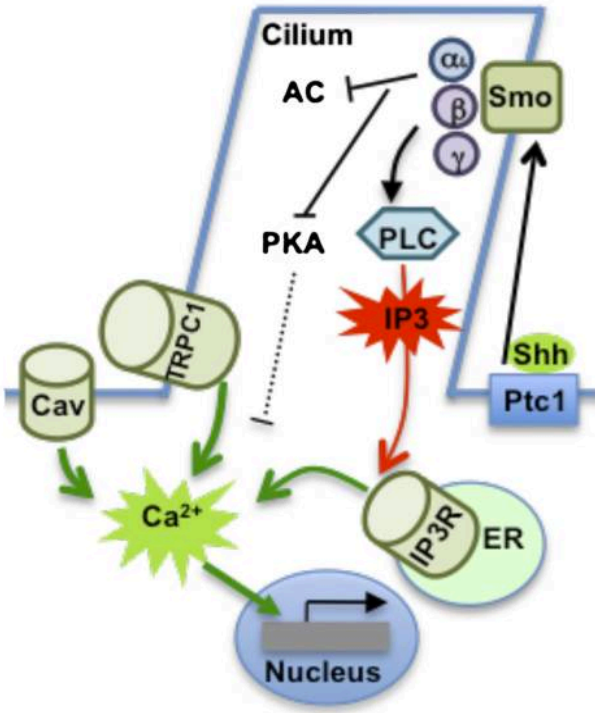

Figure 6.18: Modes of increased intracellular Ca^{2+} as a result of Shh pathway activation. Following binding of Shh to its receptor Ptch, Smo is activated resulting in the activation of heterotrimeric G proteins. The $G\alpha_i$ subunit inhibits AC and therefore PKA which can inhibit IP3 induced Ca^{2+} release. The Gβγ subunit can activate PLC enzymes, resulting in increased IP3 levels. This can then open IP3Rs on the ER to increase intracellular Ca^{2+} levels. Emptying of ER store can also activate of TRPC1 which can subsequently depolarise the membrane, thus leading to opening of voltage gated Ca^{2+} channels. All of these events can contribute to Ca^{2+} spike activity. Abbreviations: AC- adenylyl cyclise, Cav- Voltage gated Ca^{2+} channels, Ptch1, patched 1; Er, Endoplasmic reticulum; PKA, Protein kinase A. Image taken from Belgacem and Borodinsky, 2011.

6.5. Conclusion

This chapter has provided further insight into a mutant form of PLCη1 that is implicated in the development of HPE. A corresponding PLCη1 variant of the mouse protein was created that lacked a C-terminal tail region and was shorter by approximately 600 amino acid residues compared to WT PLCη1. Following overexpression of both variants in COS7 cells, two very different distributions were observed. Whereas the mutant form was localised in the nucleus and in vesicle-like structures, the WT form was present throughout the cytoplasm, in what appeared to be a cytoskeletal-like distribution, indicating that the C-terminal is an important factor in determining the intracellular localisation of PLCη1. Immuno-labelling of embryonic

C3H10T1/2 and N7 cells that possessed Shh pathway genes also showed a cytoskeletal localisation for endogenous PLCη1, with some degree of co-localisation with microtubules and actin filaments. The significance of this to the Shh pathway remains to be determined. The Shh pathway is present within the primary cilium of cells and requires the movement of components in and out of this compartment via motor proteins. It may be possible that PLCη1 is regulating Ca^{2+} related processes that are required for proper motor protein function.

The WT and mutant form of PLCη1 also showed different effects on the expression of Shh pathway genes. Expression of three genes, Ptch, Smo and Neo1 was lower in cells overexpressing PLCη1 compared to the mutant form, which suggests that the increase in expression of PLCη1 is causing pathway repression, potentially as a result of alterations in the cells Ca^{2+} dynamics. If the pathway is indeed regulated at a crucial point by Ca^{2+}, the mutated form that is associated with HPE may be causing disease due to its inability to generate sufficient Ca^{2+} signals. Immuno-labelling however did not show co-localisation of PLCη1 with the primary cilia which suggests that PLCη1 is influencing the Shh pathway prior to, or after events in the primary cilium. Based on the high Ca^{2+} sensitivity of PLCη1, the most promising explanation thus far is the involvement of PLCη1 downstream in the Shh pathway where it may be involved in Shh induced generation of Ca^{2+} spike activity which is essential for embryonic development. This may explain why a mutation in PLCη1 causes abnormal embryonic development. The identification of a mutant form of PLCη1 as a factor in HPE further strengthens the notion that PLCη enzymes are involved in neurodevelopmental processes.

Chapter 7

Summary of findings, future directions and conclusion

The work carried out in this thesis has strengthened the current understanding of PLCη enzymes and has clarified several questions that were in doubt. These findings have also raised questions and experimental hypotheses that can drive forward research on PLCη enzymes inorder to further understand their biochemical functions and relevance to disease. This chapter aims to summarise the research findings of this thesis by reviewing the key findings of each chapter and suggests future experiments inspired by these findings.

The activation of PLCη1 and PLCη2 by Ca^{2+} has been confirmed using the method employed by Popovics *et al.* (Popovics et al., 2011). Both isozymes showed activation by physiological levels of Ca^{2+}, showing an approximately two fold increase in activity between 0.1 μM and 1 μM free Ca^{2+} and maximal activation at 10 μM. To identify the exact Ca^{2+} concentration at which the activity of PLCη2 shows greatest elevation of activity, a more precise Ca^{2+} gradient must be set, i.e. the same experimental conditions can be used however transfected Cos7 cells should be incubated in solutions containing Ca^{2+} concentrations ranging from 0.1 μM to 1 μM, with 100 nM increments in concentration. The Ca^{2+}-binding properties of the EF-hand domain may also be understood more clearly if this domain was purified and crystalised, then used in downstream experiments such as Isothermal Titration Calorimetry (ITC) which is able to detect with high sensitivity, the interactions between proteins and small molecules (Bounds et al. 2002).

Using viral 2A sequencies and performing an inositol phosphate release assay, it was confirmed that Gβ1γ2 is indeed an activator of PLCη2 as reported by Zhou *et al*. (Zhou et al., 2005). This system can therefore be used to investigate the activation of both PLCη1 and PLCη2 by different Gβγ combinations to identify other Gβγ heterodimers that may activate them. Additionally, this system can be used to investigate the activation of other proteins by Gβγ heterodimers.

The subcellular localisation of PLCη2 has been clarified in Neuro2A cells using immuno-electron microscopy, showing presence primarily in the nucleus and to a lower extent in the cytoplasm and plasma membrane. This suggests that PLCη2 principally functions to regulate nuclear processes, while maintaining the classical role of PLC enzymes, which is to break down PtdIns(4,5)P_2 into Ins(4,5)P_3 and DAG. A number of cellular processes are regulated by nuclear

Ca^{2+} including cell division, apoptosis and gene transcription (Berridge, 2001). These processes may be assessed by utilising PLCη2 KD cells and comparing with ShRNA control cells to determine the extent of which these processes are affected. The latter has been assessed to some extent using a RARE luciferase assay, where Popovics *et al*, showed a reduction in RA induced transcription activity in PLCη2 KD cells, showing a 60% decrease in luciferase activity, which was linked to RARE (Popovics et al, 2013). It will be interesting to look at the activity of other transcription factors to get an idea of whether PLCη2 is regulating their function. It was also shown in Chapter 3 that Gβ1γ2 can activate PLCη2. It will be interesting to investigate whether this heterodimer is present in the nucleus where it may be activating PLCη2. It may be possible that PLCη2 is functioning to maintain Ca^{2+} levels in the nucleus. A good experiment would therefore be to compare the level of Ca^{2+} in the nucleus of PLCη2 KD and ShRNA control cells using Ca^{2+} sensitive fluorescent dyes.

PLCη2 was also found to localise to the mitochondria, which is interesting as its activity was previously shown to increase in response to the Na^{+}/H^{+} antiporter monensin (Popovics et al., 2011). This study has indicated the cellular compartments to which PLCη2 would localise to in neuronal cells but further immuno-EM analysis on primary neurons or RA treated Neuro2A cells that possess a more neuronal like morphology (enlarged cell body and outgrowing neurites) will give a better indication of its localisation in neuronal cells. Further analysis may be performed on brain sections to which PLCη2 localises such as the hippocampus, neocortex and olfactory bulb (Nakahara et al., 2005). This will give a better picture of PLCη2 localisation and can provide further information such as its presence at nerve endings, which can give an indication of its functional role at synapses.

Unlike PLCη2, PLCη1 was determined to have a cytoplasmic localisation and was completely absent from the nucleus. Immuno-EM analysis can be performed to identify the exact subcellular localisation of PLCη1 in Neuro2A cells. The PH and C2 domains of both variants showed 86.8% and 92.8% similarity, respectively. This suggests that these two domains, which are involved in membrane binding, are unlikely to be the cause of the altered localisation. A key residue that is required for the lipid binding specificity of the C2 domain (D861) is also onserved between the two isozymes. It is likely that the C-terminal tail region, which possesses the biggest difference in sequence, is responsible for altered localisation of the two isozymes. It will therefore be interesting to truncate the C-terminal tail regions of both isozymes and clone them into GFP expressing vectors to determine whether they would possess a similar cellular

distribution. Kim *et al*. previously reported that PLCβ1 has a nuclear localisation sequence (NLS) in its C-terminal tail region (Kim et al., 1996). It would therefore be interesting to investigate the presence of a specific NLS in the C-terminal of PLCη2. Absence of such a sequence from the C-terminal tail of PLCη1 may indicate why it does not localise to the nucleus.

Differentiation and neuritogenesis was explored in this project, as a functional role for PLCη2. A ligand proximity assay was utilised to show the direct interaction of PLCη2 and LIMK-1, which increased upon RA induced differentiation of Neuro2A cells. A better model may be to perform this experiment on mouse brain sections to determine the regions in which this interaction is most prevalent. It is well known that LIMK-1 phosphorylates cofilin family proteins. Following phosphorylation, cofilin family proteins are inactivated and cannot resume with their actin severing function (Endo et al., 2007). It will be interesting to confirm the phosphorylation of cofilin family members in RA treated PLCη2 KD and ShRNA control cells to confirm that this is the mechanism by which neuritogenesis is occurring. One way in which PLCη2 is causing phosphorylation of LIMK-1 may be through raising the cytosolic concentrations of Ca^{2+}, which subsequently activates CaMKIV. This can then lead to phosphorylation of LIMK-1. Western blot analysis using several time points can be utilised to confirm this.

By creating stable cell lines expressing mutant forms of PLCη2 and treating them with RA, it was shown that the catalytic domain of PLCη2 is essential for RA mediated neurite outgrowth. Stable cell lines exhibiting a mutation in the Ca^{2+} sensing EF hand domain however did not show any difference in neuritogenesis, in relation to the EV control stable cell line. A stable cell line that overexpressed PLCη2 however showed a slight increase in neuritogenesis in comparison to control cells, again indicating that PLCη2 is involved in neuritogenesis. A further experiment to solidify the fact that PLCη2 is essential in this process will be to transfect PLCη2 KD cells with PLCη2 and perform the four day RA treatment to see if neuritogenesis will be rescued.

Several interesting proteins that have been previously implicated in cellular differentiation and neurite formation were also identied using 2D gel electrophoresis. The high number of proteins that were identified to be expressed differentially in differentiated and undifferentiated cells

indicates that numerous pathways are involved in RA induced neuritogenesis and further studies are required to determine which other pathways PLCη2 is affecting.

In a short chapter investigating the relevance of PLCη2 to AD, it was shown that the expression of PLCη2 remains unaltered following treatment of differentiated Neuro2A cells with Aβ1-42. This suggests that the enzyme remains active in the disease state and could be contributing to the rise in intracellular Ca^{2+} by causing further release from the ER through binding of $Ins(4,5)P_3$ to its receptor. PKC may also become activated by DAG, leading to NMDA channel opening (Lin et al., 2010). Such mechanisms may contribute to the Ca^{2+} dysregulation that occurs in AD. Additional experiments are required to determine whether PLCη2 is involved in this so called "caciumopathy". It is known that PLCη2 levels increase as the mouse brain develops (Nakahara et al. 2005) and this may be the case throughout life. It will therefore be worthwhile to to look at expression levels of PLCη2 in animal models of AD or in clinical samples from individuals diagnosed with the disorder. Such a rise in PLCη2 would lead to increased accumulation of cytosolic Ca^{2+}, which could aid in disease proression. The cellular distribution of PLCη2 was altered upon 8 hrs of treatment with Aβ1-42, becoming completely absent from the nucleus. The significance of this is unclear and must be explored further. It will therefore be interesting to look at the localisation of PLCη2 in post mortem samples taken from AD patients and to compare its localisation with healthy samples. An altered localisation in the disease state would mean that PLCη2 is no longer able to carry out its normal function and may contribute to disease pathogenesis. It may be of interest to investigate whether the absence of PLCη2 from the nucleus causes increased interaction with LIMK-1 in the cytoplasm and whether this increase in interaction harbours any adverse effects.

The discovery of a C-terminal truncation mutation in PLCη1, in clinical cases of HPE strengthened the notion that PLCη enzymes are involved in brain development. Following transfection into COS7 cells, the mutated form of PLCη1 showed a nuclear localisation whereas the WT form was completely absent from the nucleus. This suggests that the C-terminal tail region is extremely important for cellular localisation. This finding further implies that the C-terminal tail region of PLCη1 and PLCη2 enzymes is the reason for their altered cellular localisation as shown in Chapter 4. Endogenous PLCη1 appeared to have a cytoskeletal localisation. It would be of interest to investigate why PLCη1 is localised to the cytoskeleton and what effects the mislocalisation would have on the cells cytoskeleton. The effect of the mutated form of PLCη1 on the Shh pathway was next determined as this pathway is involved

in embryonic development and cranial patterning. It was shown that the mutant form resulted in altered effects on the Shh pathway as determined by qPCR. Further experiments however are required to identify the exact point of the pathway at which PLCη1 is causing an effect. It may be possible that PLCη1 is regulating a certain Ca^{2+} regulated process in the Shh pathway. The qPCR assay showed that the level of Shh pathway genes were very low following overexpression of WT PLCη1 but increased greatly upon addition of the Shh ligand. This warrants further experiments to determine whether PLCη1 is involved in releasing the Shh ligand from producing cells, and whether this may be a Ca^{2+} regulated process. An additional experiment will be to perform a Gli-luciferase reporter assay to determine the extent of Gli transcription factor activation following transfection of cells with WT and mutant PLCη1. Furthermore, there exists a non-canonical Shh pathway that is responsive to the Shh ligand but is independent of Gli transcription factor activation (Jenkins D., 2009). It will be worth studying the role of PLCη1 in this non-canonical Shh pathway.

The main conclusions of this study are:

1) PLCη1 and PLCη2 are both activated by physiological levels of Ca^{2+} and show maximal activation at 10 μM free Ca^{2+}.
2) PLCη2 is activated by Gβ1γ2. In the process, it has been shown that the 2A co-expression system is an efficient tool for studying the activation of proteins by different Gβγ combinations.
3) PLCη2 localises primarily to the nucleus but is also present in other cellular compartments, mainly the cytosol and mitochondria, and the plasma membrane to a lower extent.
4) PLCη1 possess an altered cellular localisation compared with PLCη2, showing complete absence from the nucleus.
5) PLCη2 interacts directly with LIMK-1 and this interaction increases upon retinoic acid induced differentiation of Neuro2A cells.
6) PLCη2 is essential for retinoic acid induced differentiation of Neuro2A cells, but this is not dependent on its high Ca^{2+} sensing ability.
7) The expression of PLCη2 is not affected by Aβ1-42 treatment of differentiated Neuro2A cells.
8) The localisation of PLCη2 is altered upon Aβ1-42 treatment of differentiated Neuro2A cells, becoming completely absent from the nucleus.

9) The mutated form of PLCη1 (N1075X), which was identified in clinical cases of holoprosencephaly shows a nuclear localisation compared with WT PLCη1, which is cytoplasmic.

10) PLCη1 has a cytoskeletal distribution in embryonic C3H10T1/2 cells.

11) Mutant PLCη1 (N1075X) has altered effects on the Shh pathway compared with WT PLCη1.

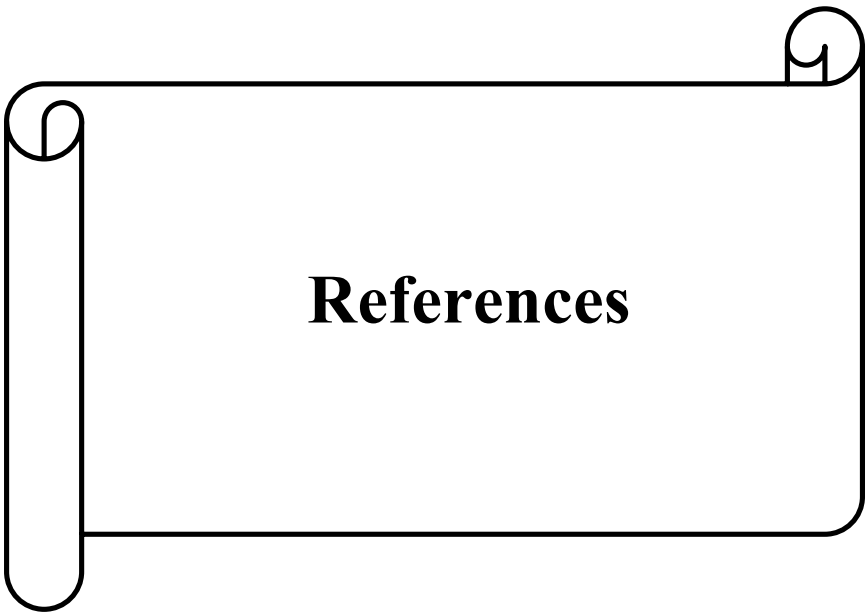

References

References

ABDEL-LATIF, A. A., GREEN, K., SMITH, J. P., MCPHERSON, J. C., JR. & MATHENY, J. L. 1978. Norepinephrine-stimulated breakdown of triphosphoinositide of rabbit iris smooth muscle: effects of surgical sympathetic denervation and in vivo electrical stimulation of the sympathetic nerve of the eye. *J Neurochem,* 30**,** 517-22.

ABRAHAM, C. R., SHIRAHAMA, T. & POTTER, H. 1990. Alpha 1-antichymotrypsin is associated solely with amyloid deposits containing the beta-protein. Amyloid and cell localization of alpha 1-antichymotrypsin. *Neurobiol Aging,* 11**,** 123-9.

ADEBANJO, O. A., ANANDATHEERTHAVARADA, H. K., KOVAL, A. P., MOONGA, B. S., BISWAS, G., SUN, L., SODAM, B. R., BEVIS, P. J., HUANG, C. L., EPSTEIN, S., LAI, F. A., AVADHANI, N. G. & ZAIDI, M. 1999. A new function for CD38/ADP-ribosyl cyclase in nuclear Ca2+ homeostasis. *Nat Cell Biol,* 1**,** 409-14.

AKASU, T., HASUO, H. & TOKIMASA, T. 1987. Activation of 5-HT3 receptor subtypes causes rapid excitation of rabbit parasympathetic neurones. *Br J Pharmacol,* 91**,** 453-5.

ALESSI, D. R. 2001. Discovery of PDK1, one of the missing links in insulin signal transduction. Colworth Medal Lecture. *Biochem Soc Trans,* 29**,** 1-14.

ALLAN, D. & MICHELL, R. H. 1978. A calcium-activated polyphosphoinositide phosphodiesterase in the plasma membrane of human and rabbit erythrocytes. *Biochim Biophys Acta,* 508**,** 277-86.

ALLEN, V., SWIGART, P., CHEUNG, R., COCKCROFT, S. & KATAN, M. 1997. Regulation of inositol lipid-specific phospholipase cdelta by changes in Ca2+ ion concentrations. *Biochem J,* 327 (Pt 2)**,** 545-52.

ALONSO, M. T., VILLALOBOS, C., CHAMERO, P., ALVAREZ, J. & GARCIA-SANCHO, J. 2006. Calcium microdomains in mitochondria and nucleus. *Cell Calcium,* 40**,** 513-25.

AMAKYE, D., JAGANI, Z. & DORSCH, M. 2013. Unraveling the therapeutic potential of the Hedgehog pathway in cancer. *Nat Med,* 19**,** 1410-22.

ANANTHANARAYANAN, B., DAS, S., RHEE, S. G., MURRAY, D. & CHO, W. 2002. Membrane targeting of C2 domains of phospholipase C-delta isoforms. *J Biol Chem,* 277**,** 3568-75.

ANIS, Y., NURNBERG, B., VISOCHEK, L., REISS, N., NAOR, Z. & COHEN-ARMON, M. 1999. Activation of Go-proteins by membrane depolarization traced by in situ photoaffinity labeling of galphao-proteins with [alpha32P]GTP-azidoanilide. *J Biol Chem,* 274**,** 7431-40.

AOKI, J., INOUE, A., MAKIDE, K., SAIKI, N. & ARAI, H. 2007. Structure and function of extracellular phospholipase A1 belonging to the pancreatic lipase gene family. *Biochimie,* 89**,** 197-204.

ARISPE, N., ROJAS, E. & POLLARD, H. B. 1993. Alzheimer disease amyloid beta protein forms calcium channels in bilayer membranes: blockade by tromethamine and aluminum. *Proc Natl Acad Sci U S A,* 90**,** 567-71.

ARSHAVSKY, V. Y., LAMB, T. D. & PUGH, E. N., JR. 2002. G proteins and phototransduction. *Annu Rev Physiol,* 64**,** 153-87.

AVAZERI, N., COURTOT, A. M., PESTY, A., DUQUENNE, C. & LEFEVRE, B. 2000. Cytoplasmic and nuclear phospholipase C-beta 1 relocation: role in resumption of meiosis in the mouse oocyte. *Mol Biol Cell,* 11**,** 4369-80.

AVILA, J., PEREZ, M., LIM, F., GOMEZ-RAMOS, A., HERNANDEZ, F. & LUCAS, J. J. 2004. Tau in neurodegenerative diseases: tau phosphorylation and assembly. *Neurotox Res,* 6**,** 477-82.

AZZI, M., CHAREST, P. G., ANGERS, S., ROUSSEAU, G., KOHOUT, T., BOUVIER, M. & PINEYRO, G. 2003. Beta-arrestin-mediated activation of MAPK by inverse agonists

reveals distinct active conformations for G protein-coupled receptors. *Proc Natl Acad Sci U S A,* 100**,** 11406-11.

BACSKAI, B. J., HOCHNER, B., MAHAUT-SMITH, M., ADAMS, S. R., KAANG, B. K., KANDEL, E. R. & TSIEN, R. Y. 1993. Spatially resolved dynamics of cAMP and protein kinase A subunits in Aplysia sensory neurons. *Science,* 260**,** 222-6.

BAE, J. H., LEW, E. D., YUZAWA, S., TOME, F., LAX, I. & SCHLESSINGER, J. 2009. The selectivity of receptor tyrosine kinase signaling is controlled by a secondary SH2 domain binding site. *Cell,* 138**,** 514-24.

BAE, Y. S., CANTLEY, L. G., CHEN, C. S., KIM, S. R., KWON, K. S. & RHEE, S. G. 1998. Activation of phospholipase C-gamma by phosphatidylinositol 3,4,5-trisphosphate. *J Biol Chem,* 273**,** 4465-9.

BAIROCH, A. & COX, J. A. 1990. EF-hand motifs in inositol phospholipid-specific phospholipase C. *FEBS Lett,* 269**,** 454-6.

BARE, D. J., KETTLUN, C. S., LIANG, M., BERS, D. M. & MIGNERY, G. A. 2005. Cardiac type 2 inositol 1,4,5-trisphosphate receptor: interaction and modulation by calcium/calmodulin-dependent protein kinase II. *J Biol Chem,* 280**,** 15912-20.

BARON, U., FREUNDLIEB, S., GOSSEN, M. & BUJARD, H. 1995. Co-regulation of two gene activities by tetracycline via a bidirectional promoter. *Nucleic Acids Res,* 23**,** 3605-6.

BARTEL, D. P. 2009. MicroRNAs: target recognition and regulatory functions. *Cell,* 136**,** 215-33.

BECCHETTI, A. & WHITAKER, M. 1997. Lithium blocks cell cycle transitions in the first cell cycles of sea urchin embryos, an effect rescued by myo-inositol. *Development,* 124**,** 1099-107.

BELCHEVA, M. M., CLARK, A. L., HAAS, P. D., SERNA, J. S., HAHN, J. W., KISS, A. & COSCIA, C. J. 2005. Mu and kappa opioid receptors activate ERK/MAPK via different protein kinase C isoforms and secondary messengers in astrocytes. *J Biol Chem,* 280**,** 27662-9.

BELGACEM, Y. H. & BORODINSKY, L. N. 2011. Sonic hedgehog signaling is decoded by calcium spike activity in the developing spinal cord. *Proc Natl Acad Sci U S A,* 108**,** 4482-7.

BERNARDI, P. & FORTE, M. 2007. The mitochondrial permeability transition pore. *Novartis Found Symp,* 287**,** 157-64; discussion 164-9.

BERRIDGE, M. J. 1998. Neuronal calcium signaling. *Neuron,* 21**,** 13-26.

BERRIDGE, M. J. 2001. The versatility and complexity of calcium signalling. *Novartis Found Symp,* 239**,** 52-64; discussion 64-7, 150-9.

BERRIDGE, M. J. 2009. Inositol trisphosphate and calcium signalling mechanisms. *Biochim Biophys Acta,* 1793**,** 933-40.

BERRIDGE, M. J. 2011. Calcium signalling and Alzheimer's disease. *Neurochem Res,* 36**,** 1149-56.

BERRIDGE, M. J. 2012. *cell signalling biology*, portland press limited.

BERRIDGE, M. J., BOOTMAN, M. D. & LIPP, P. 1998. Calcium--a life and death signal. *Nature,* 395**,** 645-8.

BERRIDGE, M. J., BOOTMAN, M. D. & RODERICK, H. L. 2003. Calcium signalling: dynamics, homeostasis and remodelling. *Nat Rev Mol Cell Biol,* 4**,** 517-29.

BERRIDGE, M. J., DAWSON, R. M., DOWNES, C. P., HESLOP, J. P. & IRVINE, R. F. 1983. Changes in the levels of inositol phosphates after agonist-dependent hydrolysis of membrane phosphoinositides. *Biochem J,* 212**,** 473-82.

BERRIDGE, M. J. & IRVINE, R. F. 1989. Inositol phosphates and cell signalling. *Nature,* 341**,** 197-205.

BERRIDGE, M. J., LIPP, P. & BOOTMAN, M. D. 2000. The versatility and universality of calcium signalling. *Nat Rev Mol Cell Biol,* 1**,** 11-21.

BEZANILLA, F. 2005. Voltage-gated ion channels. *IEEE Trans Nanobioscience,* 4**,** 34-48.

BHAT, M. B. & MA, J. 2002. The transmembrane segment of ryanodine receptor contains an intracellular membrane retention signal for Ca(2+) release channel. *J Biol Chem,* 277**,** 8597-601.

BIGAY, J. & ANTONNY, B. 2012. Curvature, lipid packing, and electrostatics of membrane organelles: defining cellular territories in determining specificity. *Dev Cell,* 23**,** 886-95.

BITTNER, M. A. & HOLZ, R. W. 2005. Phosphatidylinositol-4,5-bisphosphate: actin dynamics and the regulation of ATP-dependent and -independent secretion. *Mol Pharmacol,* 67**,** 1089-98.

BLAUSTEIN, M. P. & LEDERER, W. J. 1999. Sodium/calcium exchange: its physiological implications. *Physiol Rev,* 79**,** 763-854.

BLENNOW, K., DE LEON, M. J. & ZETTERBERG, H. 2006. Alzheimer's disease. *Lancet,* 368**,** 387-403.

BOGATCHEVA, N. V., SERGEEVA, M. G., DUDEK, S. M. & VERIN, A. D. 2005. Arachidonic acid cascade in endothelial pathobiology. *Microvasc Res,* 69**,** 107-27.

BOGUSLAVSKY, V., REBECCHI, M., MORRIS, A. J., JHON, D. Y., RHEE, S. G. & MCLAUGHLIN, S. 1994. Effect of monolayer surface pressure on the activities of phosphoinositide-specific phospholipase C-beta 1, -gamma 1, and -delta 1. *Biochemistry,* 33**,** 3032-7.

BOHDANOWICZ, M. & GRINSTEIN, S. 2013. Role of phospholipids in endocytosis, phagocytosis, and macropinocytosis. *Physiol Rev,* 93**,** 69-106.

BOOTMAN, M. D., COLLINS, T. J., PEPPIATT, C. M., PROTHERO, L. S., MACKENZIE, L., DE SMET, P., TRAVERS, M., TOVEY, S. C., SEO, J. T., BERRIDGE, M. J., CICCOLINI, F. & LIPP, P. 2001a. Calcium signalling--an overview. *Semin Cell Dev Biol,* 12**,** 3-10.

BOOTMAN, M. D., LIPP, P. & BERRIDGE, M. J. 2001b. The organisation and functions of local Ca(2+) signals. *J Cell Sci,* 114**,** 2213-22.

BORCHELT, D.R., THINKARAN, G., ECKMAN, C.B., LEE, M.K, DAVENPORT, F., RATOVISKY, T., PRADA, C.M., KIM, G., SEEKINS, S., YAGER, D., SLUNT, HH., WANG, R., SEEGER, M., LEVEY, A.I., GANDY, S.E., COPELAND, N.G., JENKINS, N.A., PRICE, D.L., YOUNKIN, S.G. & SISODIA, S.S. 1996. Familial Alzheimer's disease-linked presenilin 1 variant elevates Aβ 1-42/1-40 ratio in vitro and in vivo. *neuron,* 17, 1005-1013.

BOUNDS, P.L., SUTTER, B. & KOPPENOL, W.H. 2002. Studies of metal-binding properties of Cu, Zn superoxide dismutase by isothermal titration calorimetry', *Methods Enzymol,* 349, 115-23.

BOYER, J. L., WALDO, G. L. & HARDEN, T. K. 1992. Beta gamma-subunit activation of G-protein-regulated phospholipase C. *J Biol Chem,* 267**,** 25451-6.

BRANDT, D. R. & ROSS, E. M. 1985. GTPase activity of the stimulatory GTP-binding regulatory protein of adenylate cyclase, Gs. Accumulation and turnover of enzyme-nucleotide intermediates. *J Biol Chem,* 260**,** 266-72.

BRILLANTES, A. B., ONDRIAS, K., SCOTT, A., KOBRINSKY, E., ONDRIASOVA, E., MOSCHELLA, M. C., JAYARAMAN, T., LANDERS, M., EHRLICH, B. E. & MARKS, A. R. 1994. Stabilization of calcium release channel (ryanodine receptor) function by FK506-binding protein. *Cell,* 77**,** 513-23.

BRINI, M. & CARAFOLI, E. 2011. The plasma membrane Ca(2)+ ATPase and the plasma membrane sodium calcium exchanger cooperate in the regulation of cell calcium. *Cold Spring Harb Perspect Biol,* 3.

BRISTOL, A., HALL, S. M., KRIZ, R. W., STAHL, M. L., FAN, Y. S., BYERS, M. G., EDDY, R. L., SHOWS, T. B. & KNOPF, J. L. 1988. Phospholipase C-148: chromosomal location and deletion mapping of functional domains. *Cold Spring Harb Symp Quant Biol,* 53 Pt 2**,** 915-20.

BROADWELL, R. D. & CATALDO, A. M. 1984. The neuronal endoplasmic reticulum: its cytochemistry and contribution to the endomembrane system. II. Axons and terminals. *J Comp Neurol,* 230**,** 231-48.

BROSTROM & BROSTROM. 1990. Calcium dependent regulation of protein synthesis in intact mammalian cells. *Annual Review of Physiology*, 52, 577-590.

BROWN, M. S. & GOLDSTEIN, J. L. 1999. A proteolytic pathway that controls the cholesterol content of membranes, cells, and blood. *Proc Natl Acad Sci U S A,* 96**,** 11041-8.

BUCK, L. B. 2000. The molecular architecture of odor and pheromone sensing in mammals. *Cell,* 100**,** 611-8.

BUNNEY, T. D. & KATAN, M. 2011. PLC regulation: emerging pictures for molecular mechanisms. *Trends Biochem Sci,* 36**,** 88-96.

BURGOYNE, R. D., O'CALLAGHAN, D. W., HASDEMIR, B., HAYNES, L. P. & TEPIKIN, A. V. 2004. Neuronal Ca2+-sensor proteins: multitalented regulators of neuronal function. *Trends Neurosci,* 27**,** 203-9.

BURKE, J. E. & DENNIS, E. A. 2009. Phospholipase A2 structure/function, mechanism, and signaling. *J Lipid Res,* 50 Suppl**,** S237-42.

BYGRAVE, F. L. & BENEDETTI, A. 1996. What is the concentration of calcium ions in the endoplasmic reticulum? *Cell Calcium,* 19**,** 547-51.

CADIGAN, K. M. & NUSSE, R. 1997. Wnt signaling: a common theme in animal development. *Genes Dev,* 11**,** 3286-305.

CARAFOLI, E., SANTELLA, L., BRANCA, D. & BRINI, M. 2001. Generation, control, and processing of cellular calcium signals. *Crit Rev Biochem Mol Biol,* 36**,** 107-260.

CAREY, M. B. & MATSUMOTO, S. G. 1999. Spontaneous calcium transients are required for neuronal differentiation of murine neural crest. *Dev Biol,* 215**,** 298-313.

CASEY, D. M., INABA, K., PAZOUR, G. J., TAKADA, S., WAKABAYASHI, K., WILKERSON, C. G., KAMIYA, R. & WITMAN, G. B. 2003. DC3, the 21-kDa subunit of the outer dynein arm-docking complex (ODA-DC), is a novel EF-hand protein important for assembly of both the outer arm and the ODA-DC. *Mol Biol Cell,* 14**,** 3650-63.

CATTERALL, W. A., PEREZ-REYES, E., SNUTCH, T. P. & STRIESSNIG, J. 2005. International Union of Pharmacology. XLVIII. Nomenclature and structure-function relationships of voltage-gated calcium channels. *Pharmacol Rev,* 57**,** 411-25.

CHACINSKA, A., KOEHLER, C. M., MILENKOVIC, D., LITHGOW, T. & PFANNER, N. 2009. Importing mitochondrial proteins: machineries and mechanisms. *Cell,* 138**,** 628-44.

CHALMERS, K. A. & LOVE, S. 2007. Neurofibrillary tangles may interfere with Smad 2/3 signaling in neurons. *J Neuropathol Exp Neurol,* 66**,** 158-67.

CHAMBERLAIN, C. E., JEONG, J., GUO, C., ALLEN, B. L. & MCMAHON, A. P. 2008. Notochord-derived Shh concentrates in close association with the apically positioned basal body in neural target cells and forms a dynamic gradient during neural patterning. *Development,* 135**,** 1097-106.

CHAN, S. L., MAYNE, M., HOLDEN, C. P., GEIGER, J. D. & MATTSON, M. P. 2000. Presenilin-1 mutations increase levels of ryanodine receptors and calcium release in PC12 cells and cortical neurons. *J Biol Chem,* 275**,** 18195-200.

CHANG, D. T., LOPEZ, A., VON KESSLER, D. P., CHIANG, C., SIMANDL, B. K., ZHAO, R., SELDIN, M. F., FALLON, J. F. & BEACHY, P. A. 1994. Products, genetic linkage and limb patterning activity of a murine hedgehog gene. *Development,* 120**,** 3339-53.

CHEN, A. E., GINTY, D. D. & FAN, C. M. 2005. Protein kinase A signalling via CREB controls myogenesis induced by Wnt proteins. *Nature,* 433**,** 317-22.

CHEN, S. R. & MACLENNAN, D. H. 1994. Identification of calmodulin-, Ca(2+)-, and ruthenium red-binding domains in the Ca2+ release channel (ryanodine receptor) of rabbit skeletal muscle sarcoplasmic reticulum. *J Biol Chem,* 269**,** 22698-704.

CHEN, S. R., ZHANG, L. & MACLENNAN, D. H. 1992. Characterization of a Ca2+ binding and regulatory site in the Ca2+ release channel (ryanodine receptor) of rabbit skeletal muscle sarcoplasmic reticulum. *J Biol Chem,* 267**,** 23318-26.

CHEN, W., BURGESS, S. & HOPKINS, N. 2001. Analysis of the zebrafish smoothened mutant reveals conserved and divergent functions of hedgehog activity. *Development,* 128**,** 2385-96.

CHEN, W., REN, X. R., NELSON, C. D., BARAK, L. S., CHEN, J. K., BEACHY, P. A., DE SAUVAGE, F. & LEFKOWITZ, R. J. 2004. Activity-dependent internalization of smoothened mediated by beta-arrestin 2 and GRK2. *Science,* 306**,** 2257-60.

CHENG, H., LEDERER, M. R., XIAO, R. P., GOMEZ, A. M., ZHOU, Y. Y., ZIMAN, B., SPURGEON, H., LAKATTA, E. G. & LEDERER, W. J. 1996. Excitation-contraction coupling in heart: new insights from Ca2+ sparks. *Cell Calcium,* 20**,** 129-40.

CHENG, H. F., JIANG, M. J., CHEN, C. L., LIU, S. M., WONG, L. P., LOMASNEY, J. W. & KING, K. 1995. Cloning and identification of amino acid residues of human phospholipase C delta 1 essential for catalysis. *J Biol Chem,* 270**,** 5495-505.

CHEUNG, K. H., MEI, L., MAK, D. O., HAYASHI, I., IWATSUBO, T., KANG, D. E. & FOSKETT, J. K. 2010. Gain-of-function enhancement of IP3 receptor modal gating by familial Alzheimer's disease-linked presenilin mutants in human cells and mouse neurons. *Sci Signal,* 3**,** ra22.

CHIANG, C., LITINGTUNG, Y., LEE, E., YOUNG, K. E., CORDEN, J. L., WESTPHAL, H. & BEACHY, P. A. 1996. Cyclopia and defective axial patterning in mice lacking Sonic hedgehog gene function. *Nature,* 383**,** 407-13.

CHO, W. & STAHELIN, R. V. 2006. Membrane binding and subcellular targeting of C2 domains. *Biochim Biophys Acta,* 1761**,** 838-49.

CHOI, W. C., GERFEN, C. R., SUH, P. G. & RHEE, S. G. 1989. Immunohistochemical localization of a brain isozyme of phospholipase C (PLC III) in astroglia in rat brain. *Brain Res,* 499**,** 193-7.

CHOO, A. Y., ROUX, P. P. & BLENIS, J. 2006. Mind the GAP: Wnt steps onto the mTORC1 train. *Cell,* 126**,** 834-6.

CHUN, J. 1999. Lysophospholipid receptors: implications for neural signaling. *Crit Rev Neurobiol,* 13**,** 151-68.

CHURCHILL, G. C., OKADA, Y., THOMAS, J. M., GENAZZANI, A. A., PATEL, S. & GALIONE, A. 2002. NAADP mobilizes Ca(2+) from reserve granules, lysosome-related organelles, in sea urchin eggs. *Cell,* 111**,** 703-8.

CITRON, M., OLTERSDORF, T., HAASS, C., McCONLOGUE, L., HUNG, AY., SEUBERT, P., VIGO-PELFREY, C.,LIEBERBURG, I., & SELKOE, dj. 1992. Mutation of the beta-amyloid precursor protein in familial Alzheimer's disease increases beta-protein production. *Nature,* 360, 672-674.

CLAPHAM, D. E. & NEER, E. J. 1997. G protein beta gamma subunits. *Annu Rev Pharmacol Toxicol,* 37**,** 167-203.

CLEVERS, H. 2006. Wnt/beta-catenin signaling in development and disease. *Cell,* 127**,** 469-80.

COCCO, L., GILMOUR, R. S., OGNIBENE, A., LETCHER, A. J., MANZOLI, F. A. & IRVINE, R. F. 1987. Synthesis of polyphosphoinositides in nuclei of Friend cells. Evidence for polyphosphoinositide metabolism inside the nucleus which changes with cell differentiation. *Biochem J,* 248**,** 765-70.

COCCO, L., MARTELLI, A. M., GILMOUR, R. S., OGNIBENE, A., MANZOLI, F. A. & IRVINE, R. F. 1988. Rapid changes in phospholipid metabolism in the nuclei of Swiss 3T3 cells induced by treatment of the cells with insulin-like growth factor I. *Biochem Biophys Res Commun,* 154**,** 1266-72.

COCKCROFT, S. 2006. The latest phospholipase C, PLCeta, is implicated in neuronal function. *Trends Biochem Sci,* 31**,** 4-7.

COHEN, M. M., JR. 1989. Perspectives on holoprosencephaly: Part I. Epidemiology, genetics, and syndromology. *Teratology,* 40**,** 211-35.

COLEGROVE, S. L., ALBRECHT, M. A. & FRIEL, D. D. 2000. Quantitative analysis of mitochondrial Ca2+ uptake and release pathways in sympathetic neurons. Reconstruction of the recovery after depolarization-evoked [Ca2+]i elevations. *J Gen Physiol,* 115**,** 371-88.

COTE, J. F., MOTOYAMA, A. B., BUSH, J. A. & VUORI, K. 2005. A novel and evolutionarily conserved PtdIns(3,4,5)P3-binding domain is necessary for DOCK180 signalling. *Nat Cell Biol,* 7**,** 797-807.

CRESPO, P., XU, N., SIMONDS, W. F. & GUTKIND, J. S. 1994. Ras-dependent activation of MAP kinase pathway mediated by G-protein beta gamma subunits. *Nature,* 369**,** 418-20.

CROMPTON, M., VIRJI, S., DOYLE, V., JOHNSON, N. & WARD, J. M. 1999. The mitochondrial permeability transition pore. *Biochem Soc Symp,* 66**,** 167-79.

CROSSLEY, I., SWANN, K., CHAMBERS, E. & WHITAKER, M. 1988. Activation of sea urchin eggs by inositol phosphates is independent of external calcium. *Biochem J,* 252**,** 257-62.

CROUCH, M. F. 1991. Growth factor-induced cell division is paralleled by translocation of Gi alpha to the nucleus. *FASEB J,* 5**,** 200-6.

CULLEN, P. J., HSUAN, J. J., TRUONG, O., LETCHER, A. J., JACKSON, T. R., DAWSON, A. P. & IRVINE, R. F. 1995. Identification of a specific Ins(1,3,4,5)P4-binding protein as a member of the GAP1 family. *Nature,* 376**,** 527-30.

CURTHOYS, N. M., FREITTAG, H., CONNOR, A., DESOUZA, M., BRETTLE, M., POLJAK, A., HALL, A., HARDEMAN, E., SCHEVZOV, G., GUNNING, P. W. & FATH, T. 2014. Tropomyosins induce neuritogenesis and determine neurite branching patterns in B35 neuroblastoma cells. *Mol Cell Neurosci,* 58**,** 11-21.

DE FELIPE, P., LUKE, G. A., HUGHES, L. E., GANI, D., HALPIN, C. & RYAN, M. D. 2006. E unum pluribus: multiple proteins from a self-processing polyprotein. *Trends Biotechnol,* 24**,** 68-75.

DE SOUZA, L. E., MOURA COSTA, M. D., BILEK, E. S., LOPES, M. H., MARTINS, V. R., PUSCHEL, A. W., MERCADANTE, A. F., NAKAO, L. S. & ZANATA, S. M. 2014. STI1 antagonizes cytoskeleton collapse mediated by small GTPase Rnd1 and regulates neurite growth. *Exp Cell Res,* 324**,** 84-91.

DEGUCHI, R., SHIRAKAWA, H., ODA, S., MOHRI, T. & MIYAZAKI, S. 2000. Spatiotemporal analysis of Ca(2+) waves in relation to the sperm entry site and animal-vegetal axis during Ca(2+) oscillations in fertilized mouse eggs. *Dev Biol,* 218**,** 299-313.

DEJDA, A., JOZWIAK-BEBENISTA, M. & NOWAK, J. Z. 2006. PACAP, VIP, and PHI: effects on AC-, PLC-, and PLD-driven signaling systems in the primary glial cell cultures. *Ann N Y Acad Sci,* 1070**,** 220-5.

DEKROON, R. M. & ARMATI, P. J. 2002. The effects of oxidative stress and altered intracellular calcium levels on vesicular transport of apoE-EGFP. *Cell Biol Int,* 26**,** 407-20.

DELON, C., MANIFAVA, M., WOOD, E., THOMPSON, D., KRUGMANN, S., PYNE, S. & KTISTAKIS, N. T. 2004. Sphingosine kinase 1 is an intracellular effector of phosphatidic acid. *J Biol Chem,* 279**,** 44763-74.

DEMURO, A., MINA, E., KAYED, R., MILTON, S. C., PARKER, I. & GLABE, C. G. 2005. Calcium dysregulation and membrane disruption as a ubiquitous neurotoxic mechanism of soluble amyloid oligomers. *J Biol Chem,* 280**,** 17294-300.

DEMURO, A., PARKER, I. & STUTZMANN, G. E. 2010. Calcium signaling and amyloid toxicity in Alzheimer disease. *J Biol Chem,* 285**,** 12463-8.

DESHPANDE, A., MINA, E., GLABE, C. & BUSCIGLIO, J. 2006. Different conformations of amyloid beta induce neurotoxicity by distinct mechanisms in human cortical neurons. *J Neurosci,* 26**,** 6011-8.

DEY, J., DITZLER, S., KNOBLAUGH, S. E., HATTON, B. A., SCHELTER, J. M., CLEARY, M. A., MECHAM, B., RORKE-ADAMS, L. B. & OLSON, J. M. 2012. A distinct Smoothened mutation causes severe cerebellar developmental defects and medulloblastoma in a novel transgenic mouse model. *Mol Cell Biol,* 32**,** 4104-15.

DI PAOLO, G. & DE CAMILLI, P. 2006. Phosphoinositides in cell regulation and membrane dynamics. *Nature,* 443**,** 651-7.

DIAZ, J., BAIER, G., MARTINEZ-MEKLER, G. & PASTOR, N. 2002. Interaction of the IP(3)-Ca(2+) and the FGF-MAPK signaling pathways in the Xenopus laevis embryo: a qualitative approach to the mesodermal induction problem. *Biophys Chem,* 97**,** 55-72.

DIVECHA, N., BANFIC, H. & IRVINE, R. F. 1991. The polyphosphoinositide cycle exists in the nuclei of Swiss 3T3 cells under the control of a receptor (for IGF-I) in the plasma membrane, and stimulation of the cycle increases nuclear diacylglycerol and apparently induces translocation of protein kinase C to the nucleus. *EMBO J,* 10**,** 3207-14.

DIVECHA, N., LETCHER, A. J., BANFIC, H. H., RHEE, S. G. & IRVINE, R. F. 1995. Changes in the components of a nuclear inositide cycle during differentiation in murine erythroleukaemia cells. *Biochem J,* 312 (Pt 1)**,** 63-7.

DIVECHA, N., RHEE, S. G., LETCHER, A. J. & IRVINE, R. F. 1993. Phosphoinositide signalling enzymes in rat liver nuclei: phosphoinositidase C isoform beta 1 is specifically, but not predominantly, located in the nucleus. *Biochem J,* 289 (Pt 3)**,** 617-20.

DOI, T., PURI, P., BANNIGAN, J. & THOMPSON, J. 2010. Disruption of noncanonical Wnt/CA2+ pathway in the cadmium-induced omphalocele in the chick model. *J Pediatr Surg,* 45**,** 1645-9.

DONNELLY, M. L., HUGHES, L. E., LUKE, G., MENDOZA, H., TEN DAM, E., GANI, D. & RYAN, M. D. 2001a. The 'cleavage' activities of foot-and-mouth disease virus 2A site-directed mutants and naturally occurring '2A-like' sequences. *J Gen Virol,* 82**,** 1027-41.

DONNELLY, M. L., LUKE, G., MEHROTRA, A., LI, X., HUGHES, L. E., GANI, D. & RYAN, M. D. 2001b. Analysis of the aphthovirus 2A/2B polyprotein 'cleavage' mechanism indicates not a proteolytic reaction, but a novel translational effect: a putative ribosomal 'skip'. *J Gen Virol,* 82**,** 1013-25.

DOYLE, D. A., LEE, A., LEWIS, J., KIM, E., SHENG, M. & MACKINNON, R. 1996. Crystal structures of a complexed and peptide-free membrane protein-binding domain: molecular basis of peptide recognition by PDZ. *Cell,* 85**,** 1067-76.

DUNLAP, K., LUEBKE, J. I. & TURNER, T. J. 1995. Exocytotic Ca2+ channels in mammalian central neurons. *Trends Neurosci,* 18**,** 89-98.

DUPONT, G., COMBETTES, L. & LEYBAERT, L. 2007. Calcium dynamics: spatio-temporal organization from the subcellular to the organ level. *Int Rev Cytol,* 261**,** 193-245.

EBASHI, S. 1991. Excitation-contraction coupling and the mechanism of muscle contraction. *Annu Rev Physiol,* 53**,** 1-16.

ECHELARD, Y., EPSTEIN, D. J., ST-JACQUES, B., SHEN, L., MOHLER, J., MCMAHON, J. A. & MCMAHON, A. P. 1993. Sonic hedgehog, a member of a family of putative signaling molecules, is implicated in the regulation of CNS polarity. *Cell,* 75**,** 1417-30.

ECHEVARRIA, W., LEITE, M. F., GUERRA, M. T., ZIPFEL, W. R. & NATHANSON, M. H. 2003. Regulation of calcium signals in the nucleus by a nucleoplasmic reticulum. *Nat Cell Biol,* 5**,** 440-6.

ELLIS, M. V., JAMES, S. R., PERISIC, O., DOWNES, C. P., WILLIAMS, R. L. & KATAN, M. 1998. Catalytic domain of phosphoinositide-specific phospholipase C (PLC). Mutational analysis of residues within the active site and hydrophobic ridge of plcdelta1. *J Biol Chem,* 273**,** 11650-9.

ENDO, M., OHASHI, K. & MIZUNO, K. 2007. LIM kinase and slingshot are critical for neurite extension. *J Biol Chem,* 282**,** 13692-702.

ERICKSON, E. S., MOOREN, O. L., MOORE-NICHOLS, D. & DUNN, R. C. 2004. Activation of ryanodine receptors in the nuclear envelope alters the conformation of the nuclear pore complex. *Biophys Chem,* 112**,** 1-7.

ERTEL, E. A., CAMPBELL, K. P., HARPOLD, M. M., HOFMANN, F., MORI, Y., PEREZ-REYES, E., SCHWARTZ, A., SNUTCH, T. P., TANABE, T., BIRNBAUMER, L., TSIEN, R. W. & CATTERALL, W. A. 2000. Nomenclature of voltage-gated calcium channels. *Neuron,* 25**,** 533-5.

ESPINDOLA, F. S., SUTER, D. M., PARTATA, L. B., CAO, T., WOLENSKI, J. S., CHENEY, R. E., KING, S. M. & MOOSEKER, M. S. 2000. The light chain composition of chicken brain myosin-Va: calmodulin, myosin-II essential light chains, and 8-kDa dynein light chain/PIN. *Cell Motil Cytoskeleton,* 47**,** 269-81.

ESSEN, L. O., PERISIC, O., CHEUNG, R., KATAN, M. & WILLIAMS, R. L. 1996. Crystal structure of a mammalian phosphoinositide-specific phospholipase C delta. *Nature,* 380**,** 595-602.

ESSEN, L. O., PERISIC, O., KATAN, M., WU, Y., ROBERTS, M. F. & WILLIAMS, R. L. 1997a. Structural mapping of the catalytic mechanism for a mammalian phosphoinositide-specific phospholipase C. *Biochemistry,* 36**,** 1704-18.

ESSEN, L. O., PERISIC, O., LYNCH, D. E., KATAN, M. & WILLIAMS, R. L. 1997b. A ternary metal binding site in the C2 domain of phosphoinositide-specific phospholipase C-delta1. *Biochemistry,* 36**,** 2753-62.

ETCHEBERRIGARAY, R., HIRASHIMA, N., NEE, L., PRINCE, J., GOVONI, S., RACCHI, M., TANZI, R. E. & ALKON, D. L. 1998. Calcium responses in fibroblasts from asymptomatic members of Alzheimer's disease families. *Neurobiol Dis,* 5**,** 37-45.

EVANKO, D. S., THIYAGARAJAN, M. M., SIDEROVSKI, D. P. & WEDEGAERTNER, P. B. 2001. Gbeta gamma isoforms selectively rescue plasma membrane localization and palmitoylation of mutant Galphas and Galphaq. *J Biol Chem,* 276**,** 23945-53.

EVANS, J. H., GERBER, S. H., MURRAY, D. & LESLIE, C. C. 2004. The calcium binding loops of the cytosolic phospholipase A2 C2 domain specify targeting to Golgi and ER in live cells. *Mol Biol Cell,* 15**,** 371-83.

EXTON, J. H. 1996. Regulation of phosphoinositide phospholipases by hormones, neurotransmitters, and other agonists linked to G proteins. *Annu Rev Pharmacol Toxicol,* 36**,** 481-509.

FAENZA, I., MATTEUCCI, A., BAVELLONI, A., MARMIROLI, S., MARTELLI, A. M., GILMOUR, R. S., SUH, P. G., MANZOLI, L. & COCCO, L. 2002. Nuclear

PLCbeta(1) acts as a negative regulator of p45/NF-E2 expression levels in Friend erythroleukemia cells. *Biochim Biophys Acta,* 1589**,** 305-10.

FALASCA, M., LOGAN, S. K., LEHTO, V. P., BACCANTE, G., LEMMON, M. A. & SCHLESSINGER, J. 1998. Activation of phospholipase C gamma by PI 3-kinase-induced PH domain-mediated membrane targeting. *EMBO J,* 17**,** 414-22.

FANNING, A. S. & ANDERSON, J. M. 1996. Protein-protein interactions: PDZ domain networks. *Curr Biol,* 6**,** 1385-8.

FAUQUIER, T., GUERINEAU, N. C., MCKINNEY, R. A., BAUER, K. & MOLLARD, P. 2001. Folliculostellate cell network: a route for long-distance communication in the anterior pituitary. *Proc Natl Acad Sci U S A,* 98**,** 8891-6.

FERGUSON, K. M., LEMMON, M. A., SCHLESSINGER, J. & SIGLER, P. B. 1995. Structure of the high affinity complex of inositol trisphosphate with a phospholipase C pleckstrin homology domain. *Cell,* 83**,** 1037-46.

FERREIRO, E., OLIVEIRA, C. R. & PEREIRA, C. 2004. Involvement of endoplasmic reticulum Ca2+ release through ryanodine and inositol 1,4,5-triphosphate receptors in the neurotoxic effects induced by the amyloid-beta peptide. *J Neurosci Res,* 76**,** 872-80.

FERRI, K. F. & KROEMER, G. 2001. Organelle-specific initiation of cell death pathways. *Nat Cell Biol,* 3**,** E255-63.

FESENKO, E. E., KOLESNIKOV, S. S. & LYUBARSKY, A. L. 1985. Induction by cyclic GMP of cationic conductance in plasma membrane of retinal rod outer segment. *Nature,* 313**,** 310-3.

FESKE, S., GILTNANE, J., DOLMETSCH, R., STAUDT, L. M. & RAO, A. 2001. Gene regulation mediated by calcium signals in T lymphocytes. *Nat Immunol,* 2**,** 316-24.

FESSENDEN, J. D., CHEN, L., WANG, Y., PAOLINI, C., FRANZINI-ARMSTRONG, C., ALLEN, P. D. & PESSAH, I. N. 2001. Ryanodine receptor point mutant E4032A reveals an allosteric interaction with ryanodine. *Proc Natl Acad Sci U S A,* 98**,** 2865-70.

FINCH, E. A., TURNER, T. J. & GOLDIN, S. M. 1991. Calcium as a coagonist of inositol 1,4,5-trisphosphate-induced calcium release. *Science,* 252**,** 443-6.

FLEISCHER, S., OGUNBUNMI, E. M., DIXON, M. C. & FLEER, E. A. 1985. Localization of Ca2+ release channels with ryanodine in junctional terminal cisternae of sarcoplasmic reticulum of fast skeletal muscle. *Proc Natl Acad Sci U S A,* 82**,** 7256-9.

FLUCK, R., ABRAHAM, V., MILLER, A. & GALIONE, A. 1999. Microinjection of cyclic ADP-ribose triggers a regenerative wave of Ca2+ release and exocytosis of cortical alveoli in medaka eggs. *Zygote,* 7**,** 285-92.

FORD, C. E., SKIBA, N. P., BAE, H., DAAKA, Y., REUVENY, E., SHEKTER, L. R., ROSAL, R., WENG, G., YANG, C. S., IYENGAR, R., MILLER, R. J., JAN, L. Y., LEFKOWITZ, R. J. & HAMM, H. E. 1998. Molecular basis for interactions of G protein betagamma subunits with effectors. *Science,* 280**,** 1271-4.

FOSKETT, J. K., WHITE, C., CHEUNG, K. H. & MAK, D. O. 2007. Inositol trisphosphate receptor Ca2+ release channels. *Physiol Rev,* 87**,** 593-658.

FREDRIKSSON, R., LAGERSTROM, M. C., LUNDIN, L. G. & SCHIOTH, H. B. 2003. The G-protein-coupled receptors in the human genome form five main families. Phylogenetic analysis, paralogon groups, and fingerprints. *Mol Pharmacol,* 63**,** 1256-72.

FU, H., SUBRAMANIAN, R. R. & MASTERS, S. C. 2000. 14-3-3 proteins: structure, function, and regulation. *Annu Rev Pharmacol Toxicol,* 40**,** 617-47.

FUJII, M., YI, K. S., KIM, M. J., HA, S. H., RYU, S. H., SUH, P. G. & YAGISAWA, H. 2009. Phosphorylation of phospholipase C-delta 1 regulates its enzymatic activity. *J Cell Biochem,* 108**,** 638-50.

FUKAMI, K. 2002. Structure, regulation, and function of phospholipase C isozymes. *J Biochem,* 131**,** 293-9.

FUKUHARA, S., MURGA, C., ZOHAR, M., IGISHI, T. & GUTKIND, J. S. 1999. A novel PDZ domain containing guanine nucleotide exchange factor links heterotrimeric G proteins to Rho. *J Biol Chem,* 274**,** 5868-79.

FURLER, S., PATERNA, J. C., WEIBEL, M. & BUELER, H. 2001. Recombinant AAV vectors containing the foot and mouth disease virus 2A sequence confer efficient bicistronic gene expression in cultured cells and rat substantia nigra neurons. *Gene Ther,* 8**,** 864-73.

GARCIA, D. E., LI, B., GARCIA-FERREIRO, R. E., HERNANDEZ-OCHOA, E. O., YAN, K., GAUTAM, N., CATTERALL, W. A., MACKIE, K. & HILLE, B. 1998. G-protein beta-subunit specificity in the fast membrane-delimited inhibition of Ca2+ channels. *J Neurosci,* 18**,** 9163-70.

GASSAMA-DIAGNE, A., ROGALLE, P., FAUVEL, J., WILLSON, M., KLAEBE, A. & CHAP, H. 1992. Substrate specificity of phospholipase B from guinea pig intestine. A glycerol ester lipase with broad specificity. *J Biol Chem,* 267**,** 13418-24.

GEORGIEV, P., GARCIA-MURILLAS, I., ULAHANNAN, D., HARDIE, R. C. & RAGHU, P. 2005. Functional INAD complexes are required to mediate degeneration in photoreceptors of the Drosophila rdgA mutant. *J Cell Sci,* 118**,** 1373-84.

GERASIMENKO, J. V., MARUYAMA, Y., YANO, K., DOLMAN, N. J., TEPIKIN, A. V., PETERSEN, O. H. & GERASIMENKO, O. V. 2003. NAADP mobilizes Ca2+ from a thapsigargin-sensitive store in the nuclear envelope by activating ryanodine receptors. *J Cell Biol,* 163**,** 271-82.

GERASIMENKO, O. V., GERASIMENKO, J. V., TEPIKIN, A. V. & PETERSEN, O. H. 1995. ATP-dependent accumulation and inositol trisphosphate- or cyclic ADP-ribose-mediated release of Ca2+ from the nuclear envelope. *Cell,* 80**,** 439-44.

GIANNINI, G., CONTI, A., MAMMARELLA, S., SCROBOGNA, M. & SORRENTINO, V. 1995. The ryanodine receptor/calcium channel genes are widely and differentially expressed in murine brain and peripheral tissues. *J Cell Biol,* 128**,** 893-904.

GIL, O. D., ZANAZZI, G., STRUYK, A. F. & SALZER, J. L. 1998. Neurotrimin mediates bifunctional effects on neurite outgrowth via homophilic and heterophilic interactions. *J Neurosci,* 18**,** 9312-25.

GILROY, D. W., NEWSON, J., SAWMYNADEN, P., WILLOUGHBY, D. A. & CROXTALL, J. D. 2004. A novel role for phospholipase A2 isoforms in the checkpoint control of acute inflammation. *FASEB J,* 18**,** 489-98.

GLUZMAN, Y. 1981. SV40-transformed simian cells support the replication of early SV40 mutants. *Cell,* 23**,** 175-82.

GOETZ, S. C. & ANDERSON, K. V. 2010. The primary cilium: a signalling centre during vertebrate development. *Nat Rev Genet,* 11**,** 331-44.

GOETZ, S. C., OCBINA, P. J. & ANDERSON, K. V. 2009. The primary cilium as a Hedgehog signal transduction machine. *Methods Cell Biol,* 94**,** 199-222.

GORDON, M. D. & NUSSE, R. 2006. Wnt signaling: multiple pathways, multiple receptors, and multiple transcription factors. *J Biol Chem,* 281**,** 22429-33.

GORELICK, F. S. & SHUGRUE, C. 2001. Exiting the endoplasmic reticulum. *Mol Cell Endocrinol,* 177**,** 13-8.

GOUD, P. T., GOUD, A. P., VAN OOSTVELDT, P. & DHONT, M. 1999. Presence and dynamic redistribution of type I inositol 1,4,5-trisphosphate receptors in human oocytes

and embryos during in-vitro maturation, fertilization and early cleavage divisions. *Mol Hum Reprod,* 5**,** 441-51.

GRABAREK, Z. 2006. Structural basis for diversity of the EF-hand calcium-binding proteins. *J Mol Biol,* 359**,** 509-25.

GRANGE, M., SETTE, C., CUOMO, M., CONTI, M., LAGARDE, M., PRIGENT, A. F. & NEMOZ, G. 2000. The cAMP-specific phosphodiesterase PDE4D3 is regulated by phosphatidic acid binding. Consequences for cAMP signaling pathway and characterization of a phosphatidic acid binding site. *J Biol Chem,* 275**,** 33379-87.

GRAY, A., OLSSON, H., BATTY, I. H., PRIGANICA, L. & PETER DOWNES, C. 2003. Nonradioactive methods for the assay of phosphoinositide 3-kinases and phosphoinositide phosphatases and selective detection of signaling lipids in cell and tissue extracts. *Anal Biochem,* 313**,** 234-45.

GREEN, K. N. & LAFERLA, F. M. 2008. Linking calcium to Abeta and Alzheimer's disease. *Neuron,* 59**,** 190-4.

GREEN, K. N. & PEERS, C. 2001. Amyloid beta peptides mediate hypoxic augmentation of Ca(2+) channels. *J Neurochem,* 77**,** 953-6.

GRENNINGLOH, G., SOEHRMAN, S., BONDALLAZ, P., RUCHTI, E. & CADAS, H. 2004. Role of the microtubule destabilizing proteins SCG10 and stathmin in neuronal growth. *J Neurobiol,* 58**,** 60-9.

GRESSET, A., HICKS, S. N., HARDEN, T. K. & SONDEK, J. 2010. Mechanism of phosphorylation-induced activation of phospholipase C-gamma isozymes. *J Biol Chem,* 285**,** 35836-47.

GROBLER, J. A., ESSEN, L. O., WILLIAMS, R. L. & HURLEY, J. H. 1996. C2 domain conformational changes in phospholipase C-delta 1. *Nat Struct Biol,* 3**,** 788-95.

GROBLER, J. A. & HURLEY, J. H. 1998. Catalysis by phospholipase C delta1 requires that Ca2+ bind to the catalytic domain, but not the C2 domain. *Biochemistry,* 37**,** 5020-8.

GROIGNO, L. & WHITAKER, M. 1998. An anaphase calcium signal controls chromosome disjunction in early sea urchin embryos. *Cell,* 92**,** 193-204.

GUILD, S. 1991. Effects of adenosine 3':5'-cyclic monophosphate and guanine nucleotides on calcium-evoked ACTH release from electrically permeabilized AtT-20 cells. *Br J Pharmacol,* 104**,** 117-22.

GUNTESKI-HAMBLIN, A. M., CLARKE, D. M. & SHULL, G. E. 1992. Molecular cloning and tissue distribution of alternatively spliced mRNAs encoding possible mammalian homologues of the yeast secretory pathway calcium pump. *Biochemistry,* 31**,** 7600-8.

GUO, Q., FURUKAWA, K., SOPHER, B. L., PHAM, D. G., XIE, J., ROBINSON, N., MARTIN, G. M. & MATTSON, M. P. 1996. Alzheimer's PS-1 mutation perturbs calcium homeostasis and sensitizes PC12 cells to death induced by amyloid beta-peptide. *Neuroreport,* 8**,** 379-83.

HADDOCK, P. S., COETZEE, W. A. & ARTMAN, M. 1997. Na+/Ca2+ exchange current and contractions measured under Cl(-)-free conditions in developing rabbit hearts. *Am J Physiol,* 273**,** H837-46.

HAGA, T., HAGA, K. & KAMEYAMA, K. 1994. G protein--coupled receptor kinases. *J Neurochem,* 63**,** 400-12.

HAGIWARA, S., OZAWA, S. & SAND, O. 1975. Voltage clamp analysis of two inward current mechanisms in the egg cell membrane of a starfish. *J Gen Physiol,* 65**,** 617-44.

HAKAMATA, Y., NAKAI, J., TAKESHIMA, H. & IMOTO, K. 1992. Primary structure and distribution of a novel ryanodine receptor/calcium release channel from rabbit brain. *FEBS Lett,* 312**,** 229-35.

HAMMERSCHMIDT, M. & MCMAHON, A. P. 1998. The effect of pertussis toxin on zebrafish development: a possible role for inhibitory G-proteins in hedgehog signaling. *Dev Biol,* 194**,** 166-71.

HAMMOND, G. R., FISCHER, M. J., ANDERSON, K. E., HOLDICH, J., KOTECI, A., BALLA, T. & IRVINE, R. F. 2012. PI4P and PI(4,5)P2 are essential but independent lipid determinants of membrane identity. *Science,* 337**,** 727-30.

HANNAN, A. J., BLAKEMORE, C., KATSNELSON, A., VITALIS, T., HUBER, K. M., BEAR, M., RODER, J., KIM, D., SHIN, H. S. & KIND, P. C. 2001. PLC-beta1, activated via mGluRs, mediates activity-dependent differentiation in cerebral cortex. *Nat Neurosci,* 4**,** 282-8.

HANNAN, A. J., KIND, P. C. & BLAKEMORE, C. 1998. Phospholipase C-beta1 expression correlates with neuronal differentiation and synaptic plasticity in rat somatosensory cortex. *Neuropharmacology,* 37**,** 593-605.

HANOUNE, J. & DEFER, N. 2001. Regulation and role of adenylyl cyclase isoforms. *Annu Rev Pharmacol Toxicol,* 41**,** 145-74.

HANSON, M. G. & LANDMESSER, L. T. 2004. Normal patterns of spontaneous activity are required for correct motor axon guidance and the expression of specific guidance molecules. *Neuron,* 43**,** 687-701.

HARDEN, J., BERTONI, G. & KLEINSMITH, L. 2012. *Becker's world of the cell*, Pearson education inc.

HARDEN, T. K., HICKS, S. N. & SONDEK, J. 2009. Phospholipase C isozymes as effectors of Ras superfamily GTPases. *J Lipid Res,* 50 Suppl**,** S243-8.

HARDEN, T. K. & SONDEK, J. 2006. Regulation of phospholipase C isozymes by ras superfamily GTPases. *Annu Rev Pharmacol Toxicol,* 46**,** 355-79.

HARDY & SELKOE. 2002. .The amyloud hypothesis of Alzheimer's disease: progress and problems on the road to therapeutics. *Science,* 297, 353-356.

HARGREAVES, A. C., LUMMIS, S. C. & TAYLOR, C. W. 1994. Ca2+ permeability of cloned and native 5-hydroxytryptamine type 3 receptors. *Mol Pharmacol,* 46**,** 1120-8.

HARRIS, B. Z. & LIM, W. A. 2001. Mechanism and role of PDZ domains in signaling complex assembly. *J Cell Sci,* 114**,** 3219-31.

HASEGAWA, K., COWAN, A. B., NAKATSUJI, N. & SUEMORI, H. 2007. Efficient multicistronic expression of a transgene in human embryonic stem cells. *Stem Cells,* 25**,** 1707-12.

HASSINGER, T. D., ATKINSON, P. B., STRECKER, G. J., WHALEN, L. R., DUDEK, F. E., KOSSEL, A. H. & KATER, S. B. 1995. Evidence for glutamate-mediated activation of hippocampal neurons by glial calcium waves. *J Neurobiol,* 28**,** 159-70.

HAWKES, M. J., NELSON, T. E. & HAMILTON, S. L. 1992. [3H]ryanodine as a probe of changes in the functional state of the Ca(2+)-release channel in malignant hyperthermia. *J Biol Chem,* 267**,** 6702-9.

HEINZ, D. W., ESSEN, L. O. & WILLIAMS, R. L. 1998. Structural and mechanistic comparison of prokaryotic and eukaryotic phosphoinositide-specific phospholipases C. *J Mol Biol,* 275**,** 635-50.

HEISENBERG, C. P., TADA, M., RAUCH, G. J., SAUDE, L., CONCHA, M. L., GEISLER, R., STEMPLE, D. L., SMITH, J. C. & WILSON, S. W. 2000. Silberblick/Wnt11 mediates convergent extension movements during zebrafish gastrulation. *Nature,* 405**,** 76-81.

HELFMAN, D. M., CHELEY, S., KUISMANEN, E., FINN, L. A. & YAMAWAKI-KATAOKA, Y. 1986. Nonmuscle and muscle tropomyosin isoforms are expressed from a single gene by alternative RNA splicing and polyadenylation. *Mol Cell Biol,* 6**,** 3582-95.

HENNECKE, M., KWISSA, M., METZGER, K., OUMARD, A., KROGER, A., SCHIRMBECK, R., REIMANN, J. & HAUSER, H. 2001. Composition and arrangement of genes define the strength of IRES-driven translation in bicistronic mRNAs. *Nucleic Acids Res,* 29**,** 3327-34.

HERLITZE, S., GARCIA, D. E., MACKIE, K., HILLE, B., SCHEUER, T. & CATTERALL, W. A. 1996. Modulation of Ca2+ channels by G-protein beta gamma subunits. *Nature,* 380**,** 258-62.

HILES, I. D., OTSU, M., VOLINIA, S., FRY, M. J., GOUT, I., DHAND, R., PANAYOTOU, G., RUIZ-LARREA, F., THOMPSON, A., TOTTY, N. F. & ET AL. 1992. Phosphatidylinositol 3-kinase: structure and expression of the 110 kd catalytic subunit. *Cell,* 70**,** 419-29.

HIROKAWA, N., NODA, Y. & OKADA, Y. 1998. Kinesin and dynein superfamily proteins in organelle transport and cell division. *Curr Opin Cell Biol,* 10**,** 60-73.

HIRONO, M., SUGIYAMA, T., KISHIMOTO, Y., SAKAI, I., MIYAZAWA, T., KISHIO, M., INOUE, H., NAKAO, K., IKEDA, M., KAWAHARA, S., KIRINO, Y., KATSUKI, M., HORIE, H., ISHIKAWA, Y. & YOSHIOKA, T. 2001. Phospholipase Cbeta4 and protein kinase Calpha and/or protein kinase CbetaI are involved in the induction of long term depression in cerebellar Purkinje cells. *J Biol Chem,* 276**,** 45236-42.

HOFMANN, S. L. & MAJERUS, P. W. 1982. Identification and properties of two distinct phosphatidylinositol-specific phospholipase C enzymes from sheep seminal vesicular glands. *J Biol Chem,* 257**,** 6461-9.

HOKIN, M. R. & HOKIN, L. E. 1953. Enzyme secretion and the incorporation of P32 into phospholipides of pancreas slices. *J Biol Chem,* 203**,** 967-77.

HONG, M., SCHACHTER, K. A., JIANG, G. & KRAUSS, R. S. 2012. Neogenin regulates Sonic Hedgehog pathway activity during digit patterning. *Dev Dyn,* 241**,** 627-37.

HOPKINS, A. L. & GROOM, C. R. 2002. The druggable genome. *Nat Rev Drug Discov,* 1**,** 727-30.

HORCH, H. L. & SARGENT, P. B. 1995. Perisynaptic surface distribution of multiple classes of nicotinic acetylcholine receptors on neurons in the chicken ciliary ganglion. *J Neurosci,* 15**,** 7778-95.

HORSTMAN, D. A., CHATTOPADHYAY, A. & CARPENTER, G. 1999. The influence of deletion mutations on phospholipase C-gamma 1 activity. *Arch Biochem Biophys,* 361**,** 149-55.

HOTH, M. & PENNER, R. 1992. Depletion of intracellular calcium stores activates a calcium current in mast cells. *Nature,* 355**,** 353-6.

HSIA, J. A., MOSS, J., HEWLETT, E. L. & VAUGHAN, M. 1984. ADP-ribosylation of adenylate cyclase by pertussis toxin. Effects on inhibitory agonist binding. *J Biol Chem,* 259**,** 1086-90.

HUBBARD, S. R. & TILL, J. H. 2000. Protein tyrosine kinase structure and function. *Annu Rev Biochem,* 69**,** 373-98.

HUBER, A., SANDER, P., BAHNER, M. & PAULSEN, R. 1998. The TRP Ca2+ channel assembled in a signaling complex by the PDZ domain protein INAD is phosphorylated through the interaction with protein kinase C (ePKC). *FEBS Lett,* 425**,** 317-22.

HUBER, F., SCHNAUSS, J., RONICKE, S., RAUCH, P., MULLER, K., FUTTERER, C. & KAS, J. 2013. Emergent complexity of the cytoskeleton: from single filaments to tissue. *Adv Phys,* 62**,** 1-112.

HUI, C. C. & JOYNER, A. L. 1993. A mouse model of greig cephalopolysyndactyly syndrome: the extra-toesJ mutation contains an intragenic deletion of the Gli3 gene. *Nat Genet,* 3**,** 241-6.

HUMBERT, J. P., MATTER, N., ARTAULT, J. C., KOPPLER, P. & MALVIYA, A. N. 1996. Inositol 1,4,5-trisphosphate receptor is located to the inner nuclear membrane vindicating regulation of nuclear calcium signaling by inositol 1,4,5-trisphosphate. Discrete distribution of inositol phosphate receptors to inner and outer nuclear membranes. *J Biol Chem,* 271**,** 478-85.

HUNG, M. C. & LINK, W. 2011. Protein localization in disease and therapy. *J Cell Sci,* 124**,** 3381-92.

HUTTON, M., BUSFIELD, F., WRAGG, M., CROOK, R., PEREZ-TUR, J., CLARK, R. F., PRIHAR, G., TALBOT, C., PHILLIPS, H., WRIGHT, K., BAKER, M., LENDON, C., DUFF, K., MARTINEZ, A., HOULDEN, H., NICHOLS, A., KARRAN, E., ROBERTS, G., ROQUES, P., ROSSOR, M., VENTER, J. C., ADAMS, M. D., CLINE, R. T., PHILLIPS, C. A., GOATE, A. & ET AL. 1996. Complete analysis of the presenilin 1 gene in early onset Alzheimer's disease. *Neuroreport,* 7**,** 801-5.

HWANG, J. I., HEO, K., SHIN, K. J., KIM, E., YUN, C., RYU, S. H., SHIN, H. S. & SUH, P. G. 2000. Regulation of phospholipase C-beta 3 activity by Na+/H+ exchanger regulatory factor 2. *J Biol Chem,* 275**,** 16632-7.

HWANG, J. I., OH, Y. S., SHIN, K. J., KIM, H., RYU, S. H. & SUH, P. G. 2005. Molecular cloning and characterization of a novel phospholipase C, PLC-eta. *Biochem J,* 389**,** 181-6.

ICHAS, F. & MAZAT, J. P. 1998. From calcium signaling to cell death: two conformations for the mitochondrial permeability transition pore. Switching from low- to high-conductance state. *Biochim Biophys Acta,* 1366**,** 33-50.

IGWE, O. J. & FILLA, M. B. 1997. Aging-related regulation of myo-inositol 1,4,5-trisphosphate signal transduction pathway in the rat striatum. *Brain Res Mol Brain Res,* 46**,** 39-53.

INCARDONA, J. P., LEE, J. H., ROBERTSON, C. P., ENGA, K., KAPUR, R. P. & ROELINK, H. 2000. Receptor-mediated endocytosis of soluble and membrane-tethered Sonic hedgehog by Patched-1. *Proc Natl Acad Sci U S A,* 97**,** 12044-9.

INGHAM, P. W. 1998. The patched gene in development and cancer. *Curr Opin Genet Dev,* 8**,** 88-94.

INGHAM, P. W. & MCMAHON, A. P. 2001. Hedgehog signaling in animal development: paradigms and principles. *Genes Dev,* 15**,** 3059-87.

INOKI, K., OUYANG, H., ZHU, T., LINDVALL, C., WANG, Y., ZHANG, X., YANG, Q., BENNETT, C., HARADA, Y., STANKUNAS, K., WANG, C. Y., HE, X., MACDOUGALD, O. A., YOU, M., WILLIAMS, B. O. & GUAN, K. L. 2006. TSC2 integrates Wnt and energy signals via a coordinated phosphorylation by AMPK and GSK3 to regulate cell growth. *Cell,* 126**,** 955-68.

INUI, M., SAITO, A. & FLEISCHER, S. 1987. Purification of the ryanodine receptor and identity with feet structures of junctional terminal cisternae of sarcoplasmic reticulum from fast skeletal muscle. *J Biol Chem,* 262**,** 1740-7.

IQBAL, K., ALONSO ADEL, C., CHEN, S., CHOHAN, M. O., EL-AKKAD, E., GONG, C. X., KHATOON, S., LI, B., LIU, F., RAHMAN, A., TANIMUKAI, H. & GRUNDKE-IQBAL, I. 2005. Tau pathology in Alzheimer disease and other tauopathies. *Biochim Biophys Acta,* 1739**,** 198-210.

IRVINE, R. F. 2003. Nuclear lipid signalling. *Nat Rev Mol Cell Biol,* 4**,** 349-60.

ITOH, K., ISHIMA, T., KEHLER, J. & HASHIMOTO, K. 2011. Potentiation of NGF-induced neurite outgrowth in PC12 cells by papaverine: role played by PLC-gamma, IP3 receptors. *Brain Res,* 1377**,** 32-40.

IZUMI, Y., OHTA, N., ITOH-FURUYA, A., FUSE, N. & MATZUSAKI, F. 2004. Differential functions of G protein and Baz-aPKC signalling pathways in Drosophila neuroblast assymetric division. *J. cell Biol*. 164, 729-738.

JANG, H. J., YANG, Y. R., KIM, J. K., CHOI, J. H., SEO, Y. K., LEE, Y. H., LEE, J. E., RYU, S. H. & SUH, P. G. 2013. Phospholipase C-gamma1 involved in brain disorders. *Adv Biol Regul,* 53**,** 51-62.

JANMEY, P. A. & KINNUNEN, P. K. 2006. Biophysical properties of lipids and dynamic membranes. *Trends Cell Biol,* 16**,** 538-46.

JENKINS, D. 2009. Hedgehog signalling: emerging evidence for non-canonical pathways. *Cell signal,* 21, 1023-34.

JI, T. H., GROSSMANN, M. & JI, I. 1998. G protein-coupled receptors. I. Diversity of receptor-ligand interactions. *J Biol Chem,* 273**,** 17299-302.

JIA, J., KOLTERUD, A., ZENG, H., HOOVER, A., TEGLUND, S., TOFTGARD, R. & LIU, A. 2009. Suppressor of Fused inhibits mammalian Hedgehog signaling in the absence of cilia. *Dev Biol,* 330**,** 452-60.

JIANG, D., ZHAO, L. & CLAPHAM, D. E. 2009. Genome-wide RNAi screen identifies Letm1 as a mitochondrial Ca2+/H+ antiporter. *Science,* 326**,** 144-7.

JONES, K. T. 1998. Ca2+ oscillations in the activation of the egg and development of the embryo in mammals. *Int J Dev Biol,* 42**,** 1-10.

JUNG, H., KIM, H. J., LEE, S. K., KIM, R., KOPACHIK, W., HAN, J. K. & JHO, E. H. 2009. Negative feedback regulation of Wnt signaling by Gbetagamma-mediated reduction of Dishevelled. *Exp Mol Med,* 41**,** 695-706.

KABACHINSKI, G., YAMAGA, M., KIELAR-GREVSTAD, D. M., BRUINSMA, S. & MARTIN, T. F. 2014. CAPS and Munc13 utilize distinct PIP2-linked mechanisms to promote vesicle exocytosis. *Mol Biol Cell,* 25**,** 508-21.

KAMAT, A. & CARPENTER, G. 1997. Phospholipase C-gamma1: regulation of enzyme function and role in growth factor-dependent signal transduction. *Cytokine Growth Factor Rev,* 8**,** 109-17.

KAMMERMEIER, P. J., RUIZ-VELASCO, V. & IKEDA, S. R. 2000. A voltage-independent calcium current inhibitory pathway activated by muscarinic agonists in rat sympathetic neurons requires both Galpha q/11 and Gbeta gamma. *J Neurosci,* 20**,** 5623-9.

KAMP, F., ZAKIM, D., ZHANG, F., NOY, N. & HAMILTON, J. A. 1995. Fatty acid flip-flop in phospholipid bilayers is extremely fast. *Biochemistry,* 34**,** 11928-37.

KANEMARU, K., NAKAHARA, M., NAKAMURA, Y., HASHIGUCHI, Y., KOUCHI, Z., YAMAGUCHI, H., OSHIMA, N., KIYONARI, H. & FUKAMI, K. 2010. Phospholipase C-eta2 is highly expressed in the habenula and retina. *Gene Expr Patterns,* 10**,** 119-26.

KATAN, M. 2005. New insights into the families of PLC enzymes: looking back and going forward. *Biochem J,* 391**,** e7-9.

KAUFMAN, R. J. 1999. Stress signaling from the lumen of the endoplasmic reticulum: coordination of gene transcriptional and translational controls. *Genes Dev,* 13**,** 1211-33.

KELLEY, G. G., REKS, S. E., ONDRAKO, J. M. & SMRCKA, A. V. 2001. Phospholipase C(epsilon): a novel Ras effector. *EMBO J,* 20**,** 743-54.

KELLY, B. L. & FERREIRA, A. 2006. beta-Amyloid-induced dynamin 1 degradation is mediated by N-methyl-D-aspartate receptors in hippocampal neurons. *J Biol Chem,* 281**,** 28079-89.

KENT, C. 1995. Eukaryotic phospholipid biosynthesis. *Annu Rev Biochem,* 64**,** 315-43.

KHACHATURIAN, Z. S. 1987. Hypothesis on the regulation of cytosol calcium concentration and the aging brain. *Neurobiol Aging,* 8**,** 345-6.

KILIAN, B., MANSUKOSKI, H., BARBOSA, F. C., ULRICH, F., TADA, M. & HEISENBERG, C. P. 2003. The role of Ppt/Wnt5 in regulating cell shape and movement during zebrafish gastrulation. *Mech Dev,* 120**,** 467-76.

KIM, C. G., PARK, D. & RHEE, S. G. 1996. The role of carboxyl-terminal basic amino acids in Gqalpha-dependent activation, particulate association, and nuclear localization of phospholipase C-beta1. *J Biol Chem,* 271**,** 21187-92.

KIM, D., JUN, K. S., LEE, S. B., KANG, N. G., MIN, D. S., KIM, Y. H., RYU, S. H., SUH, P. G. & SHIN, H. S. 1997. Phospholipase C isozymes selectively couple to specific neurotransmitter receptors. *Nature,* 389**,** 290-3.

KIM, J., KATO, M. & BEACHY, P. A. 2009. Gli2 trafficking links Hedgehog-dependent activation of Smoothened in the primary cilium to transcriptional activation in the nucleus. *Proc Natl Acad Sci U S A,* 106**,** 21666-71.

KIM, J. K., CHOI, J. W., LIM, S., KWON, O., SEO, J. K., RYU, S. H. & SUH, P. G. 2011. Phospholipase C-eta1 is activated by intracellular Ca(2+) mobilization and enhances GPCRs/PLC/Ca(2+) signaling. *Cell Signal,* 23**,** 1022-9.

KIM, J. W., SIM, S. S., KIM, U. H., NISHIBE, S., WAHL, M. I., CARPENTER, G. & RHEE, S. G. 1990. Tyrosine residues in bovine phospholipase C-gamma phosphorylated by the epidermal growth factor receptor in vitro. *J Biol Chem,* 265**,** 3940-3.

KINZLER, K. W. & VOGELSTEIN, B. 1990. The GLI gene encodes a nuclear protein which binds specific sequences in the human genome. *Mol Cell Biol,* 10**,** 634-42.

KLEBE, R. J. & RUDDLE, F. H. 1969. 'Neuroblastoma: Cell culture analysis of a differentiating stem cell system. *J Cell Biol*.

KLECKNER, N. W. & DINGLEDINE, R. 1988. Requirement for glycine in activation of NMDA-receptors expressed in Xenopus oocytes. *Science,* 241**,** 835-7.

KOBILKA, B. K. 2007. G protein coupled receptor structure and activation. *Biochim Biophys Acta,* 1768**,** 794-807.

KOHN, A. D. & MOON, R. T. 2005. Wnt and calcium signaling: beta-catenin-independent pathways. *Cell Calcium,* 38**,** 439-46.

KOMURO, H. & RAKIC, P. 1996. Intracellular Ca2+ fluctuations modulate the rate of neuronal migration. *Neuron,* 17**,** 275-85.

KOUCHI, Z., IGARASHI, T., SHIBAYAMA, N., INANOBE, S., SAKURAI, K., YAMAGUCHI, H., FUKUDA, T., YANAGI, S., NAKAMURA, Y. & FUKAMI, K. 2011. Phospholipase Cdelta3 regulates RhoA/Rho kinase signaling and neurite outgrowth. *J Biol Chem,* 286**,** 8459-71.

KOUCHI, Z., SHIKANO, T., NAKAMURA, Y., SHIRAKAWA, H., FUKAMI, K. & MIYAZAKI, S. 2005. The role of EF-hand domains and C2 domain in regulation of enzymatic activity of phospholipase Czeta. *J Biol Chem,* 280**,** 21015-21.

KOVAL, A. & KATANAEV, V. L. 2011. Wnt3a stimulation elicits G-protein-coupled receptor properties of mammalian Frizzled proteins. *Biochem J,* 433**,** 435-40.

KRAUSS, S., CONCORDET, J. P. & INGHAM, P. W. 1993. A functionally conserved homolog of the Drosophila segment polarity gene hh is expressed in tissues with polarizing activity in zebrafish embryos. *Cell,* 75**,** 1431-44.

KRETSINGER, R. H. & NOCKOLDS, C. E. 1973. Carp muscle calcium-binding protein. II. Structure determination and general description. *J Biol Chem,* 248**,** 3313-26.

KUCHIBHOTLA, K. V., GOLDMAN, S. T., LATTARULO, C. R., WU, H. Y., HYMAN, B. T. & BACSKAI, B. J. 2008. Abeta plaques lead to aberrant regulation of calcium homeostasis in vivo resulting in structural and functional disruption of neuronal networks. *Neuron,* 59**,** 214-25.

KUHL, M., SHELDAHL, L. C., MALBON, C. C. & MOON, R. T. 2000. Ca(2+)/calmodulin-dependent protein kinase II is stimulated by Wnt and Frizzled homologs and promotes ventral cell fates in Xenopus. *J Biol Chem,* 275**,** 12701-11.

KUMAR, V., JONG, Y. J. & O'MALLEY, K. L. 2008. Activated nuclear metabotropic glutamate receptor mGlu5 couples to nuclear Gq/11 proteins to generate inositol 1,4,5-trisphosphate-mediated nuclear Ca2+ release. *J Biol Chem,* 283**,** 14072-83.

KUME, S., MUTO, A., OKANO, H. & MIKOSHIBA, K. 1997. Developmental expression of the inositol 1,4,5-trisphosphate receptor and localization of inositol 1,4,5-trisphosphate during early embryogenesis in Xenopus laevis. *Mech Dev,* 66**,** 157-68.

KURIAN, M. A., MEYER, E., VASSALLO, G., MORGAN, N. V., PRAKASH, N., PASHA, S., HAI, N. A., SHUIB, S., RAHMAN, F., WASSMER, E., CROSS, J. H., O'CALLAGHAN, F. J., OSBORNE, J. P., SCHEFFER, I. E., GISSEN, P. & MAHER, E. R. 2010. Phospholipase C beta 1 deficiency is associated with early-onset epileptic encephalopathy. *Brain,* 133**,** 2964-70.

KUROSE, H. 2003. Galpha12 and Galpha13 as key regulatory mediator in signal transduction. *Life Sci,* 74**,** 155-61.

KUWAJIMA, G., FUTATSUGI, A., NIINOBE, M., NAKANISHI, S. & MIKOSHIBA, K. 1992. Two types of ryanodine receptors in mouse brain: skeletal muscle type exclusively in Purkinje cells and cardiac muscle type in various neurons. *Neuron,* 9**,** 1133-42.

LAGERSTROM, M. C. & SCHIOTH, H. B. 2008. Structural diversity of G protein-coupled receptors and significance for drug discovery. *Nat Rev Drug Discov,* 7**,** 339-57.

LAI, F. A., ERICKSON, H. P., ROUSSEAU, E., LIU, Q. Y. & MEISSNER, G. 1988. Purification and reconstitution of the calcium release channel from skeletal muscle. *Nature,* 331**,** 315-9.

LAMBERT, M. P., BARLOW, A. K., CHROMY, B. A., EDWARDS, C., FREED, R., LIOSATOS, M., MORGAN, T. E., ROZOVSKY, I., TROMMER, B., VIOLA, K. L., WALS, P., ZHANG, C., FINCH, C. E., KRAFFT, G. A. & KLEIN, W. L. 1998. Diffusible, nonfibrillar ligands derived from Abeta1-42 are potent central nervous system neurotoxins. *Proc Natl Acad Sci U S A,* 95**,** 6448-53.

LANE, M. A. & BAILEY, S. J. 2005. Role of retinoid signalling in the adult brain. *Prog Neurobiol,* 75**,** 275-93.

LEDEEN, R. W. & WU, G. 2004. Nuclear lipids: key signaling effectors in the nervous system and other tissues. *J Lipid Res,* 45**,** 1-8.

LEE, H. J., WANG, N. X., SHAO, Y. & ZHENG, J. J. 2009a. Identification of tripeptides recognized by the PDZ domain of Dishevelled. *Bioorg Med Chem,* 17**,** 1701-8.

LEE, H. J., WANG, N. X., SHI, D. L. & ZHENG, J. J. 2009b. Sulindac inhibits canonical Wnt signaling by blocking the PDZ domain of the protein Dishevelled. *Angew Chem Int Ed Engl,* 48**,** 6448-52.

LEE, H. J. & ZHENG, J. J. 2010. PDZ domains and their binding partners: structure, specificity, and modification. *Cell Commun Signal,* 8**,** 8.

LEE, S. B. & RHEE, S. G. 1996. Molecular cloning, splice variants, expression, and purification of phospholipase C-delta 4. *J Biol Chem,* 271**,** 25-31.

LEE, S. B., VARNAI, P., BALLA, A., JALINK, K., RHEE, S. G. & BALLA, T. 2004. The pleckstrin homology domain of phosphoinositide-specific phospholipase Cdelta4 is not a critical determinant of the membrane localization of the enzyme. *J Biol Chem,* 279**,** 24362-71.

LEE, W. K., KIM, J. K., SEO, M. S., CHA, J. H., LEE, K. J., RHA, H. K., MIN, D. S., JO, Y. H. & LEE, K. H. 1999. Molecular cloning and expression analysis of a mouse phospholipase C-delta1. *Biochem Biophys Res Commun,* 261**,** 393-9.

LEISSRING, M. A., PAUL, B. A., PARKER, I., COTMAN, C. W. & LAFERLA, F. M. 1999. Alzheimer's presenilin-1 mutation potentiates inositol 1,4,5-trisphosphate-mediated calcium signaling in Xenopus oocytes. *J Neurochem,* 72**,** 1061-8.

LEMMON, M. A. 2003. Phosphoinositide recognition domains. *Traffic,* 4**,** 201-13.

LENGLER, J., HOLZMULLER, H., SALMONS, B., GUNZBURG, W. H. & RENNER, M. 2005. FMDV-2A sequence and protein arrangement contribute to functionality of CYP2B1-reporter fusion protein. *Anal Biochem,* 343**,** 116-24.

LESNE, S., KOH, M. T., KOTILINEK, L., KAYED, R., GLABE, C. G., YANG, A., GALLAGHER, M. & ASHE, K. H. 2006. A specific amyloid-beta protein assembly in the brain impairs memory. *Nature,* 440**,** 352-7.

LEWIT-BENTLEY, A. & RETY, S. 2000. EF-hand calcium-binding proteins. *Curr Opin Struct Biol,* 10**,** 637-43.

LI, H. S., XU, X. Z. & MONTELL, C. 1999. Activation of a TRPC3-dependent cation current through the neurotrophin BDNF. *Neuron,* 24**,** 261-73.

LI, Y., STERNWEIS, P. M., CHARNECKI, S., SMITH, T. F., GILMAN, A. G., NEER, E. J. & KOZASA, T. 1998. Sites for Galpha binding on the G protein beta subunit overlap with sites for regulation of phospholipase Cbeta and adenylyl cyclase. *J Biol Chem,* 273**,** 16265-72.

LI, Y. S., WU, P., ZHOU, X. Y., CHEN, J. G., CAI, L., WANG, F., XU, L. M., ZHANG, X. L., CHEN, Y., LIU, S. J., HUANG, Y. P. & YE, D. Y. 2008. Formyl-peptide receptor like 1: a potent mediator of the Ca2+ release-activated Ca2+ current ICRAC. *Arch Biochem Biophys,* 478**,** 110-8.

LIEBNER, S. & PLATE, K. H. 2010. Differentiation of the brain vasculature: the answer came blowing by the Wnt. *J Angiogenes Res,* 2**,** 1.

LIEM, K. F., JR., HE, M., OCBINA, P. J. & ANDERSON, K. V. 2009. Mouse Kif7/Costal2 is a cilia-associated protein that regulates Sonic hedgehog signaling. *Proc Natl Acad Sci U S A,* 106**,** 13377-82.

LIN, K., TANG, M., HAN, H., GUO, Y., LIN, Y. & MA, C. 2010. Association between the polymorphisms of CALHM1 and GOLPH2 genes and Alzheimer's disease. *Psychiatr Genet,* 20**,** 190.

LINDWALL, G. & COLE, R. D. 1984. Phosphorylation affects the ability of tau protein to promote microtubule assembly. *J Biol Chem,* 259**,** 5301-5.

LING, K., SCHILL, N. J., WAGONER, M. P., SUN, Y. & ANDERSON, R. A. 2006. Movin' on up: the role of PtdIns(4,5)P(2) in cell migration. *Trends Cell Biol,* 16**,** 276-84.

LIU, N., FUKAMI, K., YU, H. & TAKENAWA, T. 1996. A new phospholipase C delta 4 is induced at S-phase of the cell cycle and appears in the nucleus. *J Biol Chem,* 271**,** 355-60.

LIU, C.C., Kanekiyo, T., Xu, H., & Bu, G. 2013. Apolipoprotein E and Alzheimer's disease: risk, mechanisms and therapy. *Nature Reviews Neurology,* 9, 106-118.

LO VASCO, V. R. 2011. 1p36.32 rearrangements and the role of PI-PLC eta2 in nervous tumours. *J Neurooncol,* 103**,** 409-16.

LO VASCO, V. R., CARDINALE, G. & POLONIA, P. 2012. Deletion of PLCB1 gene in schizophrenia-affected patients. *J Cell Mol Med,* 16**,** 844-51.

LO VASCO, V. R., LONGO, L. & POLONIA, P. 2013. Phosphoinositide-specific Phospholipase C beta1 gene deletion in bipolar disorder affected patient. *J Cell Commun Signal,* 7**,** 25-9.

LOGAN, C. Y. & NUSSE, R. 2004. The Wnt signaling pathway in development and disease. *Annu Rev Cell Dev Biol,* 20**,** 781-810.

LOGOTHETIS, D. E., KURACHI, Y., GALPER, J., NEER, E. J. & CLAPHAM, D. E. 1987. The beta gamma subunits of GTP-binding proteins activate the muscarinic K+ channel in heart. *Nature,* 325**,** 321-6.

LOMASNEY, J. W., CHENG, H. F., WANG, L. P., KUAN, Y., LIU, S., FESIK, S. W. & KING, K. 1996. Phosphatidylinositol 4,5-bisphosphate binding to the pleckstrin homology domain of phospholipase C-delta1 enhances enzyme activity. *J Biol Chem,* 271**,** 25316-26.

LONGENECKER, K. L., LEWIS, M. E., CHIKUMI, H., GUTKIND, J. S. & DEREWENDA, Z. S. 2001. Structure of the RGS-like domain from PDZ-RhoGEF: linking heterotrimeric g protein-coupled signaling to Rho GTPases. *Structure,* 9**,** 559-69.

LOPES, M. H., HAJJ, G. N., MURAS, A. G., MANCINI, G. L., CASTRO, R. M., RIBEIRO, K. C., BRENTANI, R. R., LINDEN, R. & MARTINS, V. R. 2005. Interaction of cellular prion and stress-inducible protein 1 promotes neuritogenesis and neuroprotection by distinct signaling pathways. *J Neurosci,* 25**,** 11330-9.

LOPEZ, I., MAK, E. C., DING, J., HAMM, H. E. & LOMASNEY, J. W. 2001. A novel bifunctional phospholipase c that is regulated by Galpha 12 and stimulates the Ras/mitogen-activated protein kinase pathway. *J Biol Chem,* 276**,** 2758-65.

LORENS, J. B., PEARSALL, D. M., SWIFT, S. E., PEELLE, B., ARMSTRONG, R., DEMO, S. D., FERRICK, D. A., HITOSHI, Y., PAYAN, D. G. & ANDERSON, D. 2004. Stable, stoichiometric delivery of diverse protein functions. *J Biochem Biophys Methods,* 58**,** 101-10.

LOWERY, L. A., RUBIN, J. & SIVE, H. 2007. Whitesnake/sfpq is required for cell survival and neuronal development in the zebrafish. *Dev Dyn,* 236**,** 1347-57.

LUCKHOFF, A. & CLAPHAM, D. E. 1992. Inositol 1,3,4,5-tetrakisphosphate activates an endothelial Ca(2+)-permeable channel. *Nature,* 355**,** 356-8.

LUCOCQ, J. M. & GAWDEN-BONE, C. 2010. Quantitative assessment of specificity in immunoelectron microscopy. *J Histochem Cytochem,* 58**,** 917-27.

LUNDBERG, E., FAGERBERG, L., KLEVEBRING, D., MATIC, I., GEIGER, T., COX, J., ALGENAS, C., LUNDEBERG, J., MANN, M. & UHLEN, M. 2010. Defining the transcriptome and proteome in three functionally different human cell lines. *Mol Syst Biol,* 6**,** 450.

LUTTRELL, L. M. & LEFKOWITZ, R. J. 2002. The role of beta-arrestins in the termination and transduction of G-protein-coupled receptor signals. *J Cell Sci,* 115**,** 455-65.

MA, Q. L., YANG, F., ROSARIO, E. R., UBEDA, O. J., BEECH, W., GANT, D. J., CHEN, P. P., HUDSPETH, B., CHEN, C., ZHAO, Y., VINTERS, H. V., FRAUTSCHY, S. A. & COLE, G. M. 2009. Beta-amyloid oligomers induce phosphorylation of tau and inactivation of insulin receptor substrate via c-Jun N-terminal kinase signaling: suppression by omega-3 fatty acids and curcumin. *J Neurosci,* 29**,** 9078-89.

MAEDA, N., KAWASAKI, T., NAKADE, S., YOKOTA, N., TAGUCHI, T., KASAI, M. & MIKOSHIBA, K. 1991. Structural and functional characterization of inositol 1,4,5-trisphosphate receptor channel from mouse cerebellum. *J Biol Chem,* 266**,** 1109-16.

MANENT, J. B., DEMARQUE, M., JORQUERA, I., PELLEGRINO, C., BEN-ARI, Y., ANIKSZTEJN, L. & REPRESA, A. 2005. A noncanonical release of GABA and glutamate modulates neuronal migration. *J Neurosci,* 25**,** 4755-65.

MARAMBAUD, P., DRESES-WERRINGLOER, U. & VINGTDEUX, V. 2009. Calcium signaling in neurodegeneration. *Mol Neurodegener,* 4**,** 20.

MARCAND, S., GASSER, S. M. & GILSON, E. 1996. Chromatin: a sticky silence. *Curr Biol,* 6**,** 1222-5.

MARCHENKO, S. M. & THOMAS, R. C. 2006. Nuclear Ca2+ signalling in cerebellar Purkinje neurons. *Cerebellum,* 5**,** 36-42.

MARCHENKO, S. M., YAROTSKYY, V. V., KOVALENKO, T. N., KOSTYUK, P. G. & THOMAS, R. C. 2005. Spontaneously active and InsP3-activated ion channels in cell nuclei from rat cerebellar Purkinje and granule neurones. *J Physiol,* 565**,** 897-910.

MARGOLSKEE, R. F. 2002. Molecular mechanisms of bitter and sweet taste transduction. *J Biol Chem,* 277**,** 1-4.

MARKS, A. R., TEMPST, P., HWANG, K. S., TAUBMAN, M. B., INUI, M., CHADWICK, C., FLEISCHER, S. & NADAL-GINARD, B. 1989. Molecular cloning and characterization of the ryanodine receptor/junctional channel complex cDNA from skeletal muscle sarcoplasmic reticulum. *Proc Natl Acad Sci U S A,* 86**,** 8683-7.

MARTELLI, A. M., GILMOUR, R. S., BERTAGNOLO, V., NERI, L. M., MANZOLI, L. & COCCO, L. 1992. Nuclear localization and signalling activity of phosphoinositidase C beta in Swiss 3T3 cells. *Nature,* 358**,** 242-5.

MARTELLI, A. M., NERI, L. M., GILMOUR, R. S., BARKER, P. J., HUSKISSON, N. S., MANZOLI, F. A. & COCCO, L. 1991. Temporal changes in intracellular distribution of protein kinase C in Swiss 3T3 cells during mitogenic stimulation with insulin-like growth factor I and bombesin: translocation to the nucleus follows rapid changes in nuclear polyphosphoinositides. *Biochem Biophys Res Commun,* 177**,** 480-7.

MARTIN, K. C., MICHAEL, D., ROSE, J. C., BARAD, M., CASADIO, A., ZHU, H. & KANDEL, E. R. 1997. MAP kinase translocates into the nucleus of the presynaptic cell and is required for long-term facilitation in Aplysia. *Neuron,* 18**,** 899-912.

MASTAKOV, M. Y., BAER, K., SYMES, C. W., LEICHTLEIN, C. B., KOTIN, R. M. & DURING, M. J. 2002. Immunological aspects of recombinant adeno-associated virus delivery to the mammalian brain. *J Virol,* 76**,** 8446-54.

MASTERS, C. L., SIMMS, G., WEINMAN, N. A., MULTHAUP, G., MCDONALD, B. L. & BEYREUTHER, K. 1985. Amyloid plaque core protein in Alzheimer disease and Down syndrome. *Proc Natl Acad Sci U S A,* 82**,** 4245-9.

MASUMIYA, H., WANG, R., ZHANG, J., XIAO, B. & CHEN, S. R. 2003. Localization of the 12.6-kDa FK506-binding protein (FKBP12.6) binding site to the NH2-terminal domain of the cardiac Ca2+ release channel (ryanodine receptor). *J Biol Chem,* 278**,** 3786-92.

MATTEUCCI, A., FAENZA, I., GILMOUR, R. S., MANZOLI, L., BILLI, A. M., PERUZZI, D., BAVELLONI, A., RHEE, S. G. & COCCO, L. 1998. Nuclear but not cytoplasmic phospholipase C beta 1 inhibits differentiation of erythroleukemia cells. *Cancer Res,* 58**,** 5057-60.

MATTHEWS, R. P., GUTHRIE, C. R., WAILES, L. M., ZHAO, X., MEANS, A. R. & MCKNIGHT, G. S. 1994. Calcium/calmodulin-dependent protein kinase types II and IV differentially regulate CREB-dependent gene expression. *Mol Cell Biol,* 14**,** 6107-16.

MATTILA, P. K., PYKALAINEN, A., SAARIKANGAS, J., PAAVILAINEN, V. O., VIHINEN, H., JOKITALO, E. & LAPPALAINEN, P. 2007. Missing-in-metastasis and IRSp53 deform PI(4,5)P2-rich membranes by an inverse BAR domain-like mechanism. *J Cell Biol,* 176**,** 953-64.

MATTSON, M. P. & CHAN, S. L. 2003. Neuronal and glial calcium signaling in Alzheimer's disease. *Cell Calcium,* 34**,** 385-97.

MATTSON, M. P., CHENG, B., DAVIS, D., BRYANT, K., LIEBERBURG, I. & RYDEL, R. E. 1992. beta-Amyloid peptides destabilize calcium homeostasis and render human cortical neurons vulnerable to excitotoxicity. *J Neurosci,* 12**,** 376-89.

MAUCH, T. J. & SCHOENWOLF, G. C. 2001. Developmental Biology. Sixth Edition. By Scott F. Gilbert. *American Journal of Medical Genetics,* 99**,** 170-171.

MAYER, M. L. & WESTBROOK, G. L. 1987. Permeation and block of N-methyl-D-aspartic acid receptor channels by divalent cations in mouse cultured central neurones. *J Physiol,* 394**,** 501-27.

MCCUDDEN, C. R., HAINS, M. D., KIMPLE, R. J., SIDEROVSKI, D. P. & WILLARD, F. S. 2005. G-protein signaling: back to the future. *Cell Mol Life Sci,* 62**,** 551-77.

MCCULLAR, J. S., LARSEN, S. A., MILLIMAKI, R. A. & FILTZ, T. M. 2003. Calmodulin is a phospholipase C-beta interacting protein. *J Biol Chem,* 278**,** 33708-13.

MCDERMOTT, M., WAKELAM, M. J. & MORRIS, A. J. 2004. Phospholipase D. *Biochem Cell Biol,* 82**,** 225-53.

MCLACHLAN, D. R., WONG, L., BERGERON, C. & BAIMBRIDGE, K. G. 1987. Calmodulin and calbindin D28K in Alzheimer disease. *Alzheimer Dis Assoc Disord,* 1**,** 171-9.

MCSTAY, G. P., CLARKE, S. J. & HALESTRAP, A. P. 2002. Role of critical thiol groups on the matrix surface of the adenine nucleotide translocase in the mechanism of the mitochondrial permeability transition pore. *Biochem J,* 367**,** 541-8.

MEBERG, P. J., KINNEY, W. R., VALCOURT, E. G. & ROUTTENBERG, A. 1996. Gene expression of the transcription factor NF-kappa B in hippocampus: regulation by synaptic activity. *Brain Res Mol Brain Res,* 38**,** 179-90.

MEISENHELDER, J., SUH, P. G., RHEE, S. G. & HUNTER, T. 1989. Phospholipase C-gamma is a substrate for the PDGF and EGF receptor protein-tyrosine kinases in vivo and in vitro. *Cell,* 57**,** 1109-22.

MEISSNER, G. & EL-HASHEM, A. 1992. Ryanodine as a functional probe of the skeletal muscle sarcoplasmic reticulum Ca2+ release channel. *Mol Cell Biochem,* 114**,** 119-23.

MELLITI, K., MEZA, U., FISHER, R. & ADAMS, B. 1999. Regulators of G protein signaling attenuate the G protein-mediated inhibition of N-type Ca channels. *J Gen Physiol,* 113**,** 97-110.

MELLMAN, D. L., GONZALES, M. L., SONG, C., BARLOW, C. A., WANG, P., KENDZIORSKI, C. & ANDERSON, R. A. 2008. A PtdIns4,5P2-regulated nuclear poly(A) polymerase controls expression of select mRNAs. *Nature,* 451**,** 1013-7.

MELONI, A. R., FRALISH, G. B., KELLY, P., SALAHPOUR, A., CHEN, J. K., WECHSLER-REYA, R. J., LEFKOWITZ, R. J. & CARON, M. G. 2006. Smoothened signal transduction is promoted by G protein-coupled receptor kinase 2. *Mol Cell Biol,* 26**,** 7550-60.

MERY, L., MESAELI, N., MICHALAK, M., OPAS, M., LEW, D. P. & KRAUSE, K. H. 1996. Overexpression of calreticulin increases intracellular Ca2+ storage and decreases store-operated Ca2+ influx. *J Biol Chem,* 271**,** 9332-9.

MIGNEN, O., THOMPSON, J. L. & SHUTTLEWORTH, T. J. 2003. Ca2+ selectivity and fatty acid specificity of the noncapacitative, arachidonate-regulated Ca2+ (ARC) channels. *J Biol Chem,* 278**,** 10174-81.

MIGNEN, O., THOMPSON, J. L. & SHUTTLEWORTH, T. J. 2007. STIM1 regulates Ca2+ entry via arachidonate-regulated Ca2+-selective (ARC) channels without store depletion or translocation to the plasma membrane. *J Physiol,* 579**,** 703-15.

MIGNEN, O., THOMPSON, J. L. & SHUTTLEWORTH, T. J. 2008. Both Orai1 and Orai3 are essential components of the arachidonate-regulated Ca2+-selective (ARC) channels. *J Physiol,* 586**,** 185-95.

MILLER, J. R. 2002. The Wnts. *Genome Biol,* 3**,** REVIEWS3001.

MILLIGAN, G. & KOSTENIS, E. 2006. Heterotrimeric G-proteins: a short history. *Br J Pharmacol,* 147 Suppl 1**,** S46-55.

MINICHIELLO, L. 2009. TrkB signalling pathways in LTP and learning. *Nat Rev Neurosci,* 10**,** 850-60.

MINICHIELLO, L., CALELLA, A. M., MEDINA, D. L., BONHOEFFER, T., KLEIN, R. & KORTE, M. 2002. Mechanism of TrkB-mediated hippocampal long-term potentiation. *Neuron,* 36**,** 121-37.

MITCHELL, K. J., LAI, F. A. & RUTTER, G. A. 2003. Ryanodine receptor type I and nicotinic acid adenine dinucleotide phosphate receptors mediate Ca2+ release from insulin-containing vesicles in living pancreatic beta-cells (MIN6). *J Biol Chem,* 278**,** 11057-64.

MITCHELL, K. J., PINTON, P., VARADI, A., TACCHETTI, C., AINSCOW, E. K., POZZAN, T., RIZZUTO, R. & RUTTER, G. A. 2001. Dense core secretory vesicles revealed as a dynamic Ca(2+) store in neuroendocrine cells with a vesicle-associated membrane protein aequorin chimaera. *J Cell Biol,* 155**,** 41-51.

MIYAZAKI, S., SHIRAKAWA, H., NAKADA, K. & HONDA, Y. 1993. Essential role of the inositol 1,4,5-trisphosphate receptor/Ca2+ release channel in Ca2+ waves and Ca2+ oscillations at fertilization of mammalian eggs. *Dev Biol,* 158**,** 62-78.

MONTMINY, M. R. & BILEZIKJIAN, L. M. 1987. Binding of a nuclear protein to the cyclic-AMP response element of the somatostatin gene. *Nature,* 328**,** 175-8.

MOORE, K. J. 2013. microRNAs: small regulators with a big impact on lipid metabolism. *J Lipid Res,* 54**,** 1159-60.

MORRIS, A. J., WALDO, G. L., DOWNES, C. P. & HARDEN, T. K. 1990. A receptor and G-protein-regulated polyphosphoinositide-specific phospholipase C from turkey erythrocytes. II. P2Y-purinergic receptor and G-protein-mediated regulation of the purified enzyme reconstituted with turkey erythrocyte ghosts. *J Biol Chem,* 265**,** 13508-14.

MUNDY, W., TANDON, P., ALI, S. & TILSON, H. 1991. Age-related changes in receptor-mediated phosphoinositide hydrolysis in various regions of rat brain. *Life Sci,* 49**,** PL97-102.

MURAKAMI, M. & KUDO, I. 2002. Phospholipase A2. *J Biochem,* 131**,** 285-92.

MURONE, M., LUOH, S. M., STONE, D., LI, W., GURNEY, A., ARMANINI, M., GREY, C., ROSENTHAL, A. & DE SAUVAGE, F. J. 2000. Gli regulation by the opposing activities of fused and suppressor of fused. *Nat Cell Biol,* 2**,** 310-2.

MURTHY, K. S., ZHOU, H., HUANG, J. & PENTYALA, S. N. 2004. Activation of PLC-delta1 by Gi/o-coupled receptor agonists. *Am J Physiol Cell Physiol,* 287**,** C1679-87.

MUSLIN, A. J., PETERS, K. G. & WILLIAMS, L. T. 1994. Direct activation of phospholipase C-gamma by fibroblast growth factor receptor is not required for mesoderm induction in Xenopus animal caps. *Mol Cell Biol,* 14**,** 3006-12.

MUTO, A., KUME, S., INOUE, T., OKANO, H. & MIKOSHIBA, K. 1996. Calcium waves along the cleavage furrows in cleavage-stage Xenopus embryos and its inhibition by heparin. *J Cell Biol,* 135**,** 181-90.

NAKAHARA, M., SHIMOZAWA, M., NAKAMURA, Y., IRINO, Y., MORITA, M., KUDO, Y. & FUKAMI, K. 2005. A novel phospholipase C, PLC(eta)2, is a neuron-specific isozyme. *J Biol Chem,* 280**,** 29128-34.

NAKAI, J., IMAGAWA, T., HAKAMAT, Y., SHIGEKAWA, M., TAKESHIMA, H. & NUMA, S. 1990. Primary structure and functional expression from cDNA of the cardiac ryanodine receptor/calcium release channel. *FEBS Lett,* 271**,** 169-77.

NAKAI, J., SEKIGUCHI, N., RANDO, T. A., ALLEN, P. D. & BEAM, K. G. 1998. Two regions of the ryanodine receptor involved in coupling with L-type Ca2+ channels. *J Biol Chem,* 273**,** 13403-6.

NAKANISHI, S., KUWAJIMA, G. & MIKOSHIBA, K. 1992. Immunohistochemical localization of ryanodine receptors in mouse central nervous system. *Neurosci Res,* 15**,** 130-42.

NALEFSKI, E. A. & FALKE, J. J. 1996. The C2 domain calcium-binding motif: structural and functional diversity. *Protein Sci,* 5**,** 2375-90.

NARAYANAN, D., ADEBIYI, A. & JAGGAR, J. H. 2012. Inositol trisphosphate receptors in smooth muscle cells. *Am J Physiol Heart Circ Physiol,* 302**,** H2190-210.

NEVES, S. R., RAM, P. T. & IYENGAR, R. 2002. G protein pathways. *Science,* 296**,** 1636-9.

NEYLON, C. B., RICHARDS, S. M., LARSEN, M. A., AGROTIS, A. & BOBIK, A. 1995. Multiple types of ryanodine receptor/Ca2+ release channels are expressed in vascular smooth muscle. *Biochem Biophys Res Commun,* 215**,** 814-21.

NGUYEN TLE, X., YE, K., CHO, S. W. & AHN, J. Y. 2007. Overexpression of phospholipase C-gamma1 inhibits NGF-induced neuronal differentiation by proliferative activity of SH3 domain. *Int J Biochem Cell Biol,* 39**,** 2083-92.

NICOT, A. & DICICCO-BLOOM, E. 2001. Regulation of neuroblast mitosis is determined by PACAP receptor isoform expression. *Proc Natl Acad Sci U S A,* 98**,** 4758-63.

NIGGLI, E. 1999. Localized intracellular calcium signaling in muscle: calcium sparks and calcium quarks. *Annu Rev Physiol,* 61**,** 311-35.

NIGGLI, V., ADUNYAH, E. S. & CARAFOLI, E. 1981. Acidic phospholipids, unsaturated fatty acids, and limited proteolysis mimic the effect of calmodulin on the purified erythrocyte Ca2+ - ATPase. *J Biol Chem,* 256**,** 8588-92.

NISHITA, M., YOO, S. K., NOMACHI, A., KANI, S., SOUGAWA, N., OHTA, Y., TAKADA, S., KIKUCHI, A. & MINAMI, Y. 2006. Filopodia formation mediated by receptor tyrosine kinase Ror2 is required for Wnt5a-induced cell migration. *J Cell Biol,* 175**,** 555-62.

NOMIKOS, M., BLAYNEY, L. M., LARMAN, M. G., CAMPBELL, K., ROSSBACH, A., SAUNDERS, C. M., SWANN, K. & LAI, F. A. 2005. Role of phospholipase C-zeta domains in Ca2+-dependent phosphatidylinositol 4,5-bisphosphate hydrolysis and cytoplasmic Ca2+ oscillations. *J Biol Chem,* 280**,** 31011-8.

NURNBERG, B., GUDERMANN, T. & SCHULTZ, G. 1995. Receptors and G proteins as primary components of transmembrane signal transduction. Part 2. G proteins: structure and function. *J Mol Med (Berl),* 73**,** 123-32.

NUSSLEIN-VOLHARD, C. & WIESCHAUS, E. 1980. Mutations affecting segment number and polarity in Drosophila. *Nature,* 287**,** 795-801.

ODENT, S., ATTI-BITACH, T., BLAYAU, M., MATHIEU, M., AUG, J., DELEZO DE, A. L., GALL, J. Y., LE MAREC, B., MUNNICH, A., DAVID, V. & VEKEMANS, M. 1999. Expression of the Sonic hedgehog (SHH) gene during early human development and phenotypic expression of new mutations causing holoprosencephaly. *Hum Mol Genet,* 8**,** 1683-9.

OGDEN, S. K., FEI, D. L., SCHILLING, N. S., AHMED, Y. F., HWA, J. & ROBBINS, D. J. 2008. G protein Galphai functions immediately downstream of Smoothened in Hedgehog signalling. *Nature,* 456**,** 967-70.

OHKUBO, N., MITSUDA, N., TAMATANI, M., YAMAGUCHI, A., LEE, Y. D., OGIHARA, T., VITEK, M. P. & TOHYAMA, M. 2001. Apolipoprotein E4 stimulates cAMP response element-binding protein transcriptional activity through the extracellular signal-regulated kinase pathway. *J Biol Chem,* 276**,** 3046-53.

OIKAWA, T., YAMAGUCHI, H., ITOH, T., KATO, M., IJUIN, T., YAMAZAKI, D., SUETSUGU, S. & TAKENAWA, T. 2004. PtdIns(3,4,5)P3 binding is necessary for WAVE2-induced formation of lamellipodia. *Nat Cell Biol,* 6**,** 420-6.

OTTINI, L., MARZIALI, G., CONTI, A., CHARLESWORTH, A. & SORRENTINO, V. 1996. Alpha and beta isoforms of ryanodine receptor from chicken skeletal muscle are the homologues of mammalian RyR1 and RyR3. *Biochem J,* 315 (Pt 1)**,** 207-16.

OZAWA, M & MURAMATSU, T. 1993. Reticulocalbin, a novel endoplasmic reticulum resident Ca2+ binding protein with multiple EF-hand motifs and a carboxyl-terminal HDEL sequence. *The Journal of Biological Chemistry*, 268, 699-705.

PADMANABHAN, J., LEVY, M., DICKSON, D. W. & POTTER, H. 2006. Alpha1-antichymotrypsin, an inflammatory protein overexpressed in Alzheimer's disease brain, induces tau phosphorylation in neurons. *Brain,* 129**,** 3020-34.

PALECEK, J., LIPS, M. B. & KELLER, B. U. 1999. Calcium dynamics and buffering in motoneurones of the mouse spinal cord. *J Physiol,* 520 Pt 2**,** 485-502.

PALTY, R., SILVERMAN, W. F., HERSHFINKEL, M., CAPORALE, T., SENSI, S. L., PARNIS, J., NOLTE, C., FISHMAN, D., SHOSHAN-BARMATZ, V., HERRMANN, S., KHANANSHVILI, D. & SEKLER, I. 2010. NCLX is an essential component of mitochondrial Na+/Ca2+ exchange. *Proc Natl Acad Sci U S A,* 107**,** 436-41.

PAPPA, H., MURRAY-RUST, J., DEKKER, L. V., PARKER, P. J. & MCDONALD, N. Q. 1998. Crystal structure of the C2 domain from protein kinase C-delta. *Structure,* 6**,** 885-94.

PAREKH, A. B. & PENNER, R. 1997. Store depletion and calcium influx. *Physiol Rev,* 77**,** 901-30.

PAREKH, A. B. & PUTNEY, J. W., JR. 2005. Store-operated calcium channels. *Physiol Rev,* 85**,** 757-810.

PARHAM, J. H., IANNONE, M. A., OVERTON, L. K. & HUTCHINS, J. T. 1998. Optimization of transient gene expression in mammalian cells and potential for scale-up using flow electroporation. *Cytotechnology,* 28**,** 147-55.

PARK, D., JHON, D. Y., LEE, C. W., LEE, K. H. & RHEE, S. G. 1993. Activation of phospholipase C isozymes by G protein beta gamma subunits. *J Biol Chem,* 268**,** 4573-6.

PARK, H. & POO, M. M. 2013. Neurotrophin regulation of neural circuit development and function. *Nat Rev Neurosci,* 14**,** 7-23.

PARMACEK, M. S. & LEIDEN, J. M. 1991. Structure, function, and regulation of troponin C. *Circulation,* 84**,** 991-1003.

PARSEGIAN, A. 1969. Energy of an ion crossing a low dielectric membrane: solutions to four relevant electrostatic problems. *Nature,* 221**,** 844-6.

PATEL, S., JOSEPH, S. K. & THOMAS, A. P. 1999. Molecular properties of inositol 1,4,5-trisphosphate receptors. *Cell Calcium,* 25**,** 247-64.

PATEL, S., Marchant, J. & BRAILOIU, E. 2010. Two pore channels: regulation by NAADP and customized roles in triggering calcium signals. *Cell Calcium.* 47, 480-490.

PAULUS, H. & KENNEDY, E. P. 1960. The enzymatic synthesis of inositol monophosphatide. *J Biol Chem,* 235**,** 1303-11.

PEI, Z., YANG, L. & WILLIAMSON, J. R. 1996. Phospholipase C-gamma 1 binds to actin-cytoskeleton via its C-terminal SH2 domain in vitro. *Biochem Biophys Res Commun,* 228**,** 802-6.

PEPINSKY, R. B., ZENG, C., WEN, D., RAYHORN, P., BAKER, D. P., WILLIAMS, K. P., BIXLER, S. A., AMBROSE, C. M., GARBER, E. A., MIATKOWSKI, K., TAYLOR, F. R., WANG, E. A. & GALDES, A. 1998. Identification of a palmitic acid-modified form of human Sonic hedgehog. *J Biol Chem,* 273**,** 14037-45.

PERIN, M. S., FRIED, V. A., MIGNERY, G. A., JAHN, R. & SUDHOF, T. C. 1990. Phospholipid binding by a synaptic vesicle protein homologous to the regulatory region of protein kinase C. *Nature,* 345**,** 260-3.

PERISIC, O., FONG, S., LYNCH, D. E., BYCROFT, M. & WILLIAMS, R. L. 1998. Crystal structure of a calcium-phospholipid binding domain from cytosolic phospholipase A2. *J Biol Chem,* 273**,** 1596-604.

PERRIMON, N., PITSOULI, C. & SHILO, B. Z. 2012. Signaling mechanisms controlling cell fate and embryonic patterning. *Cold Spring Harb Perspect Biol,* 4**,** a005975.

PESSAH, I. N., WATERHOUSE, A. L. & CASIDA, J. E. 1985. The calcium-ryanodine receptor complex of skeletal and cardiac muscle. *Biochem Biophys Res Commun,* 128**,** 449-56.

PIERROT, N., GHISDAL, P., CAUMONT, A. S. & OCTAVE, J. N. 2004. Intraneuronal amyloid-beta1-42 production triggered by sustained increase of cytosolic calcium concentration induces neuronal death. *J Neurochem,* 88**,** 1140-50.

PINTON, P., POZZAN, T. & RIZZUTO, R. 1998. The Golgi apparatus is an inositol 1,4,5-trisphosphate-sensitive Ca2+ store, with functional properties distinct from those of the endoplasmic reticulum. *EMBO J,* 17**,** 5298-308.

PLACZEK, M., JESSELL, T. M. & DODD, J. 1993. Induction of floor plate differentiation by contact-dependent, homeogenetic signals. *Development,* 117**,** 205-18.

PONCET, C., FRANCES, V., GRISTINA, R., SCHEINER, C., PELLISSIER, J. F. & FIGARELLA-BRANGER, D. 1996. CD24, a glycosylphosphatidylinositol-anchored molecules is transiently expressed during the development of human central nervous system and is a marker of human neural cell lineage tumors. *Acta Neuropathol,* 91**,** 400-8.

POPOVICS, P. 2012. *Biochemical and functional characterisation of Phospholipase C-eta2.* St Andrews.

POPOVICS, P., BESWICK, W., GUILD, S. B., CRAMB, G., MORGAN, K., MILLAR, R. P. & STEWART, A. J. 2011. Phospholipase C-eta2 is activated by elevated intracellular Ca(2+) levels. *Cell Signal,* 23**,** 1777-84.

POPOVICS, P., GRAY, A., ARASTOO, M., FINELLI, D. K., TAN, A. J. & STEWART, A. J. 2013. Phospholipase C-eta2 is required for retinoic acid-stimulated neurite growth. *J Neurochem,* 124**,** 632-44.

POPOVICS, P., LU, J., NADIA KAMIL, L., MORGAN, K., MILLAR, R. P., SCHMID, R., BLINDAUER, C. A. & STEWART, A. J. 2014. A canonical EF-loop directs Ca(2+) -sensitivity in phospholipase C-eta2. *J Cell Biochem,* 115**,** 557-65.

POPOVICS, P. & STEWART, A. J. 2012a. Phospholipase C-eta activity may contribute to Alzheimer's disease-associated calciumopathy. *J Alzheimers Dis,* 30**,** 737-44.

POPOVICS, P. & STEWART, A. J. 2012b. Putative roles for phospholipase Ceta enzymes in neuronal Ca2+ signal modulation. *Biochem Soc Trans,* 40**,** 282-6.

POWER, J. M. & SAH, P. 2002. Nuclear calcium signaling evoked by cholinergic stimulation in hippocampal CA1 pyramidal neurons. *J Neurosci,* 22**,** 3454-62.

POWER, M. L., HEANEY, R. P., KALKWARF, H. J., PITKIN, R. M., REPKE, J. T., TSANG, R. C. & SCHULKIN, J. 1999. The role of calcium in health and disease. *Am J Obstet Gynecol,* 181**,** 1560-9.

PRAKRIYA, M., FESKE, S., GWACK, Y., SRIKANTH, S., RAO, A. & HOGAN, P. G. 2006. Orai1 is an essential pore subunit of the CRAC channel. *Nature,* 443**,** 230-3.

PUTNEY, J. W., JR. 1982. Inositol lipids and cell stimulation in mammalian salivary gland. *Cell Calcium,* 3**,** 369-83.

PUTNEY, J. W., JR. 1986. A model for receptor-regulated calcium entry. *Cell Calcium,* 7**,** 1-12.

QUESADA, I. & VERDUGO, P. 2005. InsP3 signaling induces pulse-modulated Ca2+ signals in the nucleus of airway epithelial ciliated cells. *Biophys J,* 88**,** 3946-53.

QUIRK, J., VAN DEN HEUVEL, M., HENRIQUE, D., MARIGO, V., JONES, T. A., TABIN, C. & INGHAM, P. W. 1997. The smoothened gene and hedgehog signal transduction in Drosophila and vertebrate development. *Cold Spring Harb Symp Quant Biol,* 62**,** 217-26.

RAAM, M. S., SOLOMON, B. D. & MUENKE, M. 2011. Holoprosencephaly: a guide to diagnosis and clinical management. *Indian Pediatr,* 48**,** 457-66.

RAJADHYAKSHA, A., BARCZAK, A., MACIAS, W., LEVEQUE, J. C., LEWIS, S. E. & KONRADI, C. 1999. L-Type Ca(2+) channels are essential for glutamate-mediated CREB phosphorylation and c-fos gene expression in striatal neurons. *J Neurosci,* 19**,** 6348-59.

RAMSER, E. M., WOLTERS, G., DITYATEVA, G., DITYATEV, A., SCHACHNER, M. & TILLING, T. 2010. The 14-3-3zeta protein binds to the cell adhesion molecule L1, promotes L1 phosphorylation by CKII and influences L1-dependent neurite outgrowth. *PLoS One,* 5**,** e13462.

RANDAZZO, P. A., ANDRADE, J., MIURA, K., BROWN, M. T., LONG, Y. Q., STAUFFER, S., ROLLER, P. & COOPER, J. A. 2000. The Arf GTPase-activating protein ASAP1 regulates the actin cytoskeleton. *Proc Natl Acad Sci U S A,* 97**,** 4011-6.

RAO, V. R. & FINKBEINER, S. 2007. NMDA and AMPA receptors: old channels, new tricks. *Trends Neurosci,* 30**,** 284-91.

RAPOPORT, T. A. 2007. Protein translocation across the eukaryotic endoplasmic reticulum and bacterial plasma membranes. *Nature,* 450**,** 663-9.

REBECCHI, M. J. & PENTYALA, S. N. 2000. Structure, function, and control of phosphoinositide-specific phospholipase C. *Physiol Rev,* 80**,** 1291-335.

RECZEK, D., BERRYMAN, M. & BRETSCHER, A. 1997. Identification of EBP50: A PDZ-containing phosphoprotein that associates with members of the ezrin-radixin-moesin family. *J Cell Biol,* 139**,** 169-79.

RHEE, S. G. 2001. Regulation of phosphoinositide-specific phospholipase C. *Annu Rev Biochem,* 70**,** 281-312.

RHEE, S. G. & CHOI, K. D. 1992. Regulation of inositol phospholipid-specific phospholipase C isozymes. *J Biol Chem,* 267**,** 12393-6.

RICHMOND, G. S. & SMITH, T. K. 2011. Phospholipases A(1). *Int J Mol Sci,* 12**,** 588-612.

RIDDLE, R. D., JOHNSON, R. L., LAUFER, E. & TABIN, C. 1993. Sonic hedgehog mediates the polarizing activity of the ZPA. *Cell,* 75**,** 1401-16.

RIGATO, F., GARWOOD, J., CALCO, V., HECK, N., FAIVRE-SARRAILH, C. & FAISSNER, A. 2002. Tenascin-C promotes neurite outgrowth of embryonic hippocampal neurons through the alternatively spliced fibronectin type III BD domains via activation of the cell adhesion molecule F3/contactin. *J Neurosci,* 22**,** 6596-609.

RIOBO, N. A., SAUCY, B., DILIZIO, C. & MANNING, D. R. 2006. Activation of heterotrimeric G proteins by Smoothened. *Proc Natl Acad Sci U S A,* 103**,** 12607-12.

RITTERSON LEW, C. & TOLAN, D. R. 2013. Aldolase sequesters WASP and affects WASP/Arp2/3-stimulated actin dynamics. *J Cell Biochem,* 114**,** 1928-39.

RIZZO, M. A., SHOME, K., VASUDEVAN, C., STOLZ, D. B., SUNG, T. C., FROHMAN, M. A., WATKINS, S. C. & ROMERO, G. 1999. Phospholipase D and its product, phosphatidic acid, mediate agonist-dependent raf-1 translocation to the plasma membrane and the activation of the mitogen-activated protein kinase pathway. *J Biol Chem,* 274**,** 1131-9.

RIZZUTO, R., PINTON, P., CARRINGTON, W., FAY, F. S., FOGARTY, K. E., LIFSHITZ, L. M., TUFT, R. A. & POZZAN, T. 1998. Close contacts with the endoplasmic reticulum as determinants of mitochondrial Ca2+ responses. *Science,* 280**,** 1763-6.

ROBB-GASPERS, L. D. & THOMAS, A. P. 1995. Coordination of Ca2+ signaling by intercellular propagation of Ca2+ waves in the intact liver. *J Biol Chem,* 270**,** 8102-7.

ROELINK, H., AUGSBURGER, A., HEEMSKERK, J., KORZH, V., NORLIN, S., RUIZ I ALTABA, A., TANABE, Y., PLACZEK, M., EDLUND, T., JESSELL, T. M. & ET

AL. 1994. Floor plate and motor neuron induction by vhh-1, a vertebrate homolog of hedgehog expressed by the notochord. *Cell,* 76**,** 761-75.

ROESSLER, E., BELLONI, E., GAUDENZ, K., JAY, P., BERTA, P., SCHERER, S. W., TSUI, L. C. & MUENKE, M. 1996. Mutations in the human Sonic Hedgehog gene cause holoprosencephaly. *Nat Genet,* 14**,** 357-60.

ROHATGI, R., MILENKOVIC, L., CORCORAN, R. B. & SCOTT, M. P. 2009. Hedgehog signal transduction by Smoothened: pharmacologic evidence for a 2-step activation process. *Proc Natl Acad Sci U S A,* 106**,** 3196-201.

ROSADO, J. A. & SAGE, S. O. 2000. Protein kinase C activates non-capacitative calcium entry in human platelets. *J Physiol,* 529 Pt 1**,** 159-69.

ROSS, C. A., MACCUMBER, M. W., GLATT, C. E. & SNYDER, S. H. 1989. Brain phospholipase C isozymes: differential mRNA localizations by in situ hybridization. *Proc Natl Acad Sci U S A,* 86**,** 2923-7.

ROSS, E. M. & GILMAN, A. G. 1977. Resolution of some components of adenylate cyclase necessary for catalytic activity. *J Biol Chem,* 252**,** 6966-9.

RUAS, M., RIETDORF, K., ARREDOUANI, A., DAVIS, L. C., LLOYD-EVANS, E., KOEGEL, H., FUNNELL, T. M., MORGAN, A. J., WARD, J. A., WATANABE, K., CHENG, X., CHURCHILL, G. C., ZHU, M. X., PLATT, F. M., WESSEL, G. M., PARRINGTON, J. & GALIONE, A. 2010. Purified TPC isoforms form NAADP receptors with distinct roles for Ca(2+) signaling and endolysosomal trafficking. *Curr Biol,* 20**,** 703-9.

RYAN, M. D., DONNELLY, M., LEWIS, A., MEHROTRA, A. P., WILKIE, J. & GANI, D. 1999. A model for nonstoichiometric, cotranslational protein scission in eukaryotic ribosomes. *Bioorganic Chemistry,* 27**,** 55-79.

RYAN, M. D., KING, A. M. & THOMAS, G. P. 1991. Cleavage of foot-and-mouth disease virus polyprotein is mediated by residues located within a 19 amino acid sequence. *J Gen Virol,* 72 (Pt 11)**,** 2727-32.

RYU, S. H., CHO, K. S., LEE, K. Y., SUH, P. G. & RHEE, S. G. 1986. Two forms of phosphatidylinositol-specific phospholipase C from bovine brain. *Biochem Biophys Res Commun,* 141**,** 137-44.

SAARIKANGAS, J., ZHAO, H. & LAPPALAINEN, P. 2010. Regulation of the actin cytoskeleton-plasma membrane interplay by phosphoinositides. *Physiol Rev,* 90**,** 259-89.

SAFFITZ, J. E., NASH, J. A., GREEN, K. G., LUKE, R. A., RANSNAS, L. A. & INSEL, P. A. 1994. Immunoelectron microscopic identification of cytoplasmic and nuclear Gs alpha in S49 lymphoma cells. *FASEB J,* 8**,** 252-8.

SALLES, J., WALLACE, M. A. & FAIN, J. N. 1993. Modulation of the phospholipase C activity in rat brain cortical membranes by simultaneous activation of distinct monoaminergic and cholinergic muscarinic receptors. *Brain Res Mol Brain Res,* 20**,** 111-7.

SARAS, J. & HELDIN, C. H. 1996. PDZ domains bind carboxy-terminal sequences of target proteins. *Trends Biochem Sci,* 21**,** 455-8.

SASAKI, T., TAKASUGA, S., SASAKI, J., KOFUJI, S., EGUCHI, S., YAMAZAKI, M. & SUZUKI, A. 2009. Mammalian phosphoinositide kinases and phosphatases. *Prog Lipid Res,* 48**,** 307-43.

SAUNDERS, C. M., LARMAN, M. G., PARRINGTON, J., COX, L. J., ROYSE, J., BLAYNEY, L. M., SWANN, K. & LAI, F. A. 2002. PLC zeta: a sperm-specific trigger of Ca(2+) oscillations in eggs and embryo development. *Development,* 129**,** 3533-44.

SCHMIDT, O., PFANNER, N. & MEISINGER, C. 2010. Mitochondrial protein import: from proteomics to functional mechanisms. *Nat Rev Mol Cell Biol,* 11**,** 655-67.

SCHMITT, A. M., SHI, J., WOLF, A. M., LU, C. C., KING, L. A. & ZOU, Y. 2006. Wnt-Ryk signalling mediates medial-lateral retinotectal topographic mapping. *Nature,* 439**,** 31-7.

SCHNABEL, P. & CAMPS, M. 1998. Activation of a phospholipase Cbeta2 deletion mutant by limited proteolysis. *Biochem J,* 330 (Pt 1)**,** 461-8.

SCHNELL, D. J. & HEBERT, D. N. 2003. Protein translocons: multifunctional mediators of protein translocation across membranes. *Cell,* 112**,** 491-505.

SCHWANHAUSSER, B., BUSSE, D., LI, N., DITTMAR, G., SCHUCHHARDT, J., WOLF, J., CHEN, W. & SELBACH, M. 2011. Global quantification of mammalian gene expression control. *Nature,* 473**,** 337-42.

SEIFERT, J. P., ZHOU, Y., HICKS, S. N., SONDEK, J. & HARDEN, T. K. 2008. Dual activation of phospholipase C-epsilon by Rho and Ras GTPases. *J Biol Chem,* 283**,** 29690-8.

SEYMOUR-LAURENT, K. J. & BARISH, M. E. 1995. Inositol 1,4,5-trisphosphate and ryanodine receptor distributions and patterns of acetylcholine- and caffeine-induced calcium release in cultured mouse hippocampal neurons. *J Neurosci,* 15**,** 2592-608.

SHANKAR, G. M., LI, S., MEHTA, T. H., GARCIA-MUNOZ, A., SHEPARDSON, N. E., SMITH, I., BRETT, F. M., FARRELL, M. A., ROWAN, M. J., LEMERE, C. A., REGAN, C. M., WALSH, D. M., SABATINI, B. L. & SELKOE, D. J. 2008. Amyloid-beta protein dimers isolated directly from Alzheimer's brains impair synaptic plasticity and memory. *Nat Med,* 14**,** 837-42.

SHARP, A. H., MCPHERSON, P. S., DAWSON, T. M., AOKI, C., CAMPBELL, K. P. & SNYDER, S. H. 1993. Differential immunohistochemical localization of inositol 1,4,5-trisphosphate- and ryanodine-sensitive Ca2+ release channels in rat brain. *J Neurosci,* 13**,** 3051-63.

SHEA, C. M., EDGAR, C. M., EINHORN, T. A. & GERSTENFELD, L. C. 2003. BMP treatment of C3H10T1/2 mesenchymal stem cells induces both chondrogenesis and osteogenesis. *J Cell Biochem,* 90**,** 1112-27.

SHELDAHL, L. C., PARK, M., MALBON, C. C. & MOON, R. T. 1999. Protein kinase C is differentially stimulated by Wnt and Frizzled homologs in a G-protein-dependent manner. *Curr Biol,* 9**,** 695-8.

SHIMOHAMA, S., SUMIDA, Y., FUJIMOTO, S., MATSUOKA, Y., TANIGUCHI, T., TAKENAWA, T. & KIMURA, J. 1998. Differential expression of rat brain phospholipase C isozymes in development and aging. *Biochem Biophys Res Commun,* 243**,** 210-6.

SHISHEVA, A. 2013. PtdIns5P: news and views of its appearance, disappearance and deeds. *Arch Biochem Biophys,* 538**,** 171-80.

SHOJI, M., IWAKAMI, N., TAKEUCHI, S., WARAGAI, M., SUZUKI, M., KANAZAWA, I., LIPPA, C. F., ONO, S. & OKAZAWA, H. 2000. JNK activation is associated with intracellular beta-amyloid accumulation. *Brain Res Mol Brain Res,* 85**,** 221-33.

SIDEROVSKI, D. P., HESSEL, A., CHUNG, S., MAK, T. W. & TYERS, M. 1996. A new family of regulators of G-protein-coupled receptors? *Curr Biol,* 6**,** 211-2.

SIMON, M. I., STRATHMANN, M. P. & GAUTAM, N. 1991. Diversity of G proteins in signal transduction. *Science,* 252**,** 802-8.

SIMON, S. M. & LLINAS, R. R. 1985. Compartmentalization of the submembrane calcium activity during calcium influx and its significance in transmitter release. *Biophys J,* 48**,** 485-98.

SIMS, P. A., MENEFEE, A. L., LARSEN, T. M., MANSOORABADI, S. O. & REED, G. H. 2006. Structure and catalytic properties of an engineered heterodimer of enolase composed of one active and one inactive subunit. *J Mol Biol,* 355**,** 422-31.

SINGER, A. U., WALDO, G. L., HARDEN, T. K. & SONDEK, J. 2002. A unique fold of phospholipase C-beta mediates dimerization and interaction with G alpha q. *Nat Struct Biol,* 9**,** 32-6.

SINGH, S. M. & MURRAY, D. 2003. Molecular modeling of the membrane targeting of phospholipase C pleckstrin homology domains. *Protein Sci,* 12**,** 1934-53.

SLUSARSKI, D. C. & PELEGRI, F. 2007. Calcium signaling in vertebrate embryonic patterning and morphogenesis. *Dev Biol,* 307**,** 1-13.

SMALLRIDGE, R. C., KIANG, J. G., GIST, I. D., FEIN, H. G. & GALLOWAY, R. J. 1992. U-73122, an aminosteroid phospholipase C antagonist, noncompetitively inhibits thyrotropin-releasing hormone effects in GH3 rat pituitary cells. *Endocrinology,* 131**,** 1883-8.

SMRCKA, A. V., HEPLER, J. R., BROWN, K. O. & STERNWEIS, P. C. 1991. Regulation of polyphosphoinositide-specific phospholipase C activity by purified Gq. *Science,* 251**,** 804-7.

SOLOMON, B. D., GROPMAN, A. & MUENKE, M. 1993. Holoprosencephaly Overview. *In:* PAGON, R. A., ADAM, M. P., ARDINGER, H. H., WALLACE, S. E., AMEMIYA, A., BEAN, L. J. H., BIRD, T. D., DOLAN, C. R., FONG, C. T., SMITH, R. J. H. & STEPHENS, K. (eds.) *GeneReviews(R).* Seattle (WA).

SONG, C., SATOH, T., EDAMATSU, H., WU, D., TADANO, M., GAO, X. & KATAOKA, T. 2002. Differential roles of Ras and Rap1 in growth factor-dependent activation of phospholipase C epsilon. *Oncogene,* 21**,** 8105-13.

SONG, H., GOLOVKIN, M., REDDY, A. S. & ENDOW, S. A. 1997. In vitro motility of AtKCBP, a calmodulin-binding kinesin protein of Arabidopsis. *Proc Natl Acad Sci U S A,* 94**,** 322-7.

SONG, I. & HUGANIR, R. L. 2002. Regulation of AMPA receptors during synaptic plasticity. *Trends Neurosci,* 25**,** 578-88.

SONG, J., LU, Y. C., YOKOYAMA, K., ROSSI, J. & CHIU, R. 2004. Cyclophilin A is required for retinoic acid-induced neuronal differentiation in p19 cells. *J Biol Chem,* 279**,** 24414-9.

SPALLER, M. R. 2006. Act globally, think locally: systems biology addresses the PDZ domain. *ACS Chem Biol,* 1**,** 207-10.

SPIRES, T. L., MOLNAR, Z., KIND, P. C., CORDERY, P. M., UPTON, A. L., BLAKEMORE, C. & HANNAN, A. J. 2005. Activity-dependent regulation of synapse and dendritic spine morphology in developing barrel cortex requires phospholipase C-beta1 signalling. *Cereb Cortex,* 15**,** 385-93.

STALLINGS, J. D., TALL, E. G., PENTYALA, S. & REBECCHI, M. J. 2005. Nuclear translocation of phospholipase C-delta1 is linked to the cell cycle and nuclear phosphatidylinositol 4,5-bisphosphate. *J Biol Chem,* 280**,** 22060-9.

STAMM, S., CASPER, D., LEES-MILLER, J. P. & HELFMAN, D. M. 1993. Brain-specific tropomyosins TMBr-1 and TMBr-3 have distinct patterns of expression during development and in adult brain. *Proc Natl Acad Sci U S A,* 90**,** 9857-61.

STEINHARDT, R., ZUCKER, R. & SCHATTEN, G. 1977. Intracellular calcium release at fertilization in the sea urchin egg. *Dev Biol,* 58**,** 185-96.

STEPHENS, L. R., EGUINOA, A., ERDJUMENT-BROMAGE, H., LUI, M., COOKE, F., COADWELL, J., SMRCKA, A. S., THELEN, M., CADWALLADER, K., TEMPST, P. & HAWKINS, P. T. 1997. The G beta gamma sensitivity of a PI3K is dependent upon a tightly associated adaptor, p101. *Cell,* 89**,** 105-14.

STENH, C., NILSBERTH, C., HAMMARBACK, J., ENGVALL, B., NASLUND, J., & LANNFELT, L. 2002. The arctic mutation interferes with processing of amyloid precursor protein. *Neuroreport,* 13, 1857-1860.

STEWART, A. J., MORGAN, K., FARQUHARSON, C. & MILLAR, R. P. 2007. Phospholipase C-eta enzymes as putative protein kinase C and Ca2+ signalling components in neuronal and neuroendocrine tissues. *Neuroendocrinology,* 86**,** 243-8.

STEWART, A. J., MUKHERJEE, J., ROBERTS, S. J., LESTER, D. & FARQUHARSON, C. 2005. Identification of a novel class of mammalian phosphoinositol-specific phospholipase C enzymes. *Int J Mol Med,* 15**,** 117-21.

STRAMBIO-DE-CASTILLIA, C., NIEPEL, M. & ROUT, M. P. 2010. The nuclear pore complex: bridging nuclear transport and gene regulation. *Nat Rev Mol Cell Biol,* 11**,** 490-501.

STREB, H., IRVINE, R. F., BERRIDGE, M. J. & SCHULZ, I. 1983. Release of Ca2+ from a nonmitochondrial intracellular store in pancreatic acinar cells by inositol-1,4,5-trisphosphate. *Nature,* 306**,** 67-9.

STRICKER, S. A. 1995. Time-lapse confocal imaging of calcium dynamics in starfish embryos. *Dev Biol,* 170**,** 496-518.

STRICKER, S. A. 1999. Comparative biology of calcium signaling during fertilization and egg activation in animals. *Dev Biol,* 211**,** 157-76.

STRUYK, A. F., CANOLL, P. D., WOLFGANG, M. J., ROSEN, C. L., D'EUSTACHIO, P. & SALZER, J. L. 1995. Cloning of neurotrimin defines a new subfamily of differentially expressed neural cell adhesion molecules. *J Neurosci,* 15**,** 2141-56.

STUTZMANN, G. E. 2007. The pathogenesis of Alzheimers disease is it a lifelong "calciumopathy"? *Neuroscientist,* 13**,** 546-59.

STUTZMANN, G. E., SMITH, I., CACCAMO, A., ODDO, S., LAFERLA, F. M. & PARKER, I. 2006. Enhanced ryanodine receptor recruitment contributes to Ca2+ disruptions in young, adult, and aged Alzheimer's disease mice. *J Neurosci,* 26**,** 5180-9.

SUETSUGU, S., KURISU, S. & TAKENAWA, T. 2014. Dynamic shaping of cellular membranes by phospholipids and membrane-deforming proteins. *Physiol Rev,* 94**,** 1219-48.

SUH, P. G., PARK, J. I., MANZOLI, L., COCCO, L., PEAK, J. C., KATAN, M., FUKAMI, K., KATAOKA, T., YUN, S. & RYU, S. H. 2008. Multiple roles of phosphoinositide-specific phospholipase C isozymes. *BMB Rep,* 41**,** 415-34.

SUH, P. G., RYU, S. H., MOON, K. H., SUH, H. W. & RHEE, S. G. 1988. Cloning and sequence of multiple forms of phospholipase C. *Cell,* 54**,** 161-9.

SUNTHARALINGAM, M. & WENTE, S. R. 2003. Peering through the pore: nuclear pore complex structure, assembly, and function. *Dev Cell,* 4**,** 775-89.

SUPNET, C. & BEZPROZVANNY, I. 2010. Neuronal calcium signaling, mitochondrial dysfunction, and Alzheimer's disease. *J Alzheimers Dis,* 20 Suppl 2**,** S487-98.

SUTHERLAND, E. W. & RALL, T. W. 1958. Fractionation and characterization of a cyclic adenine ribonucleotide formed by tissue particles. *J Biol Chem,* 232**,** 1077-91.

SUTTON, R. B. & SPRANG, S. R. 1998. Structure of the protein kinase Cbeta phospholipid-binding C2 domain complexed with Ca2+. *Structure,* 6**,** 1395-405.

SVARD, J., HEBY-HENRICSON, K., PERSSON-LEK, M., ROZELL, B., LAUTH, M., BERGSTROM, A., ERICSON, J., TOFTGARD, R. & TEGLUND, S. 2006. Genetic elimination of Suppressor of fused reveals an essential repressor function in the mammalian Hedgehog signaling pathway. *Dev Cell,* 10**,** 187-97.

SWANN, K. & LAWRENCE, Y. 1996. How and why spermatozoa cause calcium oscillations in mammalian oocytes. *Mol Hum Reprod,* 2**,** 388-90.

SZENT-GYORGYI, A. G. 1975. Calcium regulation of muscle contraction. *Biophys J,* 15**,** 707-23.

SZPARA, M. L., VRANIZAN, K., TAI, Y. C., GOODMAN, C. S., SPEED, T. P. & NGAI, J. 2007. Analysis of gene expression during neurite outgrowth and regeneration. *BMC Neurosci,* 8**,** 100.

SZYMCZAK, A. L., WORKMAN, C. J., WANG, Y., VIGNALI, K. M., DILIOGLOU, S., VANIN, E. F. & VIGNALI, D. A. 2004. Correction of multi-gene deficiency in vivo using a single 'self-cleaving' 2A peptide-based retroviral vector. *Nat Biotechnol,* 22**,** 589-94.

TAKAI, Y., KISHIMOTO, A., KIKKAWA, U., MORI, T. & NISHIZUKA, Y. 1979. Unsaturated diacylglycerol as a possible messenger for the activation of calcium-activated, phospholipid-dependent protein kinase system. *Biochem Biophys Res Commun,* 91**,** 1218-24.

TAKEMURA, M., MISHIMA, T., WANG, Y., KASAHARA, J., FUKUNAGA, K., OHASHI, K. & MIZUNO, K. 2009. Ca2+/calmodulin-dependent protein kinase IV-mediated LIM kinase activation is critical for calcium signal-induced neurite outgrowth. *J Biol Chem,* 284**,** 28554-62.

TAKENAWA, T. & NAGAI, Y. 1981. Purification of phosphatidylinositol-specific phospholipase C from rat liver. *J Biol Chem,* 256**,** 6769-75.

TALL, E., DORMAN, G., GARCIA, P., RUNNELS, L., SHAH, S., CHEN, J., PROFIT, A., GU, Q. M., CHAUDHARY, A., PRESTWICH, G. D. & REBECCHI, M. J. 1997. Phosphoinositide binding specificity among phospholipase C isozymes as determined by photo-cross-linking to novel substrate and product analogs. *Biochemistry,* 36**,** 7239-48.

TANAKA, O. & KONDO, H. 1994. Localization of mRNAs for three novel members (beta 3, beta 4 and gamma 2) of phospholipase C family in mature rat brain. *Neurosci Lett,* 182**,** 17-20.

TANG, W., EHRLICH, I., WOLFF, S. B., MICHALSKI, A. M., WOLFL, S., HASAN, M. T., LUTHI, A. & SPRENGEL, R. 2009. Faithful expression of multiple proteins via 2A-peptide self-processing: a versatile and reliable method for manipulating brain circuits. *J Neurosci,* 29**,** 8621-9.

TANG, W. J., KRUPINSKI, J. & GILMAN, A. G. 1991. Expression and characterization of calmodulin-activated (type I) adenylylcyclase. *J Biol Chem,* 266**,** 8595-603.

TANG, Y., TANG, J., CHEN, Z., TROST, C., FLOCKERZI, V., LI, M., RAMESH, V. & ZHU, M. X. 2000. Association of mammalian trp4 and phospholipase C isozymes with a PDZ domain-containing protein, NHERF. *J Biol Chem,* 275**,** 37559-64.

TANIMURA, A., DAN, S. & YOSHIDA, M. 1998. Cloning of novel isoforms of the human Gli2 oncogene and their activities to enhance tax-dependent transcription of the human T-cell leukemia virus type 1 genome. *J Virol,* 72**,** 3958-64.

TAYLOR, C. W., GENAZZANI, A. A. & MORRIS, S. A. 1999. Expression of inositol trisphosphate receptors. *Cell Calcium,* 26**,** 237-51.

TAYLOR, R. S., JONES, S. M., DAHL, R. H., NORDEEN, M. H. & HOWELL, K. E. 1997. Characterization of the Golgi complex cleared of proteins in transit and examination of calcium uptake activities. *Mol Biol Cell,* 8**,** 1911-31.

TAYLOR, S. J., CHAE, H. Z., RHEE, S. G. & EXTON, J. H. 1991. Activation of the beta 1 isozyme of phospholipase C by alpha subunits of the Gq class of G proteins. *Nature,* 350**,** 516-8.

TECOTT, L. H., MARICQ, A. V. & JULIUS, D. 1993. Nervous system distribution of the serotonin 5-HT3 receptor mRNA. *Proc Natl Acad Sci U S A,* 90**,** 1430-4.

TERRY, L. J., SHOWS, E. B. & WENTE, S. R. 2007. Crossing the nuclear envelope: hierarchical regulation of nucleocytoplasmic transport. *Science,* 318**,** 1412-6.

THYAGARAJAN, K., AFSHAR, K. & GONCZY, P. 2011. Polarity mediates asymmetric trafficking of the Gbeta heterotrimeric G-protein subunit GPB-1 in C. elegans embryos. *Development*, 138, 2773-82.

THOMAS, D., LIPP, P., TOVEY, S. C., BERRIDGE, M. J., LI, W., TSIEN, R. Y. & BOOTMAN, M. D. 2000. Microscopic properties of elementary Ca2+ release sites in non-excitable cells. *Curr Biol,* 10**,** 8-15.

TIAN, Q., STEPANIANTS, S. B., MAO, M., WENG, L., FEETHAM, M. C., DOYLE, M. J., YI, E. C., DAI, H., THORSSON, V., ENG, J., GOODLETT, D., BERGER, J. P., GUNTER, B., LINSELEY, P. S., STOUGHTON, R. B., AEBERSOLD, R., COLLINS, S. J., HANLON, W. A. & HOOD, L. E. 2004. Integrated genomic and proteomic analyses of gene expression in Mammalian cells. *Mol Cell Proteomics,* 3**,** 960-9.

TJOELKER, L. W., SEYFRIED, C. E., EDDY, R. L., JR., BYERS, M. G., SHOWS, T. B., CALDERON, J., SCHREIBER, R. B. & GRAY, P. W. 1994. Human, mouse, and rat calnexin cDNA cloning: identification of potential calcium binding motifs and gene localization to human chromosome 5. *Biochemistry,* 33**,** 3229-36.

TOLAR, M., KELLER, J. N., CHAN, S., MATTSON, M. P., MARQUES, M. A. & CRUTCHER, K. A. 1999. Truncated apolipoprotein E (ApoE) causes increased intracellular calcium and may mediate ApoE neurotoxicity. *J Neurosci,* 19**,** 7100-10.

TOROK, K., COWLEY, D. J., BRANDMEIER, B. D., HOWELL, S., AITKEN, A. & TRENTHAM, D. R. 1998. Inhibition of calmodulin-activated smooth-muscle myosin light-chain kinase by calmodulin-binding peptides and fluorescent (phosphodiesterase-activating) calmodulin derivatives. *Biochemistry,* 37**,** 6188-98.

TSAI, I. C., AMACK, J. D., GAO, Z. H., BAND, V., YOST, H. J. & VIRSHUP, D. M. 2007. A Wnt-CKIvarepsilon-Rap1 pathway regulates gastrulation by modulating SIPA1L1, a Rap GTPase activating protein. *Dev Cell,* 12**,** 335-47.

TSUNEKI, H., DEZAKI, K. & KIMURA, I. 1997. Neuronal nicotinic receptor operates slow Ca2+ mobilization at mouse muscle endplate. *Neurosci Lett,* 225**,** 185-8.

TSUNODA, S., SIERRALTA, J., SUN, Y., BODNER, R., SUZUKI, E., BECKER, A., SOCOLICH, M. & ZUKER, C. S. 1997. A multivalent PDZ-domain protein assembles signalling complexes in a G-protein-coupled cascade. *Nature,* 388**,** 243-9.

TU, H., NELSON, O., BEZPROZVANNY, A., WANG, Z., LEE, S. F., HAO, Y. H., SERNEELS, L., DE STROOPER, B., YU, G. & BEZPROZVANNY, I. 2006. Presenilins form ER Ca2+ leak channels, a function disrupted by familial Alzheimer's disease-linked mutations. *Cell,* 126**,** 981-93.

TU, H., TANG, T. S., WANG, Z. & BEZPROZVANNY, I. 2004. Association of type 1 inositol 1,4,5-trisphosphate receptor with AKAP9 (Yotiao) and protein kinase A. *J Biol Chem,* 279**,** 19375-82.

TU, P., KUNERT-KEIL, C., LUCKE, S., BRINKMEIER, H. & BOURON, A. 2009. Diacylglycerol analogues activate second messenger-operated calcium channels exhibiting TRPC-like properties in cortical neurons. *J Neurochem,* 108**,** 126-38.

TYSZKIEWICZ, J. P. & YAN, Z. 2005. beta-Amyloid peptides impair PKC-dependent functions of metabotropic glutamate receptors in prefrontal cortical neurons. *J Neurophysiol,* 93**,** 3102-11.

USACHEV, Y. M., MARCHENKO, S. M. & SAGE, S. O. 1995. Cytosolic calcium concentration in resting and stimulated endothelium of excised intact rat aorta. *J Physiol,* 489 (Pt 2)**,** 309-17.

VALE, R. D. 2003. The molecular motor toolbox for intracellular transport. *Cell,* 112**,** 467-80.

VANCE, J. E. & STEENBERGEN, R. 2005. Metabolism and functions of phosphatidylserine. *Prog Lipid Res,* 44**,** 207-34.

VARJOSALO, M. & TAIPALE, J. 2008. Hedgehog: functions and mechanisms. *Genes Dev,* 22**,** 2454-72.

VEINBERGS, I., EVERSON, A., SAGARA, Y. & MASLIAH, E. 2002. Neurotoxic effects of apolipoprotein E4 are mediated via dysregulation of calcium homeostasis. *J Neurosci Res,* 67**,** 379-87.

VENKATACHALAM, K., ZHENG, F. & GILL, D. L. 2003. Regulation of canonical transient receptor potential (TRPC) channel function by diacylglycerol and protein kinase C. *J Biol Chem,* 278**,** 29031-40.

VERKHRATSKY, A. 2005. Physiology and pathophysiology of the calcium store in the endoplasmic reticulum of neurons. *Physiol Rev,* 85**,** 201-79.

VETTER, S. W. & LECLERC, E. 2003. Novel aspects of calmodulin target recognition and activation. *Eur J Biochem,* 270**,** 404-14.

VOGEL, C., ABREU RDE, S., KO, D., LE, S. Y., SHAPIRO, B. A., BURNS, S. C., SANDHU, D., BOUTZ, D. R., MARCOTTE, E. M. & PENALVA, L. O. 2010. Sequence signatures and mRNA concentration can explain two-thirds of protein abundance variation in a human cell line. *Mol Syst Biol,* 6**,** 400.

WAHL, M. I., OLASHAW, N. E., NISHIBE, S., RHEE, S. G., PLEDGER, W. J. & CARPENTER, G. 1989. Platelet-derived growth factor induces rapid and sustained tyrosine phosphorylation of phospholipase C-gamma in quiescent BALB/c 3T3 cells. *Mol Cell Biol,* 9**,** 2934-43.

WALDO, G. L., BOYER, J. L., MORRIS, A. J. & HARDEN, T. K. 1991. Purification of an AlF4- and G-protein beta gamma-subunit-regulated phospholipase C-activating protein. *J Biol Chem,* 266**,** 14217-25.

WALL, M. A., POSNER, B. A. & SPRANG, S. R. 1998. Structural basis of activity and subunit recognition in G protein heterotrimers. *Structure,* 6**,** 1169-83.

WALLACE, M. A. & CLARO, E. 1990a. Comparison of serotoninergic to muscarinic cholinergic stimulation of phosphoinositide-specific phospholipase C in rat brain cortical membranes. *J Pharmacol Exp Ther,* 255**,** 1296-300.

WALLACE, M. A. & CLARO, E. 1990b. A novel role for dopamine: inhibition of muscarinic cholinergic-stimulated phosphoinositide hydrolysis in rat brain cortical membranes. *Neurosci Lett,* 110**,** 155-61.

WALLINGFORD, J. B., EWALD, A. J., HARLAND, R. M. & FRASER, S. E. 2001. Calcium signaling during convergent extension in Xenopus. *Curr Biol,* 11**,** 652-61.

WALSH, D. M., KLYUBIN, I., FADEEVA, J. V., CULLEN, W. K., ANWYL, R., WOLFE, M. S., ROWAN, M. J. & SELKOE, D. J. 2002. Naturally secreted oligomers of amyloid beta protein potently inhibit hippocampal long-term potentiation in vivo. *Nature,* 416**,** 535-9.

WALSH, D. M. & SELKOE, D. J. 2007. A beta oligomers - a decade of discovery. *J Neurochem,* 101**,** 1172-84.

WALTON, P. D., AIREY, J. A., SUTKO, J. L., BECK, C. F., MIGNERY, G. A., SUDHOF, T. C., DEERINCK, T. J. & ELLISMAN, M. H. 1991. Ryanodine and inositol trisphosphate receptors coexist in avian cerebellar Purkinje neurons. *J Cell Biol,* 113**,** 1145-57.

WANG, J. & BEST, P. M. 1992. Inactivation of the sarcoplasmic reticulum calcium channel by protein kinase. *Nature,* 359**,** 739-41.

WANG, L. P., LIM, C., KUAN, Y., CHEN, C. L., CHEN, H. F. & KING, K. 1996. Positive charge at position 549 is essential for phosphatidylinositol 4,5-bisphosphate-hydrolyzing but not phosphatidylinositol-hydrolyzing activities of human phospholipase C delta1. *J Biol Chem,* 271**,** 24505-16.

WANG, S., GEBRE-MEDHIN, S., BETSHOLTZ, C., STALBERG, P., ZHOU, Y., LARSSON, C., WEBER, G., FEINSTEIN, R., OBERG, K., GOBL, A. & SKOGSEID, B. 1998a. Targeted disruption of the mouse phospholipase C beta3 gene results in early embryonic lethality. *FEBS Lett,* 441**,** 261-5.

WANG, S., LUKINIUS, A., ZHOU, Y., STALBERG, P., GOBL, A., OBERG, K. & SKOGSEID, B. 2000a. Subcellular distribution of phospholipase C isoforms in rodent pancreas and gastric mucosa. *Endocrinology,* 141**,** 2589-93.

WANG, S., ZHOU, Y., LUKINIUS, A., OBERG, K., SKOGSEID, B. & GOBL, A. 1998b. Molecular cloning and characterization of a cDNA encoding mouse phospholipase C-beta3. *Biochim Biophys Acta,* 1393**,** 173-8.

WANG, T., DOWAL, L., EL-MAGHRABI, M. R., REBECCHI, M. & SCARLATA, S. 2000b. The pleckstrin homology domain of phospholipase C-beta(2) links the binding of gbetagamma to activation of the catalytic core. *J Biol Chem,* 275**,** 7466-9.

WANG, T., PENTYALA, S., REBECCHI, M. J. & SCARLATA, S. 1999. Differential association of the pleckstrin homology domains of phospholipases C-beta 1, C-beta 2, and C-delta 1 with lipid bilayers and the beta gamma subunits of heterotrimeric G proteins. *Biochemistry,* 38**,** 1517-24.

WANG, X., DEVAIAH, S. P., ZHANG, W. & WELTI, R. 2006. Signaling functions of phosphatidic acid. *Prog Lipid Res,* 45**,** 250-78.

WATANABE, M., NAKAMURA, M., SATO, K., KANO, M., SIMON, M. I. & INOUE, Y. 1998. Patterns of expression for the mRNA corresponding to the four isoforms of phospholipase Cbeta in mouse brain. *Eur J Neurosci,* 10**,** 2016-25.

WATT, S. A., KULAR, G., FLEMING, I. N., DOWNES, C. P. & LUCOCQ, J. M. 2002. Subcellular localization of phosphatidylinositol 4,5-bisphosphate using the pleckstrin homology domain of phospholipase C delta1. *Biochem J,* 363**,** 657-66.

WEBB, S. E. & MILLER, A. L. 2003. Calcium signalling during embryonic development. *Nat Rev Mol Cell Biol,* 4**,** 539-51.

WEINBERGER, R. P., HENKE, R. C., TOLHURST, O., JEFFREY, P. L. & GUNNING, P. 1993. Induction of neuron-specific tropomyosin mRNAs by nerve growth factor is dependent on morphological differentiation. *J Cell Biol,* 120**,** 205-15.

WEISS, S. J., MCKINNEY, J. S. & PUTNEY, J. W., JR. 1982. Receptor-mediated net breakdown of phosphatidylinositol 4,5-bisphosphate in parotid acinar cells. *Biochem J,* 206**,** 555-60.

WELLS, A. L., LIN, A. W., CHEN, L. Q., SAFER, D., CAIN, S. M., HASSON, T., CARRAGHER, B. O., MILLIGAN, R. A. & SWEENEY, H. L. 1999. Myosin VI is an actin-based motor that moves backwards. *Nature,* 401**,** 505-8.

WESTFALL, T. A., BRIMEYER, R., TWEDT, J., GLADON, J., OLBERDING, A., FURUTANI-SEIKI, M. & SLUSARSKI, D. C. 2003. Wnt-5/pipetail functions in vertebrate axis formation as a negative regulator of Wnt/beta-catenin activity. *J Cell Biol,* 162**,** 889-98.

WETZEL, G. T., CHEN, F. & KLITZNER, T. S. 1995. Na+/Ca2+ exchange and cell contraction in isolated neonatal and adult rabbit cardiac myocytes. *Am J Physiol,* 268**,** H1723-33.

WETZKER, R., KLINGER, R., HAASE, H., VETTER, R. & BOHMER, F. D. 1987. Fast activation of Ca2+-ATPases in plasma membranes from cardiac muscle and from ascites carcinoma cells: a possible function of endogenous calmodulin. *Biomed Biochim Acta,* 46**,** S403-6.

WHITAKER, M. & IRVINE, R. F. 1984. Inositol 1,4,5-trisphosphate microinjection activates sea urchin eggs. *Nature,* 312**,** 636-639.

WHITNEY, N. P., PENG, H., ERDMANN, N. B., TIAN, C., MONAGHAN, D. T. & ZHENG, J. C. 2008. Calcium-permeable AMPA receptors containing Q/R-unedited GluR2 direct human neural progenitor cell differentiation to neurons. *FASEB J,* 22**,** 2888-900.

WICKNER, W. & SCHEKMAN, R. 2005. Protein translocation across biological membranes. *Science,* 310**,** 1452-6.

WILLIAMS, R. L. 1999. Mammalian phosphoinositide-specific phospholipase C. *Biochim Biophys Acta,* 1441**,** 255-67.

WILLIAMS, C.J., SCHULTZ, R.M., & KOPF, G.S. 1996. G protein expression during mouse oocyte growth and maturation, and preimplantation embryo development. *Mol Reprod Dev*, 44, 315-23.

WING, M. R., HOUSTON, D., KELLEY, G. G., DER, C. J., SIDEROVSKI, D. P. & HARDEN, T. K. 2001. Activation of phospholipase C-epsilon by heterotrimeric G protein betagamma-subunits. *J Biol Chem,* 276**,** 48257-61.

WINKLBAUER, R., MEDINA, A., SWAIN, R. K. & STEINBEISSER, H. 2001. Frizzled-7 signalling controls tissue separation during Xenopus gastrulation. *Nature,* 413**,** 856-60.

WOO, D. H., JUNG, S. J., ZHU, M. H., PARK, C. K., KIM, Y. H., OH, S. B. & LEE, C. J. 2008. Direct activation of transient receptor potential vanilloid 1(TRPV1) by diacylglycerol (DAG). *Mol Pain,* 4**,** 42.

WORTHYLAKE, D. K., ROSSMAN, K. L. & SONDEK, J. 2000. Crystal structure of Rac1 in complex with the guanine nucleotide exchange region of Tiam1. *Nature,* 408**,** 682-8.

WU, D., TADANO, M., EDAMATSU, H., MASAGO-TODA, M., YAMAWAKI-KATAOKA, Y., TERASHIMA, T., MIZOGUCHI, A., MINAMI, Y., SATOH, T. & KATAOKA, T. 2003. Neuronal lineage-specific induction of phospholipase Cepsilon expression in the developing mouse brain. *Eur J Neurosci,* 17**,** 1571-80.

XU, A., SUH, P. G., MARMY-CONUS, N., PEARSON, R. B., SEOK, O. Y., COCCO, L. & GILMOUR, R. S. 2001. Phosphorylation of nuclear phospholipase C beta1 by extracellular signal-regulated kinase mediates the mitogenic action of insulin-like growth factor I. *Mol Cell Biol,* 21**,** 2981-90.

XU, J. & CHUANG, D. M. 1987. Serotonergic, adrenergic and histaminergic receptors coupled to phospholipase C in cultured cerebellar granule cells of rats. *Biochem Pharmacol,* 36**,** 2353-8.

XU, R. X., PAWELCZYK, T., XIA, T. H. & BROWN, S. C. 1997. NMR structure of a protein kinase C-gamma phorbol-binding domain and study of protein-lipid micelle interactions. *Biochemistry,* 36**,** 10709-17.

XU, S., ZHAO, L., LARSSON, A. & VENGE, P. 2009. The identification of a phospholipase B precursor in human neutrophils. *FEBS J,* 276**,** 175-86.

YAGASAKI, Y., NUMAKAWA, T., KUMAMARU, E., HAYASHI, T., SU, T. P. & KUNUGI, H. 2006. Chronic antidepressants potentiate via sigma-1 receptors the brain-derived neurotrophic factor-induced signaling for glutamate release. *J Biol Chem,* 281**,** 12941-9.

YAMAGA, M., KIELAR-GREVSTAD, D. M. & MARTIN, T. F. 2015. Phospholipase Ceta2 Activation Re-directs Vesicle Trafficking By Regulating F-actin. *J Biol Chem*.

YAMAMOTO, T., TAKEUCHI, H., KANEMATSU, T., ALLEN, V., YAGISAWA, H., KIKKAWA, U., WATANABE, Y., NAKASIMA, A., KATAN, M. & HIRATA, M. 1999. Involvement of EF hand motifs in the Ca(2+)-dependent binding of the pleckstrin homology domain to phosphoinositides. *Eur J Biochem,* 265**,** 481-90.

YAMAUCHI, J., NAGAO, M., KAZIRO, Y. & ITOH, H. 1997. Activation of p38 mitogen-activated protein kinase by signaling through G protein-coupled receptors. Involvement of Gbetagamma and Galphaq/11 subunits. *J Biol Chem,* 272**,** 27771-7.

YANG, E. J., YOON, J. H., MIN, D. S. & CHUNG, K. C. 2004. LIM kinase 1 activates cAMP-responsive element-binding protein during the neuronal differentiation of immortalized hippocampal progenitor cells. *J Biol Chem,* 279**,** 8903-10.

YANG, G. Y., LIANG, B., ZHU, J. & LUO, Z. G. 2011. Calpain activation by Wingless-type murine mammary tumor virus integration site family, member 5A (Wnt5a) promotes axonal growth. *J Biol Chem,* 286**,** 6566-76.

YANG, N., HIGUCHI, O., OHASHI, K., NAGATA, K., WADA, A., KANGAWA, K., NISHIDA, E. & MIZUNO, K. 1998. Cofilin phosphorylation by LIM-kinase 1 and its role in Rac-mediated actin reorganization. *Nature,* 393**,** 809-12.

YANG, Y., WANG, M., LV, B., MA, R., HU, J., DUN, Y., SUN, S. & LI, G. 2014. Sphingosine kinase-1 protects differentiated N2a cells against beta-amyloid25-35-induced neurotoxicity via the mitochondrial pathway. *Neurochem Res,* 39**,** 932-40.

YANG, Z., ASICO, L. D., YU, P., WANG, Z., JONES, J. E., BAI, R. K., SIBLEY, D. R., FELDER, R. A. & JOSE, P. A. 2005. D5 dopamine receptor regulation of phospholipase D. *Am J Physiol Heart Circ Physiol,* 288**,** H55-61.

YASHIRO, Y. & DULING, B. R. 2000. Integrated Ca(2+) signaling between smooth muscle and endothelium of resistance vessels. *Circ Res,* 87**,** 1048-54.

YE, K., AGHDASI, B., LUO, H. R., MORIARITY, J. L., WU, F. Y., HONG, J. J., HURT, K. J., BAE, S. S., SUH, P. G. & SNYDER, S. H. 2002. Phospholipase C gamma 1 is a physiological guanine nucleotide exchange factor for the nuclear GTPase PIKE. *Nature,* 415**,** 541-4.

YIN, H. L. & JANMEY, P. A. 2003. Phosphoinositide regulation of the actin cytoskeleton. *Annu Rev Physiol,* 65**,** 761-89.

YOKOYAMA, K., SU IH, I. H., TEZUKA, T., YASUDA, T., MIKOSHIBA, K., TARAKHOVSKY, A. & YAMAMOTO, T. 2002. BANK regulates BCR-induced calcium mobilization by promoting tyrosine phosphorylation of IP(3) receptor. *EMBO J,* 21**,** 83-92.

YOON, H. S., HAJDUK, P. J., PETROS, A. M., OLEJNICZAK, E. T., MEADOWS, R. P. & FESIK, S. W. 1994. Solution structure of a pleckstrin-homology domain. *Nature,* 369**,** 672-5.

YOSHIDA, Y., KIM, S., CHIBA, K., KAWAI, S., TACHIKAWA, H. & TAKAHASHI, N. 2004. Calcineurin inhibitors block dorsal-side signaling that affect late-stage development of the heart, kidney, liver, gut and somitic tissue during Xenopus embryogenesis. *Dev Growth Differ,* 46**,** 139-52.

YUASA, T., KATAOKA, H., KINTO, N., IWAMOTO, M., ENOMOTO-IWAMOTO, M., IEMURA, S., UENO, N., SHIBATA, Y., KUROSAWA, H. & YAMAGUCHI, A. 2002. Sonic hedgehog is involved in osteoblast differentiation by cooperating with BMP-2. *J Cell Physiol,* 193**,** 225-32.

YUE, C., DODGE, K. L., WEBER, G. & SANBORN, B. M. 1998. Phosphorylation of serine 1105 by protein kinase A inhibits phospholipase Cbeta3 stimulation by Galphaq. *J Biol Chem,* 273**,** 18023-7.

YUE, C., KU, C. Y., LIU, M., SIMON, M. I. & SANBORN, B. M. 2000. Molecular mechanism of the inhibition of phospholipase C beta 3 by protein kinase C. *J Biol Chem,* 275**,** 30220-5.

ZEHENTNER, B. K., LESER, U. & BURTSCHER, H. 2000. BMP-2 and sonic hedgehog have contrary effects on adipocyte-like differentiation of C3H10T1/2 cells. *DNA Cell Biol,* 19**,** 275-81.

ZENG, M. & ZHOU, J. N. 2008. Roles of autophagy and mTOR signaling in neuronal differentiation of mouse neuroblastoma cells. *Cell Signal,* 20**,** 659-65.

ZENG, W., XU, X. & MUALLEM, S. 1996. Gbetagamma transduces [Ca2+]i oscillations and Galphaq a sustained response during stimulation of pancreatic acinar cells with [Ca2+]i-mobilizing agonists. *J Biol Chem,* 271**,** 18520-6.

ZHANG, X. M., RAMALHO-SANTOS, M. & MCMAHON, A. P. 2001. Smoothened mutants reveal redundant roles for Shh and Ihh signaling including regulation of L/R symmetry by the mouse node. *Cell,* 106**,** 781-92.

ZHOU, Y., SONDEK, J. & HARDEN, T. K. 2008. Activation of human phospholipase C-eta2 by Gbetagamma. *Biochemistry,* 47**,** 4410-7.

ZHOU, Y., WING, M. R., SONDEK, J. & HARDEN, T. K. 2005. Molecular cloning and characterization of PLC-eta2. *Biochem J,* 391**,** 667-76.

ZHU, T., GOBEIL, F., VAZQUEZ-TELLO, A., LEDUC, M., RIHAKOVA, L., BOSSOLASCO, M., BKAILY, G., PERI, K., VARMA, D. R., ORVOINE, R. & CHEMTOB, S. 2006. Intracrine signaling through lipid mediators and their cognate nuclear G-protein-coupled receptors: a paradigm based on PGE2, PAF, and LPA1 receptors. *Can J Physiol Pharmacol,* 84**,** 377-91.

ZHU, Y. J., LIN, H. & LAL, R. 2000. Fresh and nonfibrillar amyloid beta protein(1-40) induces rapid cellular degeneration in aged human fibroblasts: evidence for AbetaP-channel-mediated cellular toxicity. *FASEB J,* 14**,** 1244-54.

ZORZATO, F., FUJII, J., OTSU, K., PHILLIPS, M., GREEN, N. M., LAI, F. A., MEISSNER, G. & MACLENNAN, D. H. 1990. Molecular cloning of cDNA encoding human and rabbit forms of the Ca2+ release channel (ryanodine receptor) of skeletal muscle sarcoplasmic reticulum. *J Biol Chem,* 265**,** 2244-56.

ZOU, Y. 2004. Wnt signaling in axon guidance. *Trends Neurosci,* 27**,** 528-32.

References

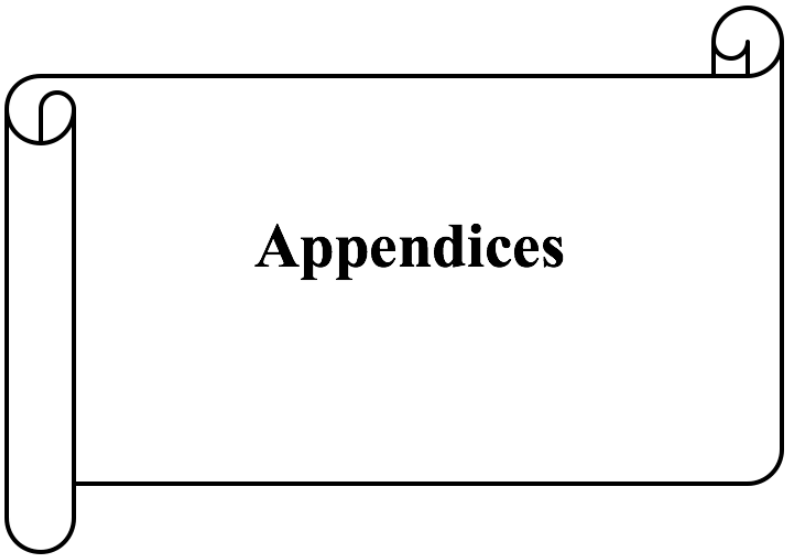
Appendices

Appendix I – PLCη1 and PLCη2 DNA and amino acid Sequences

PLCη1

DNA sequence of PLCη1 (223-3717 bp of NM_183191.3). This was inserted into PcDNA3.1.

```
   1 ATGGCAGACC TTGAAGTGTA TAAAAACTTA AGTCCAGAAA AAGTTGAAAG ATGCATGAGT
  61 GTAATGCAGT CCGGGACACA GATGATCAAA CTGAAGCGTG GCACCAAAGG GCTCGTTCGC
 121 CTCTTTTACC TGGATGAGCA CCGGACCCGC CTCCGATGGC GACCCTCTCG GAAGAGTGAG
 181 AAGGCAAAAA TACTTATTGA CTCCATCTAC AAAGTCACCG AGGGCAGGCA GTCTGAAATA
 241 TTCCACAGAC AGGCTGAGGG GAACTTTGAC CCTAGCTGCT GCTTTACCAT CTACCATGGC
 301 AACCACATGG AGTCTCTGGA CCTCATTACC TCCAACCCAG AGGAGGCACG CACCTGGATC
 361 ACGGGCCTCA AGTATCTGAT GGCTGGCATC AGTGATGAAG ACTCCCTTGC CAAGAGGCAG
 421 AGGACCCATG ACCAATGGGT GAAGCAGACC TTTGAGGAAG CTGATAAGAA CGGTGATGGC
 481 TTATTGAATA TTGAAGAGAT TCACCAGCTG ATGCATAAAC TAAATGTCAA TCTGCCCCGC
 541 AGAAAAGTCA GGCAAATGTT TCAGGAAGCA GATACAGATG AGAATCAGGG AACCTTGACA
 601 TTTGAAGAGT TCTGCGTTTT TTACAAAATG ATGTCATTGA GACGAGACCT CTATTTGCTG
 661 CTCTTGAGCT ACAGTGACAA GAAAGACCAC CTGACTGTGG AGGAGCTGGC TCAGTTTTTG
 721 AAAGTGGAAC AAAAGATGAG TAATGTGACA CTGGACTATT GTCTTGACAT CATAATGAAG
 781 TTTGAAGTTT CTGAAGAAAA CAAAGTGAAA AACGTCCTTG GTATAGAAGG CTTCACGAAC
 841 TTCATGCGTA GCCCTGCCTG TGACGTATTT AACCCGTTGC ACCATGAAGT GTACCAAGAC
 901 ATGGATCAGC CCCTGTGCAA CTACTACATT GCTTCATCTC ACAACACATA CCTGACTGGG
 961 GATCAGCTCC TTTCTCAATC TAAAGTGGAT ATGTATGCAC GGGTGCTACA AGAGGGTTGT
1021 AGATGCGTGG AAGTTGACTG TTGGGATGGC CCAGATGGAG AGCCAGTGGT CCACCATGGT
1081 TATACTCTCA CTTCAAAAAT TCTCTTCAGA GATGTTGTGG AGACCATCAA CAAGCATGCA
1141 TTCGTGAAGA ATGAGTTCCC GGTTATCCTG TCCATTGAGA ACCACTGCAG CATTCAGCAG
1201 CAGAGGAAGA TTGCTCAGTA CCTGAAAGGT ATATTGCAGG ACAAACTGGA CCTGTCTTCT
1261 GTAGACACCG GAGAGTGCAG GCAGCTTCCA AGCCCTCAGA GTCTGAAAGG CAAAATCCTA
1321 GTGAAGGGCA AGAAGTTGCC GTATCACCTT GGGGATGATG CAGAGGAAGG AGAAGTGTCC
1381 GATGAGGACA GTGCAGATGA GATTGAAGAT GAGTGCAAGT TCAAGCTGCA TTACAGTAAC
1441 GGGACCACTG AGCACCAGGT AGAATCTTTC ATACGGAAAA AGCTGGAGTC ACTGTTGAAG
1501 GAGTCTCAGA TTCGAGACAA AGAAGATCCA GACAGTTTCA CAGTGAGGGC GTTACTCAAG
1561 GCTACACATG AAGGCTTAAA TGCACACCTG AAGCAGAACC TGGATGTAAA GGAAAGTGGA
1621 AAGAAGTCCC ATGGGCGATC CCTGATGGCC AACTTTGGGA AACACAAGCA GAAAGCTACG
1681 AAATCACGTT CTAAATCCTA TAGTACTGAT GATGAGGATG ATAGCCTTCA GAATCCTGGC
1741 AAGGAGGGAG GCCAGCTGTA CAGGCTGGGC CGCCGAAGGA GAACCATGAA ACTCTGCAGA
1801 GAGCTCTCGG ACTTGGTGGT GTACACAAAC TCCGTGGCAG CCCAGGATAT TGTTGATGAT
1861 GGAACCACAG GGAATGTGTT GTCCTTCAGC GAAACAAGAG CCCATCAAGT GGTTCAGCAG
1921 AAGTCAGAGC AGTTCATGAT CTACAACCAA AAACAGCTCA CAAGGATTTA CCCCTCTGCC
1981 TACCGCATCG ATTCCAGTAA CTTCAACCCA CTGCCCTACT GGAATGCAGG CTGCCAGCTC
2041 GTGGCTCTGA ACTACCAGTC TGAAGGGCGA ATGATGCAGA TCAATCGAGC AAAATTCAAG
2101 GCGAATGGCA ACTGTGGCTA TATTCTCAAG CCCCAGCAAA TGTGCAAAGG TACTTTCAAC
2161 CCTTTCTCTG GTGACCCACT TCCTGCCAAC CCCAAAAAAC AGCTCATACT GAAAGTGATC
2221 AGTGGACAGC AACTCCCCAA ACCTCCTGAC TCTATGTTTG GAGACCGAGG CGAGATCATT
2281 GACCCTTTCG TTGAAGTTGA AATTATTGGG CTGCCAGTAG ACTGTTGCAA GGACCAAACT
2341 CGTGTGGTGG ATGACAACGG ATTTAACCCT GTGTGGGAAG AAACCCTAAC TTTTACAGTT
2401 CACATGCCAG AAATAGCTTT GGTTCGGTTC CTTGTGTGGG ATCATGATCC TATTGGAAGA
2461 GACTTTGTCG GACAAAGGAC TGTGACCTTC AGTAGCCTCG TGCCCGGCTA CCGGCATGTC
2521 TACCTGGAAG GACTCACAGA AGCATCTATT TTCGTTCACA TAACCATCAA TGAGATCTTT
2581 GGAAAGTGGA GTCCTTTAAT CCTCAACCCC AGTTATACCA TATTGCACTT TCTAGGAGCT
2641 ACAAAGAACA GACAGCTCCA AGGCCTGAAG GGGCTGTTCA ATAAGAATCC CAGGCACGCT
2701 TCTTCAGAAA ACAACTCGCA TTATGTTCGG AAGCGATCGA TTGGAGATAG GATTCTGCGA
2761 CGTACAGCTA GTGCTCCAGC CAAAGGCAGG AAAAAGAGCA AAGTGGGCTT CCAAGAAATG
```

```
2821 GTTGAGATAA AAGATTCTGT CTCTGAGGCT TCAAGAGATC AAGATGGTGT CCTGAGGAGG
2881 ACCACCCGGA GTCTGCAAGT ACGCCCTGTC TCTATGCCTG TTGACAAGAG CCTTCTGGGG
2941 GCTTTGTCGC TGCCCATATC TGAAGCAGCA AAAGACACGG ATGGAAAAGA AAACTGTCTG
3001 GCAGGAGACA AGGATGACAG AAGAAAGGGA GCCGCAACTA GAAAAGACCC ACATTTTTCA
3061 AATTTCAACA AAAAGTTATC CTCCTCCTCC AGTGCGCTCC TCCACAAAGA TGCCAACCAA
3121 GGGCCAACTG CCAGTGTATC AAACCCAGAA CAGTGTGGAG GACGAGGTGC AAAGAGTGAG
3181 AGGATCAAAC CAAATATGAC AAATGATTGC CAGGAAAACC ACAATCCCCC GAAATTCCTT
3241 TCTCCAAGGA AGCATTTGGC TCTGGATCCT GCAACGAAGG GACTGCAAGA GAGACTGCAT
3301 GGAATGAAAA CCAATGAGAA GGAGCATGCC GAGGGCTTCT TGGGAGAGAA AAGCATGCTG
3361 TCCGGAAGCG TTCTTTCTCA AAGTTCTCTG GAGGTAGAGA ACCTGGAAGG CAGCAGAGCC
3421 AAGGGCAGAG CTGCAACCTC CTTTTCTCTC TCGGACGTCT CCGCGCTCTG TTCTGACATC
3481 CCTGATTTAC ATTCAACTGC CATTCTACAG GACACTGAAA TTTCCAATCT CATTGATGAC
3541 GTGACTTTAA CAAATGAGAA TCAGTCGGGA AGTTCCATCT CGGCACTGAT TGGCCAGTTT
3601 GAAGAAAGCA ACCACCCGGC TAACGTTACT GTGGTTTCTC ATCTCAGCAC CAGTGGGGCA
3661 TCAGGAAGTG CTCCTTTCCA AACACCCTTC AAGCATGGTC TTTCCCAGGG GAACCAGAAG
3721 GCCTCCTTCT TGTGCTCATC TCCTGAGCTG AATAAGCTCT CTAGTGTTGA GACCACCAAA
3781 CTGGCAAATA ACGCAGTTCC TTGTGGAGTG ATTGGTTCTC CCATCTCTAC ACCAAAGCCA
3841 GGTGATGACC CTTCAGATAA GGCCAAGACA AGAGTCATTG AAGGCAACCT GCCTGGGTTC
3901 CCTGATGCTT CTCCTGGTCA ATTTCCCAAA AGCCCCACCC ATGGAGAGGA CCATAGTCAA
3961 GTGATGAACA GCCCTGCTCT CTCCACGGAG TTGGCCATAG AAGATATAAT TGCAGACCCT
4021 GCTCTCTCTA TAAATTCTGC AGAAAGCAGT CTTGTGGAAA TTGATGGAGA ATCTGAAAAC
4081 CTATCTCTAA CAACCTGTGA CTACAGGGAA GAAGCTCCAA GTCAACTTGT TTCTCCACTA
4141 AAACTGCAGC AGAGCCAGGA GATGGTGGAA CACATTCAGA GGGGCTTGAG GAATGGCTAC
4201 TGTAAAGAGA CTCTCCTCCC TTCTGAAATA TTCAACAATA TTCCAGGTGT CAAAAATCAC
4261 AGTATTTCTC ATCTAACCTA TCAGGGTGCT GGCTTTGTGT ATAACCATTT CTCAAGTTCA
4321 GATGCAAAAA CGAACCAAAT CTGTGAGCCC CAGCAGCCTA GGGCTCCAGA TATGCATGCC
4381 CCTACACCTA CACCATCAAC ACATGCTCCT TTGGCTGCTT TGAAACTGCC AAGCCCATGC
4441 AAATCCAAAA GTCTGGGGGA CTTAACATCA GAGGACATTG CCTGCAATTT TGAAAGCAAA
4501 TATCAATGTA TTAGTAGGAG CTTTGTGACA AACGGCATTA GGGACAAGAG CGTGACTATG
4561 AAGACAAAGT CATTAGAGCC TTTAGACGCC CTGACTGAAC AGCTCCGGAA GCTGGTGTCC
4621 TTTGACCAAG AAGACAGCTG TCAAGTGCTC TACTCAAAGC AGGATGTCAA TCAGTGTCCC
4681 AGGGCATTAG TCAGAAAGTT GTCGTCTAGA AGTCAGAGCA GAGTGCGCAA CATTGCTAGC
4741 CGTGCCAAGG AGAAGCAGGA AGCTGGCAAG CAAAAAGCTA TGGCCCAGAG CACCAGAGGA
4801 GGAGTGGTCC TTAGAAGTAA ACCGCCCGCT CCTGCTCTGG CCGTGAACCG TCACTCCACG
4861 GGCTCATACA TTGCAAGCTA CCTGAGGAAC ATGAAAGCTG GTGGCCTAGA GGGTCGAGGC
4921 ATCCCAGAGG GAGCGTGCAC GGCCCTTCGC TATGGCTACA TGGACCAGTT TTGTTCAGAT
4981 AATTCAGTTC TGCAGACTGA GCCAAGCAGC GAAGATAAAC CCGAAATTTA TTTTCTTTTG
5041 AGGCTTTGA
```

The corresponding amino acid sequence encoded by the PLCη1 plasmid (1-1681 residue of NP_ 899014.2). The sequence corresponds to the PLCη1 variant 1 splice variant.

```
   1 MADLEVYKNL SPEKVERCMS VMQSGTQMIK LKRGTKGLVR LFYLDEHRTR LRWRPSRKSE
  61 KAKILIDSIY KVTEGRQSEI FHRQAEGNFD PSCCFTIYHG NHMESLDLIT SNPEEARTWI
 121 TGLKYLMAGI SDEDSLAKRQ RTHDQWVKQT FEEADKNGDG LLNIEEIHQL MHKLNVNLPR
 181 RKVRQMFQEA DTDENQGTLT FEEFCVFYKM MSLRRDLYLL LLSYSDKKDH LTVEELAQFL
 241 KVEQKMSNVT LDYCLDIIMK FEVSEENKVK NVLGIEGFTN FMRSPACDVF NPLHHEVYQD
 301 MDQPLCNYYI ASSHNTYLTG DQLLSQSKVD MYARVLQEGC RCVEVDCWDG PDGEPVVHHG
 361 YTLTSKILFR DVVETINKHA FVKNEFPVIL SIENHCSIQQ QRKIAQYLKG ILQDKLDLSS
 421 VDTGECRQLP SPQSLKGKIL VKGKKLPYHL GDDAEEGEVS DEDSADEIED ECKFKLHYSN
 481 GTTEHQVESF IRKKLESLLK ESQIRDKEDP DSFTVRALLK ATHEGLNAHL KQNLDVKESG
 541 KKSHGRSLMA NFGKHKQKAT KSRSKSYSTD DEDDSLQNPG KEGGQLYRLG RRRRTMKLCR
 601 ELSDLVVYTN SVAAQDIVDD GTTGNVLSFS ETRAHQVVQQ KSEQFMIYNQ KQLTRIYPSA
```

```
 661 YRIDSSNFNP LPYWNAGCQL VALNYQSEGR MMQINRAKFK ANGNCGYILK PQQMCKGTFN
 721 PFSGDPLPAN PKKQLILKVI SGQQLPKPPD SMFGDRGEII DPFVEVEIIG LPVDCCKDQT
 781 RVVDDNGFNP VWEETLTFTV HMPEIALVRF LVWDHDPIGR DFVGQRTVTF SSLVPGYRHV
 841 YLEGLTEASI FVHITINEIF GKWSPLILNP SYTILHFLGA TKNRQLQGLK GLFNKNPRHA
 901 SSENNSHYVR KRSIGDRILR RTASAPAKGR KKSKVGFQEM VEIKDSVSEA SRDQDGVLRR
 961 TTRSLQVRPV SMPVDKSLLG ALSLPISEAA KDTDGKENCL AGDKDDRRKG AATRKDPHFS
1021 NFNKKLSSSS SALLHKDANQ GPTASVSNPE QCGGRGAKSE RIKPNMTNDC QENHNPPKFL
1081 SPRKHLALDP ATKGLQERLH GMKTNEKEHA EGFLGEKSML SGSVLSQSSL EVENLEGSRA
1141 KGRAATSFSL SDVSALCSDI PDLHSTAILQ DTEISNLIDD VTLTNENQSG SSISALIGQF
1201 EESNHPANVT VVSHLSTSGA SGSAPFQTPF KHGLSQGNQK ASFLCSSPEL NKLSSVETTK
1261 LANNAVPCGV IGSPISTPKP GDDPSDKAKT RVIEGNLPGF PDASPGQFPK SPTHGEDHSQ
1321 VMNSPALSTE LAIEDIIADP ALSINSAESS LVEIDGESEN LSLTTCDYRE EAPSQLVSPL
1381 KLQQSQEMVE HIQRGLRNGY CKETLLPSEI FNNIPGVKNH SISHLTYQGA GFVYNHFSSS
1441 DAKTNQICEP QQPRAPDMHA PTPTPSTHAP LAALKLPSPC KSKSLGDLTS EDIACNFESK
1501 YQCISRSFVT NGIRDKSVTM KTKSLEPLDA LTEQLRKLVS FDQEDSCQVL YSKQDVNQCP
1561 RALVRKLSSR SQSRVRNIAS RAKEKQEAGK QKAMAQSTRG GVVLRSKPPA PALAVNRHST
1621 GSYIASYLRN MKAGGLEGRG IPEGACTALR YGYMDQFCSD NSVLQTEPSS EDKPEIYFLL
1681 RL
```

PLCη1 is alternatively spliced at its C-terminus, producing three splice variants. Below is the amino acid sequences for the C-terminal tail of PLCη1 variants. Amino acid sequences obtained from NCBI protein database. C-terminus region determined by NCBI conserved domain search tool.

Variant 1

```
NEIFGKWSPLILNPSYTILHFLGATKNRQLQGLKGLFNKNPRHASSENNSHYVRKRSIGDRILRRTASAPAKGRK
KSKVGFQEMVEIKDSVSEASRDQDGVLRRTTRSLQVRPVSMPVDKSLLGALSLPISEAAKDTDGKENCLAGDKDD
RRKGAATRKDPHFSNFNKKLSSSSSALLHKDANQGPTASVSNPEQCGGRGAKSERIKPNMTNDCQENHNPPKFLS
PRKHLALDPATKGLQERLHGMKTNEKEHAEGFLGEKSMLSGSVLSQSSLEVENLEGSRAKGRAATSFSLSDVSAL
CSDIPDLHSTAILQDTEISNLIDDVTLTNENQSGSSISALIGQFEESNHPANVTVVSHLSTSGASGSAPFQTPFK
HGLSQGNQKASFLCSSPELNKLSSVETTKLANNAVPCGVIGSPISTPKPGDDPSDKAKTRVIEGNLPGFPDASPG
QFPKSPTHGEDHSQVMNSPALSTELAIEDIIADPALSINSAESSLVEIDGESENLSLTTCDYREEAPSQLVSPLK
LQQSQEMVEHIQRGLRNGYCKETLLPSEIFNNIPGVKNHSISHLTYQGAGFVYNHFSSSDAKTNQICEPQQPRAP
DMHAPTPTPSTHAPLAALKLPSPCKSKSLGDLTSEDIACNFESKYQCISRSFVTNGIRDKSVTMKTKSLEPLDAL
TEQLRKLVSFDQEDSCQVLYSKQDVNQCPRALVRKLSSRSQSRVRNIASRAKEKQEAGKQKAMAQSTRGGVVLRS
KPPAPALAVNRHSTGSYIASYLRNMKAGGLEGRGIPEGACTALRYGYMDQFCSDNSVLQTEPSSEDKPEIYFLLR
L
```

Variant 2

```
NEIFGKWSPLILNPSYTILHFLGATKNRQLQGLKGLFNKNPRHASSENNSHYVRKRSIGDRILRRTASAPAKGRK
KSKVGFQEMVEIKDSVSEASRDQDGVLRRTTRSLQVRPVSMPVDKSLLGALSLPISEAAKDTDGKENCLDLNRKQ
RKQETRMTEEREPQLEKTHIFQISTKSYPPPPVRSSTKMPTKGQLPVYQTQNSVEDEVQRVRGSNQI
```

Variant 3

```
NEIFGKWSPLILNPSYTILHFLGATKNRQLQGLKGLFNKNPRHASSENNSHYVRKRSIGDRILRRTASAPAKGRK
KSKVGFQEMVEIKDSVSEASRDQDGVLRRTTRSLQVRPVSMPVDKSLLGALSLPISEAAKDTDGKENCLVQI
```

PLCη2

DNA sequence of PLCη2 (223-3717 bp of NM_175556.4). Prof. Kiyoko Fukami inserted this sequence into PcDNA3.1 and provided this construct.

```
223                                                    ATGCCTGG TCCCCAGCCG
241  TCTGCTGCCA GCCAGACCAC AGGAGCCGTG GCTTGCCTGG CAGAGGTACT CCTCTGGGTT
301  GGAGGGAGCG TGGTAGTGTC ACCAAGATGG CAGCTCAGCC TTGTAGTGGA GCGATGCATG
361  AGTGCCATGC AAGAGGGGAC CCAGATGGTG AAGCTCCGTG GCAGCTCCAA GGGATTGGTC
421  CGCTTCTACT ACCTGGATGA GCACCGCTCC TGCCTCCGAT GGCGTCCCTC CCGCAAGAAC
481  GAGAAAGCCA AGATTTCCAT CGACTCCATC CAGGAGGTGA GTGAGGGCCG GCAGTCTGAA
541  ATCTTCCAGC GCTACCCGGA CAGCAGCTTT GACCCCAACT GCTGCTTCAG CATCTACCAT
601  GGCAGCCACA GAGAGTCGCT GGACTTGGTC TCACCCAGCA GTGAAGAGGC ACGTACCTGG
661  GTCACCGGCC TTCGCTACCT CATGGCTGGC ATCAGCGATG AAGACAGCCT AGCCCGTCGC
721  CAGCGTACCA GGGACCAGTG GCTGAAGCAG ACGTTTGATG AGGCTGACAA GAACGGGGAC
781  GGCAGCCTGA GCATCAGTGA GGTTCTGCAG CTGCTACATA AACTCAACGT GAACCTGCCC
841  CGGCAGAGGG TGAAACAGAT GTTCAGGGAG GCGGACACAG ATGACCATCA GGGGACATTA
901  GGCTTTGAGG AATTCTGCGC CTTCTACAAG ATGATGTCTA CCCGCCGAGA CCTCTACCTG
961  CTCATGCTGA CCTACAGCAA CCATAAGGAC CACTTGGATG CCTCCGACCT GCAGCGCTTT
1021 CTGGAGGTGG AGCAGAAGAT GAACGGTGTG ACCCTGGAGA GCTGTCAGAA CATCATTGAG
1081 CAGTTTGAGC CTTGCCTGGA AAATAAGAGC AAGGGGATGC TGGGGATTGA TGGCTTTACC
1141 AACTACACCC GGAGCCCCGC CGGTGACATC TTCAACCCTG AGCACAACAG AGTGCACCAA
1201 GACATGACGC AGCCGCTGAG TCACTACTTC ATCACCTCGT CCCACAACAC CTACCTCGTG
1261 GGTGACCAGC TCATGTCCCA GTCTCGGGTG GACATGTATG CCTGGGTCCT GCAGGCCGGC
1321 TGCCGCTGTG TGGAGGTGGA CTGCTGGGAC GGGCCCGATG GAGAACCCAT TGTCCATCAT
1381 GGCTACACTC TGACCTCCAA GATCCTTTTC AAAGATGTCA TCGAAACCAT CAACAAATAC
1441 GCCTTCATCA AGAATGAGTA CCCAGTGATC CTGTCCATTG AGAACCACTG TAGTGTTGTT
1501 CAGCAGAAGA AGATGGCCCA GTATCTGACT GACATCCTCG GGGACAAGCT GGACCTCTCC
1561 TCAGTGAGCA GCGAAGATGC CACCATGCTT CCATCTCCAC AGATGCTCAA GGGCAAGATC
1621 CTGGTGAAGG GGAAGAAGCT CCCTGCCAAT ATCAGTGAGG ATGCAGAAGA AGGCGAAGTA
1681 TCTGATGAGG ACAGTGCTGA TGAGATGGAG GATGACTGCA AGCTCCTCAA TGGGGATGCC
1741 TCCACCAATC GGAAGCGTGT GGAAAACATT GCAAAGAAGA AGCTGGATTC TCTGATCAAG
1801 GAGTCAAAGA TCCGTGACTG TGAAGACCCC AATGACTTCT CTGTGTCCAC ACTATCCCCC
1861 TCTGGAAAGC TTGGGCGCAA AGCAGAGGCC AAGAAGGGTC AGAGCAAGGT TGAGGAAGAC
1921 GTGGAGGCCG GGGAAGACAG CGGGGTGAGC AGGCAGAATA GCCGCCTCTT CATGAGCAGC
1981 TTCTCCAAGC GCAAGAAAAA AGGCAGCAAG ATAAAGAAGG TGGCCAGCGT GGAAGAGGGG
2041 GACGAGACCC TGGACTCCCC AGGAAGCCAG AGCCGAGGGA CTGCCCGGCA AAAGAAGACC
2101 ATGAAGCTGT CACGAGCCCT CTCGGACCTA GTGAAATATA CCAAGTCTGT GGGGACCCAT
2161 GACGTGGAGA TAGAGGTGGT ATCTAGCTGG CAGGTGTCGT CCTTCAGTGA GACCAAGGCC
2221 CATCAGATCC TGCAGCAGAA GCCCACCCAG TACCTGCGCT TCAACCAGCA CCAGCTCTCG
2281 CGCATATACC CCTCCTCCTA CCGTGTGGAC TCCAGCAACT ACAATCCACA ACCCTTCTGG
2341 AACGCTGGTT GCCAGATGGT TGCCCTGAAC TACCAGTCAG AGGGGCGGAT GCTACAGCTG
2401 AACAGGGCCA AGTTCAGCGC CAACGGTGAC TGTGGCTACG TGCTCAAACC CCAGTGCATG
2461 TGCCAGGGTG TCTTCAACCC CAACTCGGAG GATCCCCTGC CGGGGCAGCT CAAGAAGCAG
2521 CTGGCCCTGA GGATCATCAG TGGCCAGCAG CTGCCCAAAC CACGGGACTC GGTGCTGGGC
2581 GACCGTGGGG AGATCATCGA CCCCTTCGTG GAGGTGGAGG TCATTGGGCT CCCCGTGGAC
2641 TGCAGCAAGG AGCAGACCCG AGTGGTGGAC GACAACGGAT TCAACCCCAT GTGGGAGGAG
2701 ACACTGGTGT TCACCGTGCA CATGCCAGAG ATTGCGCTTG TACGCTTCCT GGTCTGGGAC
2761 CATGACCCCA TTGGACGTGA CTTCATCGGC CAGAGGACAC TAGCCTTCAG CAGCATAATG
2821 CCAGGCTACC GGCATGTGTA CCTAGAAGGG ATGGAAGAGG CCTCTATCTT TGTTCATGTG
2881 GCTGTCAGTG ACATTAGTGG TAAGGTCAAG CAGACTCTGG GTCTAAAAGG TCTCTTCCTC
2941 CGAGGCACAA AGCCAGGCTC GCTGGACAGT CATGCTGCTG GACAGCCCCT CCCCCGGCCC
3001 TCCGTTAGCC AGAGGCTCCT GCGGCGCACG GCCAGTGCCC CGACCAAAAG CCAGAAGCCA
3061 AGTCGCAAGG GCTTCCCAGA GCTGGCCCTG GGCACACAGG ACGCAGGCTC CGAGGGGGCA
3121 GCTGATGACG TGGCACCCTC TAGCCCCAAC CCAGCTCTGG AGGCCCCTAC TCAAGAGAGG
```

```
3181 TCAGGCAGCA GCAGCCCCCG AGGTAAGGCA CCAGGAGGAG AAGCAACAGA AGAGAGGACA
3241 CTGGCACAGG TGCGGTCCCC AAATGCCCCC GAAGGCCCTG GACCTGCAGG GATGGCCGCC
3301 ACATGCATGA AGTGTGTGGT GGGCTCCTGC GCCGGTATGG ACGTTGAGGG CCTTCAAAGG
3361 GAGCAACAAC CCAGCCCTGG GCCTGCAGGC AGCCACATGG CCATCAGCCA TCAGCCCAGG
3421 GCCCGGGTAG ATTCACTGGG GGGCCCTTGC TGCAGCCCAA GTCCTCGAGC CACCCCAGGG
3481 AGAAGCAAAG AGGCCCCCAA GGGTCCTAGG GCTCGGCGCC AGGGTCCAGG CGGCGGCTCT
3541 GTGTCCTCGG ACTCCAGCAG CCCAGACAGC CCAGGCAGCC CCAAGGTGGC CCCCTGCCAG
3601 CCGGAGGGTG CTCACAGGCA GCAGGGGGCG CTGCAGGGAG AGATGAACGC CTTGTTCGTT
3661 CAAAAGCTGG AGGAGATCAG GAGTCATTCC CCCATGTTCT CCACCGTTAG GGATTGA
```

The corresponding amino acid sequence encoded by the PLCη2 plasmid (75-1238 resudes of NP_780765.2). The sequence corresponds to the 21b/22/23 splice variant.

```
75                    MPGPQP SAASQTTGAV ACLAEVLLWV GGSVVVSPRW QLSLVVERCM
121     SAMQEGTQMV KLRGSSKGLV RFYYLDEHRS CLRWRPSRKN EKAKISIDSI QEVSEGRQSE
181     IFQRYPDSSF DPNCCFSIYH GSHRESLDLV SPSSEEARTW VTGLRYLMAG ISDEDSLARR
241     QRTRDQWLKQ TFDEADKNGD GSLSISEVLQ LLHKLNVNLP RQRVKQMFRE ADTDDHQGTL
301     GFEEFCAFYK MMSTRRDLYL LMLTYSNHKD HLDASDLQRF LEVEQKMNGV TLESCQNIIE
361     QFEPCLENKS KGMLGIDGFT NYTRSPAGDI FNPEHNRVHQ DMTQPLSHYF ITSSHNTYLV
421     GDQLMSQSRV DMYAWVLQAG CRCVEVDCWD GPDGEPIVHH GYTLTSKILF KDVIETINKY
481     AFIKNEYPVI LSIENHCSVV QQKKMAQYLT DILGDKLDLS SVSSEDATML PSPQMLKGKI
541     LVKGKKLPAN ISEDAEEGEV SDEDSADEME DDCKLLNGDA STNRKRVENI AKKKLDSLIK
601     ESKIRDCEDP NDFSVSTLSP SGKLGRKAEA KKGQSKVEED VEAGEDSGVS RQNSRLFMSS
661     FSKRKKKGSK IKKVASVEEG DETLDSPGSQ SRGTARQKKT MKLSRALSDL VKYTKSVGTH
721     DVEIEVVSSW QVSSFSETKA HQILQQKPTQ YLRFNQHQLS RIYPSSYRVD SSNYNPQPFW
781     NAGCQMVALN YQSEGRMLQL NRAKFSANGD CGYVLKPQCM CQGVFNPNSE DPLPGQLKKQ
841     LALRIISGQQ LPKPRDSVLG DRGEIIDPFV EVEVIGLPVD CSKEQTRVVD DNGFNPMWEE
901     TLVFTVHMPE IALVRFLVWD HDPIGRDFIG QRTLAFSSIM PGYRHVYLEG MEEASIFVHV
961     AVSDISGKVK QTLGLKGLFL RGTKPGSLDS HAAGQPLPRP SVSQRLLRRT ASAPTKSQKP
1021    SRKGFPELAL GTQDAGSEGA ADDVAPSSPN PALEAPTQER SGSSSPRGKA PGGEATEERT
1081    LAQVRSPNAP EGPGPAGMAA TCMKCVVGSC AGMDVEGLQR EQQPSPGPAG SHMAISHQPR
1141    ARVDSLGGPC CSPSPRATPG RSKEAPKGPR ARRQGPGGGS VSSDSSSPDS PGSPKVAPCQ
1201    PEGAHRQQGA LQGEMNALFV QKLEEIRSHS PMFSTVRD
```

PLCη2 is alternatively spliced at its C-terminus, producing five splice variants. All variants share the same sequence until exon 21. Amino acid sequences are shown based on findings of Zhou et al. (2005).

21a/23

VKQTLGLKGLFLRGTKPGSLDSHAAGQPLPRPSVSQRLLRRTASAPTKSQKPSRKGFPELALGTQDAGSEGAADD
VAPSSPNPALEAPTQERSGSSSPRDTRLFPLQRPISPLCSLEPIAEEPALGPGLPLQAAAPTGPSQEGSQCPVGL
GAKVTSSQQTSLGAFGTLQLRIGGGRENEEPPLRPHNGGISSGPREGTSGRQTDSKSRSRVPGHLPVVRRAKSEG
QVLSELSPTPAVYSDATGTDRLWQRLEPGSHRDSVSSSSSMSSNDTVIDLSLPSLGLCRSRESIPGVSLGRLTSR
PCLASAARPDLPPVTKSKSNPNLRVAGGLPTAPDELQPRPLAPRLTGHHPRPPWHHLTLVGLRDCPVSAKSKSLG
DLTADDFAPSFQGSTSSLSCGLGSLGVAHQVLEPGIRRDALTEQLRWLTGFQQAGDITSPTSLGPAGDGSVGGPS
FLRRSSSRSQSRVRAIASRARQAQERQQRLRGQDSRGPPEEERGTPEGACSVGHEGCVDVPMPAKGAPEQVCGAA
DGQLLLR

21a/22/23

VKQTLGLKGLFLRGTKPGSLDSHAAGQPLPRPSVSQRLLRRTASAPTKSQKPSRKGFPELALGTQDAGSEGAADD
VAPSSPNPALEAPTQERSGSSSPRVRD

21b/23

VKQTLGLKGLFLRGTKPGSLDSHAAGQPLPRPSVSQRLLRRTASAPTKSQKPSRKGFPELALGTQDAGSEGAADD
VAPSSPNPALEAPTQERSGSSSPRGKAPGGEATEERTLAQVRSPNAPEGPGPAGMAATCMKCVVGSCAGMDVEGL
QREQQPSPGPAGSHMAISHQPRARVDSLGGPCCSPSPRATPGRSKEAPKGPRARRQGPGGGSVSSDSSSPDSPGS
PKVAPCQPEGAHRQQGALQGEMNALFVQKLEEIRSHSPMFSTDTRLFPLQRPISPLCSLEPIAEEPALGPGLPLQ
AAAPTGPSQEGSQCPVGLGAKVTSSQQTSLGAFGTLQLRIGGGRENEEPPLRPHNGGISSGPREGTSGRQTDSKS
RSRVPGHLPVVRRAKSEGQVLSELSPTPAVYSDATGTDRLWQRLEPGSHRDSVSSSSSMSSNDTVIDLSLPSLGL
CRSRESIPGVSLGRLTSRPCLASAARPDLPPVTKSKSNPNLRVAGGLPTAPDELQPRPLAPRLTGHHPRPPWHHL
TLVGLRDCPVSAKSKSLGDLTADDFAPSFQGSTSSLSCGLGSLGVAHQVLEPGIRRDALTEQLRWLTGFQQAGDI
TSPTSLGPAGDGSVGGPSFLRRSSSRSQSRVRAIASRARQAQERQQRLRGQDSRGPPEEERGTPEGACSVGHEGC
VDVPMPAKGAPEQVCGAADGQLLLRL

21b/22/23

VKQTLGLKGLFLRGTKPGSLDSHAAGQPLPRPSVSQRLLRRTASAPTKSQKPSRKGFPELALGTQDAGSEGAADD
VAPSSPNPALEAPTQERSGSSSPRGKAPGGEATEERTLAQVRSPNAPEGPGPAGMAATCMKCVVGSCAGMDVEGL
QREQQPSPGPAGSHMAISHQPRARVDSLGGPCCSPSPRATPGRSKEAPKGPRARRQGPGGGSVSSDSSSPDSPGS
PKVAPCQPEGAHRQQGALQGEMNALFVQKLEEIRSHSPMFSTVRD

21c/22/23

VKQTLGLKGLFLRGTKPGSLDSHAAGQPLPRPSVSQRLLRRTASAPTKSQKPSRKGFPELALGTQDAGSEGAADD
VAPSSPNPALEAPTQERSGSSSPRGKAPGGEATEERTLAQVRSPNAPEGPGPAGMAATCMKCVVGSCAGMDVEGL
QREQQPSPGPAGSHMAISHQPRARVDSLGGPCCSPSPRATPGRSKEAPKGPRARRQGPGGGSVSSDSSSPDSPGS
PKVAPCQPEGAHRQQGALQGEMNALFVQKLEEIRSHSPMFSTGKACRSAASHALYTWHAVRD

Appendix II – Plasmid maps

Plasmid map for pcDNA3.1D/V5-His-TOPO used to clone PLCη1:

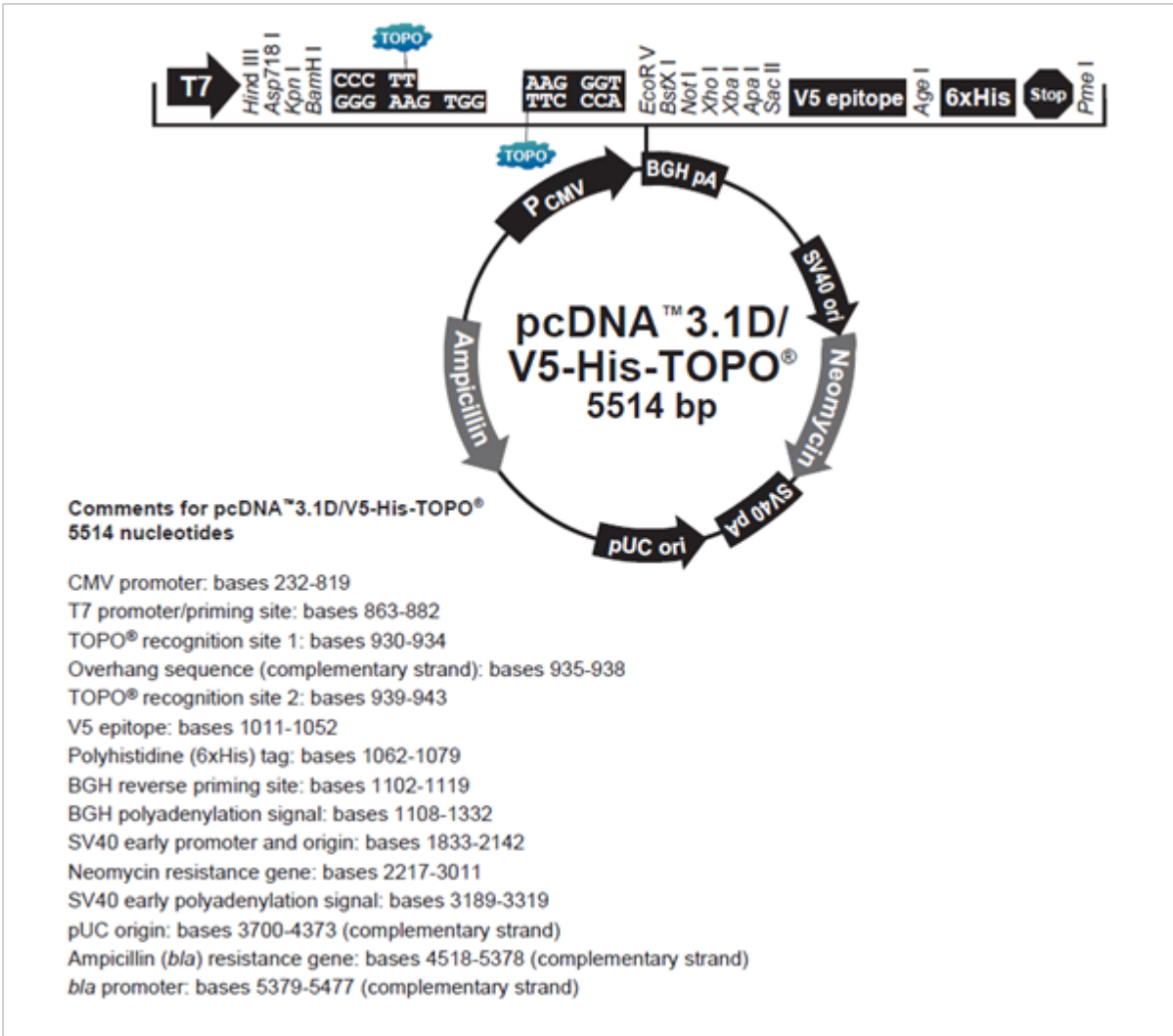

Figure B.1.: Plasmid map of pcDNA3.1D/V5-His-TOPO. Figure was downloaded from: http://www.invitrogen.com/1/1/10253-pcdna3-1-directional-topo-expression-kit.html.

Plasmid map for pcDNA3.1/NT-GFP-TOPO used to clone the PH domain of PLCη2:

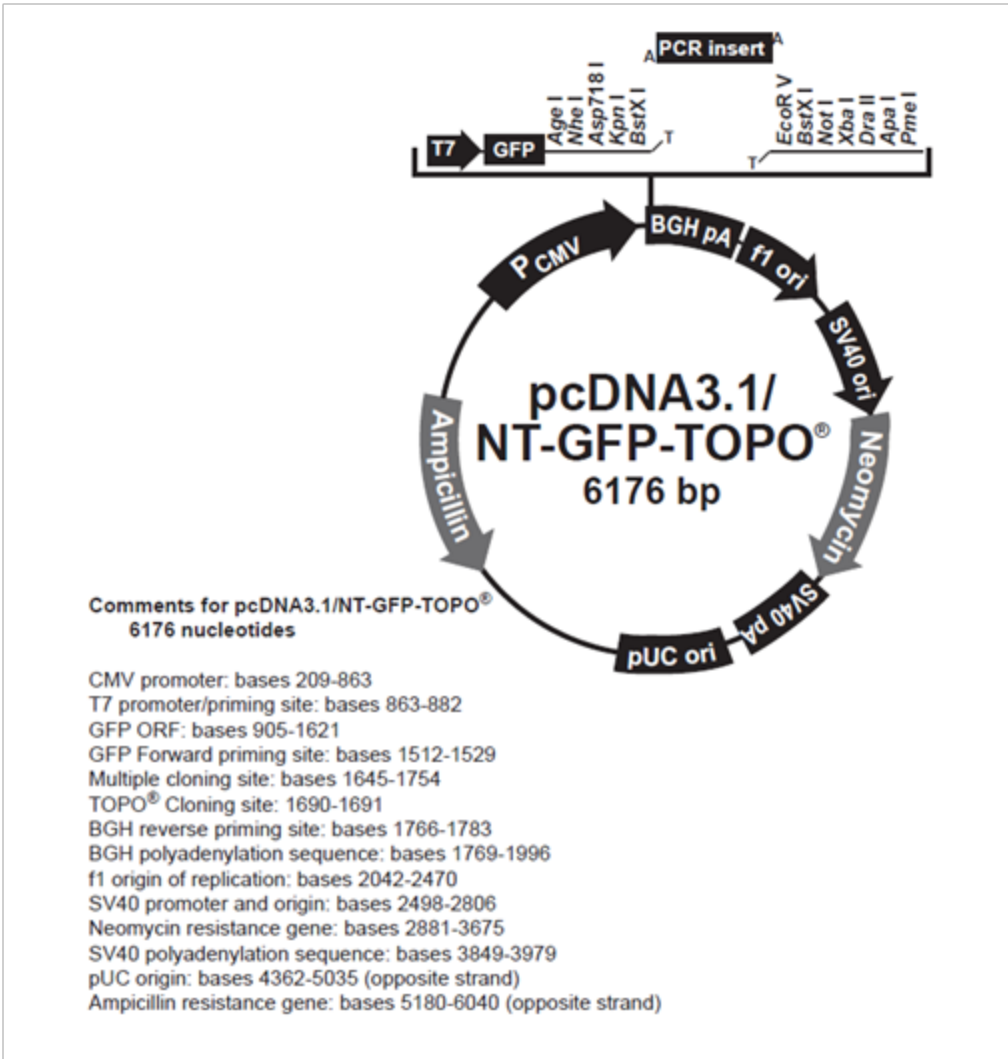

Figure B.2.: Plasmid map of pcDNA3.1/NT-GFP-TOPO. Figure was downloaded from: https://products.invitrogen.com/ivgn/product/K481001.

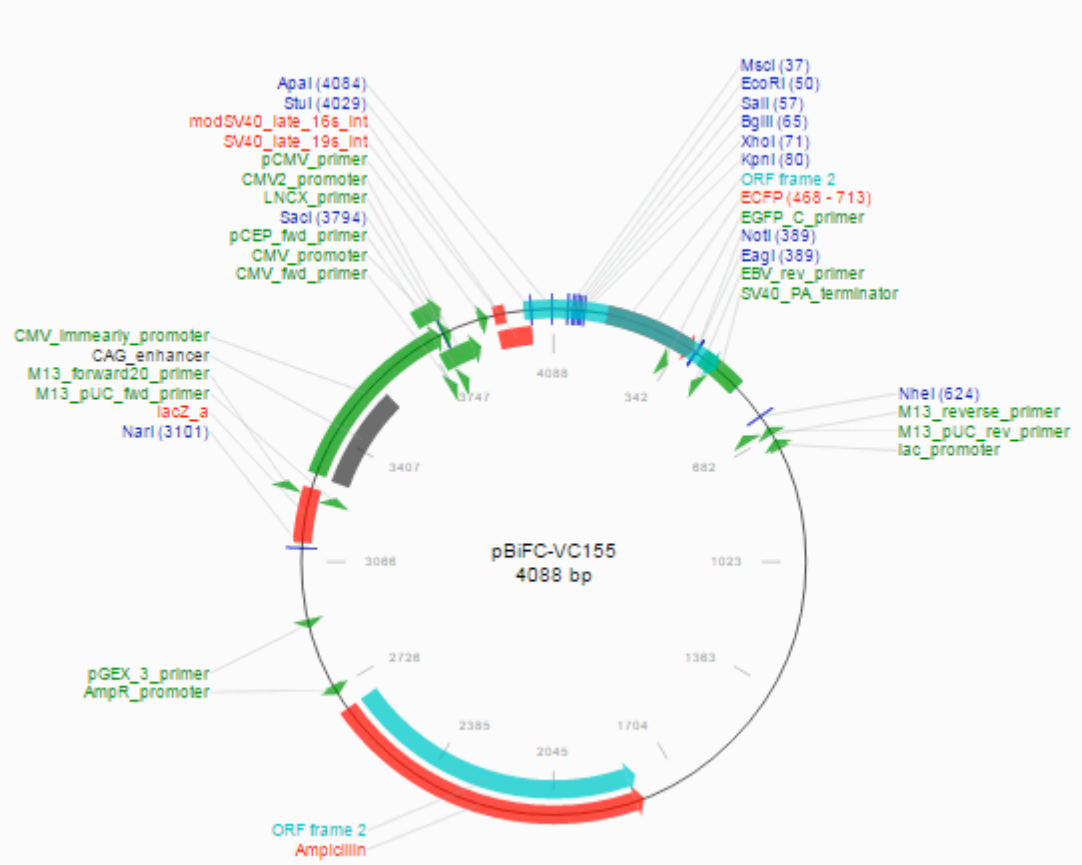

Figure B.3: plasmid map of pBiFC_VC155 containing partial sequence of the protein venus, a form of YFP. The restriction enzyme SalI was used to cut the vector and insert the full PLCη2 sequence. Figure downloaded from www.addgene.org/22011/ on 01/10/2015.

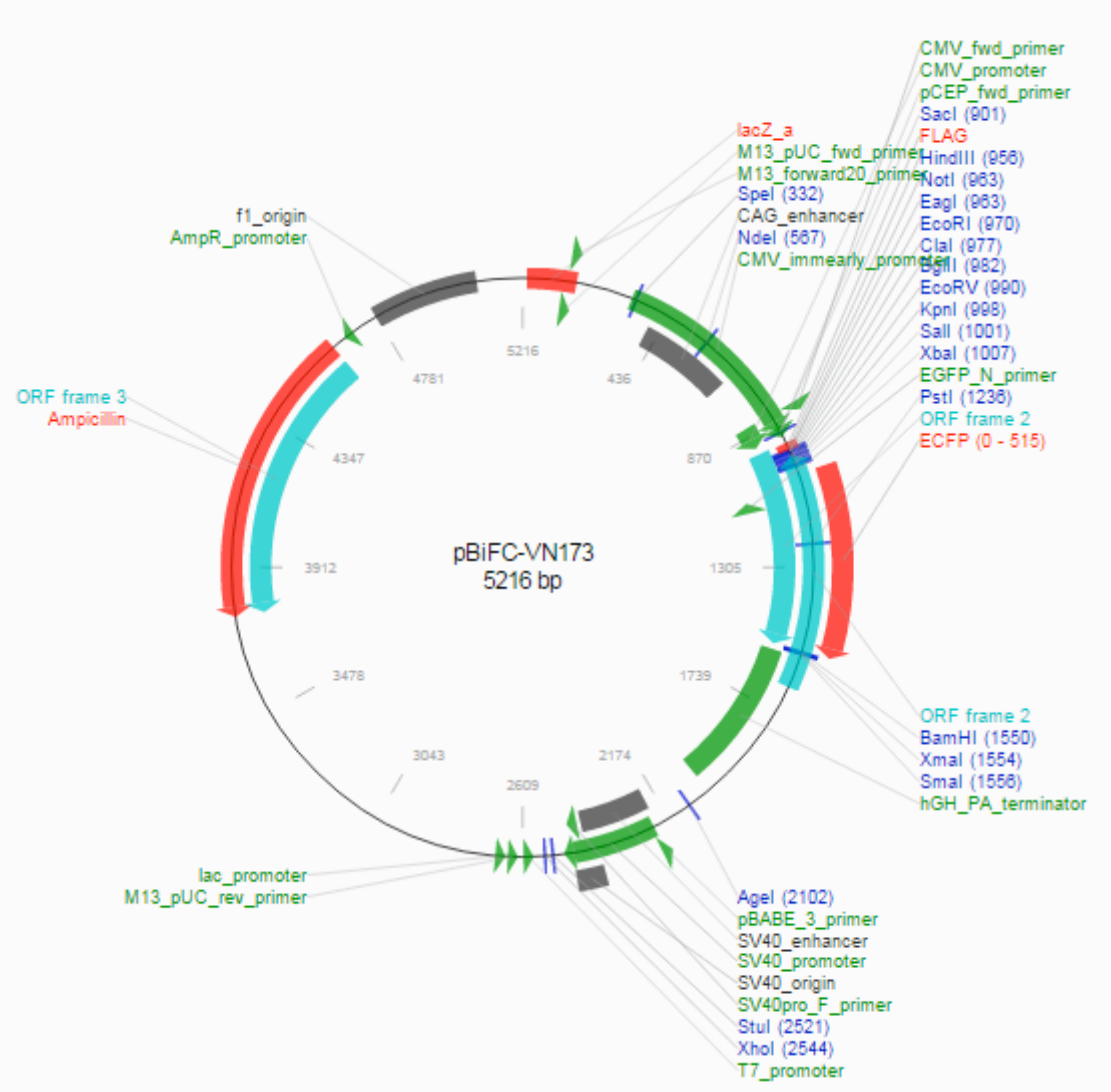

Figure B.4: Plasmid map of pBiFC_VN173 containing partial sequence of the protein venus, a form of YFP. The restriction enzyme HindIII was used to cut the vector and insert the full LIMK-1 sequence. Figure downloaded from www.addgene.org/22010/ on 01/10/2015.

Appendix III- publications

Journal of Neurochemistry

JOURNAL OF NEUROCHEMISTRY | 2013 | 124 | 632–644 doi: 10.1111/jnc.12122

ORIGINAL ARTICLE

Phospholipase C-η2 is required for retinoic acid-stimulated neurite growth

Petra Popovics,* Alexander Gray,† Mohammed Arastoo,* Deana K. Finelli,* Audrey J. L. Tan* and Alan J. Stewart*

*School of Medicine, Medical and Biological Sciences Building, North Haugh, University of St Andrews, St Andrews, Fife, UK

†College of Life Sciences, University of Dundee, Dundee, UK

Abstract

Phospholipase C-η2 is a recently identified phospholipase C (PLC) implicated in the regulation of neuronal differentiation/maturation. PLCη2 activity is triggered by intracellular calcium mobilization and likely serves to amplify Ca^{2+} signals by stimulating further Ca^{2+} release from Ins(1,4,5)P_3-sensitive stores. The role of PLCη2 in neuritogenesis was assessed during retinoic acid (RA)-induced Neuro2A cell differentiation. PLCη2 expression increased two-fold during a 4-day differentiation period. Stable expression of PLCη2-targetted shRNA led to a decrease in the number of differentiated cells and total length of neurites following RA-treatment. Furthermore, RA response element activation was perturbed by PLCη2 knock-down. Using a bacterial two-hybrid screen, we identified LIM domain kinase 1 (LIMK1) as a putative interaction partner of PLCη2. Immunostaining of PLCη2 revealed significant co-localization with LIMK1 in the nucleus and growing neurites in Neuro2A cells. RA-induced phosphorylation of LIMK1 and cAMP-responsive element-binding protein was reduced in PLCη2 knock-down cells. The phosphoinositide-binding properties of the PLCη2 PH domain, assessed using a FRET-based assay, revealed this domain to possess a high affinity toward PtdIns(3,4,5)P_3. Immunostaining of PLCη2 together with PtdIns(3,4,5)P_3 in the Neuro2A cells revealed a high degree of co-localization, indicating that PtdIns(3,4,5)P_3 levels in cellular compartments are likely to be important for the spatial control of PLCη2 signaling.

Keywords: cell differentiation, calcium signaling, neurite growth, phospholipase, nuclear receptors, neuroscience.

J. Neurochem. (2013) **124**, 632–644.

Phospholipase C-η (PLCη) enzymes are a recently identified class of phosphatidylinositol 4,5-bisphosphate (PtdIns(4,5)P_2)-hydrolyzing enzyme found in mammalian cells (Hwang *et al.* 2005; Nakahara *et al.* 2005; Stewart *et al.* 2005; Zhou *et al.* 2005). This class consists of two members, PLCη1 and PLCη2. Like other mammalian PLCs, their activity leads to the production of the second messengers Ins(1,4,5)P_3 and 1,2-diacylyglycerol (DAG), which trigger the release of Ca^{2+} from intracellular stores and the activation of protein kinase C isoforms, respectively.

Phospholipase C-η2 is most abundant in the brain and is found within the hippocampus, habenula, olfactory bulb, cerebellum, and throughout the cerebral cortex (Nakahara *et al.* 2005; Kanemaru *et al.* 2010). Activation of PLCη2 can be triggered either by intracellular Ca^{2+} immobilization (Popovics *et al.* 2011) or by Gβγ signaling (Zhou *et al.* 2005, 2008). Considering its sensitivity of toward Ca^{2+}, it is thought that PLCη2 may act synergistically with other PLCs or Ca^{2+} activated processes in neurons (Popovics and Stewart 2012). When transiently expressed in COS7 cells, PLCη2 associates with plasma and organelle membranes via its PH domain (Popovics *et al.* 2011). However, the specificity of this domain toward particular phospholipids, which is likely to control its cellular location, remains unknown.

Although a role in the amplification of PLCβ signals has recently been demonstrated for PLCη1 (Kim *et al.* 2011), a functional role has yet to be identified for PLCη2. Nakahara *et al.* previously reported that levels of PLCη2 protein increase in the brains of mice during the first few weeks after birth (Nakahara *et al.* 2005). Similarly, the retina expresses high levels of PLCη2 which also elevate from birth

Received October 8, 2012; revised manuscript received November 21, 2012; accepted December 10, 2012.

Address correspondence and reprint requests to Alan J. Stewart, School of Medicine, University of St Andrews, St Andrews, Fife, KY16 9TS, United Kingdom. E-mail: ajs21@st-andrews.ac.uk.

Abbreviation used: APC, allophycocyanin; CREB, cAMP-responsive element-binding protein; DAG, 1,2-diacylyglycerol; LIMK1, LIM domain kinase 1; PBS, phosphate-buffered saline; PLC, phospholipase C; RARE, RA response element; TBS, Tris-buffered saline.

(Kanemaru *et al.* 2010). Its expression profile hints that this enzyme might be involved in processes linked to neuronal differentiation or maturation. In this study, we examined the importance of PLCη2 during retinoic acid (RA)-induced differentiation of Neuro2A cells. This system was chosen as it provides a well-defined cellular model of neuronal differentiation that has been used to characterize the importance of various factors in this process (Pignatelli *et al.* 1999; Carter *et al.* 2003; Bryan *et al.* 2006; Kouchi *et al.* 2011), and these cells are known to express endogenous PLCη2 (Kim *et al.* 2011). Stable shRNA-mediated knockdown of PLCη2 expression in these cells revealed this enzyme to be important for RA-stimulated neurite outgrowth. Reductions in PLCη2 expression in isolated clones led to reductions in RA signaling and LIM kinase-1 (LIMK1) phosphorylation. A bacterial two-hybrid screen identified LIMK1 as a putative interaction partner for PLCη2. Furthermore, it was found that PLCη2 co-localizes with LIMK1 within the nucleus and growing neurites in Neuro2A cells and that PLCη2 associates with intracellular PtdIns(3,4,5)P_3 pools via its PH domain.

Materials and methods

Expression constructs

The GFP-tagged murine PLCη2 construct incorporating residues 75–1238 was generated as described previously (Popovics *et al.* 2011), this region of the protein includes all functional domains (PH, EF-hand, catalytic X and Y and C2 domains). Plasmids (psi-H1) encoding control and PLCη2-targeted shRNAs were purchased from GeneCopoeia (Rockville, MD, USA). These plasmids contained the 19-mer target sequences 5′-TGACTGCAAGCTCCT-CAAT-3′ or 5′-GGACCTAGTGAAATATACC-3′, which were used to generate the shRNAPLCη2-1 and shRNAPLCη2-2 cell lines, respectively. The glutathione S-transferase (GST)-tagged PLCη2 PH domain expression construct was made by inserting the corresponding cDNA fragment into pGEX6 (GE Healthcare, Buckinghamshire, UK). The same sequence was subcloned into the pcDNA3.1/NT-GFP-TOPO vector (Invitrogen, Paisley, UK) to generate a GFP-tagged PLCη2 PH domain encoding construct. The mCherry-tagged PLCδ1 PH domain expression vector was made by inserting the corresponding cDNA fragment into pmCherry-C1 (Clonetech, Saint-Germain-en-Laye, France).

Cell culture

Neuro2A cells were obtained from the European Collection of Cell Cultures (Salisbury, UK) and were maintained in Eagle's minimal essential medium (EMEM) supplemented with 10% fetal bovine serum (FBS), 2 mM L-glutamine, and 50 units/mL of penicillin/streptomycin. Differentiation of Neuro2A cells was induced as previously described by Zeng and Zhou (2008). Briefly, cells were plated at a low density (100 cells/mm^2) in complete EMEM which was changed to the differentiation medium the next day (EMEM with 2% FBS, 2 mM L-glutamine and 20 μM RA). Medium was renewed every day for 4 days. Micrographs showing cells at different stages of differentiation were collected by a Zeiss Axiovert 40 CFL microscope with a 10× objective (Carl Zeiss Ltd., Cambridge, UK). To assess neurite growth, four micrographs were taken by random selection from all experimental conditions, and experiments were repeated three times. All cells possessing at least one neurite with a length at least twice the cell body were accepted as differentiated. Results were expressed as a percentage of differentiated/total cell number. Neurite outgrowth was estimated based on a previously described stereological method (Lucocq 2008). Neuro2A cells were stably transfected with shRNA expressing plasmids to produce cell lines with reduced expression of PLCη2. In each case, 20 μg of DNA was transfected by electroporation using a Bio-Rad Gene Pulser (Hertfordshire, UK) at 230 V, 950 μF. Stably, transfected cells were selected 48 h after transfection by addition of media containing 3 μg/mL puromycin.

Western blotting

Cells were seeded onto 6-well plates and differentiated as described above. One well of cells was scraped in 50 μL radio-immunoprecipitation assay buffer containing complete protease inhibitor cocktail (Roche, Burgess Hill, UK) and cell debris was removed by centrifugation (16 000 g for 15 min). Protein concentration of the lysates was measured using the bicinchoninic acid protein assay kit (Thermo Fisher Scientific, Surrey, UK). Samples (corresponding to 10 μg total protein) were separated by NuPAGE gradient (4–12% Bis-Tris) gel electrophoresis using a MES buffer system (Life Technologies, Paisley, UK) then electro-blotted onto polyvinylidene difluoride membrane. Blots were incubated for 1 h at 20°C in blocking buffer (5% non-fat milk in TBS) before being incubated for 90 min in 1% non-fat milk and 0.5% Tween-20 in Tris-buffered saline (TBS) containing either custom-made rabbit polyclonal anti-PLCη2 antibody (1 : 5000 dilution), mouse polyclonal anti-LIMK1 or rabbit anti-phospho-LIMK1 (Thr508) antibodies (1 : 1000 dilution; Abcam, Cambridge, UK), rabbit anti-CREB or anti-phospho-CREB (Ser133) antibodies (1 : 1000 dilution; Cell Signaling Technology, Danvers, MA, USA). The custom-made antibody was raised commercially against a short peptide (SKVEEDVEA-GEDSGVSRQN; EZBiolab, Westfield, IN, USA). Blots were washed three times in TBS containing 0.5% Tween before incubating with an appropriate species-specific secondary horseradish peroxidase-conjugated antibody (1 : 10 000 dilution; Thermo Fisher Scientific) in blocking buffer containing 0.5% Tween for 1.5 h at 20°C. Blots were washed three times with TBS containing 0.5% Tween and antibody-binding was detected using the Super-Signal West Dura chemiluminescent substrate (Thermo Fisher Scientific) with a LAS-3000 phosphoimager (Fujifilm, Düsseldorf, Germany). Densitometry was performed using ImageJ software (NIH, Bethesda, MD, USA).

Inositol phosphate release assays

IP-release assays were performed in triplicate as previously described (Popovics *et al.* 2011). Briefly, cells were seeded onto 14 cm diameter dishes and treated the next day with serum- and inositol-free Dulbecco's modified Eagle's medium (MP Biomedicals, Illkirch, France) containing 1 μCi/mL myo-D-[^{3}H]inositol (GE Healthcare, Buckinghamshire, UK) for 24 h. On day 3, cells were trypsinized, counted, and collected by centrifugation. Cell pellets were diluted in buffer A (140 mM NaCl, 20 mM HEPES, 8 mM glucose, 4 mM KCl, 1 mM $MgCl_2$, 1 mM $CaCl_2$, and 1 mg/mL

bovine serum albumin) to equal cell density. Thereafter, equal cell numbers (5×10^5/tube) were transferred into buffer A containing 10 mM LiCl. Tubes were incubated for 1 h before the addition of A23187 (Ca^{2+}-ionophore) to a final concentration of 5 μM. Cells were stimulated for 3 h and reaction was terminated by the addition of a final 10 mM formic acid. This was incubated for 30 min at 4°C. Cell debris was removed by centrifugation (2 000 *g* for 3 min) and supernatant was transferred onto Dowex AG 1- resin (BioRad, Hemel Hempstead, UK). Resin was washed with water and 60 mM ammonium formate/5 mM sodium tetraborate. Inositol phosphates were eluted with 1 M ammonium formate/0.1 M formic acid and quantified by liquid scintillation counting.

RT-PCR and qPCR

Neuro2A cell mRNA was isolated by the Isolate RNA Mini Kit (Bioline, London, UK) according to the manufacturer`s instructions. DNA contamination was removed by DNAse digestion (RQ1 RNase-Free DNase, Promega, Southampton, UK). Following this 0.5 μg of mRNA was subjected to a two-step reverse transcription reaction. The mRNA was incubated with 100 pmol oligodT_{18} and 0.5 mM dNTP in Diethylpyrocarbonate (DEPC)- treated water at 65°C for 5 min and then chilled on ice. RevertAid Premium Reverse Transcriptase (200 units), RiboLock RNase Inhibitor (20 units; Thermo Fisher Scientific), and 1 × RT-buffer (Fermentas, St. Leon-Rot, Germany) were added. Mixtures were incubated at 50°C for 30 min and then 60°C for 10 min. Reactions were terminated at 85°C for 5 min. The presence of RARα, RARβ, and RARγ was detected by RT-PCR using primers designed not differentiate between splice variants (sequences are shown in Table 1). PCR reactions contained 1.25 units of GoTaq polymerase (Promega), 1 × reaction buffer, 1.5 mM $MgCl_2$, 0.2 mM dNTPs, and 250 nM of each primer. Reactions were cycled at 95°C for 15 s, 60°C for 30 s and 72°C for 1 min. The expression level of RARα in control, shRNAPLCη2-1, and shRNAPLCη2-2 cells was measured by qPCR relative to the level of the large ribosomal protein P0 mRNA. Expression was detected by Brilliant III Ultra-Fast SYBR Green mix (Agilent Technologies, Cheshire, UK) in a Rotor-Gene Q PCR machine (Qiagen, Crawley, UK). Expression levels were calculated by the ΔΔCt method.

RARE luciferase assay

RA response element (RARE) regulated transcriptional activity was measured by transiently transfected luciferase constructs. RARE reporter vector expressing luciferase and a CMV promoter driven luciferase containing construct were obtained from SABiosciences (Qiagen). Stable Neuro2A cells were seeded at 5×10^4 cell/well into a 96-well plate in antibiotic-free EMEM with 10% FBS. Cells were transfected with the luciferase constructs the next day using Lipofectamine 2000 (Life Technologies) in accordance with the manufacturer`s instructions. The media was changed to serum- and antibiotic-free EMEM after 6 h. Cells were treated the next day with RA or dimethylsulfoxide only for 4 h and reaction and luciferase activity measured using the Dual Luciferase Reporter assay kit (Promega) with a Fluostar Optima plate reader (BMG Labtech, Ortenberg, Germany). The parameters of each measurement were a combination of a 2-s pre-measurement delay and a continuous measurement for 10 s. The assays were performed in triplicates.

Table 1 Primer sequences used for semi-quantitative and quantitative assessment of RAR isoform expression

Primer	Sequence
RARα forward	5′-CACTTTTGCAGAGCGCGGTGCGG-3′
RARα reverse	5′-GCGTTTGCTGGTGATGAAGACGTGGC-3′
RARβ forward	5′-GGAAGGAGAAGGCAGTGACTCTGTGG-3′
RARβ reverse	5′-CGGTGCTGCCATTCGGCCTGG-3′
RARγ forward	5′-GCGGAGTCAGTGTGCGGTTTGGG-3′
RARγ reverse	5′-GGTCTCGGGGATGGAGCACCGC-3′
RPL0 forward	5′-GAGTGATGTGCAGCTGATAAAGACTGG-3′
RPL0 reverse	5′-CTGCTCTGTGATGTCGAGCACTTCAG-3′

Cell Imaging

Neuro2A cells were seeded onto coverslips in 6-well plates with a low cell density (100 cells/mm^2). In some cases, Neuro2A cells were transfected with GFP- or mCherry-tagged constructs using Lipofectamine 2000 transfection reagent in accordance with the manufacturer`s protocol. The next day, or after a 2-day or 4-day treatment with 20 μM retinoic acid, cells were fixed with 4% formaldehyde in phosphate-buffered saline (PBS) for 10 min. Nuclei were stained with 4′,6-diamidino-2-phenylindole and coverslips were mounted with Mowiol solution. For the detection of endogenous proteins, cells were fixed and permeabilized in one step with 4% formaldehyde and 0.2% Triton-X containing PBS. This solution was removed after 5 min and cells were washed with PBS three times. Coverslips were then incubated with blocking buffer containing 10% FBS in PBS for 1 h. Custom-made rabbit primary antibody (generated as described above) was used to stain endogenous PLCη2 (dilution: 1 : 100). Antibodies against LIMK1 (1 : 100 dilution; Abcam) and PtdIns(3,4,5)P_3 (1 : 100 dilution; Echelon Biosciences Inc., Salt Lake City, UT, USA) were also used for immunostaining. Primary and secondary antibodies were diluted into appropriate concentrations in 5% FBS in PBS. Cells were incubated with primary antibody solution for an hour followed by three washing steps with PBS. Appropriate fluorescent species-specific secondary antibodies (Dylight 488 or 594; Jackson ImmunoResearch, West Grove, PA, USA) were diluted 1 : 300 and applied onto the coverslips for 1 h. Nuclei were stained with 4′,6-diamidino-2-phenylindole and coverslips were mounted in Mowiol solution. Slides were examined with a Zeiss Axioplan fluorescent microscope system, a DeltaVision deconvolution microscope (Applied Precision, Washington, DC, USA) or a Leica TCP SP2 multiphoton confocal microscope (Leica, Heidelberg, Germany).

Bacterial two-hybrid screen

The BacterioMatch II Two-Hybrid System (Stratagene, Cambridge, UK) was used to identify putative protein interaction partners for PLCη2 according to the manufacturer`s protocol. Briefly, cDNA corresponding to the C-terminal domain of PLCη2 (residues 967-1070 of splice variant 21a/22/23) was cloned into the pBT bait plasmid and was screened against a human pancreas cDNA library (Stratagene, Cheshire, UK) encoded within the plasmid pTRG. In this system, interaction between the C-terminal domains of PLCη2 and a protein encoded by a library-derived gene product allows the transcription of *His3* and *Aad3* genes in the reporter *E. coli* strain.

This permits the selection of the interaction-pairs via the addition of 3-aminotriazole (3-AT) (an inhibitor of histidine synthesis) or by streptomycin resistance, respectively. The pBT-PLCη2-C-term and pTRG-library plasmids were co-transformed into *E. coli* reporter cells, in accordance with the manufacturer's instructions. Initially, transformed cells were spread onto plates containing minimal media with 5 mM 3-AT in the first instance. Resultant colonies were also plated on dual-selective plates containing 5 mM 3-AT and 12.5 μg/mL streptomycin to confirm a positive interaction between bait and target proteins. Colonies were picked, plasmid DNA was isolated, and pTRG plasmid inserts were sequenced commercially (Dundee Sequencing Service, Dundee, UK). The pTRG plasmid inserts were then identified using NCBI-BLAST (Altschul *et al.* 1997).

FRET-based assessment of PLCη2 PH domain–phosphoinositide binding

PH domain-phosphoinositide interactions were measured using a FRET-based assay (Gray *et al.* 2003). GST-conjugated PLCη2 PH domain was expressed in *E. coli* strain BL21 and affinity-purified using Glutathione beads (Sigma, Poole, UK). Biotinylated and non-biotinylated lipids were obtained from Cell Signals, Inc. (Lexington, KY, USA). FRET assays were performed in assay buffer (50 mM HEPES, pH 7.4, 150 mM NaCl, 5 mM $MgCl_2$, 5 mM dithiothreitol, 0.05% Chaps). PLCη2-PH (14 μL of 0.62 mg/mL) was mixed with 4 μL APC-streptavidin (2 mg/mL, Prozyme Ltd. Hayward, CA, USA), 80 μL Eu-anti-GST antibody (80 μg/mL) (Perkin-Elmer, Buckinghamshire, UK) in 2.5 mL assay buffer. From this mixture, 25 μL was added to the same volume of serially diluted (0–50 pmol in final volume) biotinylated lipids and the association of biotinylated phosphoinositide/PH domain complexes was measured in a 96-well plate (White Lumitrac 200; Greiner Ltd) in an LJL Analyst. In a separate experiment, displacement of PLCη2-PH from a pre-formed FRET complex was measured by the addition of increasing concentrations of phosphoinositides. PtdIns(4,5)P_2-PLCη2 PH domain FRET complexes were formed by mixing 4 μL (2 mg/mL) Streptavidin APC, 200 pmol biotin PtdIns(4,5)P_2, 14 μL (0.62 mg/mL) PH domain and 50 μL Eu-anti-GST (80 μg/mL) in 2.5 ml assay buffer. Displacing ligands were serially diluted from 200 μM in 5-fold steps in assay buffer, 25 μL added to 25 μL the FRET complex and any decrease in signal was measured as previously described (Gray *et al.* 2003).

Statistical analysis

Experiments were repeated independently at least three times and all assays were performed in triplicate. Data are presented as mean values ± SEM. Analyses were performed using the SigmaPlot software (Systat Software Inc, Chicago, IL, USA) with one-way ANOVA followed by the Holm-Sidak *post hoc* test or Student`s *t*-test.

Results

PLCη2 expression increases during RA-induced Neuro2A cell differentiation

Neuro2A cells were previously described as being highly susceptible to the combination of RA-treatment, reduced serum (2% FBS), and low cell plating density (100 cells/mm^2) (Zeng and Zhou 2008). Following this protocol, Neuro2A cells differentiate over a period of 4 days altering their morphology from a stem cell-like to a neuron-like shape with extended neurites and enlarged cell body (Fig. 1a). This model was used to examine PLCη2 protein levels during neuronal differentiation. The dominant expression of one splice variant was confirmed in Neuro2A cells. This was the

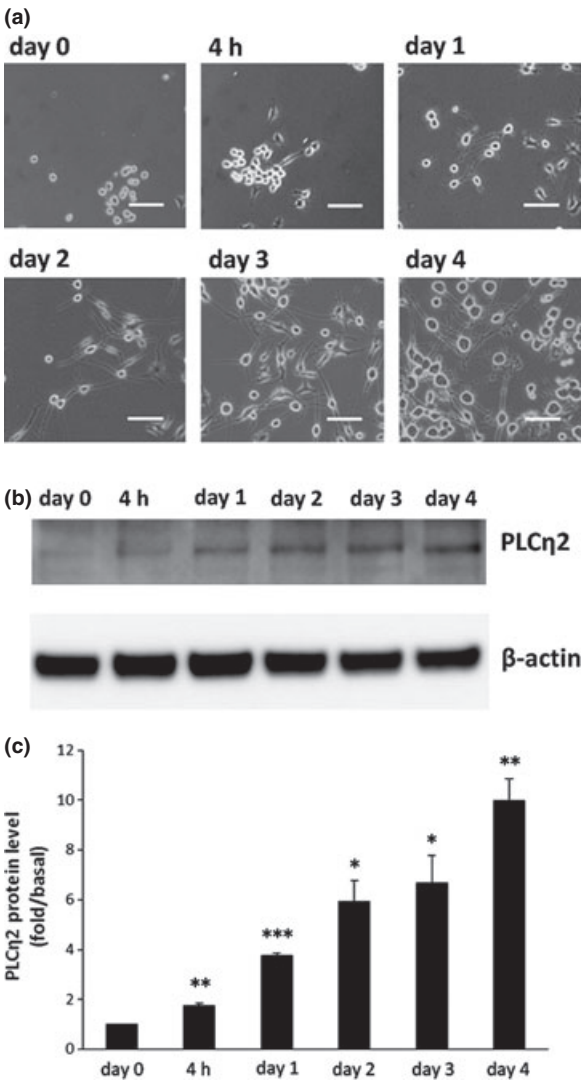

Fig. 1 Phospholipase C (PLC)-η2 protein level increases during neuronal differentiation of Neuro2A cells. (a) Bright-field images showing Neuro2A cells treated with 20 μM retinoic acid over a 4-day period. Bars correspond to 100 μm. (b) Western blot showing PLCη2 protein levels in Neuro2A cells at various times during retinoic acid-treatment. The protein levels of β-actin were used as a loading control. The blot shown is representative of three independent experiments. (c) Quantification of PLCη2 expression during Neuro2A cell differentiation. PLCη2 protein expression was normalized to β-actin protein level and the basal expression (day 0) was defined as equal to 1. Error bars represent ± SEM. Statistical significance was assessed by *t*-test (*$p < 0.05$, **$p < 0.01$, ***$p < 0.001$; $n = 3$).

21a/22/23 form, previously identified by Zhou *et al.* (2005). Short-term treatment (4 h) with RA resulted in a 76% increase in PLCη2 protein level. Moreover, PLCη2 levels gradually increased throughout the differentiation process and were ~10-fold higher than basal on day 4 (Fig. 1b and c).

PLCη2 is involved in RA-induced Neuro2A cell differentiation

We next examined whether Neuro2A cell differentiation may be affected by reducing PLCη2 expression. Appropriate 'knock-down' cell lines were generated by stable expression of shRNAs targeting PLCη2 expression. Stable clones were selected by puromycin resistance following transfection of the shRNA-encoding constructs into Neuro2A cells. PLCη2 protein levels in single-cell-derived clones for were determined by Western blot. Two lines (shRNAPLCη2-1 and shRNAPLCη2-2) were chosen for further experiments. A control cell line (shRNAcontrol) produced by the stable transfection of control shRNA was also selected. The protein level of PLCη2 in each was calculated and was found to be reduced by 67% and 39% in shRNAPLCη2-1 and shRNAPLCη2-2 cell lines, respectively (Fig. 2a and b). The cellular effects of PLCη2 knockdown in Neuro2A cells during RA-stimulated differentiation were then investigated. Control and knock-down cells were treated with RA (20 μM) for 4 days and bright images were taken with a 10× objective on each day. Representative images of each cell line following 4 days of treatment are shown in Fig. 2c. The proportion of differentiated cells was significantly affected by PLCη2 knockdown with the level of reduction largely mirroring the expression level of PLCη2. The shRNAPLCη2-1 cell line, which exhibited the greatest

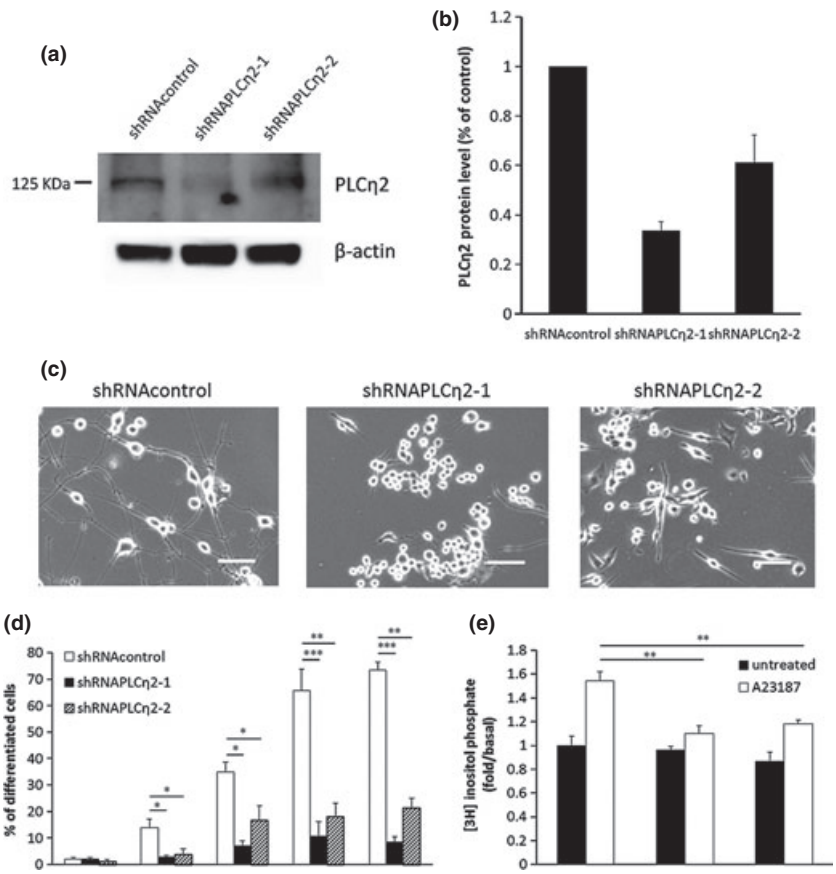

Fig. 2 Phospholipase C (PLC)η2 protein level was reduced by the stable transfection of shRNA in Neuro2A cells. (a) Representative immunoblot showing the expression of PLCη2 in control (shRNAcontrol) and PLCη2 knock-down cells (shRNAPLCη2-1, shRNAPLCη2-2). (b) Calculation of PLCη2 (21a/22/23) knock-down efficiency by densitometry (n = 2). PLCη2 levels were normalized to β-actin levels. (c) Bright-field images of control and PLCη2 knock-down cells after 4 days of retinoic acid-treatment. Bars correspond to 100 μm. (d) Percentage of differentiated control and PLCη2 knock-down cells during retinoic acid-treatment. The results are calculated from three independent experiments and at least 75 cells were measured in each group. Error bars represent ± SEM. Statistical significance was assessed by one-way ANOVA (*$p < 0.05$, **$p < 0.01$, ***$p < 0.001$; n=3). (e) Calcium induced phosphoinositide release in control and PLCη2 knock-down cells in response to 5 μM A23187. The activity of the untreated shRNA control was defined as equal to 1. Error bars represent ± SEM. Statistical significance was assessed by one-way ANOVA (**$p < 0.01$; n = 3).

decline in PLCη2 level, showed very little neurite growth, whereas the shRNAPLCη2-2 cells formed some short neurites. To better evaluate these results, the rate of differentiation was calculated from three independent experiments on each day (Fig. 2d). Cells were defined as differentiated if possessing at least one neurite with a length equal to or longer than twice the cell body diameter. Significant differences between the differentiation of control and knock-down cell lines were observed after 24 h of treatment. This difference gradually increased over the 4 days. On day 4, the proportion of differentiated shRNA-control cells was 73%, whereas only 8% and 22% of the shRNAPLCη2-1 and shRNAPLCη2-2 cells were defined as being fully differentiated. For each of the three cell lines, total neurite outgrowth (sum of neurite lengths) was also calculated based on a previously described stereological approach (Ronn *et al.* 2000; Lucocq 2008). Total neurite outgrowth was found to mirror the results obtained by calculating the percentages of differentiated cells (Figure S1). An inositol phosphate release assay was employed with the three cell lines following treatment with 5 μM A23187 (Ca^{2+} ionophore) to examine the phospholipid turnover in response to Ca^{2+}. Both the shRNAPLCη2-1 and shRNAPLCη2-2 cells exhibited a significantly decreased inositol phosphate release relative to control cells after this treatment (Fig. 2e).

PLCη2 regulates RA receptor signaling

To gain some mechanistic information as to how PLCη2 contributes to RA-induced Neuro2A differentiation, we examined whether RA signaling is affected by reduced PLCη2 expression. The cellular effects of RA are driven by its nuclear receptor (RAR) which directly regulates gene expression upon binding of its ligand. A partner, the retinoid X receptor, with which it forms a heterodimer, is also involved in this process. The receptor–ligand complex binds to specific promoter regions of the target genes, termed as RAREs (Lane and Bailey 2005). Three variants of retinoid receptors are known to exist, RARα, RARβ, and RARγ (Chambon 1996). RT-PCR analysis performed using and RAR isoform specific primers revealed that only RARα is expressed in these cells (Fig. 3a). Quantitative PCR revealed that RARα mRNA expression did not differ significantly between the shRNAPLCη2-1, shRNAPLCη2-2 and control lines (Fig. 3b). A dual-luciferase reporter assay was employed to measure RA-induced transcriptional activity in each cell line. This included the co-transfection of two expression constructs (Fig. 3c); one containing the RARE sequence (5-AGGTCACCAGGAGGTCA-3′) followed by the firefly luciferase gene and one vector constitutively expressing luciferase to allow transfection efficiency to be assessed. Interestingly, both PLCη2 knock-down cell lines exhibited reductions in basal RA-regulated signaling compared with the control cells (Fig. 3d). Luciferase activities in shRNAPLCη2-1 and shRNAPLCη2-2 cells were reduced by 60% and 30% to that of control cells, respectively. The difference between shRNAPLCη2-1 and shRNAPLCη2-2 was significant, which is likely because of the lower level of PLCη2 in shRNAPLCη2-1. RARE activation in the RA-stimulated cells was also examined (Fig. 3e). Luciferase activity increased 101-fold in shRNAcontrol cells following treatment with RA (20 μM). Under the same conditions, shRNAPLCη2-1 and shRNAPLCη2-2 cells exhibited only 35-fold and 44-fold elevations, respectively.

LIMK1 as a putative interaction partner of PLCη2

Phospholipase C-η enzymes possess an extended C-terminal domain rich in proline, serine and threonine residues, which it is thought may provide an interaction site for other proteins *in vivo* (Stewart *et al.* 2005). To identify potential binding partners for PLCη2, a bacterial 2-hybrid screen was performed. The coding sequence corresponding to the C-terminal region of the 21a/22/23 splice variant was cloned into the pBT 'bait' plasmid. This particular variant was chosen as it is the shortest and with the exception of the three C-terminal amino acids derived from exon 22 (Val-Arg-Asp), the sequence is common to all variants. A pancreas cDNA library was cloned into the pTRG 'target' plasmid for screening. Competent *E. coli* reporter cells were co-transfected with 'bait' and 'target' constructs and following dual-selection (with 3-AT and streptomycin), 18 colonies were isolated and pTRG plasmids were sequenced (Figure S2). In one colony, the pTRG plasmid was found to encode the C-terminal region (residues 519-647) of LIMK1. This region incorporates part of the protein's catalytic domain but does not contain the residues implicated in substrate binding or phosphorylation activity (residues 345-514) (Manetti 2012). To establish whether PLCη2 and LIMK1 may interact within Neuro2A cells, we examined the cellular localization of both proteins. Both undifferentiated and RA-stimulated cells were stained for endogenous PLCη2 and LIMK1 by co-immunostaining (Fig. 4a and b). LIMK1 and PLCη2 were both present in neurites and were abundant in the nucleus. This is consistent with the previous observation that LIMK1 is located within nucleus in neurons (Bernard *et al.* 1994). The localization of LIMK1 in comparison with transiently expressed GFP-PLCη2 was also assessed in transiently transfected undifferentiated and RA-treated cells (Fig. 4c and d). Both LIMK1 and GFP-PLCη2 possessed a high degree of co-localization in the nuclei of both untreated and RA-treated cells and in the neurites of the RA-treated cells.

PLCη2 is important for LIMK1/CREB signaling

To assess whether LIMK1 activity is affected by PLCη2 expression, the phosphorylation of LIMK1 was examined in shRNAPLCη2-1 and control cells at different stages of the differentiation process (Fig. 5a and b). Phosphorylated LIMK1 (pLIMK1; Thr508) was undetectable in untreated

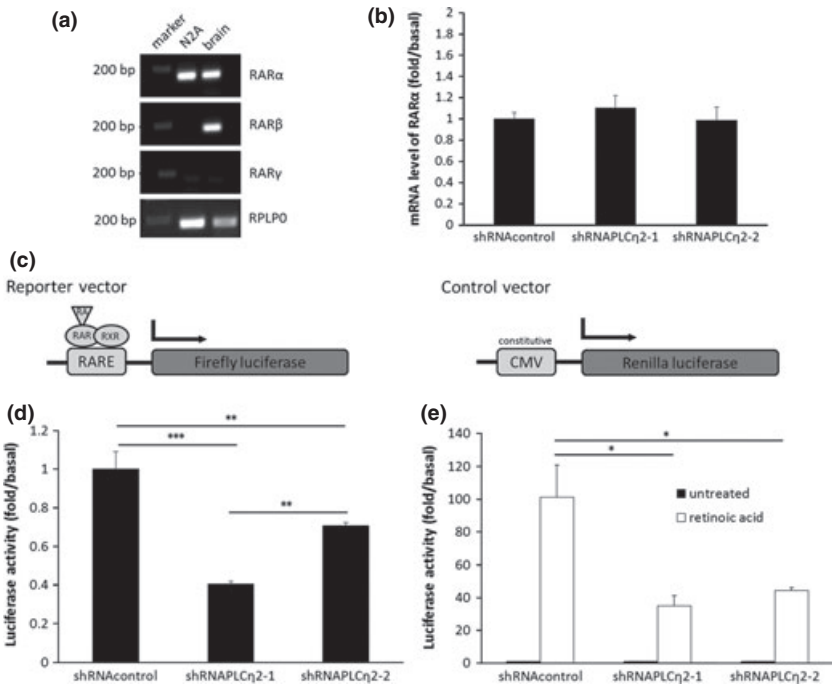

Fig. 3 (a) RT-PCR showing the expression of retinoid receptors in Neuro2A cells and in mouse brain. PCR products corresponding to RARα, RARβ, and the standard gene mRNA, RPLP0 are detected at their expected sizes (159 bp, 173 bp, and 163 bp, respectively). In the marker lane, the 200 bp band is shown. (b) Quantitative PCR showing the relative levels of RARα mRNA in control and knock-down Neuro2A cell lines. Results were normalized relative to the expression of the ribosomal mRNA, RPLP0. The RARα mRNA level in shRNAcontrol cells was defined as equal to 1. Error bars represent ± SEM. Statistical significance was assessed by one-way ANOVA ($n = 3$). (c) Luciferase reporter constructs for detection of retinoic acid (RA)-induced gene transcription. The RA-RAR-retinoid X receptor complex binds to the RA response element (RARE) sequence which induces the expression of the firefly luciferase. A control vector is co-transfected with the reporter which contains luciferase under the control of a CMV promoter. (d) Basal RARα activity in control and Phospholipase C (PLC) η2 knock-down cell lines assessed by dual-luciferase assay. The luciferase activity in shRNAcontrol cells was defined as equal to 1. Error bars represent ± SEM. Statistical significance was assessed by one-way ANOVA (**$p < 0.01$, ***$p < 0.001$; $n = 3$). (e) Retinoic acid (20 μM) stimulated RARα activity in control and PLCη2 knock-down cell lines assessed by dual-luciferase assay. The basal luciferase activities for all cell lines were defined as equal to 1. Error bars represent ± SEM. Statistical significance was assessed by one-way ANOVA (*$p < 0.05$; $n = 3$).

cells. After 4 h of RA-treatment, the level of pLIMK1 increased to detectable levels in both shRNAcontrol and shRNAPLCη2-1 cells. However, pLIMK1 levels were 75.3% lower in the shRNAPLCη2-1 cells and remained lower than the shRNAcontrol for the duration of the experiment (89% and 46.7% reduction at day 2 and 4, respectively). The phosphorylation of cAMP-responsive element-binding protein (CREB) was also examined. CREB is mainly phosphorylated (and consequently activated) by the cAMP pathway (Montminy and Bilezikjian 1987). However, in differentiating neurons, CREB is also directly phosphorylated by pLIMK1 to direct transcription of genes involved in neuronal outgrowth (Yang *et al.* 1998). A basal level of phosphorylated CREB (pCREB; Ser133) was detectable and found to be similar in the shRNAPLCη2-1 and shRNAcontrol cells. After 4 h, CREB phosphorylation in PLCη2 knock-down cells was reduced by 30% relative to the control cells, although this was not deemed a significant effect. However, at day 2 and day 4, the pCREB levels were significantly lower than the shRNAcontrol cells (reduced 69.4% and 41.7%, respectively). These results indicate that PLCη2 is involved in LIMK1 activation and the regulation of CREB-mediated gene transcription during Neuro2A cell differentiation. LIMK1 is implicated in the regulation of actin dynamics during neurite growth (Yang *et al.* 1998). The distribution of F-actin was therefore examined in RA-treated control and PLCη2 knockdown Neuro2A cells by phalloidin-tetramethylrhodamine B isothiocyanate staining (Fig. 5c). The shRNA control cells contained elongated actin filaments along the neurites. The shRNAPLCη2-1 and shRNAPLCη2-2 cells exhibit a punctate distribution of F-actin and possess multiple projections forming short neurites.

PLCη2 PH domain binds preferentially to PtdIns(3,4,5)P_3

The PH domain of PLCη2 is responsible for membrane association and is essential for activity (Nakahara *et al.* 2005; Popovics *et al.* 2011). The lipid-binding specificity of

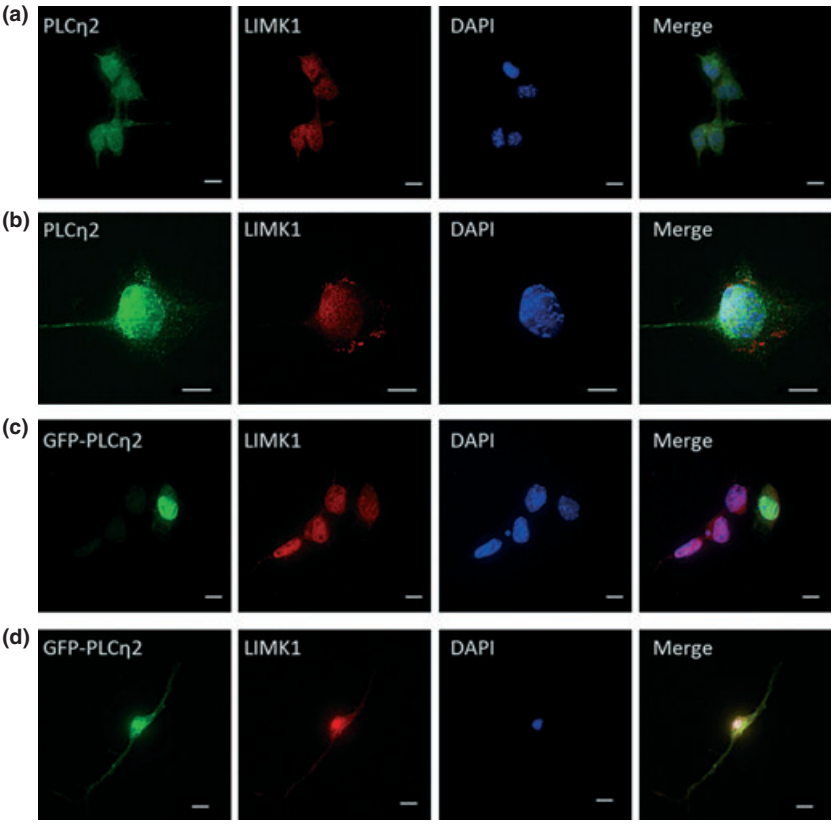

Fig. 4 Endogenous Phospholipase C (PLC)-η2 and LIM domain kinase 1 (LIMK1) co-localize in the nucleus (as visualized by 4′, 6-diamidino-2-phenylindole (DAPI) staining) of undifferentiated (a) and differentiated (b) Neuro2A cells. Fixed cells were immunostained with PLCη2 antibody (green) and LIMK1 antibody (red). Similarly, transfected GFP-PLCη2 and endogenous LIMK1 co-localize in the nucleus of undifferentiated (c) and differentiated (d) Neuro2A cells. Images were taken by a DeltaVision deconvolution microscope. Bars correspond to 10 μm.

the PH domain is highly likely to dictate the localization of the enzyme within the cell. To determine the lipid-binding properties of the PH domain, we employed a FRET-based assay which utilized a sensor complex, composed of recombinant GST-linked PLCη2 PH domain protein (GST-PLCη2PH), an Eu-labeled anti-GST antibody, streptavidin-coupled allophycocyanin (APC), and biotinylated lipid. Using this approach, biotinylated-PtdIns(3,4,5)P_3 and biotinylated-PtdIns(4,5)P_2 were able to form sensor complexes in the presence of GST-PLCη2PH, each yielding a strong concentration-dependent FRET signal (Fig. 6a). Biotinylated forms of the lipids, PtdIns(3,4)P_2, PtdIns(3)P, and PtdIns(4)P were unable to form FRET-active complexes. The binding characteristics of a range of non-biotinylated-phosphoinositides to GST-PLCη2PH were assessed via their ability to dissociate the biotinylated-PtdIns(4,5)P_2-containing sensor complex at varying concentrations. The majority of phosphoinositides examined were able to effectively and dose-dependently compete with biotinylated-PtdIns(4,5)P_2 for binding to GST–PLCη2PH (Fig. 6b). The relative IC_{50} value of each phosphoinositide is shown in Table 2. PtdIns(3,4,5)P_3 was found to be the most effective competitor (IC_{50}=0.83). The phosphoinositides in order of decreasing affinity are PtdIns(3,4,5)P_3 > PtdIns(4,5)P_2 > Ins(1,3,4,5)P_4 > Ins(1,4,5)P_3 > PtdIns(3,4)P_3 > PtdIns(3)P. PtdIns(1,3,4)P_3 was unable to compete effectively at the concentrations examined.

PLCη2 co-localizes with PtdIns(3,4,5)P_3 in Neuro2A cells

The phosphoinositide specificity of the PLCη2 PH domain suggests that PtdIns(3,4,5)P_3 may be a critical factor in defining the cellular distribution of PLCη2. With this in mind, we examined the localization of PLCη2 and PtdIns(3,4,5)P_3 in differentiated Neuro2A cells by immunostaining (Fig. 6c). Wortmannin treatment dramatically reduced PtdIns(3,4,5)P_3 immunostaining in Neuro2A cells providing evidence that the anti-PtdIns(3,4,5)P_3 antibody used acts specifically under the conditions employed (Figure S3). Interestingly, the highest level of PtdIns(3,4,5)P_3 staining was found in the nucleus where it exhibited a high degree of co-localization with endogenous PLCη2 (and with GFP-PLCη2 in transfected cells, as shown in Figure S4). PtdIns(3,4,5)P_3 was also present on the cell membrane and local elevations of both PtdIns(3,4,5)P_3 and PLCη2 were detected in growing neurites. In addition, the localization of an N-terminally GFP-tagged PH domain of PLCη2 was also assessed in undifferentiated Neuro2A cells (Figure S5). PI(4,5)P_2 content was also examined by the co-transfection of mCherry-tagged PLCδ1-PH domain. As expected, the GFP-PLCη2-PH exhibited a high co-localization rate with PI(3,4,5)P_3 in the nucleus. In contrast, the mCherry-tagged PLCδ1-PH domain (indicative of PI(4,5)P_2) mainly appeared on the plasma membrane and had a very limited co-appearance with the PH domain of PLCη2.

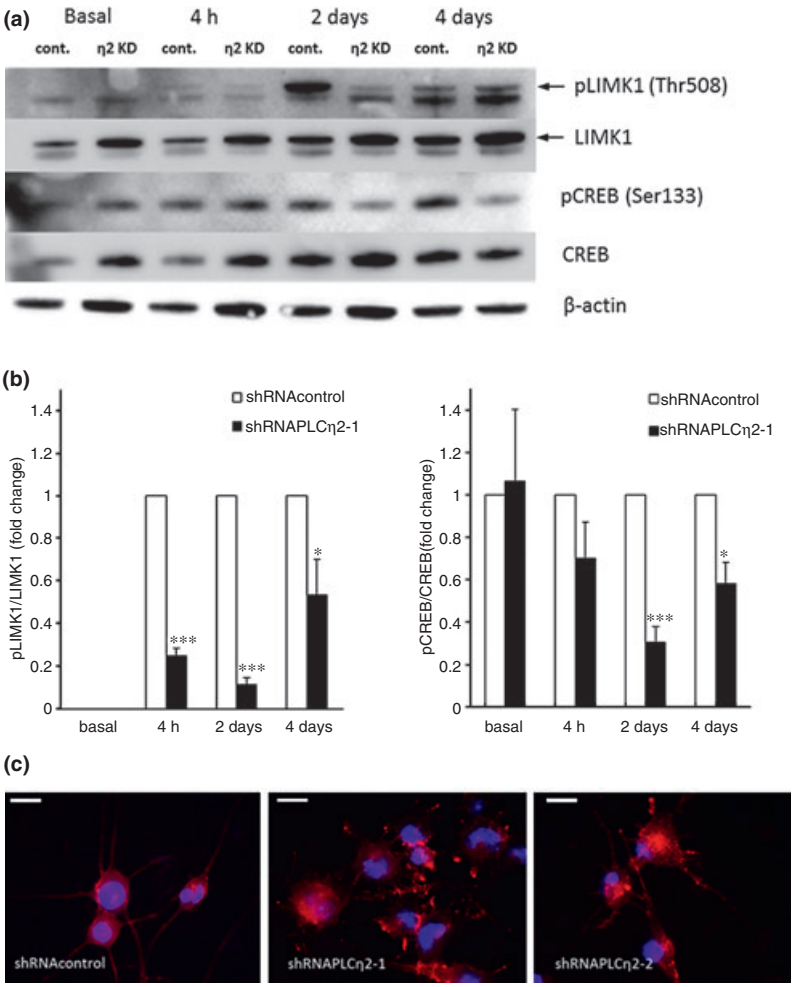

Fig. 5 Phosphorylation of LIM kinase-1 (LIMK1) and cAMP-responsive element-binding protein (CREB) following retinoic acid-treatment is altered in Phospholipase C (PLC)-η2 knock-down cells. (a) Immunoblot of total and phosphorylated LIMK1 and CREB (pLIMK1 and pCREB) at various times after addition of retinoic acid in shRNAcontrol (Cont.) and shRNAPLCη2-1 (η2 KD) cells. The levels of total LIMK1 and CREB as well as β-actin loading control were also assessed. The blot shown is representative of three independent experiments. (b) Quantification of LIMK1 and CREB phosphorylation compared with total LIMK1 and CREB levels. The pLIMK1/LIMK1 and pCREB/CREB levels were calculated relative to the shRNAcontrol level in each treatment group. The dashed lines represent the control level. Error bars represent ± SEM. Statistical significance was assessed by *t*-test (*$p <$ 0.05, ***$p < 0.001$; $n = 3$). (c) Actin filaments are distorted in PLCη2 knock-down cells. Actin was visualized by tetramethyl-rhodamine B isothiocyanate-conjugated phalloidin and nuclei were stained by DAPI. Slides were examined on a Zeiss Axioplan fluorescent microscope system. Bars correspond to 10 μm.

Discussion

Neuro2A cells represent an excellent model for the study of neuronal differentiation and were used to assess the role of PLCη2 in this process. PLCη2 protein expression was found to increase in Neuro2A cells during retinoic acid induced differentiation. The involvement of PLCη2 in this process was further indicated by an observed reduction in neurite outgrowth in shRNA-mediated PLCη2 knock-down cells (shRNAPLCη2-1 and shRNAPLCη2-2 lines). Both the percentage of differentiated cells and the total neurite growth were found to be reduced. The extent of this phenotypic effect largely mirrored the degree by which PLCη2 expression was decreased in the PLCη2 knock-down cells, highly indicative of a specific role for PLCη2 in this process. Differentiating neurons are known to exhibit spontaneous Ca^{2+} spikes and waves (Gu and Spitzer 1995) and, because of the high Ca^{2+} sensitivity of PLCη2, it is possible that the enzyme plays an important role in the generation of these signals and/or their translation into downstream effects. This is supported by the observation that inositol phosphate release is reduced in PLCη2 knock-down cells, relative to control cells, following treatment with the Ca^{2+} ionophore, A23187. It should be acknowledged that most of the inositol phosphate release triggered by this agent seems to be directed by PLCη2 with other PLCs having little residual effect. This is likely down to that fact that PLCη enzymes are more sensitive to Ca^{2+} in comparison to other isotypes likely to be present (such as PLCδ enzymes). PLCη1 has been shown to amplify PLCβ signals in Neuro2A cells following Ca^{2+} release (Kim *et al.* 2011). Whether PLCη1 and PLCη2 signals are interdependent or not is still to be established but it is possible that lowering PLCη2 protein level would greatly impact upon PLCη signaling as a whole.

To determine whether PLCη2 regulates transcriptional activity we examined its influence in the control of RAR-directed gene expression. Of the three known RAR isoforms, only RARα was found to be present in Neuro2A cells. The mRNA level corresponding to expression of this isoform was found to be similar in control and PLCη2 knock-down cells. However, PLCη2 knock-down had a substantial effect on basal and RA-stimulated retinoid

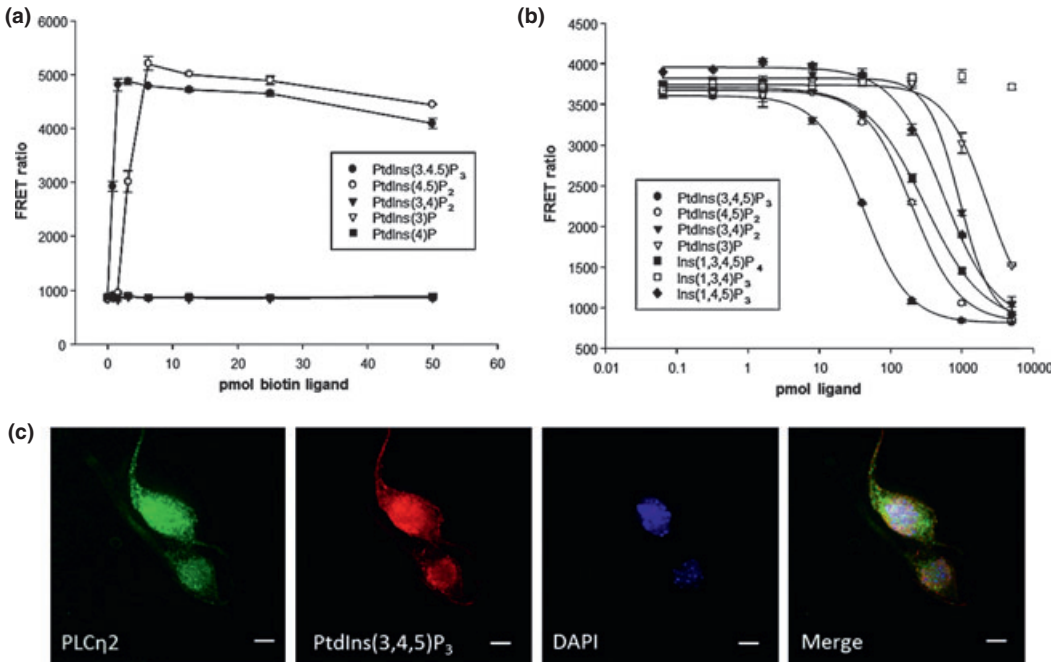

Fig. 6 (a) Generation and specificity of FRET sensor complexes. Streptavidin-tagged allophycocyanin was incubated with GST-Phospholipase C (PLC)η2PH, Eu-labeled anti-GST antibody and the indicated concentrations of biotinylated-phosphoinositides. (b) Dissociation of biotinylated-PtdIns(3,4,5)P_3-containing sensor complexes with different concentrations of non-biotinylated-phosphoinositides. (c) PtdIns(3,4,5)P_3 co-localizes with endogenous PLCη2 in differentiated Neuro2A cells. Cells were seeded onto coverslips and were differentiated for 4 days with 20 μM retinoic acid. Fixed cells were immunostained with PLCη2 antibody (green) and anti-PtdIns(3,4,5)P_3 antibody (red). 4′,6-diamidino-2-phenylindole (DAPI) was used as a marker for the nucleus. Images are representative and were taken by a DeltaVision deconvolution microscope. Bars correspond to 10 μm.

Table 2 Phosphoinositide binding of GST-PLCη2PH. IC_{50} values for various non-biotinylated-phosphoinositides based on their abilities to dissociate the biotinylated-PtdIns(4,5)P_2-containing FRET sensor complex

Ligand	IC_{50} (μM)
PtdIns(3,4,5)P_3	0.83
PtdIns(4,5)P_2	3.97
PtdIns(3,4)P_2	18.40
PtdIns(3)P	45.13
Ins(1,3,4,5)P_4	6.02
Ins(1,3,4)P_3	< 200
Ins(1,4,5)P_3	10.86

signaling. This likely contributes to the phenotype associated with the PLCη2 knock-down cells as neuronal differentiation is, as one would expect, associated with a substantial change in gene expression (Gurok *et al.* 2004). The precise mechanism(s) by which PLCη2 exerts this effect is not clear. Promoters containing RAREs have been shown to be activated by downstream regulatory element antagonist modulator, a Ca^{2+}-effector protein (Scsucova *et al.* 2005). It is possible that the absence of sufficient levels of PLCη2 in the knock-down cells negatively influences cytosolic Ca^{2+}-dynamics such that activation of downstream regulatory element antagonist modulator is compromised. PLCη2 was found to be present in the nuclei of both undifferentiated and differentiated Neuro2A cells. Other nuclear PLC enzymes are known to influence gene expression. A prime example is PLCβ1, which is present in nuclear speckles; the location of several transcription-regulating molecules (Martelli *et al.* 1992). PLCβ1 is involved in the regulation of c-Jun and AP1 promoter-binding in differentiating myogenic cells (Ramazzotti *et al.* 2008). As with cytosolic PLC enzymes, the nuclear enzymes can activate protein kinase C (PKC) (α-isoform) via the production of DAG. PKCα has been shown to phosphorylate lamin B1 to trigger the breakdown of the nuclear lamina for mitotic division in murine erythroleukemia cells (Fiume *et al.* 2009). The consequent action of PLC enzymes in the nucleus decrease PtdIns(4,5)P_2 levels, which are important for chromatin remodeling (Zhao *et al.* 1998). It has also been proposed that cells may possess Ins(1,4,5)P_3 receptors on the inner nuclear membrane that allow movement of Ca^{2+} to the nucleoplasm (Klein and Malviya 2008). Despite this, the precise roles PLC enzymes play in regulating gene expression and nuclear Ca^{2+} dynamics are still far from understood.

A putative interaction between PLCη2 and LIMK1 was identified using a bacterial two-hybrid screen. We attempted to confirm this interaction in Neuro2A cells using a co-immunoprecipitation approach but were unsuccessful (data not shown). Nevertheless, LIMK1 and PLCη2 do co-localize in both undifferentiated and differentiated Neuro2A cells. This implies that their distribution allows the interaction of these proteins. LIMK1 and CREB phosphorylation was significantly reduced in the PLCη2 knock-down cells, suggesting that PLCη2 regulates their activity. PLCη2 may potentially influence LIMK1 (and CREB) phosphorylation in two ways. First, it remains known that the phosphorylation of LIMK1 and CREB is regulated by Ca^{2+} via the Ca^{2+}/calmodulin kinase IV pathway (Matthews *et al.* 1994; Takemura *et al.* 2009), thus phosphorylation of both proteins may be altered because of aberrations in Ca^{2+}-signaling in the PLCη2 knock-down cells. Second, it is also possible that PLCη2 and LIMK1 interact directly in such a manner as to regulate activation of LIMK1. It is also possible that a PLCη2-LIMK1 interaction could simply serve such that PLCη2 is "on hand" to modulate LIMK1 activation by Ca^{2+}/calmodulin kinase IV. By whichever mechanism, both PLCη2 and LIMK1 are present in growing neurites. Reduced phosphorylation of LIMK1 (as observed in the PLCη2 knock-down cells) is likely to influence phosphorylation of cofilin. Once phosphorylated, cofilin acts to alter the F-actin/G-actin ratio, a process which is important for neurite outgrowth (Yang *et al.* 1998, 2004). Aberrations in actin dynamics were observed by phalloidin-tetramethylrhodamine B isothiocyanate staining of shRNAPLCη2-1 and shRNAPLCη2-2 cells. In these cells, a punctate distribution of F-actin was observed with multiple projections and reduced outgrowth compared to control cells. Interestingly, Endo *et al.* (2007) previously found that down-regulation of LIM kinase activity in PC12 cells significantly reduces neuronal outgrowth. Although the authors did not mention it, the number of projections also appeared to be increased in these cells. Potentially, the observed phenotype of PLCη2 knock-down cells could be caused, at least in part, by an increase in cofilin activity and a consequent reduction in the polymerization rate of actin. Such effects are likely to be further compounded in PLCη2 knock-down cells by reduced expression of RARα-regulated genes involved in the differentiation process (as summarized in Fig. 7). In addition, significant staining of LIMK1 was found in the nucleus of the Neuro2A cells. Nuclear translocation LIMK1 has previously been suggested to be a process important for the control of actin dynamics (Yokoo *et al.* 2003). It is also possible that nuclear LIMK1 activity contributes to the regulation of genes involved in neuritogenesis.

The PH domain of PLCη2 has previously been shown to be responsible for association of the enzyme to intracellular membranes (Nakahara *et al.* 2005; Popovics *et al.* 2011). A GST-tagged PLCη2 PH domain was synthesized and its ability to bind a range of lipids and phosphoinositides was examined. The PLCη2 PH domain bound preferentially to PtdIns(3,4,5)P_3. Furthermore, PLCη2 was found to co-localize with PtdIns(3,4,5)P_3 in the nucleus and to some extent at the cell membrane in Neuro2A cells, suggesting that it predominantly interacts with this lipid *in vivo*. Neuronal cells have previously been reported to possess high levels of PtdIns(3,4,5)P_3 levels in the nucleus (Neri *et al.* 1999; Kwon *et al.* 2010). This likely explains why PLCη2 is present in the nucleus of Neuro2A cells and why its cellular distribution differs in other non-neuronal cell types (Popovics *et al.* 2011). It is important to point out that the PLCη2 PH domain was also able to bind PtdIns(4,5)P_2, although with a somewhat lower

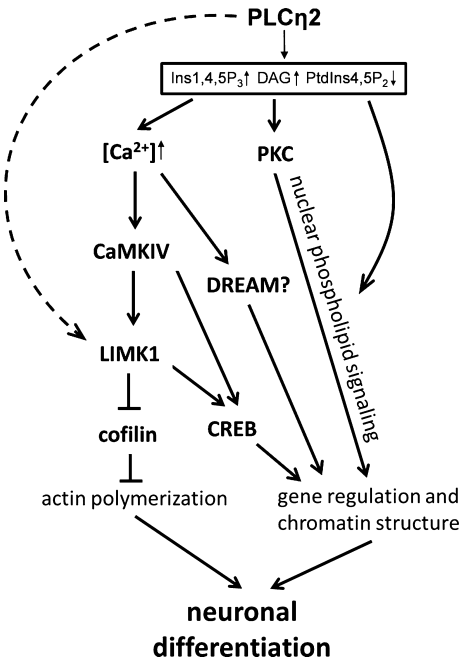

Fig. 7 Summary of pathways by which Phospholipase C (PLC)-η2 may regulate neuronal differentiation. Upon PLCη2 activation, the level of the substrate PtdIns(4,5)P_2 will decrease with subsequent elevations in Ins(1,4,5)P_3 and 1,2-diacylyglycerol (DAG). Ins(1,4,5)P_3 triggers Ca^{2+}-release from the endoplasmic reticulum to activate LIM kinase-1 (LIMK1) and subsequently cAMP-responsive element-binding protein (CREB) through stimulation of CaMKIV activity. PLCη2 could also potentially activate LIMK1 by direct association. Activated CREB initiates gene transcription. Activated LIMK1 also inhibits actin depolymerization leading to the assembly of actin filaments necessary for neuronal differentiation. Changes in the nuclear DAG and PtdIns(4,5)P_2 levels may also affect the transcriptional activity through DAG-PKC or PtdIns(4,5)P_2-chromatin interactions. Abbreviations: PLCη2: Phospholipase C-η2, InsP_3: Inositol 1,4,5-trisphosphate, PtdIns(4,5)P_2: Phosphatidylinositol 4,5-bisphosphate, DAG: diacylglycerol, CaMKIV: Ca^{2+}/Calmodulin-dependent protein kinase IV, LIMK1: LIM domain kinase 1, cAMP response element-binding protein, PKC: Protein kinase C.

affinity. However, co-expression of GFP-PLCη2-PH with mCherry-tagged PLCδ1-PH domain in Neuro2A cells revealed the cellular locations of these proteins to be distinct. The PH domain of PLCδ1 is known to associate with cellular PtdIns(4,5)P_2 very specifically (Watt *et al.* 2002), it is therefore unlikely that PLCη2 interacts to any great extent with this phospholipid in these cells. An interesting feature of the PtdIns(3,4,5)P_3 headgroup resides in its larger size and additional negative charge compared with other phosphoinositide headgroups. This triggers its projection from the lipid bilayer which might facilitate the interaction between PtdIns (3,4,5)P_3 and PH domains though little penetration of the lipid bilayer is required for docking (Chen *et al.* 2012). Consequently, PtdIns(3,4,5)P_3-binding PLCs such as PLCη2 might represent a subgroup, which respond quicker to extracellular stimuli. Interestingly, the PLCη2 PH domain exhibited a relatively low affinity toward Ins(1,4,5)P_3 as demonstrated by the high IC_{50} value (10.86 μM). Ins(1,4,5)P_3-binding is known to regulate PLCδ1 activity, such that it competes with PtdIns(4,5)P_2 to displace the PH domain (and thus the enzyme) from the plasma membrane upon its production (Hirose *et al.* 1999). Given the low affinity of the PLCη2 PH domain toward Ins(1,4,5)P_3, it is unlikely that the hydrolyzed headgroup will be able to effectively compete with PtdIns (3,4,5)P_3. Consequently, the phospholipid/phosphoinositide-binding specificity of PLCη2 likely make this enzyme particularly well-suited for the modulation of transient Ca^{2+}-signals through sustained generation of Ins(1,4,5)P_3 (and DAG) in the nucleus and in growing neurites during the differentiation process.

Acknowledgements

We gratefully acknowledge the University of St Andrews in providing a PhD studentship for Petra Popovics. We thank Dr Kevin Morgan (MRC Human Reproductive Sciences Unit, Edinburgh, UK) for cloning the pancreas cDNA library. The authors declare no conflicts of interest.

Supporting information

Additional supporting information may be found in the online version of this article at the publisher's web-site.

Figure S1. Total neurite outgrowth is markedly reduced in Neuro2A cells with reduced PLCη2 expression.

Figure S2. Summary of pTRG inserts from 18 positive colonies isolated following the bacterial two-hybrid screen.

Figure S3. Anti-PtdIns(3,4,5)P_3 antibody staining in retinoic acid- and wortmannin-treated Neuro2A cells.

Figure S4. GFP-PLCη2 co-localizes with PtdIns(3,4,5)P_3 in differentiated Neuro2A cells.

Figure S5. GFP-PLCη2 PH co-localizes with PtdIns(3,4,5)P_3 but not with PtdIns(4,5)P_2 in Neuro2A cells.

References

Altschul S. F., Madden T. L., Schaffer A. A., Zhang J., Zhang Z., Miller W. and Lipman D. J. (1997) Gapped BLAST and PSI-BLAST: a new generation of protein database search programs. *Nucleic Acids Res.* **25**, 3389–3402.

Bernard O., Ganiatsas S., Kannourakis G. and Dringen R. (1994) Kiz-1, a protein with LIM zinc finger and kinase domains, is expressed mainly in neurons. *Cell Growth Differ.* **5**, 1159–1171.

Bryan B. A., Cai Y. and Liu M. (2006) The Rho-family guanine nucleotide exchange factor GEFT enhances retinoic acid- and cAMP-induced neurite outgrowth. *J. Neurosci. Res.* **83**, 1151–1159.

Carter J. M., Waite K. A., Campenot R. B., Vance J. E. and Vance D. E. (2003) Enhanced expression and activation of CTP: phosphocholine cytidyltransferase β2 during neurite outgrowth. *J. Biol. Chem.* **278**, 44988–44994.

Chambon P. (1996) A decade of molecular biology of retinoic acid receptors. *FASEB J.* **10**, 940–954.

Chen H. C., Ziemba B. P., Landgraf K. E., Corbin J. A. and Falke J. J. (2012) Membrane docking geometry of GRP1 PH domain bound to a target lipid bilayer: an EPR site-directed spin-labeling and relaxation study. *PLoS ONE* **7**, e33640.

Endo M., Ohashi K. and Mizuno K. (2007) LIM kinase and slingshot are critical for neurite extension. *J. Biol. Chem.* **282**, 13692–13702.

Fiume R., Ramazzotti G., Teti G., Chiarini F., Faenza I., Mazzotti G., Billi A. M. and Cocco L. (2009) Involvement of nuclear PLCbeta1 in lamin B1 phosphorylation and G2/M cell cycle progression. *FASEB J.* **23**, 957–966.

Gray A., Olsson H., Batty I. H., Priganica L. and Downes C. P. (2003) Nonradioactive methods for the assay of phosphoinositide 3-kinases and phosphoinositide phosphatases and selective detection of signaling lipids in cell and tissue extracts. *Anal. Biochem.* **313**, 234–245.

Gu X. and Spitzer N. C. (1995) Distinct aspects of neuronal differentiation encoded by frequency of spontaneous Ca^{2+} transients. *Nature* **375**, 784–787.

Gurok U., Steinhoff C., Lipkowitz B., Ropers H. H., Scharff C. and Nuber U. A. (2004) Gene expression changes in the course of neural progenitor cell differentiation. *J. Neurosci.* **24**, 5982–6002.

Hirose K., Kadowacki S., Tanabe M., Takeshima H. and Iino M. (1999) Spatiotemporal dynamics of inositol 1,4,5-triphosphate that underlies complex Ca^{2+} mobilization patterns. *Science* **284**, 1527–1530.

Hwang J. I., Oh Y. S., Shin K. J., Kim H., Ryu S. H. and Suh P. G. (2005) Molecular cloning and characterization of a novel phospholipase C, PLC-η. *Biochem. J.* **389**, 181–186.

Kanemaru K., Nakahara M., Nakamura Y., Hashiguchi Y., Kouchi Z., Yamaguchi H., Oshima N., Kiyonari H. and Fukami K. (2010) Phospholipase C-η2 is highly expressed in the habenula and retina. *Gene Expr. Patterns* **10**, 119–126.

Kim J. K., Choi J. W., Lim S., Kwon O., Seo J. K., Ryu S. H. and Suh P. G. (2011) Phospholipase C-η1 is activated by intracellular Ca^{2+} mobilization and enhances GPCRs/PLC/Ca^{2+} signaling. *Cell. Signal.* **23**, 1022–1029.

Klein C. and Malviya A. N. (2008) Mechanism of nuclear calcium signaling by inositol 1,4,5-trisphosphate produces in the nucleus, nuclear located protein kinase C and cAMP-dependent protein kinase. *Front. Biosci.* **13**, 1206–1226.

Kouchi Z., Igarshi T., Shibayama N., Inanobe S., Sakurai K., Yamaguchi H., Fukada T., Yanagi S., Nakamura Y. and Fukami K. (2011)

Phospholipase Cδ3 regulates RhoA/Rho kinase signaling and neurite outgrowth. *J. Biol. Chem.* **286**, 8459–8471.

Kwon I. S., Lee K. H., Choi J. W. and Ahn J. Y. (2010) PI(3,4,5)P3 regulates the interaction between Akt and B23 in the nucleus. *BMB Rep.* **43**, 127–132.

Lane M. A. and Bailey S. J. (2005) Role of retinoid signalling in the adult brain. *Prog. Neurobiol.* **75**, 275–293.

Lucocq J. (2008) Quantification of Structures and Gold Labeling in Transmission Electron Microscopy. *Methods Cell Biol.* **88**, 59–82.

Manetti F. (2012) LIM kinases are attractive targets with many macromolecular partners and only a few small molecule regulators. *Med. Res. Rev.* **32**, 968–998.

Martelli A. M., Gilmour R. S., Bertagnolo V., Neri L. M., Manzoli L. and Cocco L. (1992) Nuclear localization and signalling activity of phosphoinositidase C-beta in Swiss 3T3 cells. *Nature* **358**, 242–245.

Matthews R. P., Guthrie C. R., Wailes L. M., Zhao X., Means A. R. and McKnight G. S. (1994) Calcium/calmodulin-dependent protein kinase types II and IV differentially regulate CREB-dependent gene expression. *Mol. Cell. Biol.* **14**, 6107–6116.

Montminy M. R. and Bilezikjian L. M. (1987) Binding of a nuclear protein to the cyclic-AMP response element of the somatostatin gene. *Nature* **328**, 175–178.

Nakahara M., Shimozawa M., Nakamura Y., Irino Y., Morita M., Kudo Y. and Fukami K. (2005) A novel phospholipase C, PLCη2, is a neuron-specific isozyme. *J. Biol. Chem.* **280**, 29128–29134.

Neri L. M., Martelli A. M., Borgatti P., Colamussi M. L., Marchisio M. and Capitani S. (1999) Increase in nuclear phosphatidylinositol 3-kinase activity and phosphatidylinositol 3,4,5-trisphosphate synthesis precede PCK-zeta translocation to the nucleus of NGF-treated PC12 cells. *FASEB J.* **13**, 2299–2310.

Pignatelli M., Cortes-Canteli M., Santos A. and Perez-Castillo A. (1999) Involvement of the NGFI-A gene in the differentiation of neuroblastoma cells. *FEBS Lett.* **461**, 37–42.

Popovics P. and Stewart A. J. (2012) Putative roles for phospholipase C-η enzymes in neuronal Ca^{2+} signal modulation. *Biochem. Soc. Trans.* **40**, 282–286.

Popovics P., Beswick W., Guild S. B., Cramb G., Morgan K., Millar R. P. and Stewart A. J. (2011) Phospholipase C-η2 is activated by elevated intracellular Ca^{2+} levels. *Cell. Signal.* **23**, 1777–1784.

Ramazzotti G., Faenza I., Gaboardi G. C., Piazzi M., Bavelloni A., Fiume R., Manzoli L., Martelli A. M. and Cocco L. (2008) Catalytic activity of nuclear PLC-β1 is required for its signalling function during C2C12 differentiation. *Cell. Signal.* **20**, 2013–2021.

Ronn L. C., Ralets I., Hartz B. P., Bech M., Berezin A., Berezin V., Moller A. and Bock E. (2000) A simple procedure for quantification of neurite outgrowth based on stereological principles. *J. Neurosci. Methods* **100**, 25–32.

Scsucova S., Palacios D., Savignac M., Mellström B., Naranjo J. R. and Aranda A. (2005) The repressor DREAM acts as a transcriptinal activator on vitamin D and retinoic acid response elements. *Nucleic Acids Res.* **33**, 2269–2279.

Stewart A. J., Mukherjee J., Roberts S. J., Lester D. and Farquharson C. (2005) Identification of a novel class of mammalian phosphoinositol-specific phospholipase C enzymes. *Int. J. Mol. Med.* **15**, 117–121.

Takemura M., Mishima T., Wang Y., Kasahara J., Fukunaga K., Ohashi K. and Mizuno K. (2009) Ca^{2+}/calmodulin-dependent protein kinase IV-mediated LIM kinase activation is critical for calcium signal-induced neurite outgrowth. *J. Biol. Chem.* **284**, 28554–28562.

Watt S. A., Kular G., Fleming I. N., Downes C. P. and Lucocq J. M. (2002) Subcellular localization of phosphatidyl 4,5-bisphosphate using the pleckstrin homology domain of phospholipase C delta1. *Biochem. J.* **363**, 657–666.

Yang N., Higuchi O., Ohashi K., Nagata K., Wada A., Kangawa K., Nishida E. and Mizuno K. (1998) Cofilin phosphorylation by LIM-kinase 1 and its role in Rac-mediated actin reorganization. *Nature* **393**, 809–812.

Yang E. J., Yoon J. H., Min D. S. and Chung K. C. (2004) LIM kinase 1 activates cAMP-responsive element-binding protein during the neuronal differentiation of immortalized hippocampal progenitor cells. *J. Biol. Chem.* **279**, 8903–8910.

Yokoo T., Toyoshima H., Miura M. *et al.* (2003) p57Kip2 regulates actin dynamics by binding and translocating LIM-kinase 1 to the nucleus. *J. Biol. Chem.* **278**, 52919–52923.

Zeng M. and Zhou J. N. (2008) Roles of autophagy and mTOR signaling in neuronal differentiation of mouse neuroblastoma cells. *Cell. Signal.* **20**, 659–665.

Zhao K., Wang W., Rando O. J., Xue Y., Swiderek K., Kuo A. and Crabtree G. R. (1998) Rapid and phosphoinositol-dependent binding of the SWI/SNF-like BAF complex to chromatin after T lymphocyte receptor signaling. *Cell* **95**, 625–636.

Zhou Y., Wing M. R., Sondek J. and Harden T. K. (2005) Molecular cloning and characterization of PLC-η2. *Biochem. J.* **391**, 667–676.

Zhou Y., Sondek J. and Harden T. K. (2008) Activation of human phospholipase C-η2 by Gβγ. *Biochemistry* **47**, 4410–4417.

Histochem Cell Biol (2016) 145:163–173
DOI 10.1007/s00418-015-1390-7

ORIGINAL PAPER

Phospholipase C-η2 interacts with nuclear and cytoplasmic LIMK-1 during retinoic acid-stimulated neurite growth

Mohammed Arastoo[1] · Christian Hacker[1,2] · Petra Popovics[1,3] · John M. Lucocq[1] · Alan J. Stewart[1]

Accepted: 24 November 2015 / Published online: 15 December 2015

Abstract Neurite growth is central to the formation and differentiation of functional neurons, and recently, an essential role for phospholipase C-η2 (PLCη2) in neuritogenesis was revealed. Here we investigate the function of PLCη2 in neuritogenesis using Neuro2A cells, which upon stimulation with retinoic acid differentiate and form neurites. We first investigated the role of the PLCη2 calcium-binding EF-hand domain, a domain that is known to be required for PLCη2 activation. To do this, we quantified neurite outgrowth in Neuro2A cells, stably overexpressing wild-type PLCη2 and D256A (EF-hand) and H460Q (active site) PLCη2 mutants. Retinoic acid-induced neuritogenesis was highly dependent on PLCη2 activity, with the H460Q mutant exhibiting a strong dominant-negative effect. Expression of the D256A mutant had little effect on neurite growth relative to the control, suggesting that calcium-directed activation of PLCη2 is not essential to this process. We next investigated which cellular compartments contain endogenous PLCη2 by comparing immunoelectron microscopy signals over control and knockdown cell lines. When signals were analyzed to reveal specific labeling for PLCη2, it was found to be localized predominantly over the nucleus and cytosol. Furthermore in these compartments (and also in growing neurites), a proximity ligand assay revealed that PLCη2 specifically interacts with LIMK-1 in Neuro2A cells. Taken together, these data emphasize the importance of the PLCη2 EF-hand domain and articulation of PLCη2 with LIMK-1 in regulating neuritogenesis.

Keywords Calcium signaling · Cell differentiation · Electron microscopy · Neuritogenesis · Protein–protein interaction

Introduction

Phospholipase C (PLC) enzymes are a well-characterized family of hydrolytic enzymes (E.C. 3.1.4.11). In mammals, PLC enzymes are responsible for cleaving the membrane phospholipid phosphatidylinositol 4,5-bisphosphate (PtdIns(4,5)P_2), thereby generating the two essential second messengers inositol 1,4,5-trisphosphate (Ins(1,4,5)P_3) and 1,2-diacylglycerol (DAG) following receptor activation. Consequently, Ins(1,4,5)P_3 triggers calcium discharge from the endoplasmic reticulum and DAG together with calcium activates effector proteins, most notably protein kinase C (PKC; Berridge et al. 1983; Hokin and Hokin 1953; Streb et al. 1983). Six classes of PLCs have been identified based on their amino acid sequence, domain structure, and mechanism of activation. These include the β, γ, δ, ε, ζ and η classes (Suh et al. 2008). The most recently identified is the η class of which there are two isoforms, PLCη1 and PLCη2 (Hwang et al. 2005; Nakahara et al. 2005; Stewart et al. 2005; Zhou et al. 2005), encoded by the *PLCH1* and *PLCH2* genes, respectively. A number of spliceforms of both PLCη1 and PLCη2 exist, which vary in length at the C-terminal end (Hwang et al. 2005; Zhou et al. 2005). This region is rich in serine and proline residues, and it is thought that this part of the protein may

✉ Alan J. Stewart
ajs21@st-andrews.ac.uk

[1] School of Medicine, Medical and Biological Sciences Building, North Haugh, University of St Andrews, St Andrews, Fife KY16 9TF, UK

[2] Bioimaging Centre, Geoffrey Pope Building, College of Life and Environmental Sciences, University of Exeter, Exeter EX4 4QD, UK

[3] Veterans Affairs Medical Center, Miami, FL 33125, USA

facilitate protein–protein interactions (Suh et al. 2008). Both PLCη enzymes can be activated directly by mobilization of intracellular calcium (Kim et al. 2011; Popovics et al. 2011, 2014). We recently reported that mutation of a putative calcium-binding residue (D256A) within EF-loop 1 of the EF-hand domain of PLCη2 reduces the sensitivity to calcium by tenfold, indicating this domain to be responsible for calcium-induced activation (Popovics et al. 2014). In addition, it has also been shown that PLCη2, but not PLCη1, can be activated by Gβγ, which is released from trimeric G-protein complexes following G-protein-coupled receptor activation (Zhou et al. 2005, 2008).

The isozyme PLCη2 is expressed in neurons with highest expression in the olfactory bulb, cerebral cortex and pyramidal cells of the hippocampus (Nakahara et al. 2005). It is also expressed within the habenula, the retina (Kanemura et al. 2010), in the pituitary and neuroendocrine cells (Stewart et al. 2007) as well as in non-nervous tissue such as the intestine and pancreatic islets (Stewart et al. 2005). Its specific function(s) within neurons is still unclear, although considering its sensitivity toward calcium, it is thought that PLCη2 may act synergistically with other PLCs or calcium-activated processes (Popovics and Stewart 2012). PLCη2 is expressed in the brain of mice after birth and increases until 4 weeks of age. Cultured hippocampal pyramidal cells showed a high level of PLCη2, whereas astrocyte-enriched cultures did not show any expression (Nakahara et al. 2005), indicating a functional role in neuronal formation and physiology. In accordance, deletion of the chromosomal region 1p36.32 in which PLCη2 is located, leads to mental retardation (Fitzgibbon et al. 2008; Lo Vasco 2011). Previously, using a targeted knockdown approach, we found PLCη2 to be essential for retinoic acid-induced neurite growth in Neuro2A cells (Popovics et al. 2013). Despite this, the precise mechanism by which PLCη2 facilitates neurite growth in these cells is not known. In our previous study, through use of a bacterial two-hybrid assay we identified Lim-domain kinase-1 (LIMK-1) as a putative C-terminal interaction partner of PLCη2 (Popovics et al. 2013). LIMK-1 acts primarily downstream of Rho GTPases to phosphorylate and inactivate cofilin family proteins (cofilin1, cofilin2 and destrin), which promote actin depolymerization and the severing of actin filaments during neurite outgrowth (Arber et al. 1998; Yang et al. 1998; Endo et al. 2007). LIMK-1 has also been shown to be a substrate for calcium/calmodulin-dependent kinase-IV (CaMKIV) during neurite growth (Takemura et al. 2009). Although it was revealed that PLCη2 and LIMK-1 do indeed co-localize in Neuro2A cells (Popovics et al. 2013), it is not known whether these two proteins directly interact in the cell, or whether such interactions occur during neurite outgrowth.

To gain a better understanding of the role of PLCη2 in neuritogenesis, we examine the importance of PLCη2 activity and calcium-mediated activation of the enzyme for neurite outgrowth in Neuro2A cells stably overexpressing wild-type and mutant PLCη2 proteins. In addition, we examine the intracellular localization of PLCη2 in Neuro2A cells at the ultrastructural level and, through use of a proximity ligand assay, probe the interaction of PLCη2 and LIMK-1 in differentiating Neuro2A cells.

Materials and methods

Growth and retinoic acid-induced differentiation of Neuro2A cells

Neuro2A cells were obtained from the European Collection of Cell Cultures (Salisbury, UK). Eagle's minimal essential medium (EMEM) supplemented with 10 % fetal bovine serum (FBS), 2 mM L-glutamine and 50 units/ml of penicillin/streptomycin (complete EMEM) was used to maintain Neuro2A cells and stable transfected clones. Neuro2A cells were differentiated as previously described by Zeng and Zhou (2008). Briefly, cells were plated at a low density (100 cells/mm^2) in 6-well plates in complete EMEM which was changed to the differentiation medium the next day (EMEM with 2 % FBS, 2 mM L-glutamine and 20 μM retinoic acid). Medium was replaced every day for 4 days. Micrographs showing cells at 4-day differentiation were collected by a Zeiss Axiovert 40 CFL microscope with a 10× objective (Carl Zeiss Ltd., Cambridge, UK). Images were taken using an AxioCam ICc 1 digital camera (Carl Zeiss Ltd.). Neurite outgrowth was assessed by taking four micrographs by random selection from all experimental conditions (in each case, at least 220 cells were sampled per experiment), and experiments were repeated three times. All cells possessing at least one neurite with a length at least twice the cell body were considered differentiated. Results were expressed as a percentage of differentiated/total cell number.

Generation of stable Neuro2A cell lines overexpressing wild-type and mutant PLCη2

An expression construct encoding residues 75-1238 of mouse PLCη2 (isoform a; NP_780765) in pcDNA3.1 (as used in Nakahara et al. 2005) was a gift from Prof. Kiyoko Fukami (Tokyo University of Pharmacy and Life Science, Japan). The pcDNA3.1-PLCη2 expression construct was used to synthesize D256A and H460Q mutants using the Quikchange Site-Directed Mutagenesis Kit (Stratagene, Amsterdam, The Netherlands). Neuro2A cells were stably transfected with empty pcDNA3.1 vector (control) and wild-type and mutant PLCη2

expressing plasmids to produce cell lines overexpressing each protein. In each case, 20 μg of DNA was transfected by electroporation using a Bio-Rad Gene Pulser (Hertfordshire, UK) at 230 V, 950 μF. Stably transfected cells were selected after 48 h by adding 500 μg/ml G418 (InvivoGen, San Diego, CA, USA) and single cell-derived clones were picked and cultured for further experiments.

Measurement of PLCH2 mRNA levels in stable Neuro2A cell lines

The mRNA expression levels of *PLCH2* (OMIM *612836) forms in stable Neuro2A cell lines were measured using quantitative PCR. Briefly, mRNA was isolated using the Isolate RNA Mini Kit (Bioline, London, UK) according to the manufacturer's instructions. DNA contamination was removed by DNAse digestion (RQ1 RNase-Free DNase, Promega, Southampton, UK). This was followed by a two-step reverse transcription reaction using 0.5 μg of mRNA. The mRNA was incubated with 100 pmol oligod T_{18} and 0.5 mM dNTP in DEPC-treated water at 65 °C for 5 min. RevertAid Premium Reverse Transcriptase (200 units), RiboLock RNase Inhibitor (20 units; Thermo Fisher Scientific, Surrey, UK) and 1× RT-buffer (Fermentas, St. Leon-Rot, Germany) were added. Mixtures were incubated for 30 min at 50 °C followed by 10 min at 60 °C. Reactions were terminated at 85 °C for 5 min. *PLCH2* and *RPLP0* mRNA expression levels were detected by RT-PCR using primers obtained from Eurofins Scientific (Luxembourg). The sequences of corresponding primers used were: *PLCH2*, 5′-GGCTACACTCTGACCT CCAAGATCC-3′ (forward) and 5′-GGAAGCATGGT GGCATCTTCGCTGC-3′ (reverse); *RPLP0*, 5′-GAGTG ATGTGCAGCTGATAAAGACTGG-3′ (forward) and 5′-CTGCTCTGTGATGTCGAGCACTTCAG-3′ (reverse). The *RPLP0* primers were used previously as described (Popovics et al. 2013). The *PLCH2* primers were designed in house and checked for specificity using adequate positive and negative controls. PCR reactions contained 1× reaction buffer, 1.5 mM $MgCl_2$, 0.2 mM dNTPs, 250 nM of each primer and 1.25 units of GoTaq polymerase (Promega). Reactions were cycled at 95 °C for 15 s, 60 °C for 30 s and 72 °C for 1 min. The expression level of PLCη2 was measured by qPCR relative to the level of the large ribosomal protein P0 (RPLP0) mRNA. Expression was detected by Brilliant III Ultra-Fast SYBR Green mix (Agilent Technologies, Cheshire, UK) using a 7300 Real-Time PCR system (Applied Biosystems, Massachusetts, USA). Expression levels were calculated by the ΔC_t method. At least four colonies were chosen from each stably transfected cell group, and qPCR analysis was performed simultaneously on their cDNA to evaluate the expression of inserted gene. Based on the gene expression, colonies that possessed comparable levels of *PLCH2* in each transfection group were chosen for differentiation studies.

Immunogold labeling and electron microscopy (EM)

Samples were processed according to the Tokuyasu thawed frozen section method (Tokuyasu 1973). Briefly, Neuro2A cells stably expressing a PLCη2-targetted shRNA (PLCη2 KD) or non-target shRNA control (referred to as shRNAPLCη2-1 and shRNA control, respectively, in Popovics et al. 2014) were grown to full confluency in a T-75 flask before fixation with 4 % *p*-formaldehyde, 0.05 % glutaraldehyde, buffered with 0.2 M PIPES, pH 7.2, for 15 min at ambient temperature. Cells were then scraped, collected and centrifuged at 16,000×*g* for 15 min to form a pellet before cryoprotection in 2.3 M sucrose in PBS (overnight at 4 °C). Small blocks were prepared from the pellets and mounted onto specimen carriers before plunge-freezing in liquid N_2. Sections (80 nm thick) were cut at −100 °C (Leica EM FC7 ultracryomicrotome; Vienna, Austria) and retrieved using droplets of 2.1 M sucrose:2 % (w/v) methyl cellulose (mixed 1:1) and mounted in the same solution on pioloform-coated EM copper grids (Agar Scientific, Stanstead, UK) and stored at 4 °C. Prior to immunogold labeling, grids were washed three times in ice-cold distilled water (5 min each) and once in PBS (5 min) at ambient temperature. Sections were then incubated in 0.5 % fish skin gelatin (Sigma-Aldrich) in PBS and labeled using a custom polyclonal rabbit antibody raised commercially against a short peptide of PLCη2 (60 min; SKVEEDVEAGEDSGVSRQN; EZBiolab, Westfield, IN, USA), followed by three washes in PBS (15 min total) and 10 nm protein A-gold (20 min; BBI Solutions, Dundee, UK). After washing in PBS and distilled water, the sections were contrasted using 2 % (w/v) methylcellulose/3 % (w/v) uranyl acetate (mixed 9:1), and after air-drying the sections were visualized using a JEOL 1200 EX transmission electron microscope operated at 80 kV and images observed and recorded using an Orius 200 digital camera (Gatan, Abingdon, UK). Sections from shRNAPLCη2-1 and shRNA control samples were always run in parallel using the same solutions, dilutions and under environmental conditions.

Cell structures were identified according to the following criteria: The nuclear envelope was a double membrane that separated the nucleus from the cytosol. Mitochondria were elongated or circular profiles with double membranes and at least one double-membraned crista profile. ER was defined as a double-membraned cisterna decorated by ribosomes. The plasma membrane was a single membrane layer at the cell periphery. The Golgi apparatus cisternal stack was identified as at least two closely stacked cisternal membranes each with an axial ratio of at least 3:1 (groups of vesiculotubular structures were considered as belonging to Golgi

if they were closer than two vesicle widths from Golgi cisternal structures). MVBs were round structures containing at least one round structure within it. Isolated vesicles were small round structures (50–100 nm) within the cytosol.

To analyze specific labeling, the control and knockdown preparations were fixed, sectioned and labeled in parallel using identical solutions. For quantification, labeled sections were visualized at a nominal magnification of 5000× and analyzed in a series of scans placed systematic uniform random (SUR; Lucocq 2008, 2012), across the ribbon of sections. Gold particles were counted and assigned to different cellular compartments. To compare the intensity of labeling, membranes of the endoplasmic reticulum or nuclear envelope were used as a standard to which gold labeling of various organelles/compartments was related. These standard membranes were assessed during scanning by counting intersections of these membranes with the edge of a marker feature that was placed on the display screen. The density of gold particles was then expressed as a labeling index by dividing the number of gold particles by the membrane intersections. In the case of gold labeling situated over volume occupying compartments such as nucleoplasm and cytosol, the gold counts were related to the number of nuclear envelope and plasma membrane intersections, respectively.

Proximity ligand assay of PLCη2-LIMK-1 interactions

Ligand proximity assays as described by Söderberg et al. (2006) were performed using the Duolink proximity ligand assay system (Sigma-Aldrich). Two sets of experiments were performed; the first with Neuro2A cells stably expressing PLCη2-targeted shRNA and the corresponding non-target shRNA-expressing control cells and the second, with untransfected Neuro2A cells grown for 4 days in the presence and absence of 20 μM retinoic acid. In all cases, cells were seeded at a low density (100 cells/mm^2) and grown on coverslips overnight. The PLA assay was performed in accordance with the manufacturer's instructions. For specific visualization of the PLCη2-LIMK-1 interaction in cells, a custom rabbit anti-PLCη2 antibody (as described above; 1:100 dilution) and a mouse polyclonal anti-LIMK-1 antibody (Abcam, Cambridge, UK; 1:100 dilution) were used. Samples were analyzed using the Leica TCS SP8 confocal microscope with a 63× objective (Leica Microsystems, Heidelberg, Germany).

Results

PLCη2 activity is important for neurite growth

A characteristic property of PLCη enzymes is their ability to be directly activated by calcium released from intracellular stores (Kim et al. 2011; Popovics et al. 2011). To assess the importance of PLCη2 activity in neurite outgrowth and to determine whether calcium-induced activation of PLCη2 plays a role in this process, Neuro2A cells stably overexpressing wild-type PLCη2 and mutant forms of the enzyme (D256A and H460Q) were created and analyzed together. Neuro2A cells stably transfected with empty vector only (EV) were used as a control. The D256A mutation has been demonstrated previously to abolish the ability of calcium to activate PLCη2 through perturbation of calcium binding at EF-loop 1 of the EF-hand domain (Popovics et al. 2014). His460 corresponds to a key active site residue that is highly conserved within PLC isozymes (Heinz et al. 1998), and mutation of the corresponding His residue in PLCδ1 (His356) has been shown to abolish the activity of this enzyme (Stallings et al. 2005). Quantitative PCR analysis revealed PLCη2 mRNA levels to be increased 3–4-fold in all cell lines stably expressing PLCη2 forms relative to control cells (Fig. 1a). The cell lines were treated with retinoic acid for 4 days, and the proportion of cells showing signs of differentiation was assessed (Fig. 1b–f). Following retinoic acid treatment, there was a slight but significant increase in the average percentage of differentiated cells observed in the wild-type PLCη2 stably transfected cells (55.9 ± 0.9 %), relative to controls cells (49.0 ± 1.1 %), $p = 0.0285$, $n = 3$. Conversely, cells stably transfected with the H460Q mutant exhibited a dramatic reduction in the proportion of differentiated cells (2.4 ± 0.3 %) relative to control cells after stimulation with retinoic acid, $p = 0.0003$, $n = 3$. A comparable degree of differentiation was observed in the cells stably transfected with the D256A mutant (44.9 ± 0.9 %) relative to control after the treatment, $p = 0.9195$, $n = 3$. Note that errors quoted above represent S.E.M from three separate experiments. To reduce the possibility of type 1 errors, p values were corrected by applying Bonferroni's correction.

Immunogold localization of PLCη2 in Neuro2A cells

Because of the compartmentalized nature of cells, determining a protein's localization can provide a good indication of its functional role. Therefore, we examined the intracellular localization of endogenous PLCη2 in Neuro2A cells using quantitative immunoelectron microscopy (EM). We used two previously generated Neuro2A cell lines (Popovics et al. 2013): one stably expressing PLCη2-targeted shRNA plasmid (PLCη2 KD) and the other a non-target shRNA (control). As determined by Western blotting, the cell line expressing the PLCη2-targetted shRNA plasmid was shown to exhibit a 67 % reduction in PLCη2 expression at the protein level, and a ninefold reduction in retinoic acid-induced neuritogenesis after 4 days, relative to the control cells (Popovics et al. 2013). The

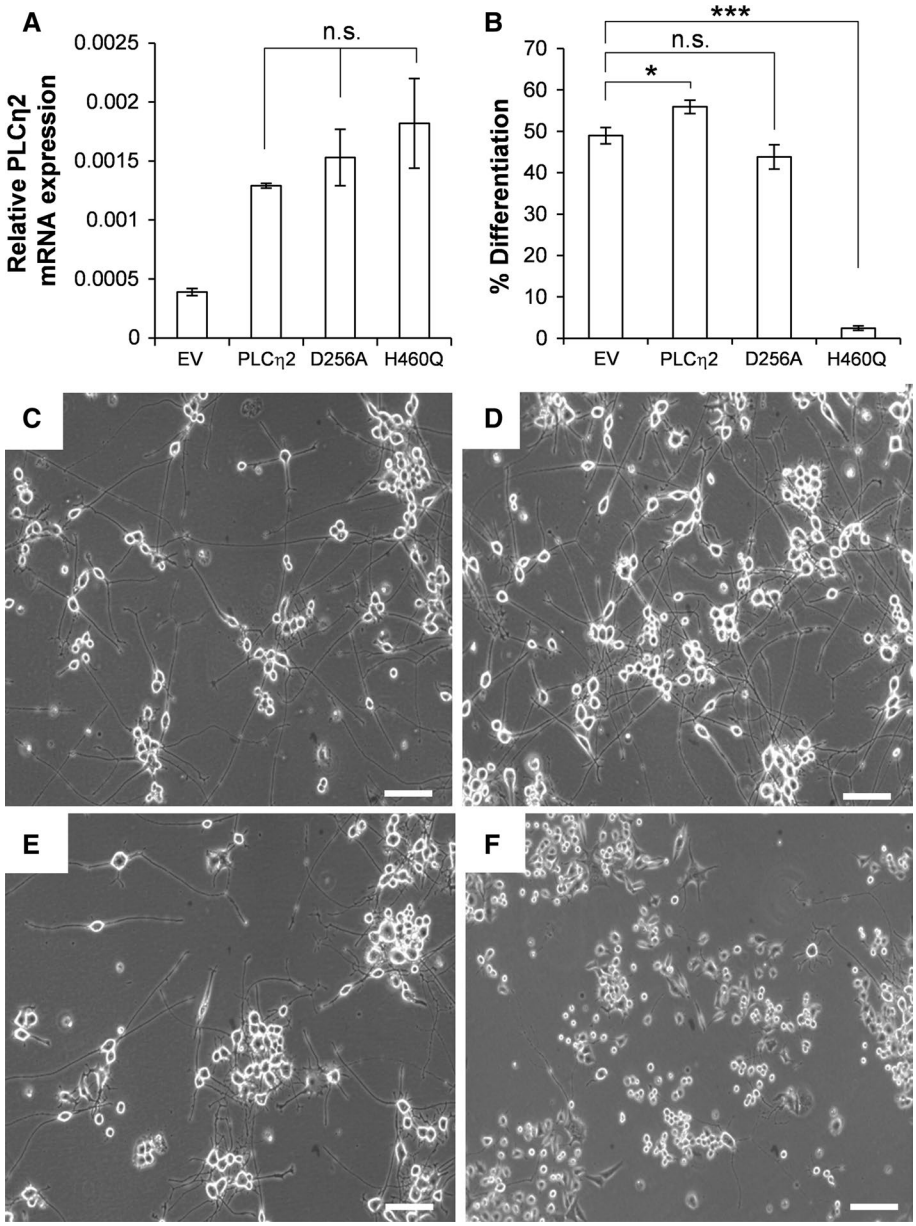

Fig. 1 **a** *Graph* showing mRNA expression levels of PLCη2 relative to RPLP0 in stably transfected cell lines. *Error bars* represent S.E.M. The statistical significance was established by one-way ANOVA using Tukey's honest significance test. Differences in PLCη2 mRNA expression (relative to RPLP0 mRNA expression) in cell lines stably expressing PLCη2 forms were nonsignificant as indicated by n.s; where $p > 0.05$. **b** *Graph* showing percentage of differentiation in different stable cell lines. *Error bars* represent S.E.M. The statistical significance (as determined by unpaired *t* test with applied Bonferroni's correction) is indicated as $***p < 0.001$ and $*p < 0.05$. **c**–**f** Representative *bright-field* images of stable cells expressing empty vector (EV), wild-type PLCη2 (PLCη2) and D256A and H460Q mutants, respectively, after 4 days of retinoic acid treatment. *Scale bars* correspond to 10 µm

signal intensities over a range of cellular compartments were compared as shown in Fig. 2a. The majority of organelles were found to exhibit a higher signal in the control compared with PLCη2 KD cells. The specific percentage of gold particles attributed to each organelle was then calculated in order to assess the degree of specific staining (Fig. 2b; Table 1). The majority of specific signal, corresponding to the presence of PLCη2, was found in the cell nucleus (54.4 ± 3.5 %) and to a lesser degree, the cytosol (27.4 ± 1.4 %) and mitochondria (8.8 ± 2.6 %), A smaller specific signal was observed at plasma membrane (5.5 ± 1.3 %), nuclear envelope (2.2 ± 1.0 %), endoplasmic reticulum (1.7 ± 1.5 %). No specific staining was observed over the Golgi apparatus or multivesicular bodies. Note that errors quoted above represent S.E.M from three separate experiments.

PLCη2 interacts directly with LIMK-1

LIMK-1 was previously identified as an interaction partner of PLCη2 using a bacterial hybrid screen (Popovics et al. 2013). In order to attempt to clarify the direct interaction of PLCη2 with LIMK-1, proximity ligand assays were performed using control and PLCη2 KD cells. In each of these cell lines, fluorescent particles, corresponding to interactions between PLCη2 and LIMK-1, were observed and were predominantly located within the cytosol, but some were also present in the cell nucleus (Fig. 3a–c).

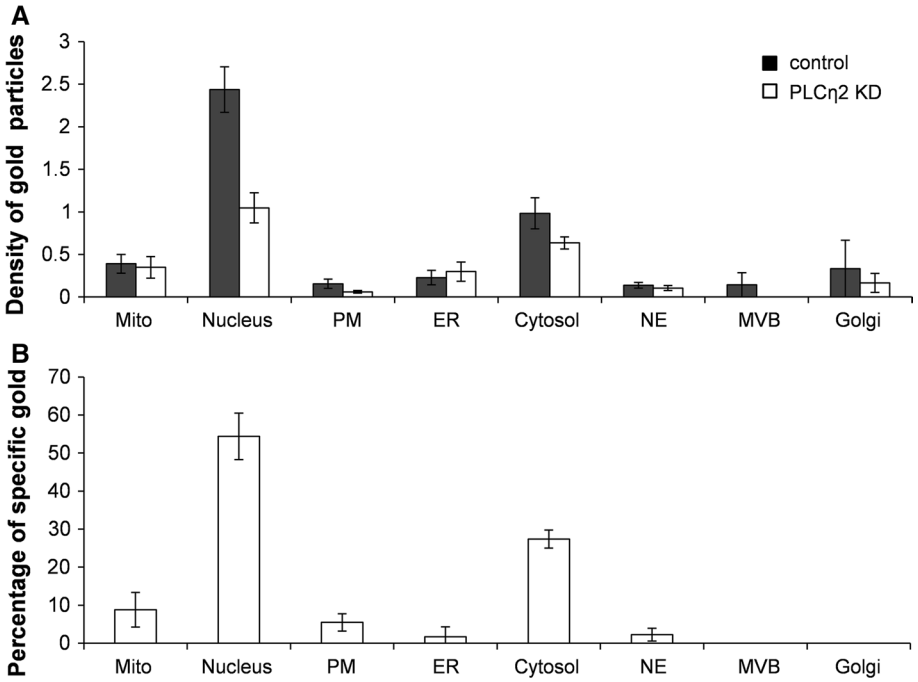

Fig. 2 **a** *Graph* showing the labeling index for PLCη2 localization over cell compartments and organelles in non-target shRNA control cells (*black bars*) and PLCη2 KD cells (*white bars*). The index was calculated by dividing the number of counted gold particles counted over each organelle by the number of intercepts that a set reference point made with standard membrane features during scanning. *Error bars* represent S.E.M from three experiments. *Filled bars* control cells and *open bars* knockdown. **b** *Graph* showing the percentage of specific gold in each compartment/organelle as derived from Table 1. *Error bars* represent S.E.M from three experiments. *Mito* mitochondria, *PM* plasma membrane, *ER* endoplasmic reticulum, *NE* nuclear envelope, *MVB* multivesicular body, *Golgi* Golgi apparatus

Table 1 Data used to calculate the specific percentage of gold particles in cellular compartments/organelles

	Specific density (SD)	Fraction specific (FS)	Total raw gold	Specific gold (SG)	% Specific
Mitochondria	0.16	0.48	25.33	9.59	8.82
Nucleus	1.74	0.72	102.00	71.60	54.38
PM	0.12	0.75	9.67	7.15	5.47
ER	0.04	0.21	19.67	1.23	1.71
Cytosol	0.56	0.57	62.67	35.77	27.38
NE	0.07	0.53	5.00	2.29	2.25
MVB	0.14	0.33	1.00	0.00	0.00
Golgi	0.22	0.22	0.33	0.00	0.00

Specific labeling density was calculated from the difference between control and knockdown. The number of specific gold particles attributed to each organelle was calculated as described previously (Lucocq and Gawden-Bone 2010). Briefly, specific density (SD) of gold particles was calculated by subtracting the average density of labeling for each organelle in PLCη2 KD Neuro2A cells from that of control cells. SD was then divided by the average density in control cells to determine the fraction specific (FS) gold particles. Next, specific gold (SG) was calculated by multiplying FS by the total number of raw gold particles counted in each organelle in control cells. This was then divided by the total SG across all compartments and multiplied by 100 to establish the percentage of specific gold in each organelle. Data are expressed as average values across three experiments

The number of fluorescent particles in the PLCη2 control cells was eightfold higher than in PLCη2 KD cells, indicating the staining to be specific. The assay was also performed with non-transfected Neuro2A cells grown for 4 days in the presence or absence of 20 μM retinoic acid. The retinoic acid-treated Neuro2A cells underwent normal differentiation, characterized by an enlargement of the cell body and neurite outgrowth (Fig. 3d–h). The number of fluorescent particles in retinoic acid-treated cells was approximately eightfold greater than the untreated cells. Particles were observed mainly in the cytoplasm and within growing neurites, as well as in the nucleus to a lower degree.

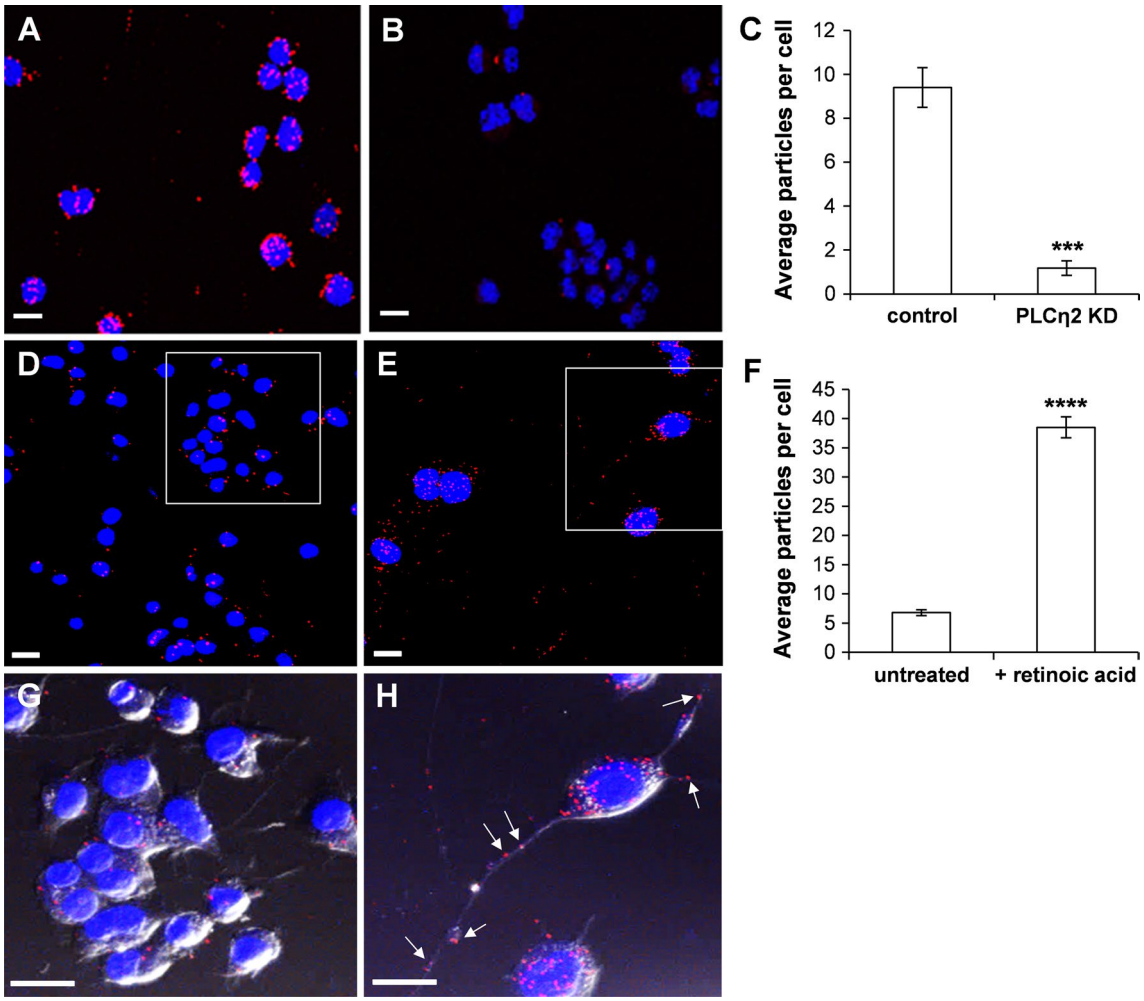

Fig. 3 Proximity ligand assay allowing visualization and quantification of PLCη2-LIMK-1 interactions in Neuro2A cells. Fluorescent images in (**a**) and (**b**) are taken from control and PLCη2 KD Neuro2A cells, respectively. Fluorescent particles corresponding to PLCη2-LIMK-1 interactions appear in *red* and DAPI-staining of nuclei in *blue*. These micrographs are representative of the quantitative data shown in (**c**). **c** *Graph* showing the average number of fluorescent particles in each cell for control and PLCη2 KD groups. Five images were taken at random locations on the coverslip and nuclei and fluorescent particles which indicate PLCη2 interaction with LIMK-1 were counted according to a randomized counting method. **d**, **e** Fluorescent images [representative of quantitation in (**f**)] are taken from untreated and retinoic acid-treated Neuro2A cells, respectively (fluorescent particles corresponding to PLCη2-LIMK-1 interactions appear in *red*; DAPI-staining of nuclei in *blue*). **f** *Graph* showing the average number of fluorescent particles in untreated and retinoic acid-treated Neuro2A cells. Five micrographs were taken at random. Nuclei and fluorescent particles which indicate PLCη2 interaction with LIMK-1 were counted according to a randomized counting method. **g**, **h** Respective "close-up" images of the cells in (**d**, **e**) as indicated, where fluorescence is merged with *bright-field* view such that individual cells can be more easily visualized. *Error bars* represent standard error of the coefficient for five micrographs. The statistical significance (as determined by unpaired *t* test) is indicated as ****$p < 0.0001$. *Scale bars* correspond to 15 µm

These results confirm that PLCη2 and LIMK-1 do indeed interact and provide a strong indication that their interaction is important for retinoic acid-induced Neuro2A cell differentiation.

Discussion

The Neuro2A cell is an established cell model for the examination of molecular events that regulate neuronal differentiation (Pankratova et al. 1994; Riboni et al. 1995; Carter et al. 2003; Kouchi et al. 2011), and upon stimulation with retinoic acid, they change from a stem cell-like morphology to a neuronal one, including formation and extension of neurites. An essential role for PLCη2 in neurite growth was previously demonstrated in Neuro2A cells (Popovics et al. 2014), which was further investigated in this study. Unlike most PLCs which comprise a non-calcium-sensing EF-hand-like domain (Bairoch and Cox 1990), PLCη2 has a functional EF-hand domain containing

a canonical 12-residue loop (EF-loop 1) (Popovics et al. 2014). We reported that EF-loop 1 is responsible for activation of the enzyme by calcium through mutation of D256 (to Ala), a key calcium-binding residue in this domain, which resulted in an apparent ~tenfold reduction in calcium sensitivity in transfected COS-7 cells (Popovics et al. 2014). In an attempt to assess both whether PLCη2 activity is important for neurite growth and whether such involvement may be due to activation by calcium, we generated Neuro2A cells stably overexpressing wild-type PLCη2 and mutant forms of the enzyme (D256A and H460Q). Following retinoic acid treatment, there was a slight but significant increase in the percentage of differentiated cells observed in the wild-type PLCη2 stably transfected cells, relative to controls cells. Conversely, cells stably transfected with the H460Q mutant exhibited a dramatic reduction in the proportion of differentiated cells (~25-fold) relative to control cells after stimulation with retinoic acid. A comparable degree of differentiation was observed in the cells stably transfected with the D256A mutant relative to control after the treatment. These results reveal that expression of the H460Q mutant has a strong dominant-negative effect on neurite outgrowth. These results further highlight the essential role of PLCη2 in neurite outgrowth. In addition, they suggest that modulation of PLCη2 activity by calcium binding at the EF-hand domain may enhance, presumably through positive feedback of calcium signaling, but is not essential to retinoic acid-stimulated neurite growth. It is therefore likely that the principal mechanism by which PLCη2 is activated is not through calcium binding, but through another unknown mechanism. Recently, a new role has emerged for PLCη2 in secretion of cytoplasmic dense core vesicles in neuroendocrine cells. This is accomplished by PLCη2-mediated PtdIns(4,5)P_2 hydrolysis following its activation by Ca^{2+}. The decrease in PtdIns(4,5)P_2 causes dysregulation of actin binding proteins which results in F-actin disassembly, thereby removing the physical barrier which would otherwise prevent dense core vesicle up-regulation to the plasma membrane (Yamaga et al. 2015). In this process, reorganization of the actin cytoskeleton is therefore dependent on Ca^{2+} activation of PLCη2. The authors did, however, show that this occurs only when intracellular Ca^{2+} levels are very high (~800 nM), and showed exocytosis of plasma membrane dense core vesicles at lower Ca^{2+} levels (~400 nM). This suggests that Ca^{2+} activation of PLCη2 may be involved in actin reorganization under certain conditions that significantly elevate intracellular Ca^{2+} levels.

To establish where in Neuro2A cells PLCη2 is specifically located, we examined the subcellular localization of endogenous PLCη2 by quantitative immuno-EM. This approach revealed the majority of endogenous PLCη2 to reside in the nucleus. We also observed a relatively high degree of PLCη2 to be present in the cytosol and to a lower extent, at the plasma membrane. The presence of PLCη2 in the nucleus and cytosol is consistent with previous immunofluorescent studies which also revealed a high degree of nuclear staining, corresponding to the presence of PLCη2, in these cells (Popovics et al. 2011). The PH domain of PLCη2 has been shown to bind phosphatidylinositol 3,4,5-trisphosphate (PtdIns(3,4,5)P_3) with high affinity, a phospholipid which is abundant in Neuro2A cell nuclei (Popovics et al. 2011). Indeed PLCη2 and PtdIns(3,4,5)P_3 were shown to co-localize in these cells to a large degree (Popovics et al. 2011), and hence this interaction could govern the cellular localization of PLCη2. If so, then it is also likely that PLCη2 resides in the nucleus of neuronal cells as they have also been reported to possess high levels of PtdIns(3,4,5)P_3 in their nuclei (Neri et al. 1999; Kwon et al. 2010). The presence of other phospholipases such as PLCγ1, PLCδ4 and PLCβ1 in eukaryotic cell nuclei is well established (Martelli et al. 1992; Divecha et al. 1993; Matteucci et al. 1998; Ye et al. 2002; Liu et al. 1996). PLCβ1 is perhaps the best characterized of these and has proposed roles in mediating differentiation of C2C12 myoblasts (Faenza et al. 2003) and erythroleukemia cells (Fiume et al. 2005), mainly through regulation of gene expression. It is therefore possible that PLCη2 plays a similar role in neuronal differentiation. Evidence for a role in regulation of gene expression is supported by the observation that activation of retinoic acid response element (RARE)-associated gene expression is dramatically reduced in PLCη2 KD cells (Popovics et al. 2011). As with the cytoplasm, PLCη2 may also be responsible for regulating actin dynamics in the nucleus. Although β-actin has been identified in the nucleus, actin filaments have not been detected at interphase by common F-actin detecting methods (Sellers 2004). It has, however, been reported that ~20 % of nuclear actin forms polymeric structures, with rapid turnover (McDonald et al. 2006). Both cofilin and LIMK-1 possess nuclear localization sequences and are present in the nucleus (Abe et al. 1993; Goyal et al. 2006). More recently, it has emerged that cofilin is required for RNA polymerase II functioning and transcription elongation (Obrdlik and Percipalle 2011). It is therefore likely that PLCη2 is involved in regulating gene expression and actin-related processes in the nucleus; however, the precise role of nuclear PLCη2 remains to be established and must be probed further.

Another potential mechanism by which PLCη2 may contribute to neurite growth is through regulation of cytoskeletal dynamics. LIMK-1, a specific regulator of actin polymerization, was previously identified using a bacterial-2-hybrid screen as a putative interaction partner of PLCη2; however, a specific interaction of these two proteins within the cell was not shown (Popovics et al. 2011).

It is well established that LIMK-1 deactivates cofilin family proteins by phosphorylation, which in turn prevents actin depolymerization and contributes to reorganization of the actin cytoskeleton (Ghosh et al. 2004; Lorenz et al. 2004). Accordingly, neurons from LIMK-1 knockout mice show reduced or deficient growth cones as well as abnormal dendritic morphology, synapse structures and spine development which manifest in behavioral changes such as the relearning of spatial information (Meng et al. 2002). LIMK-1 also appears to have contradictory roles; activation of LIMK-1 by Semaphorin 3A (Aizawa et al. 2001), or fibrillar amyloid beta (Heredia et al. 2006) for example, leads to growth cone collapse and neurite deformation, respectively. Based on these studies, it appears that LIMK-1 is an essential protein for correct central nervous system development, but its regulation is important for normal physiology and alterations to its normal functioning leads to human diseases such as William's syndrome, which is characterized by mild to moderate mental retardation (Meyer-Lindenberg et al. 2006).

To establish whether PLCη2 and LIMK-1 interact directly, we utilized a proximity ligand interaction assay which allowed quantification and localization of interactions between the two proteins. To attain a positive signal using this approach, proteins must be in the proximity of <30–40 nm; this distance is a good indication that proteins are close enough to one another to interact, or at the very least, participate in cross talk. By looking at compiled Z-stack images, we were able to determine that this putative interaction took place mainly in the cytosol and within growing neurites, suggestive of a role in regulating actin dynamics. Putative PLCη2-LIMK-1 interactions were also observed in the nucleus, albeit to a lower degree. Accordingly, LIMK-1 has a nuclear localization signal which drives translocation into the nucleus, and shuttling between the nucleus and the cytoplasm is indicated by presence of nuclear import and export sequences (Goyal et al. 2006). Upon cell differentiation, we observed a ~six-fold increase in fluorescent particles in Neuro2A cells, suggesting that these proteins interact to a higher degree during differentiation. This may in part be due the fact that PLCη2 protein expression is increased in Neuro2A cells following retinoic acid treatment (Popovics et al. 2013). Some evidence that PLCη2 activation occurs upstream from LIMK-1 comes from the observation that phosphorylation of LIMK-1 and CREB, a substrate of LIMK-1, is significantly reduced in retinoic acid-treated PLCη2 KD cells relative to control cells (Popovics et al. 2013). Also down-regulation of either of these genes significantly decreases neurite outgrowth in cultured cells (Endo et al. 2007; Popovics et al. 2013).

We previously proposed a model by which PLCη2 may regulate neuronal differentiation (Popovics et al. 2011), whereby the generation of secondary messengers, Ins(1,4,5)P_3 and DAG impact upon cytoskeletal dynamics and gene expression, respectively. PLCη2 can be activated by Gβγ dimers, but as retinoic acid acts upon nuclear receptors rather than GPCRs, it would seem unlikely that the enzyme is activated this way in the current context. PLC isozymes such as PLCδ1 can be activated by kinases (Fujii et al. 2009), of which PLCη2 may also be a target. It is in theory possible that PLCη2 may be activated by LIMK-1; however, without knowledge of a specific activating phosphorylation site on PLCη2, this will be difficult to establish.

Upon PLCη2 activation, the level of PtdIns(4,5)P_2 will likely decrease with subsequent elevations in Ins(1,4,5)P_3 and DAG. Ins(1,4,5)P_3 triggers calcium release from the intracellular stores to activate CaMKIV. The consequent stimulation of LIMK-1 activity leads to activation of CREB which initiates transcription of genes directing neuronal differentiation (Popovics et al. 2013). Here, we have clarified part of this model by demonstrating the direct association of PLCη2 and LIMK-1 in differentiating Neuro2A cells. This direct association could allow PLCη2 to directly activate LIMK-1 by promoting an active conformation upon association, or it is possible that this interaction simply allows PLCη2 to be "on hand" to modulate LIMK-1 activation via Ins(1,4,5)P_3 release and CaMKIV activation. Changes in the nuclear DAG and PtdIns(4,5)P_2 levels may also influence transcriptional activity through modulation of DAG-PKC or PtdIns(4,5)P_2-chromatin interactions.

In conclusion, we reveal that PLCη2 activity in Neuro2A cells is important for retinoic acid-induced neurite growth but is not dependent upon calcium binding at EF-loop 1, highlighting the fact that activation of PLCη2 during this process does not primarily occur through calcium binding, but via another unknown mechanism. We also demonstrate that PLCη2 is present in the nucleus and cytosol of Neuro2A cells and reveal that the enzyme interacts directly with LIMK-1 in the cytosol and within growing neurites as well as inside the nucleus. This interaction has important implications for regulation of actin dynamics and expression of genes implicated in neuronal differentiation.

Acknowledgments We gratefully acknowledge financial support from the Wellcome Trust (Grant No. WT089803MA to J.M.L.) and the School of Medicine, University of St Andrews.

References

Abe H, Nagaoka R, Obinata T (1993) Cytoplasmic localization and nuclear transport of cofilin in cultured myotubes. Exp Cell Res 206:1–10

Aizawa H, Wakatsuki S, Ishii A, Moriyama K, Sasaki Y, Ohashi K, Sekine-Aizawa Y, Sehara-Fujisawa A, Mizuno K, Goshima Y, Yahara I (2001) Phosphorylation of cofilin by LIM-kinase is necessary for semaphorin 3A-induced growth cone collapse. Nat Neurosci 4:367–373

Arber S, Barbayannis FA, Hanser H, Schneider C, Stanyon CA, Bernard O, Caroni P (1998) Regulation of actin dynamics through phosphorylation of cofilin by LIM-kinase. Nature 393:805–809

Bairoch A, Cox JA (1990) EF-hand motifs in inositol phospholipid-specific phospholipase C. FEBS Lett 269:454–456

Berridge MJ, Dawson RM, Downes CP, Heslop JP, Irvine RF (1983) Changes in the levels of inositol phosphates after agonist-dependent hydrolysis of membrane phosphoinositides. Biochem J 2121:473–482

Carter JM, Waite KA, Campenot RB, Vance JE, Vance DE (2003) Enhanced expression and activation of CTP:phosphocholine cytidylyltransferase β2 during neurite outgrowth. J Biol Chem 278:44988–44994

Divecha N, Rhee SG, Letcher AJ, Irvine RF (1993) Phosphoinositide signalling enzymes in rat liver nuclei: phosphoinositidase C isoform β1 is specifically, but not predominately, located in the nucleus. Biochem J 289:617–620

Endo M, Ohasi K, Mizuno K (2007) LIM kinase and slingshot are critical for neurite extension. J Biol Chem 282:13692–13702

Faenza I, Bavelloni A, Fiume R, Lattanzi G, Maraldi NM, Gilmour RS, Martelli AM, Suh PG, Billi AM, Cocco L (2003) Up-regulation of nuclear PLCβ1 in myogenic differentiation. J Cell Physiol 195:446–452

Fitzgibbon GJ, Clayton-Smith J, Banka S, Hamilton SJ, Needham MM, Dore JK, Miller JT, Pawson D, Gaunt L (2008) Array comparative genomic hybridization-based identification of two imbalances of chromosome 1p in a 9-year-old girl with a monosomy 1p36-related phenotype and a family history of learning difficulties: a case report. J Med Case Rep 2:355

Fiume R, Faenza I, Matteucci A, Astolfi A, Vitale M, Martelli AM, Cocco L (2005) Nuclear phospholipase C β1 (PLCβ1) affects CD24 expression in murine erythroleukemia cells. J Biol Chem 280:24221–24226

Fujii M, Yi KS, Kim MJ, Ha SH, Ryu SH, Suh PG, Yagisawa H (2009) Phosphorylation of phospholipase C-δ1 regulates its enzymatic activity. J Cell Biochem 108:638–650

Ghosh M, Song X, Mouneimne G, Sidani M, Lawrence DS, Condeelis JS (2004) Cofilin promotes actin polymerization and defines the direction of cell motility. Science 304:743–746

Goyal P, Pandey D, Siess W (2006) Phosphorylation-dependent regulation of unique nuclear and nucleolar localization signals of LIM-kinase 2 in endothelial cells. J Biol Chem 281:25223–25230

Heinz DW, Essen LO, Williams RL (1998) Structural and mechanistic comparison of prokaryotic and eukaryotic phosphoinositide-specific phospholipase C. J Mol Biol 275:635–650

Heredia L, Helguera P, de Olmos S, Kedikian G, Sola Vigo F, LaFerla F, Staufenbiel M, de Olmos J, Busciglio J, Caceres A, Lorenzo A (2006) Phosphorylation of actin-depolymerizing factor/cofilin by LIM-kinase mediates amyloid β-induced degeneration: a potential mechanism of neuronal dystrophy in Alzheimer's disease. J Neurosci 26:6533–6542

Hokin MR, Hokin LE (1953) Enzyme secretion and the incorporation of P32 into phospholipides of pancreas slices. J Biol Chem 203:967–977

Hwang JI, Oh YS, Shin KJ, Kim H, Ryu SH, Suh PG (2005) Molecular cloning and characterization of a novel phospholipase C, PLC-η. Biochem J 389:181–186

Kanemaru K, Nakahara M, Nakamura Y, Hashiguchi Y, Kouchi Z, Yamaguchi H, Oshima N, Kiyonari H, Fukami K (2010) Phospholipase C-η2 is highly expressed in the habenula and retina. Gene Expr Patterns 10:119–126

Kim JK, Choi JW, Lim S, Kwon O, Seo JK, Ryu SH, Suh PG (2011) Phospholipase C-η1 is activated by intracellular Ca^{2+} mobilization and enhances GPCRs/PLC/Ca^{2+} signaling. Cell Signal 23:1022–1029

Kouchi Z, Igarashi T, Shibayama N, Inanobe S, Sakurai K, Yamaguchi H, Fukada T, Yanagi S, Nakamura Y, Fukami K (2011) Phospholipase Cδ3 regulates RhoA/Rho kinase signalling and neurite outgrowth. J Biol Chem 286:8459–8471

Kwon IS, Lee KH, Choi JW, Ahn JY (2010) PI(3,4,5)P_3 regulates the interaction between Akt and B23 in the nucleus. BMB Rep 43:127–132

Liu N, Fukami K, Yu H, Takenawa T (1996) A new phospholipase C-δ4 is induced at S-phase of the cell cycle and appears in the nucleus. J Biol Chem 271:355–360

Lo Vasco VR (2011) Role of phosphoinositide-specific phospholipase C η2 in isolated and syndromic mental retardation. Eur Neurol 65:264–269

Lorenz M, DesMarais V, Macaluso F, Singer RH, Condeelis J (2004) Measurement of barbed ends, actin polymerization, and motility in live carcinoma cells after growth factor stimulation. Cell Motil Cytoskeleton 57:207–217

Lucocq J (2008) Quantification of structures and gold labeling in transmission electron microscopy. Methods Cell Biol 88:59–82

Lucocq J (2012) Can data provenance go the full monty? Trends Cell Biol 22:229–230

Lucocq JM, Gawden-Bone C (2010) Quantitative assessment of specificity in immunoelectron microscopy. J Histochem Cytochem 58:917–927

Martelli AM, Alberto M, Martelli R, Gilmour S, Bertagnolo V, Neri LM, Manzoli L, Cocco L (1992) Nuclear localisation and signaling activity of phosphoinositidase Cβ in Swiss 3T3 cells. Nature 358:242–244

Matteucci A, Faenza I, Gilmour S, Manzoli L, Billi AM, Peruzzi D, Bavelloni A, Rhee S, Cocco L (1998) Nuclear but not cytoplasmic phospholipase C-β1 inhibits differentiation of erythroleukemia cells. Cancer Res 58:5057–5060

McDonald D, Carrero G, Andrin C, De Vries G, Hendzel MJ (2006) Nucleoplasmic beta-actin exists in a dynamic equilibrium between low-mobility polymeric species and rapidly diffusing populations. J Cell Biol 172:541–552

Meng Y, Zhang Y, Tregoubov V, Janus C, Cruz L, Jackson M, Lu WY, MacDonald JF, Wang JY, Falls DL, Jia Z (2002) Abnormal spine morphology and enhanced LTP in LIMK-1 knockout mice. Neuron 35:121–133

Meyer-Lindenberg A, Mervis CB, Faith Berman K (2006) Neural mechanisms in Williams syndrome: a unique window to genetic influences on cognition and behaviour. Nat Rev Neurosci 7:380–393

Nakahara M, Shimozawa M, Nakamura Y, Irino Y, Morita M, Kudo Y, Fukami K (2005) A novel phospholipase C, PLCη2, is a neuron-specific isozyme. J Biol Chem 280:29128–29134

Neri LM, Martelli AM, Borgatti P, Colamussi ML, Marchisio M, Capitani S (1999) Increase in nuclear phosphatidylinositol 3-kinase activity and phosphatidylinositol (3,4,5) trisphosphate synthesis precede PCK-ζ translocation to the nucleus of NGF-treated PC12 cells. FASEB J 13:2299–2310

Obrdlik A, Percipalle P (2011) The F-actin severing protein cofilin-1 is required for RNA polymerase II transcription elongation. Nucleus 2:72–79

Pankratova EV, Sytina EV, Stepchenko AG (1994) Cell differentiation in vitro and the expression of Oct-2 protein and *oct*-2 RNA. FEBS Lett 24:81–84

Popovics P, Stewart AJ (2012) Putative roles for phospholipase C-η enzymes in neuronal Ca^{2+} signal modulation. Biochem Soc Trans 40:282–286

Popovics P, Beswick W, Guild SB, Cramb G, Morgan K, Millar RP, Stewart AJ (2011) Phospholipase C-η2 is activated by elevated intracellular Ca^{2+} levels. Cell Signal 23:1777–1784

Popovics P, Gray A, Arastoo M, Finelli D, Tan AJL, Stewart AJ (2013) Phospholipase C-η2 is required for retinoic acid-stimulated neurite growth. J Neurochem 124:638–644

Popovics P, Lu J, Kamil LN, Morgan K, Millar RP, Schmid R, Blindauer CA, Stewart AJ (2014) A canonical EF-loop directs Ca^{2+}-sensitivity in phospholipase C-η2. J Cell Biochem 115:557–565

Riboni L, Prinetti A, Bassi R, Caminiti A, Tettamanti G (1995) A mediator role of ceramide in the regulation of neuroblastoma Neuro2A cell differentiation. J Biol Chem 270:26868–26875

Sellers JR (2004) Fifty years of contractility research post sliding filament hypothesis. J Muscle Cell Motil 25:475–482

Stallings JD, Tall EG, Pentyala S, Rebecchi MJ (2005) Nuclear translocation of phospholipase C-δ1 is linked to the cell cycle and nuclear phosphatidylinositol 4,5-bisphosphate. J Biol Chem 280:22060–22069

Stewart AJ, Mukherjee J, Roberts SJ, Lester D, Farquharson C (2005) Identification of a novel class of mammalian phosphoinositol-specific phospholipase C enzymes. Int J Mol Med 15:117–121

Stewart AJ, Morgan K, Farquharson C, Millar RP (2007) Phospholipase C-eta enzymes as putative protein kinase C and Ca^{2+} signaling components in neuronal and neuroendocrine tissues. Neuroendocrinology 86:243–248

Streb H, Irvine RF, Berridge MJ, Schulz I (1983) Release of Ca^{2+} from a nonmitochondrial intracellular store in pancreatic acinar cells by inositol-1,4,5-trisphosphate. Nature 306:67–69

Suh PG, Park JI, Manzoli L, Cocco L, Peak JC, Katan M, Fukami K, Kataoka T, Yun S, Ryu SH (2008) Multiple roles of phosphoinositide-specific phospholipase C. BMB Rep 41:415–434

Söderberg O, Gullberg M, Jarvius M, Ridderstråle K, Leuchowius KJ, Jarvius J, Wester K, Hydbring P, Bahram F, Larsson LG, Landegren U (2006) Direct observation of individual endogenous protein complexes in situ by proximity ligation. Nat Methods 3:995–1000

Takemura M, Mishima T, Wang Y, Kasahara J, Fukunaga K, Ohashi K, Mizuno K (2009) Ca^{2+}/calmodulin-dependent protein kinase IV-mediated LIM kinase activation is critical for calcium signal-induced neurite outgrowth. J Biol Chem 284:28554–28562

Tokuyasu KT (1973) A technique for ultracryotomy of cell suspensions and tissues. J Cell Biol 57:551–565

Yamaga M, Kielar-Grevstad DM, Martin TF (2015) Phospholipase Cη2 activation re-directs vesicle trafficking by regulating F-actin. J Biol Chem 290:29010–29021

Yang N, Higuchi O, Ohashi K, Nagata K, Wada A, Kangawa K, Nishida E, Mizuno K (1998) Cofilin phosphorylation by LIM-kinase 1 and its role in Rac-mediated actin reorganization. Nature 393:809–812

Ye K, Aghdasi B, Luo H, Moriarity JL, Wu FY, Hong JJ, Hurt KJ, Bae SS, Suh P, Snyder SH (2002) Phospholipase C-γ1 is a physiological guanine nucleotide exchange factor for the nuclear GTPase PIKE. Nature 415:541–544

Zeng M, Zhou JN (2008) Roles of autophagy and mTOR signaling in neuronal differentiation of mouse neuroblastoma cells. Cell Signal 20:659–665

Zhou Y, Wing MR, Sondek J, Harden TK (2005) Molecular cloning and characterization of PLC-η2. Biochem J 391:667–676

Zhou Y, Sondek J, Harden TK (2008) Activation of human phospholipase C-η2 by Gβγ. Biochemistry 47:4410–4417